HIGH-RESOLUTION CARBON ISOTOPE STRATIGRAPHY, PENNSYLVANIAN SNAKY CANYON FORMATION, EAST-CENTRAL IDAHO: IMPLICATIONS FOR REGIONAL AND GLOBAL CORRELATIONS

A Thesis

by

CASEY GIBSON JOLLEY

Submitted to the Office of Graduate Studies of
Texas A&M University
in partial fulfillment of the requirements for the degree of

MASTER OF SCIENCE

May 2012

Major Subject: Geology

High-Resolution Carbon Isotope Stratigraphy, Pennsylvanian Snaky Canyon Formation,

East-Central Idaho: Implications for Regional and Global Correlations

HIGH-RESOLUTION CARBON ISOTOPE STRATIGRAPHY, PENNSYLVANIAN SNAKY CANYON FORMATION, EAST-CENTRAL IDAHO: IMPLICATIONS FOR REGIONAL AND GLOBAL CORRELATIONS

A Thesis

by

CASEY GIBSON JOLLEY

Submitted to the Office of Graduate Studies of
Texas A&M University
in partial fulfillment of the requirements for the degree of

MASTER OF SCIENCE

Approved by:

Chair of Committee,	Michael C. Pope
Committee Members,	Ethan L. Grossman
	Debbie J. Thomas
Head of Department,	Rick Giardino

May 2012

Major Subject: Geology

ABSTRACT

High-Resolution Carbon Isotope Stratigraphy, Pennsylvanian
Snaky Canyon Formation, East-Central Idaho:
Implications for Regional and Global Correlations. (May 2012)
Casey Gibson Jolley, B.S., Brigham Young University
Chair of Advisory Committee: Dr. Michael C. Pope

Nearly 550 samples of fine grained carbonates, collected every 0.5 to 1.0 m from the Bloom Member of the Snaky Canyon Formation at Gallagher Peak, Idaho, were analyzed to determine the high-resolution carbon isotope stratigraphy. To constrain for diagenesis, thin sections were petrographically analyzed and viewed using cathodoluminescence microscopy. Chemical analyses were performed using an electron microprobe.

Average $\delta^{18}O$ and $\delta^{13}C$ values from the Bloom Member are -4.5‰ ± 1.6‰ (1σ) and 2.1‰ ± 1.1‰, respectively. Maximum $\delta^{13}C$ values are about 1‰ higher for the Desmoinesian and Missourian than the Morrowan and Atokan, similar to results from the Yukon Territory. $\delta^{18}O$ and $\delta^{13}C$ values are lowest for crystalline mosaic limestones and siltstones, moderate for packstones, wackestones, and mudstones, and highest for boundstones and grainstones.

The $\delta^{13}C$ profile from Gallagher Peak consists of high frequency 1‰ oscillations with several larger excursions. No large $\delta^{13}C$ increase at the base of the section suggests

the Mid-Carboniferous boundary is in the underlying Bluebird Mountain formation. $\delta^{13}C$ of Gallagher Peak and Arrow Canyon, NV, correlate well from 318 to 310 Ma, but correlation becomes more difficult around 310 Ma. This may result from increased restriction of the Snaky Canyon platform beginning in the Desmoinesian. Most of the short term (<1 Ma) isotopic excursions are the result of diagenesis. Two of the largest negative excursions at Gallagher Peak correlate with two large negative excursions at Big Hatchet Peak, NM, possibly due to sea level lowstands of the Desmoinesian. Phylloid algal mounds at Gallagher Peak are associated with positive excursions because of original aragonite composition and increased open marine influence. Positive excursions related to other facies characteristics also result from increased marine influence. The $\delta^{13}C$ curve for the upper half of Gallagher Peak contains three repeated cycles of increasing $\delta^{13}C$ over 1-1.5 Ma, which are possibly related to long-term sea level fluctuations. Given the complexity of each local environment, without detailed biostratigraphy, detailed rock descriptions, and analysis of the various rock components, $\delta^{13}C$ stratigraphy of whole rocks can be misinterpreted.

ACKNOWLEDGEMENTS

I would like to thank my committee chair, Dr. Michael Pope, and my committee members, Dr. Ethan Grossman and Dr. Debbie Thomas, for their time and guidance. Special thanks goes to my primary advisor, Dr. Pope, for his extra guidance and time away from family collecting samples. Additionally, I'd like to thank Dr. Grossman for his thorough reviews of my thesis, adding his expert knowledge and style to my work.

I want to thank those that made sample collection and analysis possible. The American Association of Petroleum Geologists and Geological Society of America gave financial support. Josiah Tingey of Brigham Young University spent six days hiking up and down more than 2000 vertical feet. He volunteered his time and energy without complaint. No words can express my gratitude for his contribution to this project. I'm grateful for the efforts of the staff at the Texas A&M Stable Isotope Geoscience Facility, who in in spite of equipment failure, found a way to run hundreds of samples for me.

Finally, I need to thank my friends and family for all their support on this project. My parents gave much time and support to help me get this far in school. Dean Jolley, my father, gave his time and vehicles to support the field work. Celia Jolley, my mother, checked drafts of this thesis for spelling and grammar. I thank all my peers or those that may not be mentioned specifically for their help with classes and other aspects of this project. Finally, I must not forget to thank my wife for being my inspiration, my motivation, and my love. She spent many lonely hours caring for our home and children while I worked on this project. Thank you.

TABLE OF CONTENTS

Page

ABSTRACT iii

ACKNOWLEDGEMENTS v

TABLE OF CONTENTS vi

LIST OF FIGURES viii

LIST OF TABLES ix

1. INTRODUCTION 1

2. BACKGROUND 5

    2.1 Biostratigraphy 6
    2.2 Stratigraphy 11
    2.3 Depositional Setting 13
    2.4 Previously Identified Pennsylvanian Carbon Isotope Trends 16

3. METHODS 21

4. RESULTS 31

    4.1 Petrographic Results 31
    4.2 $\delta^{18}O$ and $\delta^{13}C$ Averages 32
    4.3 Stratigraphic $\delta^{13}C$ trends 35
    4.4 Cathodoluminescence Microscopy and Chemical Analyses 37

5. DISCUSSION 42

    5.1 Diagenesis 42
    5.2 Excursions Related to Facies 47
    5.3 Arrow Canyon Compared to Gallagher Peak 52
    5.4 Future Work 58

6. CONCLUSIONS 59

REFERENCES 61

Page

APPENDIX A 78

APPENDIX B 109

APPENDIX C 253

APPENDIX D 254

APPENDIX E 257

APPENDIX F 258

APPENDIX G 259

VITA 260

LIST OF FIGURES

Page

Figure 1 Study locations with paleogeography modified from Blakey (2005) 5

Figure 2 Stratigraphy and carbon isotope stratigraphy of the Bloom Member of the Snaky Canyon Formation at Gallagher Peak, Idaho(A) with key 7

Figure 3 Compilation of previous carbon isotope curves along with data from this study 17

Figure 4 Carbon and oxygen isotopes for all analyzed samples from Gallagher Peak, Idaho 33

Figure 5 Average $\delta^{18}O$ and $\delta^{13}C$ based on rock classification of fine grained carbonate samples from Gallagher Peak, Idaho 34

Figure 6 Five-point running average in blue ($\delta^{18}O$) and red ($\delta^{13}C$) 36

Figure 7 Microprobe analyses of matrix calcite and other calcite components of samples from Gallagher Peak, Idaho, plotted vs. $\delta^{18}O$ 44

Figure 8 Carbon isotope stratigraphy of Gallagher Peak, Idaho, and Arrow Canyon, Nevada 49

Figure 9 Alternate correlation between Arrow Canyon, Nevada, (Saltzman, 2003) and Gallagher Peak, Idaho, using carbon isotopes of fine grained carbonate 57

LIST OF TABLES

Page

Table 1 $\delta^{18}O$ and $\delta^{13}C$ of Gallagher Peak, Idaho 25

Table 2 Average $\delta^{18}O$ and $\delta^{13}C$ by rock classification and age 34

Table 3 Electron microprobe analyses of carbonate matrix and skeletal grains 38

Table 4 North American and International stage boundary ages 53

1. INTRODUCTION

In order to more accurately correlate stratigraphic sections, carbon and oxygen stable isotopes have been used improve correlation. Carbon and oxygen stable isotope data of the Paleozoic have been used as local and global correlation tools and paleoenvironment proxies (e.g., Compston, 1960; Lowenstam, 1961; Mii et al., 1999; Saltzman, 2005). Perhaps the most successful application of stable isotope stratigraphy is the correlation across entire oceans of oxygen isotopes in benthic and planktonic foraminifera in deep sea cores, with reliable stratigraphy throughout the Cenozoic (Miller et al., 1987; Zachos et al., 2001; 2008). Positive and negative excursions of carbon isotopes were also correlated in some of these deep sea cores (Shackleton and Hall, 1984). Carbon isotope records for the Paleozoic can be quite variable (Saltzman et al., 2005), yet some excursions in well preserved sediments are recognized globally (Saltzman et al., 2000; 2004; Saltzman, 2005; Dilliard et al., 2007; Katz et al., 2007). Beyond correlating stratigraphically, stable isotopes also provide information regarding paleoenvironment and diagenesis. Oxygen isotopes in carbonate fossils and microfossils are used to indicate depositional paleotemperature (Shackleton, 1967; 1977; 1987; Grossman and Ku, 1986; Böhm et al., 2000; Zachos et al., 2008), paleodepth (Adlis et al., 1988), and original ocean chemistry (Came et al., 2007). Carbon isotopes in carbonate rocks can reflect changes in productivity (Zachos et al., 1989), oxidation of organic matter (Scholle and Arthur, 1980), carbon burial rates, weathering rates (Berner and Kothavola, 2001), ocean circulation (Mii et al., 1999), meteoric diagenesis (Allan

---

This thesis follows the style of Palaeogeography, Palaeoclimatology, Palaeoecology.

and Matthews, 1982), and original mineralogy (Swart and Eberli, 2005; Swart, 2008). Carbon isotope reservoirs and fluxes are summarized in Kump and Arthur (1999).

Local effects and/or diagenesis can dramatically disrupt the global isotopic signal and have brought the validity of correlating deep time isotopic stratigraphy records into question. For example, $\delta^{13}C$ of the shallow water setting at the Bahama Banks tends to be depleted 4‰ relative in the open ocean due to freshwater discharge, evaporation, and $CaCO_3$ withdrawal (Patterson and Walter, 1994). Also isotopic excursions can sometimes be correlated to ramp position and facies, suggesting an overriding local signal (Immenhauser et al., 2002). Thus, isotopic excursions that appear age equivalent between two sections may just be coincidental (Panchuk et al., 2005). Additionally, the effects of meteoric and burial diagenesis, which tend to lower both $\delta^{13}C$ and $\delta^{18}O$ values, are well documented (e.g. Allen and Matthews, 1977; Hudson, 1977; Dickson and Coleman, 1980).

Well preserved brachiopods are used to determine the isotopic signal of Paleozoic oceans due to their abundance and resistance to diagenesis (Popp et al., 1986; Grossman et al., 1991). Also, clumped isotopes in brachiopods and mollusks provide paleotemperatures independent of assumptions about original sea-water $\delta^{18}O$ (Came et al., 2007). However, the rarity of pristine fossils leads to two major drawbacks: (1) loss of stratigraphic continuity and (2) limited spatial distribution. Additionally, the $\delta^{13}C$ of well-preserved specimens are still subject to local carbon isotope variations of up to 4‰, which may mask global isotope excursions (Patterson and Walters, 1994; Panchuk et al., 2006).

Bulk carbonate has a powerful advantage over pristine fossils in that sampling can be stratigraphically continuous and distributed. This allows for high-resolution carbon isotope profiles to be constructed temporally at various locations (Saltzman, 2003). Closely spaced sampling can help resolve short-lived isotope excursions (Scholle and Arthur, 1980). However, it is recognized that bulk carbonate $\delta^{18}O$ and $\delta^{13}C$ values tend to be altered during early burial as the unstable carbonate minerals change to more stable mineralogies (Dicksen and Coleman, 1980; Batt et al., 2008). This alteration tends to make $\delta^{18}O$ values unreliable in whole rock samples, but $\delta^{13}C$ is still useful because of carbon buffering within the carbonate rocks (Marshall, 1992). Evidence suggests that even though $\delta^{13}C$ values may not be completely preserved, stratigraphic trends likely represent general $\delta^{13}C$ trends of original depositional waters (Stoll and Schrag, 2000).

If trends in the $\delta^{13}C$ of carbonate rocks are preserved then we might expect two locations with similar age, open ocean connectivity, and depositional setting to have similar profiles. This can only be achieved if resolution of both profiles is sufficient to identify even short term excursions. Additionally detailed notes of each material sampled will be needed to distinguish between local, diagenetic, and global signals. However, if two locations meeting these conditions show dissimilar trends, then some of the limitations of carbon isotope stratigraphy are revealed. Previous studies have attempted correlation of various locations to a high-resolution dataset from a Pennsylvanian section at Arrow Canyon, Nevada (Brand and Brenckle, 2001; Saltzman, 2003; Grossman et al., 2008; Flake, 2011). However, few of these studies have the resolution or similar depositional setting to provide a robust comparison.

We compare a high-resolution $\delta^{13}C$ profile of bulk carbonate for the Bloom Member of the Snaky Canyon Formation in east-central Idaho with the published data from a Pennsylvanian section at Arrow Canyon, Nevada (Saltzman, 2003). Both sections cover the majority of the Pennsylvanian, have similar fossil assemblages, facies, and conodont zones, and both border the ancient Panthalassan ocean. Similar depositional environments, relatively continuous deposition, and relative time equivalence make these sections good candidates to determine the utility of carbon isotope stratigraphy of fine grained carbonate samples for regional and global correlation.

2. BACKGROUND

As the Global Stratotype Section and Point (GSSP) for the Mississippian-Pennsylvanian boundary, the Carboniferous section at Arrow Canyon, southeastern Nevada (Fig. 1), is well studied (Lane et al., 1999). Its biostratigraphy, facies,

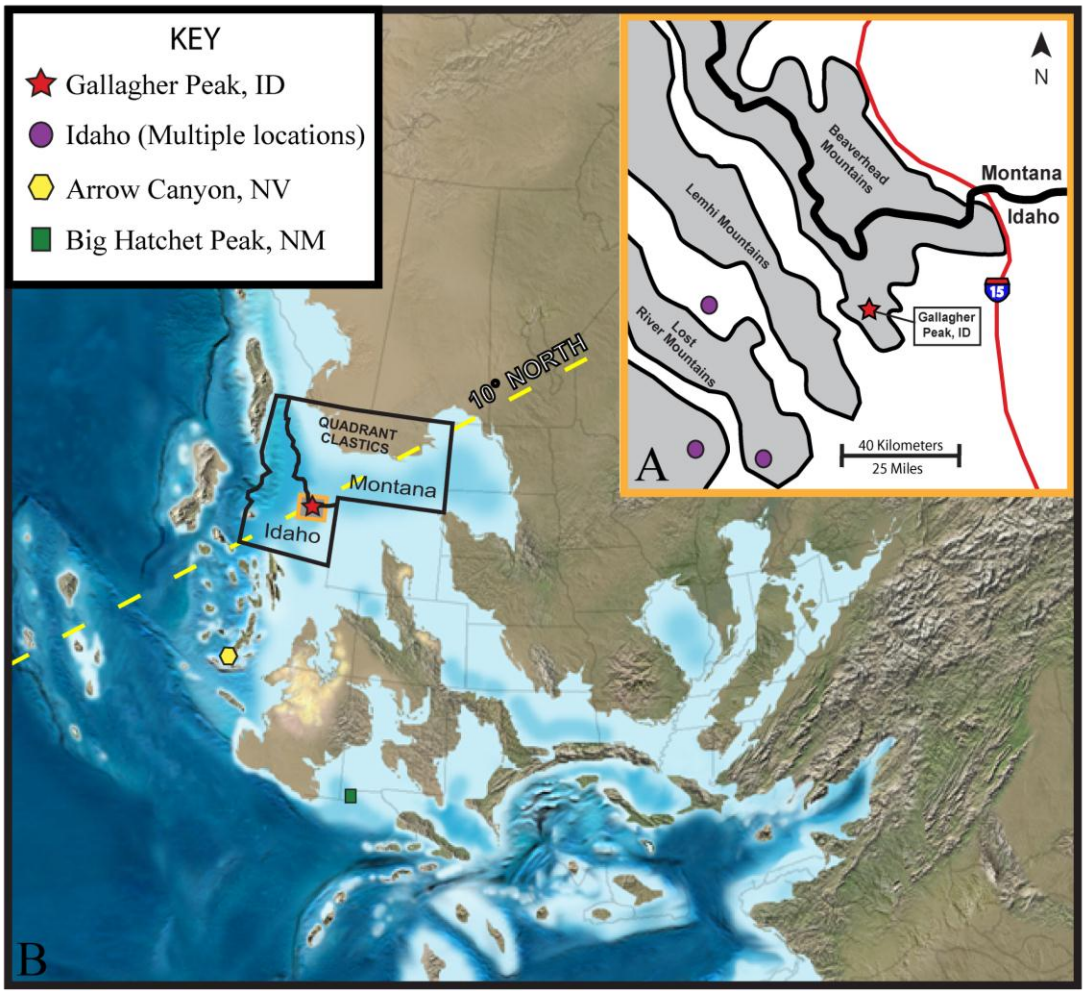

Fig. 1. Study locations (A) with paleogeography (B) modified from Blakey (2005). The upper right (A) illustrates the location of the study area with respect to modern mountain ranges and state borders. Study locations are represented by the following symbols: a red star for Gallagher Peak (this study), a purple circle for multiple sections in Idaho (Batt et al., 2007), a yellow hexagon for Arrow Canyon (Saltzman, 2003), and a green square for Big Hatchet Peak (Magaritz and Holser, 1990).

depositional environment, and carbon isotopes were previously documented (Cassity and Langenheim, 1966; Poole and Sandberg, 1991; Pierce and Langenheim, 1974; Lane et al., 1999; and Saltzman, 2003). The coeval Pennsylvanian Bloom Member of the Snaky Canyon Formation located in east-central Idaho (Fig. 1) is less studied. The biostratigraphy, sequence stratigraphy, and depositional environments of the Bloom Member are outlined here to establish the framework of the carbon isotope stratigraphy.

Upper Carboniferous mixed carbonate and siliciclastic deposits of the Snaky Canyon Formation (600-1200 m thick) outcrop in the White Knob Mountains, southern Lost River, and Lemhi Ranges of east-central Idaho near southwestern Montana (Skipp et al., 1979). The Snaky Canyon Formation was deposited directly on top of the quartzose sandstone, limestone, and dolostone of the Mississippian Bluebird Mountain Formation and is capped conformably by the Phosphoria Formation (Skipp et al., 1979). The Snaky Canyon Formation consists of the lower Bloom Member, the medial Gallagher Peak Sandstone, and the upper Juniper Gulch Member (Skipp et al., 1979). The measured section of this study encompasses the entire Bloom Member located in the southern Beaverhead Mountains near Gallagher Peak, Idaho (Fig. 2). The measured section begins at 44°10’15.91”N, 112°48’20.37”W, and ends at 44°10’5.52”N, 112°47’33.66”W. This section is located approximately 850 km (528 mi) north-northwest of the Arrow Canyon Section in Nevada (Fig 1).

2.1 *Biostratigraphy*

Conodont and foraminiferal biostratigraphy indicate the Bloom Member is Morrowan to Missourian (Fig. 2), similar in age to deposits at Arrow Canyon (Skipp et

Fig. 2. Stratigraphy and carbon isotope stratigraphy of the Bloom Member of the Snaky Canyon Formation at Gallagher Peak, Idaho(A) with key (B). Original biostratigraphy was based on North American Stages. International stages relative to North American stages are based on Menning et al. (2006). The $\delta^{13}C$ profile is a five-point running average of data from this study. The key presents rock type and biostratigraphic symbols (B). Conodont zones according to Isaacson (Isaacson, personal comm., 2011).

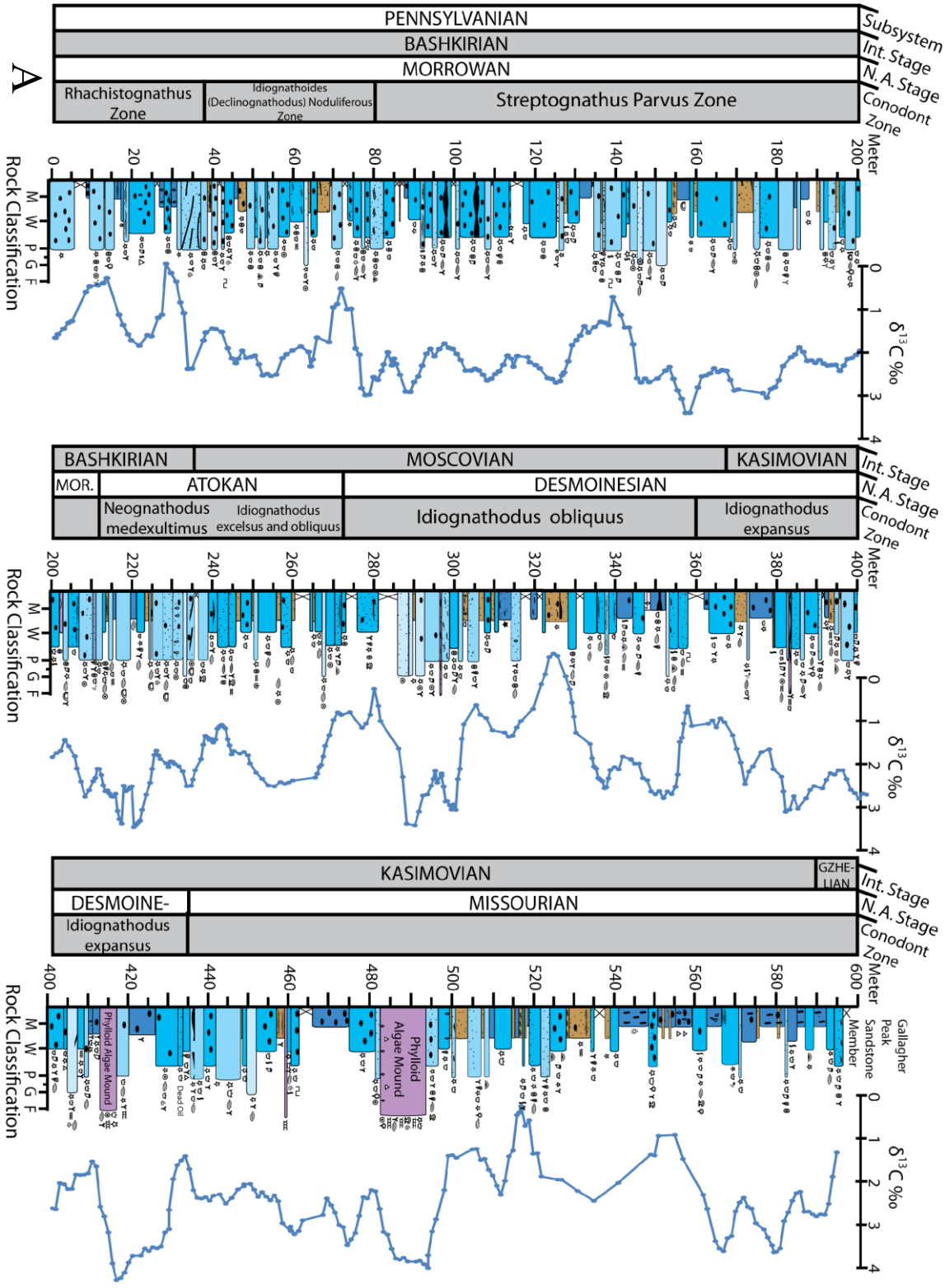
A
PENNSYLVANIAN
BASHKIRIAN
MORROWAN
Rhachistognathus Zone
Idiognathoides (Declinognathodus) Noduliferous Zone
Streptognathus Parvus Zone
Subsystem
Int. Stage
N. A. Stage
Conodont Zone
Meter
Rock Classification
M W P G F
δ13C ‰
BASHKIRIAN
MOSCOVIAN
KASIMOVIAN
MOR.
ATOKAN
DESMOINESIAN
Neognathodus medexultimus
Idiognathodus excelsus and obliquus
Idiognathodus obliquus
Idiognathodus expansus
KASIMOVIAN
GZHE-LIAN
DESMOINE-
MISSOURIAN
Idiognathodus expansus
Phylloid Algae Mound
Dead Oil
Gallagher Peak Sandstone Member

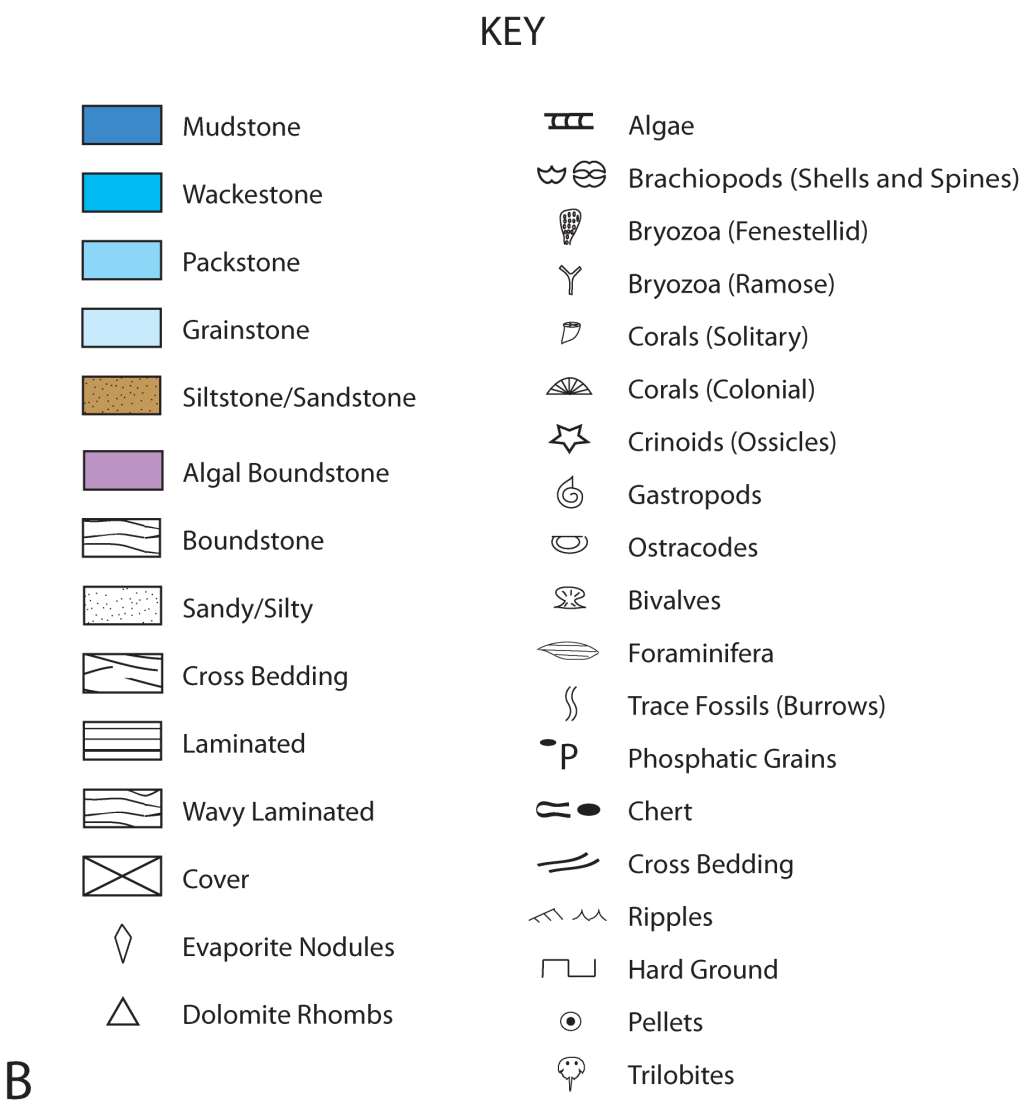

B

Figure 2 - Continued

al., 1979; Archuleta et al., 2006; Pope et al., 2007). Late Mississippian foraminifera were identified in the lower 15 m of the Gallagher Peak section, suggesting that the Mid-Carboniferous Boundary may occur within the section (Skipp et al., 1979). However, a sharp increase in $\delta^{13}C$ in the Bluebird Mountain Formation was interpreted to be the Mid-Carboniferous Boundary (Batt et al., 2008). Sampling of the Gallagher Peak section began just above the Bluebird Mountain Formation, and thus likely excludes the Mid-carboniferous boundary.

Morrowan to Atokan conodont species identified in the Snaky Canyon Formation include: *Adetognathus lautus, Adetognathus gigantus, Hindeodus minutes, Idiognathodus delicates, Neognathodus bassleri,* and *Neognathodus symmetricus* (Archuleta et al., 2006). The presence of *Hindeodus* could indicate a more stable marine environment during the Morrowan (Heckel, 1994). Morrowan foraminifera in the section include *Eoschubertella* and *Pseudostaffela* (Groves, 1986, Archuleta et al., 2006). Atokan to Desmoinesian foraminifera *Beedeina sp*., *Wedekindellina sp.*, *Fusulinella sp.*, *Globivalvulina sp., Millerella Sp., Profusulinella sp., Staffella sp.,* and *Palaeotextulariid* were previously identified about 215 to 550 m above the base of the Bloom Member near Gallagher Peak (Skipp et al., 1979; Groves, 1986). Also recovered from the Atokan was the conodont *Streptognathodus n sp.* (Groves, 1986). Desmoinesian conodont species identified around 270 m and 360 m above the base of the section include *Idiognathodus obliquus* and *Idiognathodus expansus* respectively (Isaacson, personal comm., 2011). Desmoinesian foraminifera *Wedekindellina henbesti* was also noted 168 m below the top of the Bloom Member at Gallagher Peak (Verville et al., 1990). Middle

to Late Missourian fusulinid *Triticites* was collected just below the Gallagher Peak Sandstone at Gallagher Peak with Early Virgilian *Triticites sp*. collected above the Gallagher Peak Sandstone southeast of Gallagher Peak (Verville et al., 1990). Similar conodonts and foraminifera to those described in the Snaky Canyon Formation were identified at Arrow Canyon (Skipp et al., 1985; Lane et al., 1999).

2.2 *Stratigraphy*

The Bloom Member makes up about one half of the deposits of the Snaky Canyon Formation. The Bloom Member is around 550 m of limestone with interbedded very fine quartzose sandstone and siltstone (Skipp et al., 1979). Sandstone and siltstone increase eastward from the White Knob Mountains to the Beaverhead Mountains (Skipp et al., 1979). Eventually these interfinger with the coeval Quadrant Formation to the east (Skipp et al., 1979).

The Gallagher Peak section of the Bloom Member (Fig. 2) consists primarily of medium-dark-gray skeletal wackestone (≈44%), skeletal packstone (≈26%), mudstone (≈13%), and siltstone (≈11%), with the remaining 6% composed of grainstone, calcisiltstone, algal boundstone, and bedded chert (See Appendix A for detailed descriptions of samples) deposited on a shallow subtidal carbonate ramp. Fine quartz sand and silt are pervasive throughout the entire section and some beds contain up to 40% chert in both nodular and bedded forms. Stromatolites, foraminifera, phylloid algae, *Paleoaplysina*, brachiopods, solitary and colonial corals, bryozoans, ostracods, trilobites, mollusks, and crinoids all occur within the Bloom Member (Skipp et al., 1979; Pope et al., 2007). A shallow subtidal ramp with algal mounds facies, a restricted

carbonate facies, a cherty deep subtidal facies, and an eolian facies were previously described within the Bloom Member (Isaacson et al., 1988; Archuleta et al., 2006; Pope et al., 2007). Observations of this study indicate that the shallow subtidal facies consists of skeletal wackestone and packstone, which comprise the majority of the section. Abundant evaporites and ostracods mark the restricted carbonate facies. The cherty deep subtidal facies is characterized by mudstone with few skeletal grains. The eolian facies consist of finely laminated quartz siltstone with less than 50% carbonate and often contains marine skeletal grains, usually crinoids. Increased evaporites, mudstone, and dolomudstone, and a decrease in open marine facies in the upper 200 m of the section suggest that this carbonate ramp environment was becoming more restricted toward the Gallagher Peak Sandstone. Phylloid algal mounds may have also enhanced restriction for landward deposits (Skipp et al., 1979; Archuleta et al., 2006).

The Bloom Member consists of high-frequency, high-amplitude depositional cycles imprinted on a longer-term second or third order transgressive systems tract (TST) and highstand systems tract (HST) (Archuleta et al., 2006). Parasequences (meter-scale cycles) are composed of shallowing upward cycles of 2-16 m thickness grouped into 5-10 parasequence sets, each 50-80 m thick (Pope et al., 2007). Cyclothems in the section were identified by flooding surfaces and have durations of 200-250 ky (Archuleta et al., 2006; Pope et al., 2007). The longer term TST occurred from the Morrowan to the Atokan with the HST deposited during the upper Desmoinesian to Missourian (Pope et al., 2007). The upper Missourian Gallagher Peak sandstone represents the subsequent lowstand system tract (LST). However, the Gallagher Peak

Sandstone was not preserved in all sections since it is a discontinuous unit (Skipp et al., 1979). Siliciclastics in other sections were noted to decrease in the upper half of the Bloom Member, suggesting that sea level fluctuations were less dramatic in the Late Pennsylvanian and/or that the siliciclastic source was less available due to changes in wind direction, source proximity, or tectonics (Archuleta et al., 2006). However, a consistent increase or decrease of siliciclastic input was not noted in this section. Systems tract interpretations of coeval Arrow Canyon deposits indicate a TST during the Morrowan that was followed by continual shallowing from the upper Morrowan through the Missourian (Heath et al., 1967). Carbon isotope fluctuations of this study support that Missourian depositional environments were more restricted than Morrowan settings.

2.3 *Depositional Setting*

The Snaky Canyon Formation (Fig. 1) was deposited on a shallow dipping homoclinal carbonate ramp along the western margin of Laurentia around paleolatitude 10° N (Breuninger et al., 1988; Canter and Isaacson, 1991; Batt et al., 2007). Silty shallow water deposits in the western margins of the ramp and silty subtidal carbonates deposited to the east indicate that the paleoshoreline fluctuated laterally between the Beaverhead Mountain outcrops and the Quadrant Formation in southwestern Montana (Tremblay, 1996; Batt et al., 2007). Paleowind direction indicators from the Quadrant Sandstone suggest southwest transport of sediment, indicating the Quadrant Sandstone was the likely source for quartz silt grains in the Snaky Canyon carbonates (Breuninger et al., 1976; 1988; Canter and Isaacson, 1991; Archuleta et al., 2006; Batt et al., 2007; Pope et al., 2007). Shifts in wind direction or distance from the sediment source could

have affected sand input during deposition of the Snaky Canyon Formation (Saperstone and Ethridge, 1984).

The depositional environments of the Gallagher Peak and Arrow Canyon sections are similar with a few notable exceptions. The Arrow Canyon section was interpreted as shallow marine deposits open to the ocean (Lane et al., 1999), while connectivity to the open ocean of the east-central Idaho section is unclear (Skipp et al., 1979). However, stenohaline crinoids throughout the Gallagher Peak section suggest salinities did not fluctuate dramatically (Boardman et al., 1987). Additionally, pervasive brachiopods through the entire section indicate normal marine salinities (Richardson, 1997; Brand et al., 2003). Yet, phylloid algal mound complexes in the upper 200 m of the Idaho section restricted the flow of marine water to deposits on the eastern side of the platform (Skipp et al., 1979). Mounds capped by *Paleoaplysina* are hypothesized to have grown below average low tide, while sandstone filled lows between the mounds (Breuninger et al., 1976; 1988; Rankey, 1997). The presence of evaporites and ostracods in some of the deposits indicates that this region was at times partly restricted (Hughes-Clarke and Keij, 1973; West, 1975). Likely, the Morrowan to Atokan units record a more open shallow marine ramp with peritidal and subtidal facies. Next, algal mounds of Paleoaplysina developed basinward (Archuleta et al., 2006). Atokan to Late Desmoinesian uplift of the Antler foreland basin created the Copper Basin Highlands and further restricted the Snaky Canyon carbonate platform by separating it from the Wood River Basin (Skipp et al., 1979). This resulted in more abundant peritidal facies and less subtidal facies coinciding with an increase of Paleoaplysina and phylloid algal

mounds (Archuleta et al., 2006). Increased restriction of the Snaky Canyon carbonate ramp in the Late Desmoinesian increases the possibility of an altered isotopic signal relative to open marine conditions (Patterson and Walter, 1994; Kievman, 1998).

The high frequency cycles (100-400 ky) identified at Gallagher Peak, Arrow Canyon, Paradox Basin, and the US Midcontinent are the result of glacio-eustatic sea level fluctuations (Goldhammer et al., 1991; Heckel, 1994; Archuleta et al., 2006). Sharp basal contacts could indicate that transgressive phases were much more rapid than those deposited in the US Mid-continent (Archuleta et al., 2006). Glacio-eustatic fluctuations for this region are estimated to be a minimum of 16 meters, based on algal mound height without consideration for sediment compaction (Breuninger, 1976; Archuleta et al., 2006). However, the majority of estimates for the amplitude of sea-level fluctuations during the Pennsylvanian range from 40 to 200 m based on ice-sheet volume calculations, conodont $\delta^{18}0$, and facies juxtapositions (Heckel, 1977; Veevers and Powell, 1987; Crowley & Baum, 1991; Soreghan and Giles; 1999; Butts, 2005; and Joachimski et al., 2006). High-frequency sea level oscillations likely began in the early Visean (Wright and Vanstone, 2001) and decreased into the Desmoinesian (Moscovian) (Klein, 1994). In previous studies, sea level fluctuations and stage boundaries were correlated to $\delta^{13}C$ excursions, as excursions may be the result of oceanic anoxic events, extinctions, flooding, or other events at stage boundary (Schlanger and Jenkyns, 1976; Fischer and Arthur, 1977; Scholle and Arthur, 1980).

In general, arid climate conditions prevailed in Idaho during the Pennsylvanian (Baars, 1962; Mack et al., 1979; Blakey et al., 1988; Cecil et al., 2003). However, the

Late Mississippian (Chesterian) records major climate change due to the transition from greenhouse to icehouse conditions (Isbell et al., 2003). Additionally, interglacial periods (sea level highs) resulted in more humid conditions during the Late Pennsylvanian, whereas glacial periods record more arid deposits (Soreghan, 1994; Rankey, 1997). These interpretations are consistent with the US Midcontinent transitioning from ever-wet conditions to seasonally dry climates during the changeover from the Mississippian to the Pennsylvanian (Tabor and Montañez, 2002; Raymond and Metz, 2004). Weathering and siliciclastic input also may be higher with increased seasonal rainfall (Cecil, 1990). Arrow Canyon was likely more humid with less seasonality than the Snaky Canyon section as it was located nearer the equator during the Pennsylvanian (Lane et al., 1999; Brand and Bruckschen, 2002).

2.4 *Previously Identified Pennsylvanian Carbon Isotope Trends*

In order to avoid vital affects and other differences in fractionation different records are reported for brachiopods and fine grained carbonate. However, similar $\delta^{13}C$ trends expected to be preserved in both (Saltzman, 2005). Based on brachiopod analyses long term carbon isotope trends for the Pennsylvanian, including U.S. Midcontinent data (Fig. 3), begin with an increase of 1-2‰ across the Mid-Carboniferous boundary (Grossman et al., 1993; 2008). This is followed by a gentle increase until reaching a maximum value near the mid-Desmoinesian (Mii et al., 1999; 2001; Grossman et al., 2008). A 1‰ decrease to a Kasimovian minimum is followed by a gradual 1‰ increase through the Virgilian (Grossman et al., 2008). These average trends, however, disregard spatial variability of $\delta^{13}C$ through time which complicate carbon isotope stratigraphy.

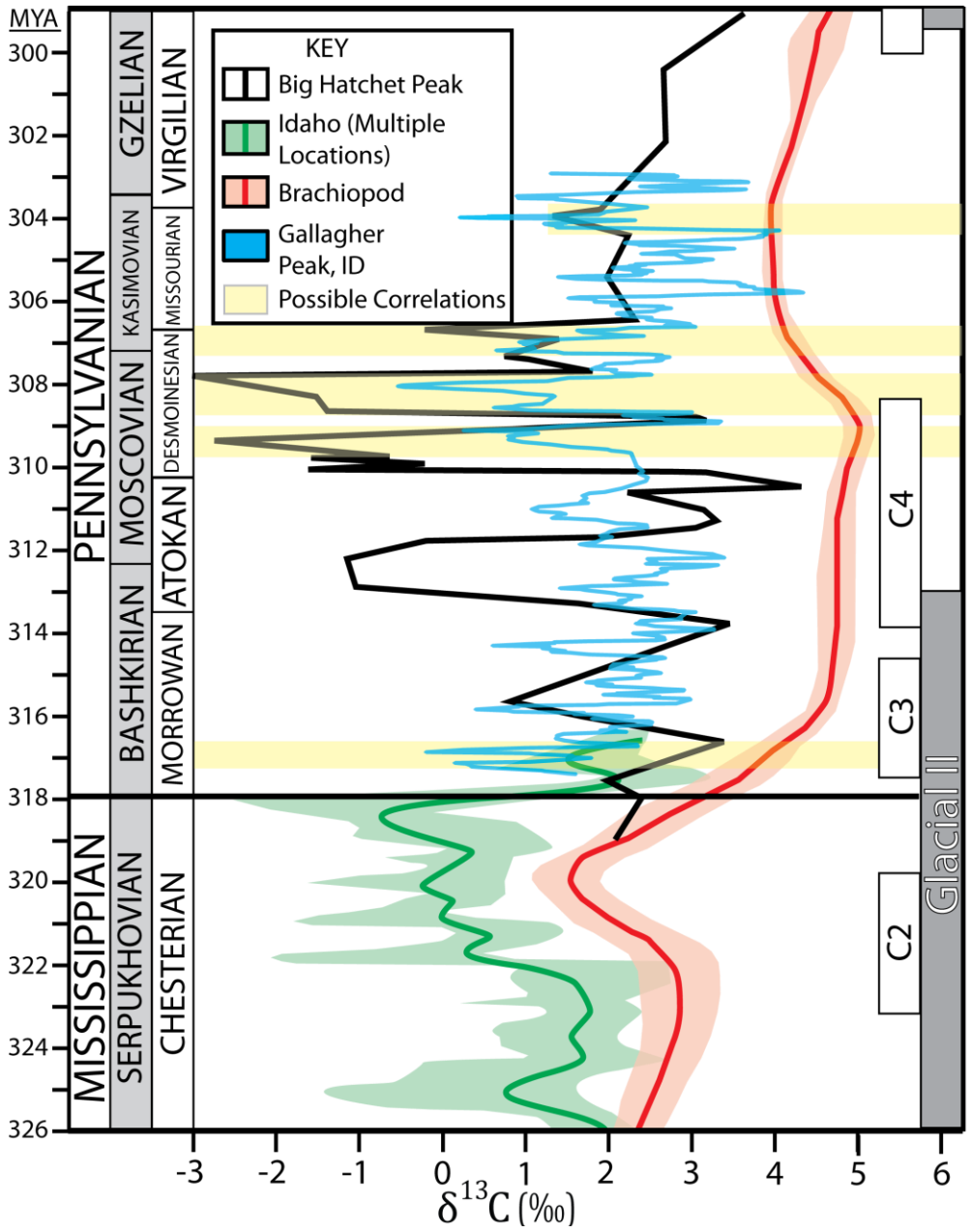

Fig. 3. Compilation of previous carbon isotope curves along with data from this study. Isotopic values for Big Hatchet Peak, NM (Magaritz and Holser, 1990), Idaho (Batt et al., 2007), and Gallagher Peak, ID (this study) are based on whole rock and fine grained carbonate analyses, while the brachiopod curve is a combination of brachiopod data from various locations (Grossman et al., 2008). Relative ages of North American stages as they relate to European stages are based on Menning et al. (2006). Glacial events are presented along the right side: Fielding et al. (2008; white boxes) and Isbell et al., 2003 (modified by Montanez et al., 2007; gray boxes). Ages are according to Gradstein et al. (2004).

For example, isotope analyses of early Pennsylvanian brachiopods indicate that the $\delta^{13}C$ of the Paleo-Tethys Ocean and Panthalassan Ocean differed by up to 1.5‰, likely reflecting paleo-oceanic circulation patterns (Mii et al., 1999). It is hypothesized that upwelling of ^{13}C-depleated waters along the west coast of Laurentia resulted in a 1.5‰ depletion relative to the Paleo-Tethys waters (Mii et al., 1999).

Carboniferous isotopic research in the US has focused primarily on the US Midcontinent (e.g. Grossman et al., 1991; 1993; 2008; Korte et al., 2005; Mii et al., 1999) with fewer studies conducted along the Western US passive margin (Saltzman, 2003; Batt et al., 2007; Katz et al., 2007). Trends from the Midcontinent can be misleading if they are interpreted as proxies to open ocean waters, as restricted circulation can dramatically alter the chemistry of these water bodies (Holmden et al., 1998; Panchuk et al., 2005; Algeo et al., 2008a; 2008b). Stable isotope studies in Canada, Idaho, and New Mexico have sampled closer to the western margins of the US (Fig. 1). In Canada, average $\delta^{13}C$ for micritic carbonate values were determined in the Sverdrup Basin, the northern Yukon territories, and eastern British Columbia (Beauchamp et al., 1987). The $\delta^{13}C$ values decreased from the northeast to the southwest. The farthest north values measured 4 to 7‰ for the Morrowan through the Desmoinesian (Beauchamp et al., 1987). Values in the Yukon Territory range from 1 to 4‰ during the Morrowan to Atokan and 3 to 5‰ during the Atokan to Desmoinesian (Beauchamp et al., 1987). Similarities between these sections and the study location could establish an increasing isotopic trend from the Morrowan to Desmoinesian along the western margin of the US.

A Late Mississippian to Early Pennsylvanian $\delta^{13}C$ profile based on micritic limestone was determined about 50 miles south of Gallagher Peak (Figs. 1, 3; Batt et al., 2007). The $\delta^{13}C$ profile stopped at the top of the Bluebird Mountain Formation (Batt et al., 2007), whereas sampling at Gallagher Peak began above the Bluebird Mountain Formation. Samples from the Bluebird Mountain Formation show a 2.5‰ increase across the mid-Carboniferous boundary that is immediately followed by a short 0.5‰ decrease then an increase (Batt et al., 2007). Although a direct correlation between the two Idaho $\delta^{13}C$ profiles is unlikely, they could still be combined into a single high-resolution profile for Idaho that spans nearly the entire Carboniferous (Appendix C).

Whole-rock $\delta^{13}C$ isotopic data were determined for a Pennsylvanian section at Big Hatchet Peak in southwestern New Mexico (Fig. 1) and Arrow Canyon in southern Nevada (Magaritz and Holser, 1990). Carbon isotope values for the Big Hatchet Peak range from -2 to 4‰ (Fig. 3). Large negative excursions of $\delta^{13}C$ at Big Hatchet Peak (Fig. 1) were correlated with fluctuations at the Arrow Canyon section around 600 km away (Magaritz and Holser, 1990). Trends in this Big Hatchet Peak section begin at 2‰ at the base of the Pennsylvanian, rising to 4‰ in the Atokan and then returning to 2‰ during the Desmoinesian before peaking again near the Pennsylvanian-Permian boundary (Magaritz and Holser, 1990).

The whole-rock $\delta^{13}C$ curve from Arrow Canyon (Saltzman, 2003; 2005) is a high-resolution data set. Additionally, continuous deposition with few exposure surfaces and a limited number of negative $\delta^{18}O$ values indicate the Arrow Canyon section underwent minimal diagenetic resetting (Saltzman, 2003). Brachiopods across the Mid-

Carboniferous boundary in Arrow Canyon had Mississippian and Pennsylvanian $\delta^{13}C$ values of 2.0 ± 0.8‰ and 2.4 ± 0.8‰ respectively (Brand and Brenckle, 2001). Micrite values for Arrow Canyon averaged 1.7 to 2.8‰ lower than pristine brachiopods (Brand and Brenckle, 2001; Jones et al., 2003). Micrite samples that have retain general isotopic trends may be used to correlate stratigraphic sections at a higher resolution than biostratigraphy (Brand and Brenckle, 2001; Saltzman, 2005). Similarities between the Arrow Canyon and Snaky Canyon isotopic records could help distinguish between long-term global trends and local variations. Additionally, differences between the Arrow Canyon section and this study area could provide evidence of restriction and/or local diagenesis of the study area.

3. METHODS

Stratigraphy and biostratigraphy of the section were refined over multiple visits by Michael Pope, Jason Aplanalp, and Bonny Archuleta (Pope et al., 2007). Rock descriptions, rock types, and fossils were further updated in this study by analyzing hand samples and thin sections. Originally the Gallagher Peak section was measured to be 647 m thick (Skipp et al., 1979). However, some beds were repeated due to minor internal faulting and is now 595 m thick (Pope et al., 2007).

The Bloom Member of the Snaky Canyon Formation near Gallagher Peak, Idaho, was sampled at meter to sub-meter intervals beginning around 9,400 ft above sea level. A meter-by-meter measured section (Pope et al., 2007) was used as a guide for sample collection. Partial and total silicification of most brachiopods prevented collection of well-preserved brachiopods in the Gallagher Peak section. All samples were sorted and cut into billets and polished to 600 grit. In order to determine what material was being sampled, two hundred sixty billets distributed throughout the section were chosen for thin section analysis (Appendix A) based on textural maturity, larger skeletal abundance, and unique features (fractures, large fossils, stylolites, laminations, etc.). Thin sections were prepared from billets by National Petrographic Services. Because of possible oil-based contamination during processing, billets were washed in an ultrasonic bath with ethanol for 60 seconds, followed by methanol for 60 seconds, and then rinsed with distilled deionized water and dried in a 70°C oven for 24 hours. No significant difference in isotopic composition between thin-section billets and non-thin-sectioned billets indicate contamination was not an issue. Prior to drilling, sample powder, all

billets were etched for 1-3 seconds in a 20% HCl solution, rinsed in distilled deionized water, and dried for at least 24 hours to ensure each sample was free of any possible debris or cross contamination.

A binocular microscope was used to evaluate the degree of alteration of carbonate components and to ensure sampling of fine-grained sediment (Brand and Brenckle, 2001; Saltzman, 2005). The amount of skeletal components, quartz silt, and dolomite in each billet were noted, while sampling focused on micrite. However, fracture cements, skeletal components, and sparse dolomite were also analyzed to understand the effects of diagenetic events on the isotopic results.

In order to screen for diagenesis, 88 thin sections were polished with 0.3 μm grit and cleaned in an ultrasonic bath of distilled water in preparation for cathodoluminescence microscopy (Dickson, 1966; Popp et al., 1986). Operating conditions for cathodoluminescence were gun currents of 200-300 mA, voltages of 10-15 kV, 20 second exposure, and a 0.07- 0.05 torr chamber pressure.

Around 565 carbonate powders were analyzed at Texas A&M's Stable Isotope Geoscience Facility. Powders were collected from four to ten ½-mm deep holes drilled in each billet using 1-mm carbide tipped drill bits in a Servo drill press. Low drill speed ensured minimal heat and sample loss. Sample powders were weighed individually to achieve the required amount of carbonate material. As each sample contained some quartz silt, additional powder was weighed to adjust for decreasing percentage of carbonate (up to 500 μg). For example, samples with 80-89% carbonate had 110-140 μg of powder analyzed, while samples with 20-29% carbonate had 350-400 μg of powder.

For about 411 samples, 60-80 μg of carbonate was reacted with 100% phosphoric acid at 70° C using a Kiel IV Carbonate Preparation Device coupled with a ThermoFisher Scientific MAT 253 isotope ratio mass spectrometer. About 154 samples, spanning the mid-Desmoinesian to mid-Missourian (342 to 495 m), were analyzed as part of an undergraduate thesis (Wood, 2011). For these samples, about 100 to 150 μg of carbonate was reacted with 100% phosphoric acid at 70° C on a Thermo Finnigan Gas Bench II on-line gas preparation and introduction system. The resultant gases were analyzed with a Thermo Electron DeltaPlus isotope ratio mass spectrometer.

Results were calibrated to VPDB using the NBS-19 standard ($\delta^{13}C$ = 1.95‰, $\delta^{18}O$ = -2.20‰) and an in-house standard. Nearly all reported $\delta^{18}O$ and $\delta^{13}C$ values had an internal and external precision of 0.1‰ or better. One sample (159 B) was simply reported with a higher standard deviation (0.24‰). The standard deviation is still small when compared to intra sample variations of oxygen isotopes.

Thirty thin sections were analyzed for chemical composition using a four spectrometer Cameca SX50 electron microprobe. Microprobe analysis were conducted using accelerating voltages of 15 KV and a beam current of 50 nA. Backscattered electron (BSE) and cathodoluminescent digital images were acquired using the microprobe. Analyses were carried out after standardization using very well characterized compounds or pure elements; standard checks were run to verify standardizations (Guillemette, 2008). For this procedure thin sections were polished to 0.3 μm and cleaned in an ultrasonic bath and then coated with ~ 15 nm of pure carbon prior to analysis to eliminate charging.

Typical accuracy for major elements (> 10 wt. %) is about ± 1 to 2%. Uncertainty at low concentrations increases as the concentration decreases, reaching 100% at the lower limit of detection (LLD). The LLD for elements in this analysis were between 0.004 and 0.02 weight %. Values below LLD were not reported.

Table 1
$\delta^{18}O$ and $\delta^{13}C$ of Gallagher Peak, Idaho. Age according to Gradstein et al. (2004). Sample types A and C are fine grained carbonate samples, D is duplicates, and B is everything else (skeletal, fracture cements, etc.). Material of type B samples is listed in Appendix.

Sample		N.A. Stage	Age (MYA)	$\delta^{13}C$ (‰ vs. VPDB)	$\delta^{18}O$ (‰ vs. VPDB)
0	A	Morrowan	318.10	1.61	-3.81
0.8	A	Morrowan	318.08	1.57	-3.80
0.8	B	Morrowan	318.08	-20.35	-7.38
1.5	A	Morrowan	318.07	1.75	-3.33
2.1	A	Morrowan	318.05	1.80	-3.59
3	A	Morrowan	318.03		
3.5	A	Morrowan	318.02	1.32	-0.87
4.7	A	Morrowan	317.99	1.19	-0.55
5.6	A	Morrowan	317.97	0.91	1.19
9	A	Morrowan	317.90	1.02	-2.88
10	A	Morrowan	317.87	1.58	-2.66
11	A	Morrowan	317.85		
12	A	Morrowan	317.83	-2.18	-8.57
12	B	Morrowan	317.83	-13.44	-5.34
13.3	A	Morrowan	317.80	0.51	-5.99
14.2	A	Morrowan	317.78	0.76	-4.62
17.2	A	Morrowan	317.71	0.80	-4.28
18.2	A	Morrowan	317.69	0.96	-4.01
19.4	A	Morrowan	317.66	2.25	-3.85
19.4	D	Morrowan	317.66	2.27	-3.79
19.4	D	Morrowan	317.66	2.24	-3.92
20.2	A	Morrowan	317.64	1.73	-4.79
21.2	A	Morrowan	317.62		
22.2	A	Morrowan	317.59	1.90	-3.39
23.3	A	Morrowan	317.57		
24.2	A	Morrowan	317.55	1.51	-4.26
25.2	A	Morrowan	317.53	1.60	-5.81
26.8	A	Morrowan	317.49	0.99	-2.03
27.8	A	Morrowan	317.47	1.86	-4.21
28.8	A	Morrowan	317.44	-0.33	-8.23
30	A	Morrowan	317.42	1.16	0.08
30	B	Morrowan	317.42	-6.61	-5.17
31.3	A	Morrowan	317.39	-4.57	-13.21
32.3	A	Morrowan	317.37	2.11	-5.07
33.2	A	Morrowan	317.34	2.91	-4.55
34.2	A	Morrowan	317.32	2.18	-4.91
35.2	A	Morrowan	317.30	2.44	-4.56
36.2	A	Morrowan	317.28		
37.2	A	Morrowan	317.25		
38	A	Morrowan	317.24	2.16	-4.39
38.6	A	Morrowan	317.22	2.05	-4.35
40.2	A	Morrowan	317.19	-0.48	-6.64
41	A	Morrowan	317.17	1.25	-5.65
42.5	A	Morrowan	317.13	1.95	-5.12
44	A	Morrowan	317.10	2.22	-4.14
45	A	Morrowan	317.08	2.41	-3.97
46	A	Morrowan	317.05	1.48	-4.86
46.6	A	Morrowan	317.04	2.47	-2.44
47.6	A	Morrowan	317.02	2.52	-2.75
48.6	A	Morrowan	316.99	1.69	-6.42
49.7	A	Morrowan	316.97	1.45	-4.82
50.7	A	Morrowan	316.95	2.34	-5.28
51.7	A	Morrowan	316.92	2.38	-4.59
52.7	A	Morrowan	316.90	2.33	-4.10
53.7	A	Morrowan	316.88	2.76	-4.34
54.7	A	Morrowan	316.86	2.79	-4.03
56	A	Morrowan	316.83	2.15	-4.23
57.5	A	Morrowan	316.79	2.63	-4.50
57.5	B	Morrowan	316.79	-1.57	-12.47
58.5	A	Morrowan	316.77	2.16	-4.24
60	A	Morrowan	316.74	0.77	-5.54
62	A	Morrowan	316.69	2.32	-4.10
64	A	Morrowan	316.64	1.71	-4.66
64.5	A	Morrowan	316.63	2.15	-4.59
64.5	D	Morrowan	316.63	2.21	-4.53
64.5	D	Morrowan	316.63	2.08	-4.66
65	A	Morrowan	316.62	2.80	-4.54
66	A	Morrowan	316.60	2.52	-4.53
69	A	Morrowan	316.53	1.49	-6.26
70	A	Morrowan	316.51	-0.95	-9.75
71	A	Morrowan	316.48	2.71	-3.99
72	A	Morrowan	316.46	-1.41	-13.48
72	B	Morrowan	316.46	-4.57	-5.52
73.5	A	Morrowan	316.43	2.14	-3.84
74.5	A	Morrowan	316.41	-0.39	-8.26
75.5	A	Morrowan	316.38	1.58	-2.14
76.5	A	Morrowan	316.36	2.62	-4.86
77	A	Morrowan	316.35	3.37	-4.85
78	A	Morrowan	316.33	2.88	-6.20
79	A	Morrowan	316.30	3.67	-4.27
80	A	Morrowan	316.28	2.43	-5.09
81	A	Morrowan	316.26	2.56	-5.77
82	A	Morrowan	316.23	1.27	-6.20
82.5	A	Morrowan	316.22	3.20	-3.94
83.5	A	Morrowan	316.20	2.55	-4.44
84.5	A	Morrowan	316.18	1.69	-6.51
85	A	Morrowan	316.17	1.06	-6.02
85	D	Morrowan	316.17	1.02	-5.99
85	D	Morrowan	316.17	1.11	-6.06
85.5	A	Morrowan	316.15	2.87	-2.51
86.5	A	Morrowan	316.13	2.39	-0.68
86.5	D	Morrowan	316.13	2.44	-0.62
86.5	D	Morrowan	316.13	2.33	-0.75
86.5	B	Morrowan	316.13	0.56	-4.17
86.5	D	Morrowan	316.13	0.50	-4.26
86.5	D	Morrowan	316.13	0.62	-4.09
88	A	Morrowan	316.10	3.21	-0.88
89	A	Morrowan	316.08	2.99	-3.87
90	A	Morrowan	316.05	3.10	-3.95
91	A	Morrowan	316.03	2.74	-4.58
92	A	Morrowan	316.01	1.19	-6.56
93	A	Morrowan	315.98	2.55	-3.62
94	A	Morrowan	315.96	1.68	-3.94
94	B	Morrowan	315.96	3.32	-3.26
95	A	Morrowan	315.94	1.65	-4.67
96.2	A	Morrowan	315.91	2.32	-3.03
97.5	A	Morrowan	315.88	2.07	-3.57
98.5	A	Morrowan	315.86	1.70	-3.83
99.5	A	Morrowan	315.84	1.00	-4.71
100.5	A	Morrowan	315.81	2.16	-4.97
101.5	A	Morrowan	315.79	2.47	-3.70
102.7	A	Morrowan	315.76	2.65	-3.58
104	A	Morrowan	315.73	2.46	-3.53
105	A	Morrowan	315.71	2.24	-3.64
106	A	Morrowan	315.69	2.17	-3.58
107	A	Morrowan	315.67	2.25	-3.53
108	A	Morrowan	315.64	2.85	-3.83
109	A	Morrowan	315.62	3.00	-3.69
110	A	Morrowan	315.60	2.91	-4.49
111	A	Morrowan	315.57	1.96	-3.97
112	A	Morrowan	315.55	1.69	-4.07
113	A	Morrowan	315.53	2.51	-3.76
114	A	Morrowan	315.51	2.24	-3.78
114.5	A	Morrowan	315.50	1.78	-4.36
115.5	A	Morrowan	315.47	2.34	-4.05
115.5	B	Morrowan	315.47	1.97	-4.16
118	A	Morrowan	315.42	2.65	-3.90
118.5	A	Morrowan	315.40	1.21	-6.41
120	A	Morrowan	315.37	2.39	-5.81
120	D	Morrowan	315.37	2.32	-5.86

Table 1 - Continued

Sample		N.A. Stage	Age (MYA)	$\delta^{13}C$ (‰ vs. VPDB)	$\delta^{18}O$ (‰ vs. VPDB)
120	D	Morrowan	315.37	2.45	-5.75
121	A	Morrowan	315.35	2.41	-3.67
122	A	Morrowan	315.32		
123	A	Morrowan	315.30	2.69	-4.86
124	A	Morrowan	315.28	3.03	-3.86
125	A	Morrowan	315.26	2.41	-3.71
126	A	Morrowan	315.23	2.49	-3.75
126.5	A	Morrowan	315.22	2.82	-4.24
127	A	Morrowan	315.21	2.54	-4.15
128	A	Morrowan	315.19	2.31	-4.32
129	A	Morrowan	315.17	2.06	-3.55
129	D	Morrowan	315.17	2.02	-3.60
129	D	Morrowan	315.17	2.10	-3.51
129	B	Morrowan	315.17	2.08	-4.86
130	A	Morrowan	315.14	1.16	-4.72
131	A	Morrowan	315.12	0.87	-4.62
132	A	Morrowan	315.10	1.92	-0.72
133	A	Morrowan	315.07	1.76	-0.35
134.5	A	Morrowan	315.04	0.93	-4.54
136	A	Morrowan	315.01	1.95	-4.00
137	A	Morrowan	314.98	0.19	-7.40
138	A	Morrowan	314.96	1.27	-7.04
139	A	Morrowan	314.94	1.87	-4.18
141	A	Morrowan	314.89	1.20	-8.12
142	A	Morrowan	314.87	-1.41	-8.23
143	A	Morrowan	314.85	2.37	-4.51
144	A	Morrowan	314.82	2.79	-4.77
145	A	Morrowan	314.80	1.86	-5.94
146	A	Morrowan	314.78	3.24	-4.10
147	A	Morrowan	314.76	2.68	-4.32
148	A	Morrowan	314.73	2.87	-3.98
150	A	Morrowan	314.69	2.35	-4.28
152	A	Morrowan	314.64	2.26	-4.27
153	A	Morrowan	314.62	2.82	-3.56
154	A	Morrowan	314.60	1.70	-5.40
155	A	Morrowan	314.57	2.43	-5.42
156	A	Morrowan	314.55	3.80	-4.57
157	A	Morrowan	314.53	3.64	-4.16
158	A	Morrowan	314.51	3.83	-3.73
159	B	Morrowan	314.48	2.68	-6.10
160	A	Morrowan	314.46	2.41	-4.48
161	A	Morrowan	314.44	2.50	-3.67
162	A	Morrowan	314.41	2.47	-3.65
163	A	Morrowan	314.39	2.78	-4.22
164	A	Morrowan	314.37	2.41	-3.36
165	A	Morrowan	314.35	2.18	-3.55
166	A	Morrowan	314.32	1.88	-2.84
167	A	Morrowan	314.30	2.90	-4.06
168	A	Morrowan	314.28	2.56	-6.42
169	A	Morrowan	314.26	2.48	-9.20
170	A	Morrowan	314.23	3.32	-4.53
170	D	Morrowan	314.23	3.36	-4.48
170	D	Morrowan	314.23	3.28	-4.57
176	A	Morrowan	314.10	3.14	-4.06
177	A	Morrowan	314.07	2.78	-4.17
178	A	Morrowan	314.05	3.01	-4.18
179	A	Morrowan	314.03	3.03	-3.43
180	A	Morrowan	314.01	2.27	-3.48
181	A	Morrowan	313.98	2.91	-3.37
183	A	Morrowan	313.94	1.96	-3.89
184	A	Morrowan	313.91	1.32	-6.18
185	A	Morrowan	313.89	1.94	-4.63
186	A	Morrowan	313.87	1.91	-5.53
187	A	Morrowan	313.85	2.09	-4.41
188	A	Morrowan	313.82	2.50	-3.49
189	A	Morrowan	313.80	2.43	-3.80
190	A	Morrowan	313.78	1.85	-4.54
190	D	Morrowan	313.78	1.87	-4.45
190	D	Morrowan	313.78	1.82	-4.64
190	B	Morrowan	313.78	1.77	-4.69
191	A	Morrowan	313.75	2.23	-3.97
191	D	Morrowan	313.75		
191	D	Morrowan	313.75		
192	A	Morrowan	313.73	1.71	-4.79
193	A	Morrowan	313.71	2.95	-3.41
194	A	Morrowan	313.69	2.67	-4.34
194	D	Morrowan	313.69		
194	D	Morrowan	313.69		
195	A	Morrowan	313.66	1.79	-4.69
195	D	Morrowan	313.66		
195	D	Morrowan	313.66		
196	A	Morrowan	313.64	2.19	-4.08
197	A	Morrowan	313.62	2.43	-4.09
198	A	Morrowan	313.60	2.33	-4.60
199	A	Morrowan	313.57	1.86	-4.13
199	D	Morrowan	313.57		
199	D	Morrowan	313.57		
200	A	Morrowan	313.55	1.67	-3.74
201	A	Morrowan	313.53	1.80	-3.41
202	A	Morrowan	313.50	1.95	-4.49
203	A	Morrowan	313.48	1.83	-5.69
203	D	Morrowan	313.48		
203	D	Morrowan	313.48		
204	A	Morrowan	313.46	1.40	-3.52
205	A	Morrowan	313.44	1.40	-4.25
206.5	A	Morrowan	313.40	0.59	-7.13
206.5	D	Morrowan	313.40	0.54	-7.21
206.5	D	Morrowan	313.40	0.64	-7.05
207	A	Morrowan	313.39	2.65	-3.11
208	A	Morrowan	313.37	2.98	-3.50
209	A	Morrowan	313.35	2.78	-3.81
210	A	Morrowan	313.32	2.87	-3.80
211	A	Atokan	313.30	2.29	-4.33
211.5	A	Atokan	313.27	1.94	-4.66
212	A	Atokan	313.24	1.94	-3.82
212.5	A	Atokan	313.21	2.42	-5.69
213	A	Atokan	313.17	1.82	-5.31
213	D	Atokan	313.17	1.84	-5.33
213	D	Atokan	313.17	1.81	-5.30
213.5	A	Atokan	313.14	2.31	-4.82
214	A	Atokan	313.11	2.64	-4.60
214.5	A	Atokan	313.08	3.10	-3.74
215	A	Atokan	313.05	3.09	-3.04
215	B	Atokan	313.05	-5.54	-3.28
215.5	A	Atokan	313.02	1.73	-5.32
216	A	Atokan	312.99	2.66	-3.72
216.5	A	Atokan	312.95	2.95	-3.35
217	A	Atokan	312.92	3.13	-4.03
217.5	A	Atokan	312.89	2.77	-4.30
218	A	Atokan	312.86	3.67	-3.43
218.5	A	Atokan	312.83	3.60	-4.08
219	A	Atokan	312.80	3.46	-4.45
219.5	A	Atokan	312.77	-1.16	-9.02
220	A	Atokan	312.73	3.37	-3.65
220.5	A	Atokan	312.70	3.49	-3.79
221	A	Atokan	312.67	3.38	-4.03
221.5	A	Atokan	312.64	3.35	-3.55
222	A	Atokan	312.61	3.41	-3.65
222.5	A	Atokan	312.58	3.15	-3.68
222.5	B	Atokan	312.58	3.37	-3.76
223	A	Atokan	312.55	3.22	-3.83
224	A	Atokan	312.48	3.16	-3.58
225	A	Atokan	312.42	2.10	-2.15
225.5	A	Atokan	312.39	1.70	-3.65
226	A	Atokan	312.36	1.82	-3.62
226.5	A	Atokan	312.33	1.66	-3.31
226.5	B	Atokan	312.33	2.46	-3.71
227	A	Atokan	312.30	1.58	-3.45
227.5	A	Atokan	312.26	1.60	-3.64
229	A	Atokan	312.17	2.26	-3.93
229.5	A	Atokan	312.14	2.22	-3.72
230	A	Atokan	312.11	2.17	-3.79
230.5	A	Atokan	312.08	2.00	-5.01
231	A	Atokan	312.04	0.95	-4.63

Table 1 - Continued

Sample		N.A. Stage	Age (MYA)	$\delta^{13}C$ (‰ vs. VPDB)	$\delta^{18}O$ (‰ vs. VPDB)
232	A	Atokan	311.98	2.32	-3.56
233	A	Atokan	311.92	2.44	-4.01
234	A	Atokan	311.86	2.41	-4.02
235	A	Atokan	311.79	2.60	-3.68
235.5	A	Atokan	311.76	2.61	-3.23
236	A	Atokan	311.73	2.28	-3.61
237.5	A	Atokan	311.64	1.73	-3.59
238	A	Atokan	311.60	1.37	-3.54
238.5	A	Atokan	311.57	1.35	-3.46
239	A	Atokan	311.54	0.96	-3.36
239.5	A	Atokan	311.51	1.28	-3.43
239.5	D	Atokan	311.51	1.27	-3.46
239.5	D	Atokan	311.51	1.29	-3.40
240	A	Atokan	311.48	1.90	-4.71
240.5	A	Atokan	311.45	1.66	-4.17
241	A	Atokan	311.42	1.23	-3.64
241.5	A	Atokan	311.38	1.39	-3.14
242	A	Atokan	311.35	0.96	-3.92
242.5	A	Atokan	311.32	0.65	-4.10
243	A	Atokan	311.29	1.40	-3.88
243.5	A	Atokan	311.26	1.06	-3.38
244	A	Atokan	311.23	1.60	-3.87
244.5	A	Atokan	311.20	1.16	-3.29
245	A	Atokan	311.16	1.87	-2.85
245.5	A	Atokan	311.13	2.10	-3.32
247	A	Atokan	311.04	2.08	-2.93
248	A	Atokan	310.98	1.20	-4.36
249	A	Atokan	310.91	1.47	-4.35
249.5	A	Atokan	310.88	1.68	-3.47
251	A	Atokan	310.79	2.48	-4.00
252.5	A	Atokan	310.69	2.99	-3.44
254	A	Atokan	310.60	2.25	-5.32
255.5	A	Atokan	310.50	2.15	-4.68
255.5	D	Atokan	310.50	2.23	-4.55
255.5	D	Atokan	310.50	2.08	-4.80
257	A	Atokan	310.41	2.43	-4.18
258	A	Atokan	310.35	2.58	-3.81
258	D	Atokan	310.35	2.57	-3.80
258	D	Atokan	310.35	2.60	-3.83
259	A	Atokan	310.29	2.51	-4.01
260	A	Atokan	310.22	2.44	-3.93
265.5	A	Atokan	309.88	2.00	-3.71
266	A	Atokan	309.85	2.21	-3.64
266.5	A	Atokan	309.81	2.24	-3.62
267	A	Atokan	309.78	2.09	-3.66
267.5	A	Atokan	309.75	1.68	-3.81
268	A	Atokan	309.72	1.75	-5.36
269	A	Atokan	309.66	1.28	-3.62
270	A	Atokan	309.59	1.03	-5.66
271	A	Atokan	309.53	0.87	-3.90
271.5	A	Desmoinesian	309.50	-0.03	-6.00
272	A	Desmoinesian	309.49	0.91	-4.20
274	A	Desmoinesian	309.44	1.39	-4.93
274	D	Desmoinesian	309.44	1.42	-4.77
274	D	Desmoinesian	309.44	1.37	-5.08
277	A	Desmoinesian	309.37	1.18	-6.83
278	A	Desmoinesian	309.35	0.58	-6.81
279	A	Desmoinesian	309.32	1.72	-6.48
280	A	Desmoinesian	309.30	0.46	-7.53
281	A	Desmoinesian	309.27	0.39	-8.36
281.5	A	Desmoinesian	309.26	-1.78	-8.50
286	A	Desmoinesian	309.16	2.53	-4.79
287	A	Desmoinesian	309.13	3.44	-4.22
288	A	Desmoinesian	309.11	3.56	-3.96
290	A	Desmoinesian	309.06	3.59	-3.71
291	A	Desmoinesian	309.04	3.54	-3.53
292	A	Desmoinesian	309.01	2.68	-3.42
293	A	Desmoinesian	308.99	1.89	-3.84
294	A	Desmoinesian	308.97	1.72	-3.13
294.5	A	Desmoinesian	308.96	3.48	-3.72
295	A	Desmoinesian	308.94	2.56	-3.40
295.5	A	Desmoinesian	308.93	1.93	-2.23
296.5	A	Desmoinesian	308.91	3.04	-3.84
296.5	B	Desmoinesian	308.91	1.27	-5.10
296.5	C	Desmoinesian	308.91	0.97	-5.15
297	A	Desmoinesian	308.90	2.46	-4.31
297.5	A	Desmoinesian	308.88	2.84	-4.07
298	A	Desmoinesian	308.87	3.15	-3.97
298.5	A	Desmoinesian	308.86	2.65	-3.08
298.5	D	Desmoinesian	308.86	2.65	-3.97
298.5	D	Desmoinesian	308.86	2.65	-2.20
298.5	B	Desmoinesian	308.86	3.29	-4.66
299	A	Desmoinesian	308.85	2.96	-3.17
299.5	A	Desmoinesian	308.84	2.96	-3.03
300	A	Desmoinesian	308.82	3.32	-3.37
300.5	A	Desmoinesian	308.81	2.58	-2.88
301	A	Desmoinesian	308.80	3.07	-3.10
301.5	A	Desmoinesian	308.79	-0.52	-6.42
302	A	Desmoinesian	308.78	1.82	-4.29
305	A	Desmoinesian	308.71	-0.10	-5.65
306	A	Desmoinesian	308.68	0.97	-3.90
307.5	A	Desmoinesian	308.65	1.02	-4.10
307.5	D	Desmoinesian	308.65	1.05	-4.03
307.5	D	Desmoinesian	308.65	1.00	-4.17
309	A	Desmoinesian	308.61	0.58	-6.34
312	A	Desmoinesian	308.54	2.21	-3.06
313	A	Desmoinesian	308.52	1.30	-4.18
314	A	Desmoinesian	308.49	1.22	-3.82
315	A	Desmoinesian	308.47	1.49	-3.12
316	A	Desmoinesian	308.45	0.45	-7.48
319	A	Desmoinesian	308.37	1.30	-7.92
321	A	Desmoinesian	308.33	0.56	-4.62
322	A	Desmoinesian	308.30	-0.13	-5.78
322	D	Desmoinesian	308.30	-0.12	-6.64
322	D	Desmoinesian	308.30	-0.14	-4.92
323	A	Desmoinesian	308.28	-1.33	-7.22
324	A	Desmoinesian	308.26	-0.66	-6.61
324	D	Desmoinesian	308.26	-0.74	-6.80
324	D	Desmoinesian	308.26	-0.58	-6.41
325	A	Desmoinesian	308.23	-0.66	-6.29
327	A	Desmoinesian	308.19	0.18	-4.90
328	A	Desmoinesian	308.16	0.11	-5.29
328.5	A	Desmoinesian	308.15	1.01	-3.11
329	A	Desmoinesian	308.14	0.77	-4.05
329.5	A	Desmoinesian	308.13	0.85	-4.45
330	A	Desmoinesian	308.11		
333	A	Desmoinesian	308.04	1.76	-3.89
333.5	A	Desmoinesian	308.03	1.94	-4.87
334	A	Desmoinesian	308.02	2.29	-3.48
334.5	A	Desmoinesian	308.01	2.39	-3.45
335	A	Desmoinesian	308.00	1.78	-3.72
335.5	A	Desmoinesian	307.98	2.00	-4.96
336	A	Desmoinesian	307.97	3.00	-2.82
336.5	A	Desmoinesian	307.96	2.46	-3.32
337	A	Desmoinesian	307.95	2.58	-3.64
337	D	Desmoinesian	307.95	2.60	-3.63
337	D	Desmoinesian	307.95	2.56	-3.66
337.5	A	Desmoinesian	307.94	2.59	-3.92
338	A	Desmoinesian	307.92	1.89	-5.20
339	A	Desmoinesian	307.90	1.99	-5.60
340	A	Desmoinesian	307.88	1.51	-4.31
341	A	Desmoinesian	307.85	2.26	-3.73
342	A	Desmoinesian	307.83		-4.28
343	A	Desmoinesian	307.81	2.85	-3.29
343	A	Desmoinesian	307.81	0.45	-4.52
343	D	Desmoinesian	307.81	0.53	-4.62
343	D	Desmoinesian	307.81	0.37	-4.41
344	A	Desmoinesian	307.78	2.27	-3.48
345	A	Desmoinesian	307.76	1.56	-5.39
346	A	Desmoinesian	307.73	2.71	-3.73
346	B	Desmoinesian	307.73	0.40	-13.74
346	D	Desmoinesian	307.73	0.44	-13.86
346	D	Desmoinesian	307.73	0.36	-13.62
347	A	Desmoinesian	307.71	2.83	-4.97

Table 1 - Continued

Sample		N.A. Stage	Age (MYA)	$\delta^{13}C$ (‰ vs. VPDB)	$\delta^{18}O$ (‰ vs. VPDB)
348	A	Desmoinesian	307.69	2.10	-4.53
349	A	Desmoinesian	307.66	2.50	-4.68
349	D	Desmoinesian	307.66	2.62	-3.79
349	D	Desmoinesian	307.66	2.38	-5.57
350	A	Desmoinesian	307.64	2.84	-4.67
351	A	Desmoinesian	307.62	3.02	-3.54
352	A	Desmoinesian	307.59	2.49	-5.13
352	D	Desmoinesian	307.59	2.36	-5.38
352	D	Desmoinesian	307.59	2.62	-4.89
353	A	Desmoinesian	307.57	2.86	-1.03
353	D	Desmoinesian	307.57	2.81	-1.03
353	D	Desmoinesian	307.57	2.92	-1.04
354	A	Desmoinesian	307.55	1.77	-4.77
354.5	A	Desmoinesian	307.53	3.12	-3.27
354.5	D	Desmoinesian	307.53	3.13	-3.39
354.5	D	Desmoinesian	307.53	3.11	-3.14
355	A	Desmoinesian	307.52	2.22	-3.76
355.5	A	Desmoinesian	307.51	1.09	-5.17
356	A	Desmoinesian	307.50	-0.82	-8.63
356	D	Desmoinesian	307.50	-0.71	-8.50
356	D	Desmoinesian	307.50	-0.94	-8.76
356.5	A	Desmoinesian	307.49	1.30	-4.61
357	A	Desmoinesian	307.47	1.53	-4.79
358	A	Desmoinesian	307.45	0.98	-4.01
362	A	Desmoinesian	307.36	0.34	-4.56
362	D	Desmoinesian	307.36	0.33	-4.63
362	D	Desmoinesian	307.36	0.35	-4.49
363	A	Desmoinesian	307.33	1.43	-4.35
364	A	Desmoinesian	307.31	1.05	-5.37
365	A	Desmoinesian	307.28	1.15	-5.16
365	D	Desmoinesian	307.28	1.06	-5.15
365	D	Desmoinesian	307.28	1.24	-5.16
366	A	Desmoinesian	307.26	1.78	-3.85
368	A	Desmoinesian	307.21	-0.70	-6.36
368	D	Desmoinesian	307.21	-0.71	-6.37
368	D	Desmoinesian	307.21	-0.69	-6.34
369	A	Desmoinesian	307.19	1.87	-4.13
370	A	Desmoinesian	307.17	2.52	-5.01
371	A	Desmoinesian	307.14	2.69	-4.51
372	A	Desmoinesian	307.12	3.32	-5.35
373	A	Desmoinesian	307.10	1.75	-5.10
373	D	Desmoinesian	307.10	1.71	-5.73
373	D	Desmoinesian	307.10	1.78	-4.47
374	A	Desmoinesian	307.07		-4.18
375	A	Desmoinesian	307.05	0.47	-7.34
375	D	Desmoinesian	307.05	0.54	-6.83
375	D	Desmoinesian	307.05	0.40	-7.85
377	A	Desmoinesian	307.00	1.92	-7.01
378	A	Desmoinesian	306.98	1.08	-6.46
380	A	Desmoinesian	306.93	2.99	-3.84
380.5	A	Desmoinesian	306.92	4.02	-3.75
381	A	Desmoinesian	306.91	1.31	
382	A	Desmoinesian	306.88	3.59	-4.15
383	A	Desmoinesian	306.86	3.36	-3.38
384	A	Desmoinesian	306.83	2.76	-6.18
386	A	Desmoinesian	306.79	2.49	-4.38
387	A	Desmoinesian	306.76	2.74	
388	A	Desmoinesian	306.74	2.40	-3.76
390	A	Desmoinesian	306.69	2.41	-3.32
391	A	Desmoinesian	306.67	2.35	-3.48
392	A	Desmoinesian	306.65	2.73	-1.83
392	D	Desmoinesian	306.65	2.65	-1.97
392	D	Desmoinesian	306.65	2.82	-1.69
393	A	Desmoinesian	306.62	1.76	-3.97
394	A	Desmoinesian	306.60	1.68	-4.23
395	A	Desmoinesian	306.57	2.57	-5.53
396	A	Desmoinesian	306.55	1.85	-6.99
397	A	Desmoinesian	306.53	2.74	-3.69
397	B	Desmoinesian	306.53		-2.94
398	A	Desmoinesian	306.50	2.76	-4.23
399	A	Desmoinesian	306.48	2.89	-4.98
400	A	Desmoinesian	306.46	2.92	-4.38
401	A	Desmoinesian	306.43	2.49	-4.01
402	A	Desmoinesian	306.41	2.15	-4.86
402	D	Desmoinesian	306.41	2.12	-4.77
402	D	Desmoinesian	306.41	2.18	-4.96
403	A	Desmoinesian	306.38	2.88	-1.04
404	A	Desmoinesian	306.36	-0.19	-6.41
404	D	Desmoinesian	306.36	-0.21	-6.76
404	D	Desmoinesian	306.36	-0.16	-6.05
405	A	Desmoinesian	306.34	3.05	-3.93
406	A	Desmoinesian	306.31	3.07	-3.80
407	A	Desmoinesian	306.29	2.13	-3.88
407	D	Desmoinesian	306.29	2.18	-3.85
407	D	Desmoinesian	306.29	2.07	-3.92
408	A	Desmoinesian	306.27	1.19	-6.85
408	B	Desmoinesian	306.27		
408	D	Desmoinesian	306.27	1.33	-6.84
408	D	Desmoinesian	306.27	1.05	-6.86
409	A	Desmoinesian	306.24	-0.15	-7.18
409	D	Desmoinesian	306.24	-0.01	-7.32
409	D	Desmoinesian	306.24	-0.28	-7.05
410	A	Desmoinesian	306.22	3.02	-3.86
411	A	Desmoinesian	306.19	2.92	-4.15
412	A	Desmoinesian	306.17	0.69	-8.46
412	D	Desmoinesian	306.17	0.79	-8.62
412	D	Desmoinesian	306.17	0.76	-8.32
412	D	Desmoinesian	306.17	0.52	-8.45
413	A	Desmoinesian	306.15	1.81	-5.22
414	A	Desmoinesian	306.12	4.60	-4.64
415	A	Desmoinesian	306.10	4.17	-6.76
416	A	Desmoinesian	306.08	4.82	-4.42
417	A	Desmoinesian	306.05	4.37	-3.42
418	A	Desmoinesian	306.03	3.78	-5.28
418	D	Desmoinesian	306.03	3.73	
418	D	Desmoinesian	306.03	3.84	-5.28
419	A	Desmoinesian	306.01	4.38	-2.88
420	A	Desmoinesian	305.98	3.51	-3.71
421	A	Desmoinesian	305.96		
421	B	Desmoinesian	305.96	3.26	
422	A	Desmoinesian	305.93	3.63	-3.50
423	A	Desmoinesian	305.91	3.55	-3.97
424	A	Desmoinesian	305.89	3.75	-3.09
425	A	Desmoinesian	305.86	3.56	-3.99
425	B	Desmoinesian	305.86	3.62	-4.61
426	A	Desmoinesian	305.84	3.80	-4.34
426	D	Desmoinesian	305.84	3.82	-4.70
426	D	Desmoinesian	305.84	3.78	-3.99
427	A	Desmoinesian	305.82	3.20	-5.26
428	A	Desmoinesian	305.79	3.66	-4.96
429	A	Desmoinesian	305.77	3.56	-4.23
429	C	Desmoinesian	305.77	1.88	-6.29
430	A	Desmoinesian	305.74	3.43	-4.86
431	A	Desmoinesian	305.72	0.91	-6.24
432	A	Desmoinesian	305.70	0.00	-7.57
432	D	Desmoinesian	305.70	0.01	-7.79
432	D	Desmoinesian	305.70	0.06	-7.60
432	D	Desmoinesian	305.70	-0.07	-7.33
433	A	Desmoinesian	305.67	1.91	-6.47
433	D	Desmoinesian	305.67	2.10	-6.96
433	D	Desmoinesian	305.67	1.71	-5.97
434	A	Missourian	305.65	1.33	-5.93
434	D	Missourian	305.65	1.39	-5.98
434	D	Missourian	305.65	1.28	-5.87
435	A	Missourian	305.64	2.91	-1.13
436	A	Missourian	305.62	2.44	-4.16
437	A	Missourian	305.61	2.50	-3.17
438	A	Missourian	305.59	2.83	-2.12
439	A	Missourian	305.58	1.41	-6.15
439	D	Missourian	305.58	1.41	-6.83
439	D	Missourian	305.58	1.42	-5.48
440	A	Missourian	305.56	2.75	-1.52
441.5	A	Missourian	305.54	2.85	-2.37
443	A	Missourian	305.52	1.89	-5.44

Table 1 - Continued

Sample		N.A. Stage	Age (MYA)	$\delta^{13}C$ (‰ vs. VPDB)	$\delta^{18}O$ (‰ vs. VPDB)
443	D	Missourian	305.52	1.92	-5.63
443	D	Missourian	305.52	1.86	-5.24
444.5	A	Missourian	305.50	2.68	-4.45
446	A	Missourian	305.48	2.52	-4.31
447.5	A	Missourian	305.45	2.08	-5.10
447.5	C	Missourian	305.45	1.82	-4.19
447.5	D	Missourian	305.45	1.94	-6.12
447.5	D	Missourian	305.45	2.21	-4.08
447.5	D	Missourian	305.45	2.06	-3.97
447.5	D	Missourian	305.45	1.57	-4.41
449	A	Missourian	305.43	1.53	-5.94
449	D	Missourian	305.43	1.50	-5.89
449	D	Missourian	305.43	1.56	-5.99
449	D	Missourian	305.43	1.52	-5.64
450	A	Missourian	305.42	2.45	-4.91
451	A	Missourian	305.40	2.48	-4.59
452	A	Missourian	305.39	2.76	-3.14
453	A	Missourian	305.37	2.69	-2.40
453	D	Missourian	305.37	2.65	-2.42
453	D	Missourian	305.37	2.72	-2.38
454	A	Missourian	305.36	0.95	-6.60
454	D	Missourian	305.36	0.93	-6.80
454	D	Missourian	305.36	0.96	-6.40
454	D	Missourian	305.36	0.93	-6.40
455	A	Missourian	305.35	2.98	-2.58
455	D	Missourian	305.35	2.89	
455	D	Missourian	305.35	3.08	-2.58
456	A	Missourian	305.33	2.91	-3.69
457	A	Missourian	305.32	2.17	-5.17
459	A	Missourian	305.29	3.53	-2.99
459	B	Missourian	305.29	-10.76	-3.43
459	A	Missourian	305.29	3.40	-3.45
460	A	Missourian	305.27	3.66	-3.72
461	A	Missourian	305.26	2.63	-3.90
462	A	Missourian	305.24	3.08	-3.43
466	A	Missourian	305.19		-5.39
467	A	Missourian	305.17	3.02	-4.60
468	A	Missourian	305.16	2.26	-4.77
469	A	Missourian	305.14	3.05	-5.63
470	A	Missourian	305.13	0.65	-7.04
470	D	Missourian	305.13	0.66	-6.93
470	D	Missourian	305.13	0.64	-7.14
471	A	Missourian	305.11	3.87	-4.18
472	A	Missourian	305.10	3.92	-4.27
473	A	Missourian	305.08	3.72	-4.47
474	A	Missourian	305.07	3.29	-4.17
475	A	Missourian	305.06	2.81	-4.99
476	A	Missourian	305.04	3.17	-1.97
477	A	Missourian	305.03	3.17	-1.92
478	A	Missourian	305.01	1.69	-6.04
478	D	Missourian	305.01	1.80	-6.13
478	D	Missourian	305.01	1.57	-5.94
479	A	Missourian	305.00	1.08	-6.74
480	A	Missourian	304.98	2.96	-4.56
481	A	Missourian	304.97	2.17	-7.50
481	D	Missourian	304.97	2.34	-7.60
481	D	Missourian	304.97	2.00	-7.40
482	A	Missourian	304.95	3.32	-3.87
483	A	Missourian	304.94	3.75	-4.79
484	A	Missourian	304.92	3.83	-5.25
485	A	Missourian	304.91	3.26	-6.37
486	A	Missourian	304.90	3.87	-5.48
487	A	Missourian	304.88	4.46	-4.29
488	A	Missourian	304.87	3.90	
490	A	Missourian	304.84	3.59	-6.03
491	A	Missourian	304.82	3.74	-5.76
492	A	Missourian	304.81	3.89	-3.65
493	A	Missourian	304.79	4.30	-4.98
493	C	Missourian	304.79	4.35	-5.05
494	A	Missourian	304.78	4.04	-4.93
495	A	Missourian	304.77	2.21	-7.80
495	D	Missourian	304.77	2.16	-7.80
495	D	Missourian	304.77	2.26	
497	A	Missourian	304.74	1.09	-8.07
498	A	Missourian	304.72	2.90	1.68
499	A	Missourian	304.71	0.84	-8.21
500	A	Missourian	304.69	-0.03	-7.97
501	A	Missourian	304.68		
504	A	Missourian	304.63	2.14	-4.71
505	A	Missourian	304.62	1.40	-4.57
506	A	Missourian	304.61	1.89	-2.68
507	A	Missourian	304.59	0.80	-5.39
508	A	Missourian	304.58	1.27	-3.67
509	A	Missourian	304.56	2.01	-5.28
510	A	Missourian	304.55	2.70	-4.01
511	A	Missourian	304.53	2.58	-3.71
512	A	Missourian	304.52	2.00	-5.52
513	A	Missourian	304.50	2.34	-4.92
514	A	Missourian	304.49	0.37	-7.61
515	A	Missourian	304.48	-0.22	-8.09
515.5	A	Missourian	304.47	1.92	-6.11
516	A	Missourian	304.46	-2.22	-11.19
517	A	Missourian	304.45	2.04	-5.24
518	A	Missourian	304.43	-0.38	-6.88
519	A	Missourian	304.42	2.12	-4.52
520	A	Missourian	304.40	1.25	-5.20
521	A	Missourian	304.39	1.75	-4.53
522	A	Missourian	304.37		
523	A	Missourian	304.36		
524	A	Missourian	304.34		
525	A	Missourian	304.33	1.98	-4.02
526	A	Missourian	304.32	2.36	-4.09
527	A	Missourian	304.30		
528	A	Missourian	304.29		
530	A	Missourian	304.26	2.50	-6.46
534	A	Missourian	304.20	1.27	-6.27
538	A	Missourian	304.14		
539	A	Missourian	304.13		
540	A	Missourian	304.11	3.07	-4.51
541	A	Missourian	304.10		
542	A	Missourian	304.08		
542	B	Missourian	304.08	3.08	-4.82
543	A	Missourian	304.07		
544	A	Missourian	304.05		
545	A	Missourian	304.04		
546	A	Missourian	304.03		
547	A	Missourian	304.01		
548	A	Missourian	304.00	3.16	-4.67
548	D	Missourian	304.00	3.16	-4.67
548	D	Missourian	304.00	3.12	-4.69
549	A	Missourian	303.98	0.23	-7.45
550	A	Missourian	303.97	-0.86	-8.54
553	A	Missourian	303.92		
554	A	Missourian	303.91	1.37	-6.50
555	A	Missourian	303.89		
556	A	Missourian	303.88	0.75	-7.49
557	A	Missourian	303.87		
558	A	Missourian	303.85		
558	A	Missourian	303.85		
559	A	Missourian	303.84		
560	A	Missourian	303.82		
561	A	Missourian	303.81	3.06	-4.78
562	A	Missourian	303.79	3.07	-4.91
563	A	Missourian	303.78		
564	A	Missourian	303.76	3.38	-4.71
565	A	Missourian	303.75	3.03	-5.02
566	A	Missourian	303.74	4.60	-1.73
567	A	Missourian	303.72	3.92	-4.09
568	A	Missourian	303.71	3.38	-4.11
569	A	Missourian	303.69	1.84	-5.92
570	A	Missourian	303.68	2.79	-4.57
571	A	Missourian	303.66	1.68	-6.52
572	A	Missourian	303.65	2.87	-4.37
573	A	Missourian	303.63	2.81	-4.24

Table 1 - Continued

Sample		N.A. Stage	Age (MYA)	$\delta^{13}C$ (‰ vs. VPDB)	$\delta^{18}O$ (‰ vs. VPDB)
574	A	Missourian	303.62	2.91	-4.84
575	A	Missourian	303.60		
576	A	Missourian	303.59	3.01	-2.46
577	A	Missourian	303.58	3.40	-4.36
578	A	Missourian	303.56	3.64	-4.06
578.5	A	Missourian	303.55	3.74	-3.90
579	A	Missourian	303.55	3.86	-3.86
580	A	Missourian	303.53	3.81	-3.82
581	A	Missourian	303.52	3.35	-4.69
582	A	Missourian	303.50	3.23	-4.23
583	A	Missourian	303.49	0.49	-6.84
584	A	Missourian	303.47	2.83	-3.87
585	A	Missourian	303.46	2.45	-3.84
586	A	Missourian	303.45	2.44	-4.16
586	B	Missourian	303.45	1.63	-4.36
587	A	Missourian	303.43	3.06	-3.78
588	A	Missourian	303.42	2.87	-4.01
589	A	Missourian	303.40	2.80	-4.10
590	A	Missourian	303.39	2.78	-3.21
591	A	Missourian	303.37	2.68	-4.06
592	A	Missourian	303.36	2.82	-4.17
593	A	Missourian	303.34	2.93	-3.94
594	A	Missourian	303.33	1.50	-4.12
595	A	Missourian	303.31	-0.45	-5.87
596	A	Missourian	303.30	-0.19	-6.73

4. RESULTS

4.1 *Petrographic Results*

All thin sections are displayed in Appendix B. Detailed notes from thin section analysis are reported in Appendix A. Carbonate rock classifications are according to the Dunham classification (Dunham, 1962). Mudstone is rare in the section and has low biodiversity with the occasional ostracod, gastropod, or other skeletal grain. A wide range of skeletal packstone and wackestone exist in the section. Some contain high biodiversity while others are purely crinoids or brachiopods. Grainstone within the section tend to have high biodiversity and are often associated with pellets or coated grains. Coated grains are distinguished from pellets in that they have a skeletal core. The grainstone grains tend to be well rounded. The two boundstone samples have unique characteristics. One sample (484 A) is bound by phylloid algae, while the other (459 A) contains in-situ bryozoan and could also be classified as a bryozoan framestone. Crystalline refers to samples composed of a mosaic of calcite crystals, possibly representing highly altered skeletal packstones.

Three rock types outside of the Dunham classification were also identified: calcisiltstone, siltstone, and sandstone. The percent of quartz silt or very fine sand in each sample was visually estimated in thin-section and hand sample. Rocks with more than 50% silt/sand were classified as either siltstone or sandstone. However, the majority of these samples still contained marine skeletal grains, such as crinoids and brachiopods, while a few even contained abundant foraminifera. Calcisiltstone consists of fine grained carbonates with visible laminations or thin bedding.

Silica replacement has masked original marine textures. Botryoidal marine cements were not seen in any of the thin sections. Nodular and bedded chert is pervasive throughout all rock types. Many skeletal grains have been wholly or partially silicified. Silica replaced zones generally contain microdolomite inclusions.

4.2 *$\delta^{18}O$ and $\delta^{13}C$ Averages*

All $\delta^{18}O$ and $\delta^{13}C$ values from the Pennsylvanian Bloom Member, including fine grained carbonate and individually sampled components, range from -13.5‰ to 1.7‰ and -4.6‰ to 4.8‰, respectively (Table 1, Fig. 4). For a complete list of data, including silt content, rock type, and description, see Appendix A. Averages of $\delta^{18}O$ and $\delta^{13}C$ for fine-grained carbonate were -4.5‰ ± 1.6‰ (1σ) and 2.1‰ ± 1.1‰ (1σ). However, average $\delta^{18}O$ and $\delta^{13}C$ of samples where micrite was the primary material sampled (mudstone, wackestone, and packstone) were only slightly higher than averages of all fine grained carbonates combined (-4.4‰ and 2.2‰, respectively).

Average values based on rock type differed only slightly (Table 2; Fig. 5) with the exception of boundstone, crystalline limestone, and siltstone. $\delta^{18}O$ and $\delta^{13}C$ for the few crystalline limestones were dramatically lower than other samples and siltstones were slightly lower. The low $\delta^{18}O$ and $\delta^{13}C$ values for crystalline limestone may not be statistically significant, because only three samples have this classification (Fig. 5). Boundstone had unexpectedly higher $\delta^{13}C$ while still having similar $\delta^{18}O$ values, yet only two samples had this classification. Intra-sample variation of $\delta^{18}O$ and $\delta^{13}C$ averaged 0.4‰ ± 0.5‰ (1σ) and 0.1‰ ± 0.1‰ (1σ), respectively, with maximum

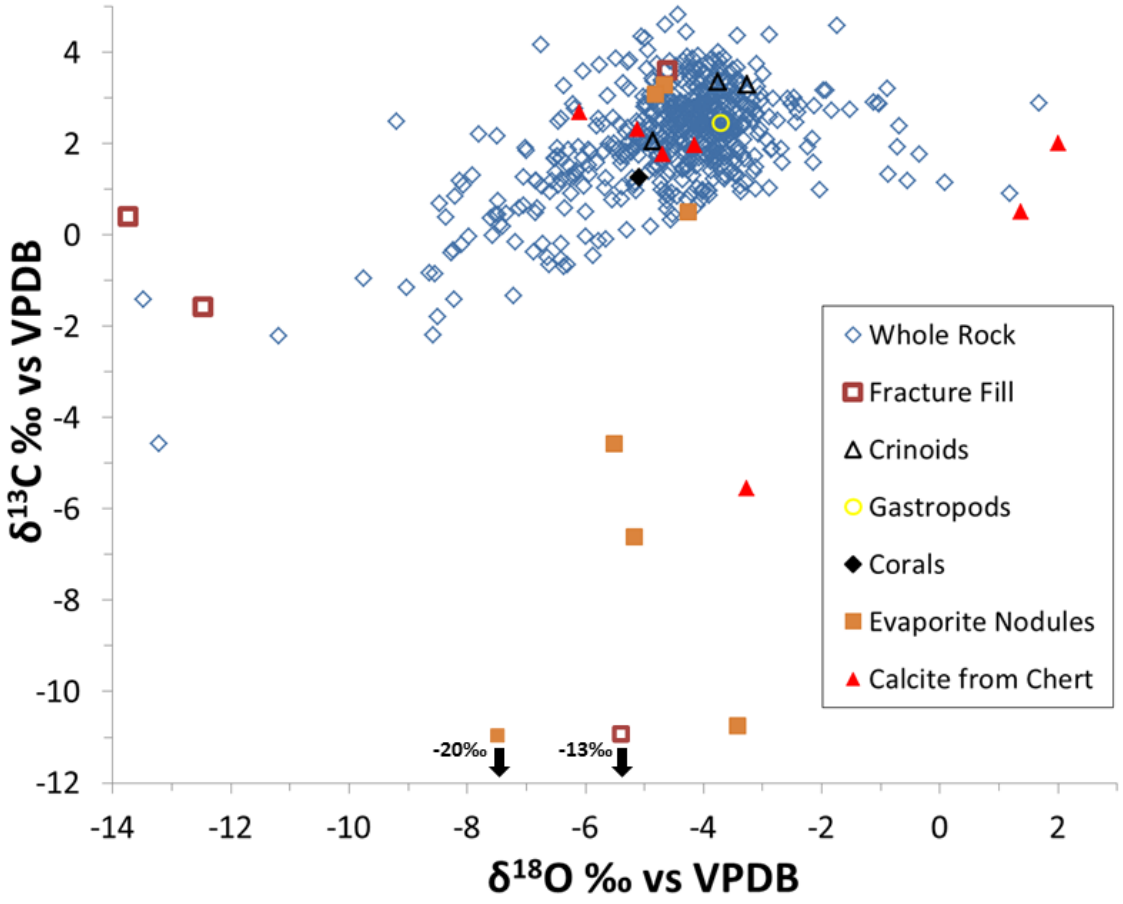

Fig. 4. Carbon and oxygen isotopes for all analyzed samples from Gallagher Peak, Idaho. Carbon isotope values of the fine grained carbonate begin to systematically decrease for oxygen values less than -5‰. The figure illustrates that $\delta^{13}C$ values less than 0‰ are likely altered by diagenesis.

Table 2

Average $\delta^{18}O$ and $\delta^{13}C$ by rock classification and age.

	$\delta^{18}O$			$\delta^{13}C$		
Rock Type	**Number**	**Avg**	**St Dev**	**Number**	**Avg**	**St Dev**
Mudstone	71	-4.31	1.70	71	2.52	1.22
Packstone	140	-4.18	1.20	141	2.20	0.99
Wackestone	228	-4.54	1.48	230	2.13	1.05
Grainstone	16	-3.91	0.33	16	2.77	0.60
Crystalline	3	-10.45	4.09	3	-1.42	2.56
Calcisiltstone	9	-5.12	2.51	9	1.68	1.09
Boundstone	2	-4.35	0.90	2	3.61	0.22
Sandstone	25	-4.59	0.98	25	1.90	0.79
Siltstone	33	-5.59	1.73	33	1.39	1.27
Wackestone/Packstone	13	-4.55	1.36	13	1.61	0.83
	540 Total			543 Total		

	$\delta^{18}O$			$\delta^{13}C$		
North American Stage	**Number**	**Avg**	**St Dev**	**Number**	**Avg**	**St Dev**
Morrowan	184	-4.44	1.77	184	2.00	1.04
Atokan	81	-3.97	0.85	81	2.11	0.83
Desmoinesian	152	-4.65	1.44	154	2.03	1.27
Missourian	123	-4.78	1.71	124	2.45	1.21
	540 Total			543 Total		
Total of All Samples	540	-4.51	1.57	543	2.13	1.13

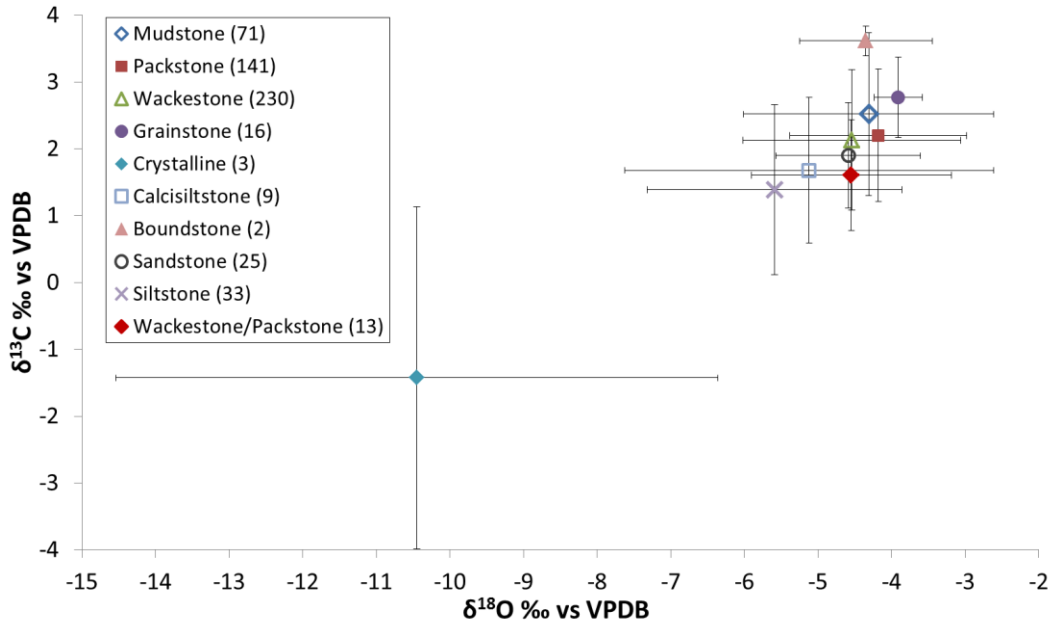

Fig. 5. Average $\delta^{18}O$ and $\delta^{13}C$ based on rock classification of fine grained carbonate samples from Gallagher Peak, Idaho. Error bars represent 1σ. Numbers in the key represent the number of samples for that rock type.

variations of 1.8‰ and 0.4‰. Regardless of rock type, $\delta^{13}C$ values decrease systematically for samples with $\delta^{18}O$ values less than -5‰ (Fig. 4).

4.3 *Stratigraphic $\delta^{13}C$ Trends*

Several long term $\delta^{13}C$ trends are delineated within the section (Fig. 6). The section begins with a gradual 1.5‰ increase over the first 80 meters, from 1.0 to 2.5‰. $\delta^{13}C$ remains around 2.5‰ for the next 100 m (80-180 m). A gradual decrease from 2.5 to -0.5‰ occurs from 180 to 325 m. This long term depletion of ^{13}C includes several large positive and negative perturbations, but the overall trend is decreasing. An increase from -0.5‰ to nearly 4.0‰ occurs over the next 165 m (325-490 m) and is followed by a sharp decrease down to 1.4‰ over 6 meters (492-498 m). This is followed by another gradual increase from 1.4 to 3.7‰ over the next 80 m (498-578 m). The uppermost 18 meters of the section (578-596 m) are marked by another rapid decrease from 3.7 to 1.3‰, just prior to deposition of the Gallagher Peak Sandstone. Many short-term ($\leq$ 20 m) positive and negative excursions of 1 to 3‰ also occur throughout the section. Further interpretation of these individual excursions is discussed below.

Little difference occurs between the average $\delta^{13}C$ of the four North America stages with the exception of the Missourian (Table 2). $\delta^{13}C$ values for North American stages in ascending order are 2.0‰ ± 1.0‰ (Morrowan), 2.1‰ ± 0.8‰ (Atokan), 2.0‰ ± 1.3‰ (Desmoinesian), and 2.5‰ ± 1.2‰ (Missourian). The Missourian averaged about 0.4‰ higher than the other three periods and is statistically significant (maximum P-value = 0.018). Not surprisingly, the most positive values of the section are within this

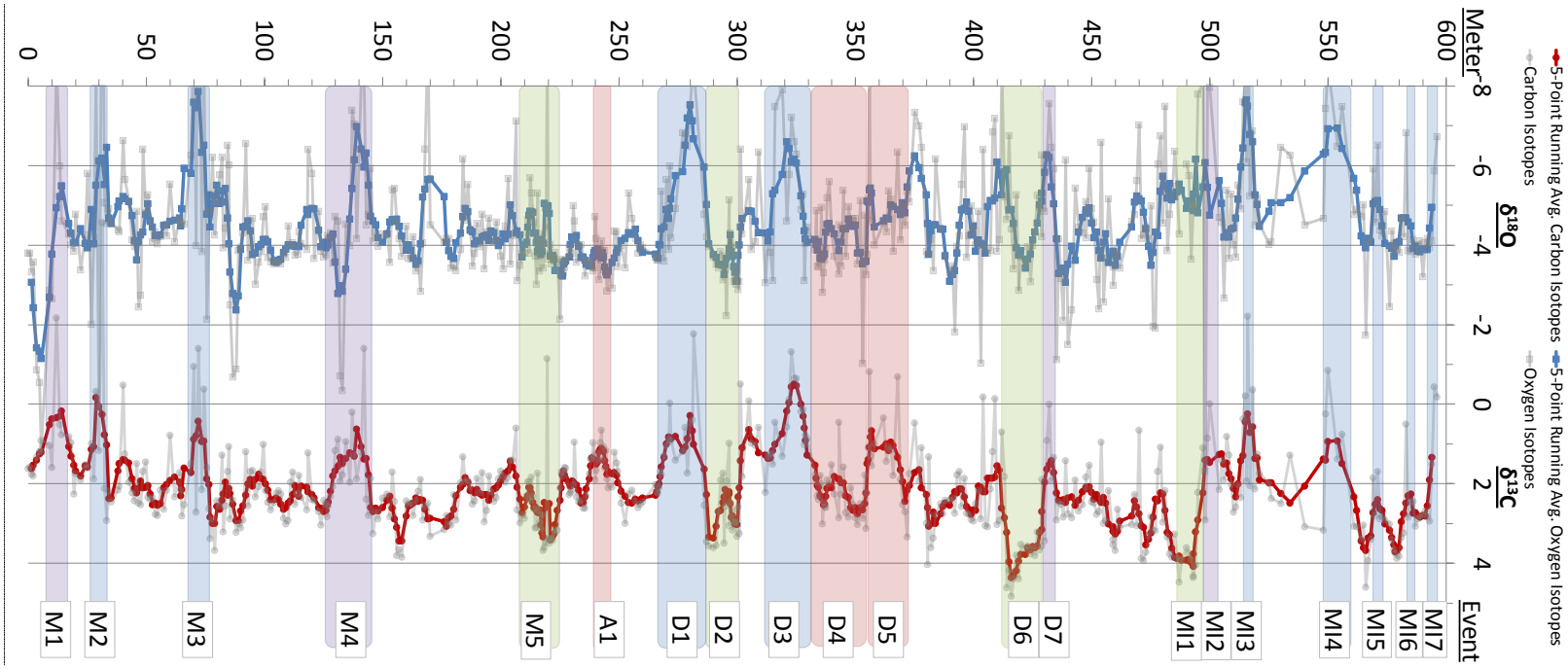

Fig. 6. Five-point running average in blue ($\delta^{18}O$) and red ($\delta^{13}C$). Oxygen and carbon isotope stratigraphies of fine grained carbonate samples from Gallagher Peak, Idaho. Individual values are plotted in gray. Major shifts (excursions) in carbon isotopes are shaded and labeled. Excursion labels begin with the letter that corresponds to their North American stage (M=Morrowan, A=Atokan, D=Desmoinesian, MI=Missourian). Each excursion is colored based on the interpreted cause of the excursion: diagenesis = blue, partial diagenesis = purple, facies characteristics = green, depositional trend (no evidence to suggest diagenesis or facies) = red.

stage. Another notable trend is that maximum values are about 1‰ higher for the upper half of the section (Desmoinesian and Missourian) than those of the Morrow and Atokan, a result similar to that from the Yukon Territory (Beauchamp et al., 1987).

No correlation of $\delta^{13}C$ and $\delta^{18}O$ values from Gallahger Peak with cyclothems and sequence boundaries (Pope et al., 2007) was observed (Appendix F). Sequence boundaries were picked at the top of major sand units (lowstands). $\delta^{13}C$ might have been expected to increase from sequence boundaries to maximum flooding surfaces, as a greater marine portion would influence deposits at maximum flooding surfaces. However, no relationship associated with sequence boundaries was evident.

4.4 *Cathodoluminescence Microscopy and Chemical Analyses*

Cathodoluminescence microscopy revealed that all samples were either non-luminescent or had minimal luminescence. Even at exposure times of 40 seconds cathodoluminescence was minimal. Cathodoluminescent images using the electron microprobe did reveal two samples with distinct zoning in a couple dolomite grains (Appendix D). Microprobe analyses also confirmed that Mn was below the detection limit in most samples and that iron only occurred in small amounts. Thus, cathodoluminescence is not a useful diagenetic indicator in these samples.

Electron probe microanalyses were performed on 30 carbonate samples (Table 3). Based on chemical composition, possible trace components include apatite, ferric hydroxide, anhydrite, clay, rutile, iron oxides, iron hydroxide, zircon, aluminum silicate, potassium feldspar, barite, strontium sulfate (celestite), fluorite, and a sodium-rich silicate (Table 3). No clear stratigraphic trends were noted for Ca, Mg, Fe, Sr, S, Na.

Table 3
Electron microprobe analyses of carbonate matrix and skeletal grains. Gray highlighting indicates values with high uncertainty (values that are less than two times the lower limit of detection (LLD). Uncertainty increases with decreasing element concentration. Most sample locations are noted on thin sections scans in Appendix B.

Lower Limit of Detection

	Ca (ppm)	Mg (ppm)	Fe (ppm)	Mn (ppm)	Sr (ppm)	S (ppm)	Na (ppm)
Reported Stat LLD	**201**	**34**	**99**	**94**	**190**	**40**	**53**

Calcite Standards

	Ca (ppm)	Mg (ppm)	Fe (ppm)	Mn (ppm)	Sr (ppm)	S (ppm)	Na (ppm)
3calcite_std#1	398850			975		74	82
3calcite_std#2	395795	46		765		77	
5CaCO3_std#1	402570			382			74
5CaCO3_std#2	399703			444			161

Calcite Analyses

	Meter	Ca (ppm)	Mg (ppm)	Fe (ppm)	Mn (ppm)	Sr (ppm)	S (ppm)	Na (ppm)	Material Analyzed	Traces Found	Notes
21.2_pt02	21.2	391414	4650	246		558	537	256	Matrix		
21.2_pt03	21.2	401068	813			469	719	178	Skeletal Grain		
23.3_pt04	23.3	397769	2168			700		56	Evaporite Nodule	Ferric hydroxide, Anhydrite in Evaporite Nodule	10-20% Dolomite
23.3_pt05	23.3	401525	1263			457	65		Evaporite Nodule		
32.3_pt01	32.3	402750	1793				75	82	Pellet		
32.3_pt02	32.3	401429	2084	241		202	210		Pellet		
32.3_pt03	32.3	402610	2191	174		273	142	538	Outer rim of crinoid		
32.3_pt04	32.3	406018	1136		239			61	Inner core of crinoid		
45_pt01	45	401028	2157			297	242		Skeletal fragment		
45_pt02	45	398806	4307			231	617	87	Outer rim of crinoid		
45_pt03	45	395166	4688	183		522	1229	404	Inner core of crinoid	Fine grained apatite in center of crinoid	
45_pt04	45	396403	3523	178		588	356	386	Coral fragment		
60_pt01	60	392971	3604	419	105		341	286	Matrix		Algae and nodules are silica
60_pt02	60	398141	3157						Calcite between grains of silica replaced algae		Small dolomite inclusions (10X5 microns) within skeletal grains
60_pt03	60	398253	2713			273	130	87	crinoid/ skeletal grain		
74.5_pt01	74.5	397705	2661				136	61	Matrix	Clay, Apatite, and Rutile	
74.5_pt02	74.5	398485	3168	135			98	74	Matrix		
74.5_pt03	74.5	401589	1992			326	110		Horn coral		
74.5_pt04	74.5	401897	1038				71		Skeletal Grains		Contains Dolomite inclusions (pts. 5 & 6)
85_pt01	85	399663	4163				240	126	Matrix		Trilobites and in situ fossils are silica replace
85_pt02	85	398850	3540				358	130	Matrix		

Table 3 – Continued

	Meter	Ca (ppm)	Mg (ppm)	Fe (ppm)	Mn (ppm)	Sr (ppm)	S (ppm)	Na (ppm)	Material Analyzed	Traces Found	Notes
85_pt03	85	397845	4965			332	106	87	Matrix		
85_pt04	85	399787	2044	188			139	69	Matrix		
137_pt01	137	390124	5602	284		261	236	108	Very fine matrix		5-10 Micron Grains
137_pt02	137	391462	5051	1364			208	130	Very fine matrix		
137_pt03	137	400844	2304						Fracture Fill		
184_pt01	184	395967	2266	1123			57		Matrix	Some form of sodium silicate	Higher silica in fossil fill, many fossil grains are calcite
184_pt02	184	396856	3255			736	3175	1332	Skeletal Grain		Darker gray material in BSE is silica
184_pt03	184	388991	5484	656	105	208	1190	434	Matrix	Apatite, Hematite, Rutile, and Clay	About 12% silica
184_pt04	184	396319	3324	1943			63		Matrix		
204_pt01	204	397016	4800	159		605	391	108	Matrix		Crinoid fossil is replaced by silica
204_pt02	204	398554	5086	116		594	433	178	Brachiopod		Material between large fossil fragments is calcite
204_pt03	204	396007	3754			843	237	529	Matrix		
204_pt04	204	401228	1790		129	231	174		Crinoid		
215_pt01	215	400452	3226				51		Algae		
215_pt02	215	400872	3869			237	222		Algae		
215_pt03	215	399463	4495				383	139	Matrix		
215_pt04	215	399719	4013				350	56	Matrix		
226.5_pt01	226.5	393748	4025	111		564	711	547	Matrix		
226.5_pt02	226.5	398389	3114	106		398	992	469	Matrix		
226.5_pt03	226.5	400792	1401			855	832	855	Large fossil fragment		
226.5_pt04	226.5	398153	4183		163		457	69	Gastropod		
271_pt01	271	400532	2520			285	180		Inner matrix of in situ coral (white material)		
271_pt02	271	396992	5086			481	651	195	Inner matrix of in situ coral (dark material)		
271_pt03	271	397240	4792			540	714	126	Matrix		
271_pt04	271	395670	6020			320	636	169	Matrix		
277_pt01	277	404364	1297		105	433			Brachiopod	Iron hydroxide spheres, Altered pyrite	In BSE image bright spots are iron hydroxide, possibly altered pyrite
277_pt02	277	399683	1655			1335	566	872	Matrix		Very little cement in sample, very porous
277_pt03	277	397737	2234	236	96	499	1626	234	Matrix		
296.5_pt01	296.5	398105	4962	304		433		91	Calcite spar in coral		
296.5_pt02	296.5	400408	2923			350	285	65	Matrix		
296.5_pt03	296.5	403391	213						Calcite rhomb in silica cement		
296.5_pt04	296.5	401669	3760	183			195		Matrix		
296.5_pt05	296.5	399014	957	487			57	82	calcite rhomb		
305_pt01	305	393035	4521	130	124	451	681	243	Matrix		lighter areas are zones of higher silica
305_pt02	305	393284	1874	685					Matrix in higher silica zone	skeletal fragments partially replaced by silica	
305_pt03	305	394033	3215			1163	1449	1306	Brachiopod		
305_pt04	305	399519	4327	111			119		Calcite core in silica replaced crinoid		
330_pt01	330	399294	2182			243		65	Skeletal fragment		Horn coral is chert

Table 3 – Continued

	Meter	Ca (ppm)	Mg (ppm)	Fe (ppm)	Mn (ppm)	Sr (ppm)	S (ppm)	Na (ppm)	Material Analyzed	Traces Found	Notes
330_pt02	330	398802	2226			1893			Skeletal fragment		Calcite around skeletal grains
330_pt03	330	398341	3036	145	100	356	566	78	Skeletal fragment		
351_pt01	351	396199	4469			350	790	226	Matrix	Apatite, Ferric hydroxide	Silt size silica
351_pt02	351	395979	3866	174		706	459	69	Matrix		
351_pt03	351	396259	4780			493	637		Skeletal fragment		
388_pt01	388	393388	4763			659	489	104	Matrix	Ferric oxide, Rutile	
388_pt02	388	398025	4238	154		226	362	130	Matrix		Silica silt visible
388_pt03	388	396403	1632			1009	1967	1033	Brachiopod		
438_pt07	438	404188	770						Matrix	K-spar, Apatite	
404_pt01	404	403759	1808			320	133	108	Matrix		
404_pt02	404	396295	4812	188		872	571	108	Matrix		
404_pt03	404	399611	2203			777			Calcite spar in nodule		
457_pt02	457	395742	4532	294		653	749	100	Matrix		
457_pt03	457	395823	4740	574			287		Calcite core of skeletal frag. with silica rim		
457_pt04	457	403155	1090	169		255			Fracture		
459_Mike Alg_pt01	459	394605	4573	135	134		522	117	Matrix (black)	Zircon, Iron oxide, and Aluminum silicate	
459_Mike Alg_pt02	459	397308	2857			979		82	White material		Lots of quartz in this area
459_pt01	459	394541	4454	689		819	556	82	Matrix	Clay, Rutile, and Apatite	
459_pt02	459	395618	4702	405	115	374	678	152	Matrix		
459_pt03	459	394645	4348	598	134				In situ fossils		Chamber walls and interior are calcite
459_pt04	459	402878	585	357	201		97		Replaced Zone	Barite, Strontium sulfide	
506_pt01	506	397524	3532	198		410	679	347	Matrix	Fluorite, K-spar, Rutile, Barite, Apatite	
506_pt02	506	402570	1032				80	161	Crinoid/ skeletal grain		
506_pt03	506	399699	1018			813	2764	555	Brachiopod with quartz rim		
506_pt04	506	393424	2932	2174	139		791		Matrix		
517_pt01	517	396992	4743	415			717	95	Matrix		
517_pt02	517	391025	6129	362		439	409	100	Matrix		
517_pt03	517	405998	946						Fracture		
517_pt04	517	396679	3269	227		605	758	664	Phylloid algae		
517_pt05	517	402986	528			469	583	113	Brachiopod		
548_pt01	548	397753	2367	304		226	159		Matrix		Partially replaced by quartz
548_pt02	548	398065	2381	241		231	124		Matrix		Some silica replacement
548_pt03	548	399050	2373	265		398	180	82	Matrix	Apatite, Ferric oxide (Goethite or Limonite), Rutile	
554_pt01	554	395078	4143	453		356	266	61	Matrix	Rutile	Evaporite nodules are quartz
554_pt02	554	397604	2128	270		356	1190	286	Matrix		
594_pt01	594	397741	2935	231		267	220		Matrix		

Table 3 – Continued

	Meter	Ca (ppm)	Mg (ppm)	Fe (ppm)	Mn (ppm)	Sr (ppm)	S (ppm)	Na (ppm)	Material Analyzed	Traces Found	Notes
594_pt02	594	395883	3575	333		237	183	143	Matrix		
594_pt03	594	400752	1476	106		611	574	87	Skeletal Grain		
594_pt04	594	399162	1499	111	134	362	48		Fracture fill		BSE and CL Images available

Dolomite Standards

	Ca (ppm)	Mg (ppm)	Fe (ppm)	Mn (ppm)	Sr (ppm)	S (ppm)	Na (ppm)
3dolomite_std#1	216670	131894	689				
3dolomite_std#2	215136	131819	752	139	243		

Dolomite Analyses

	Meter	Ca (ppm)	Mg (ppm)	Fe (ppm)	Mn (ppm)	Sr (ppm)	S (ppm)	Na (ppm)	Material Analyzed	Traces Found	Notes
23.3_pt01	23.3	225287	124090	352				56	Dolomite rhomb in matrix		BSE Image available
23.3_pt02	23.3	227606	119186	439		202	236	126	Dolomite rhomb in matrix		
23.3_pt03	23.3	224615	120391	1118	287		306	178	Dolomite rhomb in matrix		
26.8_pt01	26.8	223782	119215	3027		588	183	74	Dolomite rhomb in matrix	K-spar, Apatite, and Rutile	20% dolomite,
26.8_pt02	26.8	244156	119298	265		315	608	213	Dolomite rhomb in matrix		CL and BSE Image
74.5_pt05	74.5	223421	132050	121			51	148	Dolomite rhomb in skeletal grain		
74.5_pt06	74.5	221319	132575				60		Dolomite rhomb in skeletal grain		
404_pt04	404	229952	124148				45		Outer rim of dolomite rhomb		luminescent in CL
404_pt05	404	241085	114821	487	191	552	984	460	Dolomite in silica replaced crinoid		
404_pt06	404	227438	123779	2227	182			65	Inner rim of dolomite rhomb		less luminescent in CL
404_pt07	404	226469	121980	5722	167			61	Core of dolomite rhomb		least luminescent in CL

5. DISCUSSION

The carbon isotope profile of Pennsylvanian carbonate rocks from Gallagher Peak consists of high frequency oscillations of about 1‰, with positive and negative excursions of greater than 1.5% throughout the section (Fig. 2). Several of the most prominent excursions are named to facilitate the discussion (Fig. 6). Names consist of the first letter of the North American stage to which they correspond and an assigned number starting at 1 and increasing upward.

5.1 *Diagenesis*

Diagenetic indicators in Gallagher Peak rocks include stylolites, crystalline texture, siltstone and sandstone associated with subaerial exposure, vugs, evaporites, dolomite, and $\delta^{18}O$ values below -6‰ that are synchronous with negative $\delta^{13}C$ excursions. Stylolites and vugs indicate that dissolution of the limestone has occurred, while a crystalline texture indicates recrystallization. The siltstone/sandstone, evaporites, and dolomite could indicate shallower marine environments, with siltstone and sandstone representing eolian deposition (Breuninger et al., 1989; Canter and Isaacson, 1991; Archuleta et al., 2006). These shallow environments are often more susceptible to diagenetic alteration, which results in more negative $\delta^{18}O$ and $\delta^{13}C$ values (Immenhauser et al., 2002). Periods of higher siltstone and sandstone appear to correlate with periods of low $\delta^{18}O$ and $\delta^{13}C$ values (Appendix E). The low carbon and oxygen isotope values could be the result of meteoric and burial diagenesis (Hudson, 1977; Anderson and Arthur, 1983). For oxygen isotope values below -5‰, $\delta^{18}O$ decreases

systematically with $\delta^{13}C$ (Fig. 4). Low $\delta^{18}O$ values have been used in previous studies to indicate alteration of rock-buffered $\delta^{13}C$ values (e.g., Saltzman, 2003). In order to confirm that $\delta^{18}O$ values indicate diagenesis, t-test using $\delta^{18}O$ increments of 1‰ were performed. T-tests comparing $\delta^{13}C$ values confirmed that samples with $\delta^{18}O$ below -5‰ were significantly different than the majority of the data (samples with $\delta^{18}O$ between -5 and -3‰). However, in order avoid misinterpreting diagenesis, only $\delta^{18}O$ values less than -6‰ were used as diagenetic indicators. By excluding sample with $\delta^{18}O$ values less than -6‰ several the short term diagenetic excursions can be eliminated (Appendix G). Minimal differences between this $\delta^{13}C$ profile and a $\delta^{13}C$ profile that excludes samples with $\delta^{18}O$ values less than -5‰ confirms that -6‰ is a good diagenetic indicator that also minimizes excessive data exclusion. Additionally, $\delta^{13}C$ values of fine grained carbonate samples lower than 0‰ only occur with corresponding $\delta^{18}O$ values less than about -6‰, suggesting that carbon isotope values less than 0‰ also indicate meteoric or burial diagenetic values.

Trace elements within matrix calcite provided little evidence of preservation or diagenesis, as no clear trends were identified. Increased diagenesis may add or remove Mg, depending on original composition, and removes Na, Sr, and S (Al-Aasm and Veizer, 1982; Grossman et al., 1996; Mii et al., 1999). Calcite from seven brachiopods was analyzed and is enriched in Na, Sr, and S relative to the matrix and other samples (Fig. 7e). The preservation is likely a result of brachiopods' original low-Mg calcite mineralogy (Popp et al., 1986; Compston, 1960). Elemental analyses of matrix calcite

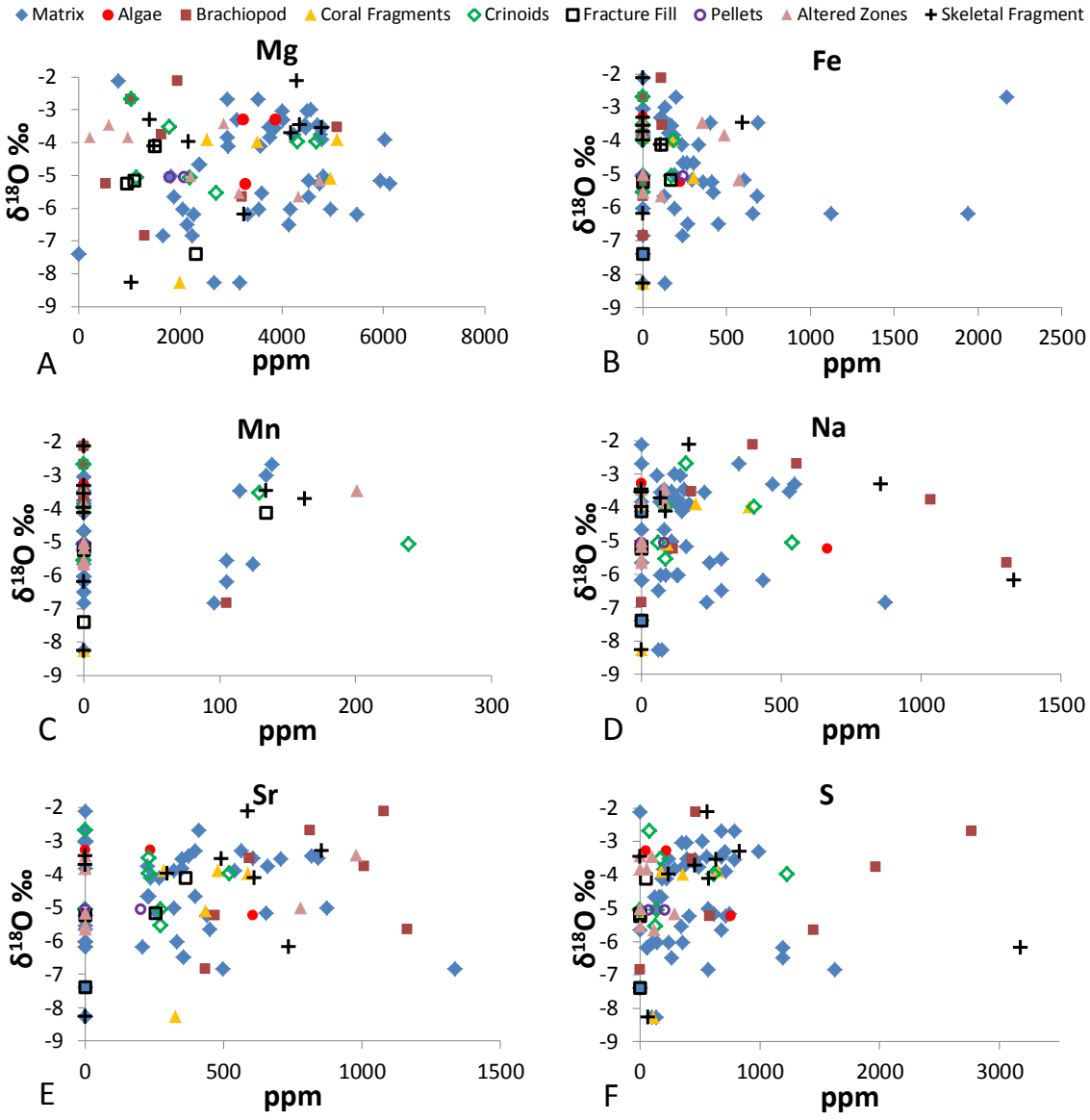

Fig. 7. Microprobe analyses of matrix calcite and other calcite components of samples from Gallagher Peak, Idaho, plotted vs. $\delta^{18}O$. These figures do not include microprobe results of dolomite from these samples. For these results see Table 3.

showed no statistical correlation of δ18O to Mg, Na, Sr, and S trends (Fig. 7e, Table 3), and provide no additional evidence for preservation or diagenesis.

Petrographic and isotopic evidence suggest that the majority of the short term (<1 Ma) negative $\delta^{13}C$ excursions can be attributed to diagenesis (Fig. 6). Some of these negative excursions are the result of, or at least enhanced by, one or two highly negative samples. M1 is mostly comprised of packstones that have slightly lower carbon and oxygen isotope values with respect to samples above and below. However, one sample (12A) contains stylolites and has extremely low $\delta^{13}C$ and $\delta^{18}O$ values of -2.2‰ and -8.6‰, respectively. This one $\delta^{13}C$ value lowers the running average of the surrounding $\delta^{13}C$ values by about 1‰. M4 and D7 are also diagenetically enhanced events similar to M1, except that the few highly negative isotopic values are associated with samples containing dark organic matter in voids. Small amount of this organic matter may have been incorporated into the carbonate powders analyzed from these samples. However, samples surrounding these events show little additional evidence suggesting alteration, consisting mainly of skeletal wackestone and packstone. Examples of isotopic excursions in the Morrowan that appear purely diagenetic are M2 and M3. M2 has two samples, 28.8A and 31.3A, with unusually low $\delta^{13}C$ values (-0.3‰ and -4.6‰, respectively). Additionally, 31.3A, has a crystalline mosaic texture with 3-5 mm vugs, suggesting more alteration than samples above and below. M3 contains three samples with very low $\delta^{18}O$ and $\delta^{13}C$ values, and each sample contains additional evidence of alteration (crystalline texture, stylolites, and about 50% silt/sand).

The two largest negative $\delta^{13}C$ excursions (D1 and D3) occur in the lower Desmoinesian and are likely related to early burial digenesis. Both events cover 10-20 m and are accompanied by large negative $\delta^{18}O$ excursions. Both events are marked by

unusually high silt content with over half the samples containing more than 30% silt. D1 contains samples with up to 60% silt, and has six consecutive samples with $\delta^{18}O$ less than -6‰. Seven out of sixteen samples in D3 contain over 70% silt. Both of these events are interpreted to be periods of deposition on the shallow platform interior during conditions of relatively low base level, possibly related to a sea level lowstand. Shallow/restricted carbonate environments have been linked to light carbon isotope values as a result of increased oxidation of organic matter (Lloyd, 1964). This could be accompanied by ^{18}O enrichment as a result of increased evaporation (Lloyd, 1964) or ^{16}O enrichment from mixing with meteoric water at these shallow water environments (Hudson, 1977; Kievman, 1998). However, the unusually low $\delta^{18}O$ of D1 and D3 suggest diagenetic alteration, making environmental interpretations untenable. Two large negative excursions also occur in lower Desmoinesian carbonate rocks at Big Hatchet Peak, NM (Fig. 3; Magaritz and Holser, 1991), suggesting that both locations could have experienced coeval increase restriction/shallowing during the early-mid Desmoinesian. However, it is highly possible that this correlation is coincidental or an artifact of resolution differences, as these two sections have few other points of correlation (Fig. 3). Higher sampling resolution and detailed sample descriptions from Big Hatchet Peak are needed in order to make a more accurate correlation.

The last six diagenetic events occur during the Missourian and are all relatively short excursions that result from a few samples. MI2 is likely a combination of diagenetic and original seawater chemistry signals. Up to 1.7‰ of the sharp decrease may actually be more of a result of the preceding highly positive values of MI1. The

silty samples of MI2 may be enhancing the negative excursion by an additional 1.3‰. The remaining five excursions (MI3, MI4, MI5, MI6, and MI7) contain samples with increased silt and $\delta^{18}O$ values less than -6‰. Some of these events are the result of multiple altered samples (MI3 and MI4), while others are the result of only one or two altered samples (MI5, MI6, MI7). MI7 samples were taken just below the Gallagher Peak Sandstone, a sea level lowstand, and the decrease may be the result of associated subaerial exposure and/or meteoric diagenesis.

5.2 *Excursions Related to Facies*

Several of the large excursions can be correlated directly to unique facies characteristics. Examples include positive excursions associated with phylloid algal mounds (D6, MI1), algal bioclastic packstones (M5), and grainstones with high biodiversity (D2). Some negative excursions are associated with increased siltstone/sandstone content, however, there also are samples with increased siltstone/sandstone content that maintain $\delta^{13}C$ and $\delta^{18}O$ values similar to those of surrounding limestone.

Phylloid algal mounds (D6 and MI1) within the section correlate with periods of ^{13}C enrichment (Fig. 2). The mounds contain high biodiversity with little silt, and their associated positive carbon isotope excursions tend to be independent of the oxygen isotopic values. Additionally, the high $\delta^{13}C$ and $\delta^{18}O$ variability decreases dramatically through these events. One explanation for this shift could be the result of higher productivity, which can increase $\delta^{13}C$ by 1-2‰ for marine environments within the photic zone (Anderson and Arthur, 1983). However, this 1-2‰ difference is a

comparison of deposits below the photic zone versus those above it. Since most of the deposits in the Gallagher Peak section were deposited within the photic zone, high verses low productivity is a less probable cause. Alternatively, these deposits could have higher $\delta^{13}C$ because they contain the greatest portion of marine carbonate. This is supported by the high biodiversity throughout these mounds. Additionally, an interpreted sea level high, based on microfacies from Arrow Canyon (Heath et al., 1967), appears to correlate with the algal mound deposits at Gallagher Peak (Fig. 8).

A third explanation for the $\delta^{13}C$ excursions related to phylloid algae in the section could represent a greater portion of aragonite relative to calcite during deposition, as phylloid algae are typically aragonitic (Scholle and Ulmer-Scholle, 2003). Carbon isotope excursions recorded in whole rock from shallow marine platforms have been shown to reflect changes in sediment mineralogy rather than changes in carbon burial or productivity (Swart and Eberli, 2005). This is because calcite-HCO_3^- and aragonite-HCO_3^- fractionation are 1.0‰ ± 0.1‰ and 2.7‰ ± 0.2‰, respectively (Romanek et al., 1992). If a higher percentage of non-algal deposits at Gallagher Peak were originally calcite, then the difference between aragonite and calcite fractionation (up to 1.7‰) could explain the 1.5-2‰ excursion. However, based on observations of aragonite cements and oolites, Pennsylvanian deposits were deposited during an aragonite sea (Sandberg, 1983; Hardie, 1996). If calcite to aragonite ratios are similar to modern Florida Bay (also an aragonite sea), then the carbonate deposits would contain 15% low-Mg calcite and 27% high-Mg calcite (Scholl, 1966). According to mass balance calculations, if aragonite increased to 100% as a result of phylloid algae

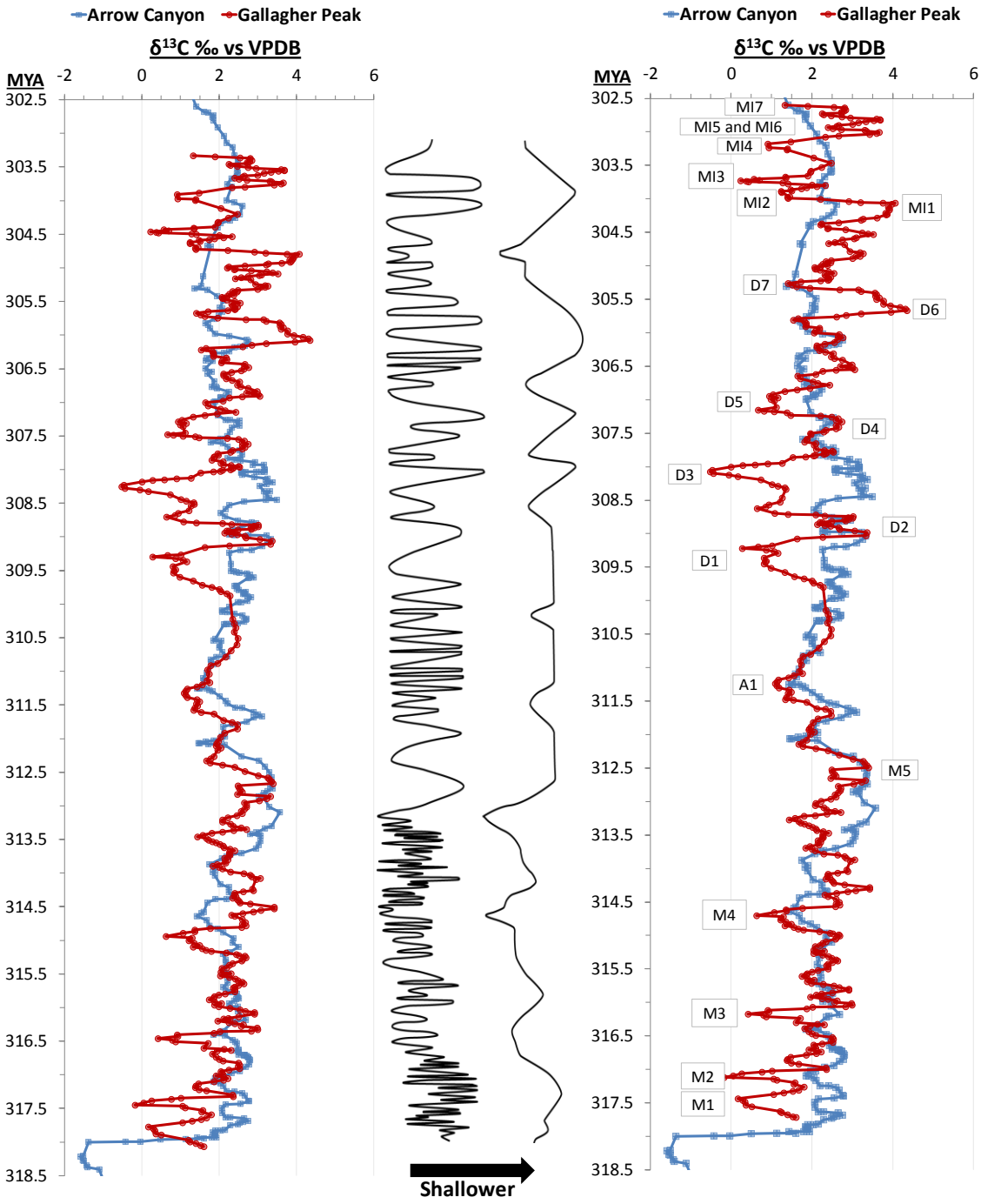

Fig. 8. Carbon isotope stratigraphy of Gallagher Peak, Idaho, and Arrow Canyon, Nevada. Curves are based on a five-point running average from both locations. The relative sea level curve is modified from Heath et al. (1967). The stratigraphy on the right (B) has a Gallagher Peak curve that has been shifted slightly for a better fit with the Arrow Canyon data. Adjustments were generally less than 0.5 Ma with a few reaching 0.75 Ma. The carbon isotope profile on the left (A) shows the data without any adjustments. Ages are according the Gradstein et al. (2004) based on North American Stage boundary ages used in Saltzman (2003).

dominance, then only a 0.5‰ increase would be expected. Yet, it is possible that in addition to their aragonite mineralogy, cement crusts on the algae could better preserve the depositional $\delta^{13}C$. Aragonite cement crusts on phylloid algae in New Mexico yielded carbon and oxygen values of 4.5‰ and -5.3‰, respectively (Dickson et al., 1991). Importantly the results from New Mexico indicate that alteration from aragonite to calcite, while lowering $\delta^{18}O$, did not affect $\delta^{13}C$ values (Dickson et al., 1991). These results are supported by the consistent $\delta^{13}C$ values observed at the Gallagher Peak section. This evidence suggests that the positive $\delta^{13}C$ excursions associated with the algal mounds are augmented by 0.5‰ or more as a result of the original aragonitic composition of the algae. The algal marine cements may also better preserve the $\delta^{13}C$ values of more open marine conditions, as they have been shown to retain their $\delta^{13}C$ while transitioning from aragonite to calcite (Dickson et al., 1991).

M5 marks a section of mostly wackestone and packstone. Most of these samples have a pelloidal texture (Appendix B, sample 215) of possible algal origin (red algae *Archaeolithophyllum* sp.). The algal texture associated with M5 appears between 214.5 and 224 m. Samples immediately above and below this texture have about 1‰ lower $\delta^{13}C$ values. This could be another example related to aragonitic algae or even increased amounts of high Mg-calcite, depending on the family of the red algae. End member high-Mg calcite can differ from low-Mg calcite by as much as 0.82‰ (Jimenez-Lopez et al., 2006). These platy red algae were often located in moderate wave energy environments (Scholle and Scholle, 2003), but the low diversity and presence of ostracods suggest it was not subject to high energy. This also correlates to an interpreted

sea level low based on thin sections from Arrow Canyon (Heath et al., 1967). Thus, the positive excursion is not likely the result of higher marine influence. The apparent drop in the middle of the positive excursion is the result of a single low carbon value from a wackestone sample (219.5A, $\delta^{13}C$ = -1.2‰, $\delta^{18}O$ = -9.0‰). M5 ends with a 1.5‰ decrease from 223 to 226 m. A carbonate-rich sandstone sample marks the beginning of the decrease, but little evidence suggests the decrease is due to diagenesis.

D2 is the largest package of consecutive skeletal grainstone/packstone in the whole section. Many of these samples contain abundant coated grains and/or pellets. Samples containing coated grains or pellets averaged around 2.8‰, similar to the grainstone average (Table 2). These are likely similar because the coated grains/pellets are associated with the grainstone facies of this section. This could be another example of the original mineralogy differences associated with the conditions in which these pellets form. However, these could simply represent a greater portion of marine deposits. The higher energy environment associated with the formation of grainstones could thus represent the greatest exposure to the open marine environment. Many of the bioclasts in the grainstone are rounded suggesting a higher energy depositional setting. Higher marine influence during D2 is also suggested by a sea level highstand (Heath et al., 1967). If D1 and D3 correlate with the two sea level lowstands (Fig. 8), then D2 would correlate with the intervening sea level highstand.

Several apparent excursions had no association with alteration or facies characteristics (A1, D4, D5). These likely represent trends of $\delta^{13}C$ of seawater DIC at Gallagher Peak, as there is no indication to suggest otherwise. Samples of event A1,

which covers meter 238 to 245, had only one sample with early stylolites. Others had high silt content, but still maintained comparable isotopic values to those without silt. D4, a positive excursion, is composed of silty wackestone and packstone. Although about half of the samples from this interval contain more than 30% silt, they still appear to have similar values as nearby samples without silt. D5 is marked by lower $\delta^{13}C$ and continues just above D4 with similar silty mudstone, wackestone, and packstone. D5 also has few diagenetic indicators with only two of the eleven having unusually low oxygen values. Most likely original depositional fluids were slightly depleted in ^{13}C. Alternatively, the oxygen isotope values could have been reset to higher values after the $\delta^{13}C$ values were already altered; however, no evidence of multistage diagenesis is visible in these thin sections.

The correlation of positive excursions with specific facies illustrates the importance of describing the individual samples and viewing them in thin sections. These facies changes may be in response to global conditions, but are partially the result of the local biota and environment. Similarly, Cenozoic nannofossil assemblages have been found to correlate directly with changes in $\delta^{13}C$ (Bralower, 2002). At least minor, shifts in the section were believed to be caused by the relative fraction of nannoplankton species (Bralower, 2002) in the sample.

5.3 *Arrow Canyon Compared to Gallagher Peak*

The carbon isotope curves for Gallagher Peak and Arrow Canyon (Saltzman, 2003) are plotted in Figure 8. The ages of the North American stages are correlated to those of the International stages (Menning et al., 2006). For better comparison, the same

North American stage boundary ages (Table 4) used by Saltzman (2003) were adopted as boundary ages for this study. Five-point running averages of the carbon isotopes from Gallagher Peak and Arrow Canyon are plotted based on North American stage boundaries in Figures 8a and 8b, but in Figure 8b the carbon isotope profile of Gallagher Peak was shifted vertically assuming a correlation between Gallagher Peak and Arrow Canyon. All adjustments were less than 750 ky (within the margin of error of the Gradstein et al. (2004) timescale). The differences between the two sections may reflect uncertainty in the time scale, differences in sedimentation rate, or errors in the biostratigraphy of two sections. The lack of a 2-3‰ increase in the lower 15 m of the Gallagher Peak section indicates that these rocks are Pennsylvanian, supporting the claim that the mid-Carboniferous boundary is contained in the uppermost part of the Bluebird Mountain Formation (Batt et al., 2007).

Table 4
North American and International stage boundary ages.

North American Stages	Age used by Saltzman (2003)
Morrowan	318.1
Atokan	313.3
Desmoinesian	309.5
Missourian	305.6
Virgilian	303.3

International Stage Boundaries	Gradstein et al. (2004)
Bashkirian	*318.1*
Moscovian	*311.7*
Kasimovian	*307.2*
Gzhelian	*303.4*

Both $\delta^{13}C$ curves fluctuate around values of 2‰, with tight correlation between the two sections from about 318 to 310 Ma (Fig. 8). However, several short lived negative excursions (Events M1, M2, M3, and M4) in the Gallagher Peak section do not

occur in the Arrow Canyon section. Around 310 Ma the Gallagher Peak $\delta^{13}C$ stratigraphy becomes more variable (Figs. 6, 8). Both positive and negative excursions increase in magnitude and extend over longer periods. Additionally, the large positive and negative excursions can be correlated with diagenetic events (i.e. D1 and D3) and facies (M5, D2, D6, MI1) characteristics, suggesting a shift to more local influences. This could be the result of increased restriction due to a combination of sea level fall, large barrier algal mounds further to the west, or the rise of the Copper Basin Highlands in the mid-Pennsylvania (Skipp et al, 1979). The rise of the Copper Basin Highlands may have separated the Wood River Basin and the Snaky Canyon carbonate platform beginning sometime in the Atokan to Late Desmoinesian (Skipp et al., 1979). These results further constrain this event, and suggest that the uplift occurred right around the Atokan-Desmoinesian boundary. Additional evidence of more restriction in the upper half of the Gallagher Peak section include evaporites, less grainstones and packstones (suggesting lower energy environments), increased presence of ostracods, and the increased appearance of the phylloid algal mounds. The lack of mound talus and grainstone around the phylloid algal mounds in Idaho, led to the interpretation that such deposits developed in the subtidal zone of a semi-restricted environment, away from strong wave action (Breuninger, 1976). However, high biodiversity within these mounds indicate that they formed in moderately open marine conditions.

The $\delta^{13}C$ curve for the upper half of Gallagher Peak section appears to consist of three cycles. Each cycle gradually becomes enriched in ^{13}C over 1-1.5 Ma and is followed by a rapid decrease of more than 1‰. The first cycle runs from about 355 to

425 m, the second from 430 to 490 m, and the third from 495 to 580 m. Another way to view the data is to exclude the algal mounds, as they might not represent general values across the carbonate platform. This would result in two increasing trends, one from 355 to 490 m and the other from 495 to 580 m, that better correlate to the sea level curve of Heath et al. (1967)(Fig. 8). The gradual increase followed by a rapid decrease could be correlated to gradual sea level regression followed by a rapid transgression. This means that flooding events (warmer) would correlate with low $\delta^{13}C$, whereas sea level lowstands (cooler) would correlate with more positive $\delta^{13}C$. This interpretation fits evidence of an observed correlation of positive excursions with cool periods in the Great Basin (Saltzman, 2005). However, comparison of these results to relative sea level interpretations based on microfacies analysis from Arrow Canyon (Heath et al., 1967), suggest that sea level highstands appear to correlate with higher $\delta^{13}C$. Higher sea level would result in greater exchange with the open ocean and thus a greater portion marine waters and sediments. This hypothesis is further supported by the high biodiversity and grainstones associated with $\delta^{13}C$ highs throughout the section.

Ignoring the two major diagenetic excursions (D1, D3) and two major facies related excursions (D6, MI1), values between the Gallagher and Arrow Canyon sections appear to be within the same range from 310 to 302.5 Ma. The larger increased variability of isotopic results and larger diagenetic and facies related excursions makes correlating specific trends in the upper half of the Gallagher Peak section more qualitative than quantitative. This suggests that even with biostratigraphy control, accurately correlating a section whose primary signal is the result of local processes is

unlikely. However, high resolution stratigraphy, coupled with careful analysis of rock types and materials sampled, can help distinguish between primary and diagenetic, and between local and regional, signals. Without biostratigraphic control and a detailed description of the individual samples, the tendency is to correlate the Gallagher Peak maximum values to those of Arrow Canyon. The result is a correlation that differs from the proposed interpretation by about 3 Ma (Fig. 9). Even this interpretation cannot be ruled out completely, as revisions of the Snaky Canyon Formation biostratigraphy could improve upon the results of the study.

The lack of a clear correlation between the $\delta^{13}C$ profiles of two similar locations near the same ocean supports that most of the excursions in the $\delta^{13}C$ profile are local or diagenetic signals with the exceptional global or regional trend visible. Even when filtering samples with indications of diagenesis, correlation is still difficult. Additionally, when individual samples are described and viewed microscopically, correlations to fossils, facies, chemical composition, and/or other local features may become apparent. This supports that the local depositional environment is the major control over the $\delta^{13}C$, rather than global carbon budget changes. However, long-term $\delta^{13}C$ trends, with the exceptional short term event, may correlate globally. In order to correlate global trends, detailed examination of each sample is necessary to rule out diagenesis. Previous whole rock studies have often failed to provide this valuable information.

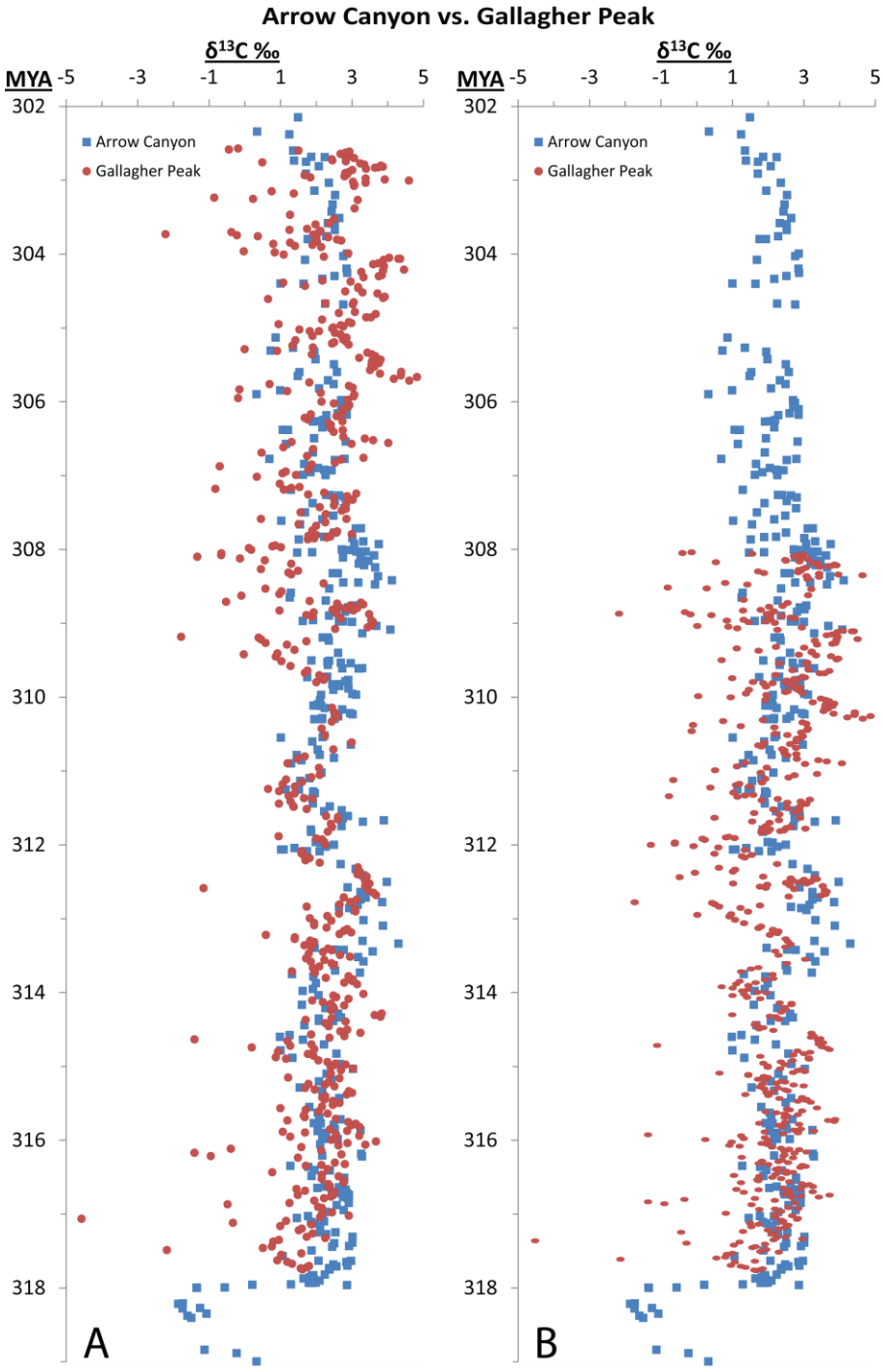

Fig. 9. Alternate correlation between Arrow Canyon, Nevada, (Saltzman, 2003) and Gallagher Peak, Idaho, using carbon isotopes of fine grained carbonate. The profile on the left (A) is plotted according to interpretation of this paper. The profile on the right (B) illustrates how correlating profiles without other stratigraphic evidence could result in dramatically different results. Ages are according to Gradstein et al., (2004).

5.4 *Future Work*

In spite of recent conodont biostratigraphy, an additional biostratigraphic study that directly correlates samples from Arrow Canyon to those of Snaky Canyon could greatly improve upon the interpretation in this study. Many well preserved foraminifera and other fossils were noted when describing thin sections for this study. However, specific species and zones were not identified as part of this work.

To test the limitations of intrabasinal carbon isotope stratigraphy, a high-resolution profile could be created for a section at Morrison Lake, located in the Beaverhead Mountains. This section ranges in age from the late Atokan to Middle Virgilian (Verville et al., 1990). This would test if two sections within the same basin can be correlated at a higher resolution.

6. CONCLUSIONS

Comparison of Arrow Canyon and the Snaky Canyon Formation stable isotope values indicate that high-resolution carbon isotope stratigraphy has its limitations. With the exception of globally recognized events, carbon isotopes curves can only provide higher resolution correlation in a tightly constrained biostratigraphic framework. Also rock type, material sampled, and regional geology need to be used to determine if the isotopic signals are controlled by local processes. Evidence of a local and/or diagenetic overprint might include increased variability of both oxygen and carbon as well as a correlation with facies. Alternatively, carbon isotope profiles from similar depositional settings that border the same water body may experience hundreds of meters of tight correlation (being within 1‰, with synchronous trends).

Carbon isotope stratigraphy thus becomes a supportive tool to previous stratigraphic correlations. The tight correlation between the bottom 270 meters of the Gallagher Peak, ID section and the Arrow Canyon, NV section illustrate the ability to correlate at a sub-Ma time scale if local conditions are not disrupting the regional signal. However, $\delta^{13}C$ profiles can still provide unique information by the presence or lack of a well-established global excursion. For example, the lack of the sharp mid-Carboniferous increase at the base of the Gallagher Peak section refutes previous suggestions that the section might include the mid-Carboniferous boundary.

The increased variability of the upper half of the Gallagher Peak section illustrates how local and diagenetic signals can easily mask regional signals. When local signals become the driving factor, the carbon isotope profile can then be used to make

inferences about the local environment. The increased variability along with other evidence was used to infer that the Pennsylvanian carbonate ramp in Idaho was becoming increasingly restricted through the Desmoinesian and Missourian.

The positive $\delta^{13}C$ excursions related to phylloid algal mounds can likely be related to original aragonite composition of Phylloid algae and encrusting cements along with better preservation of a more marine signal. This indicates that positive excursions related to phylloid algal mounds represent local environment composition rather than regional $\delta^{13}C$ trends and thus cannot be correlated across long distances. However, even though the high amplitude of these $\delta^{13}C$ excursions may not correlated to other sections, these particular algal mounds likely represent sea level highs and can be correlated with other indicators of sea level highstands. This also indicates how calcite/aragonite ratios that change with facies can affect the isotopic profile. If aragonite/calcite ratios can affect the $\delta^{13}C$ profile of whole rock 300 Ma ago, then mixing of low-Mg and high-Mg calcite could also affect the signal as well (up to 0.8‰). Whether the ratios of aragonite to calcite within micritic limestones are controlled by global processes is still under investigation (Swart, 2008). Thus, reporting the rock type and what material is sampled is increasingly important in making correlations of whole rock data.

In summary, carbon isotope profiles of fine grained carbonate have the strength to provide additional insights regarding points of correlation and regarding local environment. However, even though carbon isotope data is quantitative, correlating two locations tends to be more qualitative. Detailed sequence stratigraphy, biostratigraphy, rock type, and composition analyses are necessary to make accurate interpretations.

REFERENCES

Adlis, D.S., Grossman, E.L., Yancey, T.E., McLerran, R.D., 1988. Isotope stratigraphy and paleodepth changes of Pennsylvanian cyclical sedimentary deposits. Palaios 3, 487-506.

Al-Aasm, L.S., Veizer, J., 1982. Chemical stabilization of low-Mg calcite: an example of brachiopods. Journal of Sedimentary Petrology 52, 1101-1109.

Algeo, T.J., Heckel, P.H., 2008a. The Late Pennsylvanian Midcontinent Sea of North America: a review. Palaeogeography, Palaeoclimatology, Palaeoecology 268, 205-221.

Algeo, T.J, Heckel, P.H., Maynard, J.B., Blakely, R., Rowe, H., 2008b. Modern and ancient epieric seas and the super estuarine circulation mode of marine anoxia. Geological Association of Canada Special Publication 48. In: Holmden, C., Pratt., B.R. (Eds.), Dynamic Epeiric Seas: Sedimentological, Paleontological and Geochemical Perspectives, pp. 7-38.

Allan, J.R., Matthews, R.K., 1977. Carbon and oxygen isotopes as diagenetic and stratigraphic tools: surface and subsurface data, Barbados, West Indies. Geology 5, 16-20.

Allan, J.R., Matthews, R.K., 1982, Isotope signatures associated with early meteoric diagenesis. Sedimentology 29, 797-817.

Archuleta, B.J., Pope, M.C., Isaacson, P.E., Tremblay, M.L., Webster, G.D., 2006. Pennsylvanian cycles in East-Central Idaho: a record of sea-level fluctuations on the western margin of Laurentia. The Mountain Geologist 43, 93-114.

Baars, D. L., 1962. Permian system of the Colorado Plateau. American Association of Petroleum Geologists Bulletin 46, 146-218.

Batt, L.S., Montanez, J.P., Isaacson, P., Pope, M.C., Butts, S.H., Aplanalp, J., 2007. Multi-carbonate component reconstruction of mid-Carboniferous (Chesterian) seawater $\delta^{13}C$. Palaeogeography, Palaeoclimatolgoy, Palaeoecology 256, 298-318.

Batt, L.S. Pope, M.C., Isaacson, P.E., Montanez, I., Aplanalp, J., 2008. Upper Mississippian Antler foreland basin carbonate and siliciclastic rocks, East-Central Idaho and Southwestern Montana, U.S.A. In: Lukasik, J., Simo, J.A. (Eds.), Controls on carbonate platform and reef development. Society for Sedimentary Geology Special Publication 89, 147-170.

Beauchamp, B., Oldershaw, A.E., Krouse, H.R., 1987. Upper Carboniferous to Upper Permian ^{13}C-enriched primary carbonates in the Sverdrup Basin, Canadian Arctic: comparisons to coeval western North American ocean margins. Chemical Geology 65, 391-413.

Berner, R.A., Kothavala, Z., 2001. GEOCARB III: a revised model of atmospheric CO^2 over Phanerozoic time. American Journal of Science 301, 182-204.

Blakey, R.C., 2005. Paleogeography and tectonic evolution of late Paleozoic sedimentary basins, southwestern North America. Geological Society of America Abstracts with Program 37, 442 pp.

Blakey, R.C., Peterson, F., Kocurek, G., 1988. Synthesis of late Paleozoic and Mesozoic eolian deposits of the western interior of the United States. Sedimentary Geology 56, 3-125.

Böhm, F., Joachimski, M.M., Dullo, W-C., Eisenhauer, A., Lehnert, H., Reitner, J., Wörheide, 2000. Oxygen isotope fractionation in marine aragonite of coralline sponges. Geochimica et Cosmochimica Acta 64, 1695-1703.

Boardman, R.S., Cheetham, A.H., Rowell, A.J., 1987. Fossil Invertebrates. Blackwell Science, Cambridge, Massachusetts, 728 pp.

Bralower, T.J., 2002. Evidence of surface water oligotrophy during the Paleocene-Eocene thermal maximum: nannofossil assemblage data from Ocean Drilling Program Site 690, Maud Rise, Weddell Sea. Paleoceanography 17, 1023.

Brand, U., Brenckle, P., 2001. Chemostratigraphy of the Mid-Carboniferous boundary global stratotype section and point (GSSP), Bird Spring Formation, Arrow Canyon, Nevada, U.S.A. Palaeogeography, Palaeoclimatology, Palaeoecology 165, 321-347.

Brand, U., Bruckschen, P., 2002. Correlation of the Askyn River section, Southern Urals, Russia, with the Mid-Carboniferous Boundary GSSP, Bird Spring Formation, Arrow Canyon, Nevada, USA: implications for global paleoceanography. Palaeogeography, Palaeoclimatology, Palaeoecology 184, 177-193.

Brand, U., Logan, A., Hiller, N., Richardson, J., 2003. Geochemistry of modern brachiopods: application and implications for oceanography and paleoceanography. Chemical Geology 198, 305-334.

Breuninger, R.H., 1976. Palaeoaplysina (Hydrozoan?) carbonate buildups from Upper Paleozoic of Idaho. The American Association of Petroleum Geologists Bulletin 60, 584-607.

Breuninger, R.H., Canter, K.L., Isaacson, P.E., 1988. Pennsylvanian-Permian Palaeoaplysina and algal buildups, Snaky Canyon Formation, south-central Idaho, U.S.A. In: Geldsetzer, H.H.J., James, N.P., Tebbut, G.E. (Eds.), Reefs—Canada and adjacent areas. Canadian Society of Petroleum Geologists Memoir 13, pp. 631-637.

Butts, S.H., 2005. Latest Chesterian (Carboniferous) initiation of Gondwanan glaciation recorded in facies stacking patterns and brachiopod paleocommunities of the Antler foreland basin, Idaho. Palaeogeography, Palaeoclimatology, Palaeoecology 223, 275-289.

Came, R.E., Eiler, J.M., Veizer, J., Azmy, K., Brand, U., Weidman, C.R., 2007. Coupling of surface temperature and atmospheric CO2 concentrations during Paleozoic era. Nature 449, 198-202.

Canter, K.L., Isaacson, P.E., 1991. Depositional history and paleogeographic setting of the Juniper Gulch Member of the Middle Pennsylvanian-Lower Permian Snaky Canyon Formation of central Idaho. In: Cooper, J.D., Stevens, C.H. (Eds.), Paleozoic Paleogeography of the Western United States-II; Pacific Section.

Society of Economic Paleontologists and Mineralogists Publication 67, pp. 543-550.

Cassity, P.E., Langenheim, R.L., 1966. Pennsylvanian and Permian fusulinids of the Bird Spring Group from Arrow Canyon, Clark County, Nevada. Journal of Paleontology 40, 931-968.

Cecil, C.B., 1990. Paleoclimate controls on stratigraphic repetition of chemical and siliciclastic rocks. Geology 18, 533-536.

Cecil, B.C., Dulong, F.T., West, R.R., Stamm, R., Wardlaw, B., Edgar, N.T., 2003. Climate controls on the stratigraphy of a Middle Pennsylvanian cyclothem in North America. In Cecil, C.B., Edgar, N.T. (Eds.), Climate controls on stratigraphy. Society for Sedimentary Geology Special Publication 77, 151-182.

Compston, W., 1960. The carbon isotopic composition of certain marine invertebrates and coals from the Australian Permian. Geochimica et Cosmochima Acta 18, 1-22.

Crowley, T.J., Baum, S.K., 1991. Estimating Carboniferous sea-level fluctuations from Gondwanan ice extent. Geology 19, 975-977.

Dickson, J.A.D, Coleman, M.L., 1980. Changes in carbon and oxygen isotope compositions during limestone diagenesis. Sedimentology 27, 107-118.

Dilliard, K.A., Pope, M.C., Coniglio, M., Hosiotis, S.T. Lieberman, B.S., 2007. Stable isotope geochemistry of the lower Cambrian Sekwi Formation, Northwest Territories, Canada: Implications for ocean chemistry and seawater curve generation. Palaeogeography, Palaeoclimatology, Palaeoecology 256, 174-194.

Dunham, R.J., 1962. Classification of carbonate rocks according to depositional texture, in Ham, W.E. (Ed.), Classification of carbonate rocks. American Association of Petroleum Geologists Memoir 1, 108-121.

Emiliani, C., 1966. Paleotemperature analysis of Caribbean cores P6304-8 and P6304-9 and a generalized temperature curve for the past 425,000 years. Journal of Geology 74, 109-126.

Epstein, S., Buchsbaum, R., Lowenstam, H.A., Urey, H.C., 1953. Revised carbonate-water isotopic temperature scale. Geological Society of America Bulletin 64, 1315-1326.

Fischer, A.G., Arthur, M.A., 1977. Secular variation in the pelagic realm, in Cook, H.E., Enos, P. (Eds.), Deep marine carbonate environments. Society of Economic Paleontologists and Mineralogists Special Publication No. 25, 19-50.

Flake, R.C., 2011. Circulation of North American epicontinental seas during the carboniferous using stable isotope and trace element analysis of brachiopod shells. Master's Thesis, Texas A&M University, College Station, 74 pp.

Goldhammer, R.K., Oswald, E.J., Dunn, P.A., 1991. Hierachy of stratigraphic forcing: example from Middle Pennsylvanian shelf carbonates of the Paradox basin. Kansas Geological Survey Bulletin 233, 361-413.

Gradstein, F.M., Ogg, J.G., Smith, A.G., Agterberg, F.P., Bleeker, W., Cooper, R.A., Davydov, V., Gibbard, P., Hinnov, L.A., House, M.R., Lourens, L., Luterbacher, H.P., McArthur, J., Melchin, M.J., Robb, L.J., Shergold, J., Villeneuve, M., Wardlaw, B.R., Ali, J., Brinkhuis, H., Hilgen, F.J., Hooker, J., Howarth, R.J.,

Knoll, A.H., Laskar, J., Monechi, S., Plumb, K.A., Powell, J., Raffi, I., Röhl, U., Sadler, P., Sanfilippo, A., Schmitz, B., Shackleton, N.J., Shields, G.A., Strauss, H.,Van Dam, J., van Kolfschoten, T.,Veizer, J.,Wilson, D., 2004. A Geologic Time Scale 2004. Cambridge University Press, 589 pp.

Grossman, E.L., 1993. Stable isotopes in Late Pennsylvanian brachiopods from the United States: implications for Carboniferous paleoceanography. Geological Society of America Bulletin 105, 1284-1296.

Grossman, E. L., 1994. The carbon and oxygen isotope record during the evolution of Pangea: Carboniferous to Triassic. In: Klein, G. D. (Ed.), Pangea: paleoclimate, tectonics, and sedimentation during accretion, zenith, and breakup of a supercontinent. Geological Society of America Special Paper 288, 207-228.

Grossman, E.L., Ku, T.L., 1986. Oxygen and carbon isotope fractionation in biogenic aragonite: temperature effects. Chemical Geology 59, 59-74.

Grossman, E.L., Yancey, T.E., Jones, T.E., Bruckschen, P., Chuvashov, B., Mazzullo, S.J., Mii, H.S., 2008. Glaciation, aridification, carbon sequestration in Permo-Carboniferous: the isotopic record from low latitudes. Palaeogeography, Palaeoclimatology, Palaeoecology 268, 222-233.

Grossman, E.L., Zhang, C., Yancey, T.E., 1991. Stable-isotope stratigraphy of brachiopods from Pennsylvanian shales in Texas. Geological Society of America Bulletin 103, 953-965.

Groves, 1986. Foraminiferal characterization of the Morrowan-Atokan (lower Middle Pennsylvanian) boundary. Geological Society of America bulletin 97, 346-353.

Guillemette, R.N., 2008. Electron Microprobe Techniques, in: Drees, L.R., Ulery, A.L. (Eds.), Methods of Soil Analysis - Part 5: Mineralogical Methods. American Society of Agronomy, pp. 335-365.

Heath, C.P., Lumsden, D.N., Carozzi, A.V., 1967. Petrography of a carbonate transgressive-regressive sequence: The Bird Spring Group (Pennsylvanian), Arrow Canyon Range, Clark County, Nevada. Journal of Sedimentary Petrology 37, 377-400.

Heckel, P.H., 1977. Origin of phosphatic black shale facies in Pennsylvanian cyclothems of mid-continent North America. Bulletin of the American Association of Petroleum Geologists 61, 1045-1068.

Heckel, P.H., 1994. Evaluation of evidence for glacio-eustatic control over marine Pennsylvanian cyclothems in North America and consideration of possible tectonic effects. In: Dennison, J.M., Ettensohn, F.R. (Eds.), Tectonic and eustatic controls on sedimentary cycles. Society for Sedimentary Geology Concepts in Sedimentology and Paleontology 4, 65-87.

Holmden, C., Creaser, R.A., Muchlenbachs, K., Leslie, S.A., Bergstrom, S.M., 1998. Isotopic evidence for geochemical decoupling between ancient epeiric seas and bordering oceans. Geology 26, 567-570.

Hudson, J.D., 1977. Stable isotopes and limestone lithification. Geological Society of London 133, 637-660.

Hughes-Clarke, M.W., Keij, A.J., 1973. Organisms as Producers of Carbonate Sediments and Indicators of Environment in the Southern Persian Gulf. In: Purser, B.H. (Ed.), The Persian Gulf, pp. 33–56.

Immenhauser, A., Kenter, J.A.M., Ganssen, G., Bahamonde, J.R., Vliet, A.V., Saher, M.H., 2002. Origin and significance of isotope shifts in Pennsylvanian carbonates (Asturias, NW Spain). Journal of Sedimentary Research 72, 82-94.

Isaacson, P.E., McFaddan, M.D., Measures, E.A., Dorobek, S.L., 1988. Coralstromatoporoid carbonate buildup succession, Jefferson Formation (Late Devonian), central Idaho: U.S.A. In: Geldsetzer, H.H.J, James, N.P., Tebbutt, G.E. (Eds.), Reefs—Canada and adjacent areas. Canadian Society of Petroleum Geologists Memoir 13, 471-477.

Isbell, J.L., Miller, M.F., Wolfe, K.L., Lenarker, P.A., 2003. Timing of late Paleozoic glaciations in Gondwana: was glaciation responsible for the development of Northern Hemisphere cyclothems?. Geological Society of America Special Paper 370, 5-24.

Jimenez-Lopez, C., Romanek, C.S., Caballero, E., 2006. Carbon isotope fractionation in synthetic magnesian calcite. Geochimica et Cosmochimica Acta 70, 1163-1171.

Joachimski, M.M., Von Bitter, P.H., Buggisch, W., 2006. Constraints on Pennsylvanian glacioeustatic sea-level changes using oxygen isotopes of conodont apatite. Geology 34, 277-280.

Jones, T.E., Grossman, E.L., Yancey, T.E., 2003. Exploring the stable isotope record of global change and paleoclimate. Geological Society of America Abstracts with Programs 35, 254 pp.

Katz, Buonicoti, Montanez, Swart, Eberli, Smith, 2007. Timing and local perturbations of lower Mississippian $\delta^{13}C$ excursions in the Madison limestone. Paleogeography, Palaeclimotology, Palaeoecology 256, 231-253.

Kievman, C.M., 1998. Match between late Pleistocene Great Bahama Bank and deep-sea oxygen isotope records of sea level. Geology 26, 635-638.

Klein, G. D., 1994. Depth determination and quantitative distinction of the influence of tectonic subsidence and climate on changing sea level during deposition of midcontinent Pennsylvanian cyclothems. SEPM Concepts in Sedimentology and Paleontology 4, 35-50.

Korte, C., Jasper, T., Kozur, H.W., Veizer, J., 2005. $\delta^{18}O$ and $\delta^{13}C$ of Permian brachiopods: A record of seawater evolution and continental glaciation. Palaeogeography, Palaeoclimatology, Palaeoecology 224, 333-351.

Kump, L.R., Arthur, M.A., 1999. Interpreting carbon-isotope excursions: carbonates and organic matter. Chemical Geology 161, 181-198.

Lane, H.R., Brenckle, P.L., Baesemann, J.F., Richards, B.F., 1999. The IUGS boundary in the middle of the Carboniferous: Arrow Canyon, Nevada USA. Episodes 22, 272–283.

Langenheim, V.A.M., Langenheim, R.L., Jr., 1965. The Bird Spring Group, Chesterian through Wolfcampian at Arrow Canyon Arrow Canyon Range, Clark County, Nevada. Transactions of the Illinois Academy of Science 58: 225-240.

Lloyd, R.M., 1964. Variations in the oxygen and carbon isotope ratios of Florida Bay mollusks and their environmental significance. The Journal of Geology 72, 84-111.

Lowenstam, H.A., 1961. Mineralogy, $^{18}O/^{16}O$ ratios, and strontium and magnesium contents of recent and fossil brachiopods and their bearing on the history of the oceans. Journal of Geology 69, 241–260.

Mack, G. H., Suttner, L. J., Jennings, J. R., 1979. Permo-Pennsylvanian climatic trends on the Ancestral Rocky Mountains. Four Corners Geological Society 9th Field Conference Guidebook, 7–12.

Magaritz, M., Holser, W.T., 1990. Carbon isotopic shifts in Pennsylvanian seas. American Journal of Service 280, 977-994.

Marshall, J.D., 1992. Climate and oceanographic isotope signals from the carbonate rock record and their preservation. Geological Magazine 129, 143-160.

Menning, M., Alekseev, A.S., Chuvashov, B.I., Davydov, V.I., Devuyst, F.-X., Forke, H.C., Grunt, T.A., Hance, L., Heckel, P.H., Izokh, N.G., Jin k, Y.-G, Jones, P.J., Kotlyar, G.V., Kozur, H.W., Nemyrovska, T.I., and Schneider, J.W. Wang, X.-D., Weddige, K., Weyer, D., Work, D.M., 2006. Global time scale and regional stratigraphic reference scales of Central and West Europe, East Europe, Tethys, South China, and North America as used in the Devonian-Carboniferous-

Permian Correlation Chart 2003 (DCP 2003). Palaeogeography, Paleoclimatology, Palaeoecology 240, 318-372.

Mii, H.S., Grossman, E.L., Yancey, T.E., 1999. Carboniferous isotope stratigraphies of North America: Implications for Carboniferous paleoceanography and Mississippian glaciations. Geological Society of America Bulletin 111, 960-973.

Mii, H.S., Grossman, E.L., Yancey, T.E., Chuvashov, B., Egorov, A., 2001. Isotope records of brachiopod shells from the Russian Palatform: evidence for the onset of mid-Carboniferous glaciations. Chemical Geology 175, 133-147.

Miller, K.G., Fairbanks, R.G., Mountain, G.S., 1987. Tertiary oxygen isotope synthesis, sea level history, and continental margin erosion. Paleoceanography 2, 1-19.

Panchuk, K.M., Holmden, C., Kump, L.R., 2005. Sensitivity of the epeiric sea carbon isotope record to local-scale carbon cycle processes. Palaeogeography, Paleoclimatology, Palaeoecology 228, 320-337.

Panchuk, K.M., Holmden, C., Leslie, S.A., 2006. Local controls on carbon cycling in the Ordovician midcontinent region of North America, with implications for carbon isotope secular curves. Journal of Sedimentary Research 76, 200-211.

Patterson, W.P., and Walter, L.M., 1994. Depletion of ^{13}C in seawater ΣCO2 on modern carbonate platforms: significance for the carbon isotopic record of carbonates. Geology 22, 885-888.

Pope, M.C., Aplanalp, J., Isaacson, P.E., 2007. Eustatic variations within a Mississippian-Pennsylvanian subtidal mixed carbonate-siliciclastic succession,

Beaverhead Mountains, Idaho-Montana. Geological Society of America Abstracts with Programs 39, 86 pp.

Popp, B. N., Anderson, T. F., Sandberg, P. A., 1986. Brachiopods as indicators of original isotopic compositions in some Paleozoic limestones: Geological Society of America Bulletin 97, 1262-1269.

Rankey, E.C., 1997. Relations between relative changes in sea level and climate shifts:Pennsylvanian–Permian mixed carbonate-siliciclastic strata,western United States. Geological Society of America Bulletin 109, 1089-1100.

Raymond, A., Metz, C., 2004. Ice and its consequences: glaciation in the Late Ordovician, Late Devonian, Pennsylvanian–Permian, and Cenozoic compared. The Journal of Geology 112, 655–670.

Richardson, J.R., 1997. Ecology of articulated brachiopods. In: Kaesler, R. (Ed.), Treatise on Invertebrate Paleontology, pt. H. Brachiopoda (revised). Boulder, Colorado and Lawrence, Kansas, Geological Society of America and University of Kansas, pp. 441–462.

Romaneck, C.S., Grossman, E.L., Morse, J.W., 1992. Carbon isotopic fractionation in synthetic aragonite and calcite: effects of temperature and precipitation rate. Geochimica et Cosmochimica Acta 56, 419-430.

Saltzman, M.R., 2003. Late Paleozoic ice age: ocean gateway or pCO_2. Geology 31, 151-154.

Saltzman, M.R., 2005. Phosphorus, nitrogen, and the redox evolution of the Paleozoic oceans. Geology 33, 573-576.

Saltzman, M.R., Brasier, M.D., Ripperdan, R.L., Ergaliev, G.K., Lohmann, K.C., Robison, R.A., Chang, W.T., Peng, S., Runnegar, B., 2000. A global carbon isotope excursion during the Late Cambrian: Relation to trilobite extinctions, organic-matter burial and sea level. Palaeogeography, Palaeoceanography, Palaeoclimatology 162, 211-223.

Saltzman, M.R., Cowan, C.A., Runkel, A.C., Runnegar, B., Stewart, M.C., Palmer, A.R., 2004. The Late Cambrian SPICE ($\delta^{13}C$) event and the Sauk II-Sauk III regression: new evidence from Laurentian basins in Utah, Iowa, and Newfoundland. Journal of Sedimentary Research 74, 366-377.

Sandberg, P. A., 1983. An oscillating trend in Phanerozoic nonskeletal carbonate mineralogy. Nature 305, 19–22.

Saperstone, H.I., Ethridge, F.G., 1984. Origin and paleotectonic setting of the Previous Pennsylvanian Quadrant Sandstone, southwestern Montana. In: Goolsby, J., Morton, D. (Eds.), The Permian and Pennsylvanian Geology of Wyoming. Wyoming Geological Association 35th Annual Field Conference Guidebook, pp. 309-331.

Schlanger, S.O., Jenkyns, H.C., 1976. Cretaceous anoxic events: causes and consequences. Geologie en Mjinbouw 55, 179-184.

Scholle, P.A., Arthur, M.A., 1980. Carbon isotope fluctuations in Cretacous pelagic limestones: potential stratigraphic and petroleum tool. American Association of Petroleum Geologists Bulletin 64, 67-87.

Scholle, P.A., Ulmer-Scholle, D.S, 2003. A color guide to the petrography of carbonate rocks: Grains, textures, porosity, diagenesis. American Association of Petroleum Geologists Memoir 77, 474 pp.

Shackleton, 1967. Oxygen isotope analyses and Pleistocene temperatures re-assessed. Nature 215, 15-17.

Shackleton, 1977. Oxygen isotope stratigraphic record of the Late Pleistocene. Royal Society of London Philosophical Transactions ser. B, 280, 169-182.

Shackleton, 1987. Oxygen isotope, ice volume and sea level. Quarternary Science Reviews 6, 183-190.

Shackleton, N.J., Hall, M.A., 1984. Oxygen and carbon isotope stratigraphy of Deep Sea Drilling Project Hole 552A: Plio-Pleistocene glacial history. In: Roberts., D.G., Schnitker, D., U.S. Government Printing Office, Washington, Initial Reports of the Deep Sea Drilling Project 81, pp. 599-609.

Skipp, B., Hoggan, R.D., Schleicher, D.L., Douglas, R.C., 1979. Upper Paleozoic bank in east central Idaho-Snaky Canyon: Snaky Canyon, Bluebird Mountain, and Arco Hills Formations, and their paleotectonic significance. United States Geological Survey Bulletin 1486, 1-78.

Soreghan, G.S., 1994. Stratigraphic responses to geologic processes: late Pennsylvanian eustasy and tectonics in the Pedregosa and Orogrande basins, Ancestral Rocky Mountains. Geological Society of America Bulletin 106, 1195–1211.

Soreghan, G.S., Giles, K.A., 1999. Amplitudes of Late Pennsylvanian glacioeustasy. Geology 27, 255-258.

Stoll, H.M., Schrag, D.P., 2000. High-resolution stable isotope records from the Upper Creataceous rocks of Italy and Spain: glacial episodes in a greenhouse planet? Geological Society of America Bulletin 112, 308-319.

Swart, P.K., 2008. Global synchronous changes in the carbon isotopic composition of carbonate sediments unrelated to changes in the global carbon cycle. Proceedings of the National Academy of Sciences 105, 13741-13745.

Swart, P.K., Eberli, G., 2005. The nature of the $\delta^{13}C$ of periplatform sediments: implications for stratigraphy and the global carbon cycle. Sedimentary Geology 175, 115-129.

Tabor, N.J., Montañez, I.P., 2002. Shifts in late Paleozoic atmospheric circulation over western equatorial Pangaea: insights from pedogenic mineral $\delta^{18}O$ Compositions. Geology 30, 1127–1130.

Tremblay, M.L., 1996. Depositional controls on the Pennsylvanian-Permian Snaky Canyon carbonate platform, East-Central Idaho. Unpublished Master's Thesis, University of Idaho, Moscow, 48 pp.

Veevers, J.J., Powell, C.McA, 1987. Late Paleozoic glacial episodes in Gondwana reflected in transgressive regressive-depositional sequences in Euramerica. Geological Society of America Bulletin 98, 475-487.

Verville, G.J., Sanderson, G.A., Baesemann, J.F., Hampton, G.L., 1990. Pennsylvanian fusulinids from the Beaverhead Mountains, Morrison Lake area, Beaverhead County, Montana. The Mountain Geologist 27, 47-55.

West, I.M., 1975. Evaporites and associated sediments of the basal Purbeck Formation (Upper Jurassic) of Dorset. Proceedings of the Geologists' Association 86, 205-225.

Wood, S.G., 2011. Carbon isotope stratigraphy and diagenesis of Pennsylvanian (Desmoinesian-Missourian) carbonates in East-Central Idaho. Undergraduate Senior Scholars Thesis, Texas A&M University, College Station, 43 pp.

Wright, V.P., Vanstone, S.D., 2001. Onset of Late Palaeozoic glacio-eustasy and the evolving climates of low latitude areas: a synthesis of current understanding. Journal of the Geological Society 158, 579-582.

Zachos, J.C., Arthur, M.A., Dean, W.E., 1989. Geochemical evidence for suppression of pelagic marine productivity at the Cretaceous/Tertiary boundary. Nature 337,61-64.

Zachos, J.C., Pagani, M., Sloan, L., Thomas, E., Billups, K., 2001. Trends, rhythms, and aberrations in global climate 65 Ma to present. Science 292, 686-693.

Zachos, J.C., Dickens, G.R., Zeebe, R.E., 2008. An early Cenozoic perspective on greenhouse warming and carbon-cycle dynamics. Nature 45, 279-283.

APPENDIX A

SAMPLE DESCRIPTIONS, LOCATIONS, AGES, NOTES, AND RESULTS. BSE = BACKSCATTER ELECTRON, CL = CATHODOLUMINESCENT

Sample (Meter + Letter)		Hand Sample Number	North American Stage	Age GTS 2004	% Silt/Sand	Classification	Expanded Classification	Material Sampled in order of Abundance	Fossils and Clasts	Other Notes (Hand Sample, unless specified)	Color	Powder Weight (ug) for Analysis	$\delta^{13}C$ vs VPDB	$\delta^{18}O$ vs VPDB	$\delta^{13}C$ 1σ	$\delta^{18}O$ 1σ	Thin Section	BSE Image	CL Image
0	A	1 A	Morrowan	318.1	10	Packstone	Crinoidal Packstone	Skeletal, Other, Cement, Matrix	Crinoids, Dark grains	Hand sample is slightly crystalized	medium gray	66	1.61	-3.81	0.016	0.035	X		
0.8	A	2 A	Morrowan	318.08	10	Packstone	Skeletal Packstone	Matrix, Skeletal	Crinoids (5%), Unidentified skeletal grains	Clear cement filled voids in hand sample	light gray	98	1.57	-3.80	0.022	0.032	X		
0.8	B	2 A	Morrowan	318.08	0	Cement - Void		Cement		Cement from voids in hand sample	white		-20.35	-7.38			X		
1.5	A	3 A	Morrowan	318.07	0	Packstone	Skeletal Packstone	Calcite Spar	Recrystallized crinoids		gray	69	1.75	-3.33	0.018	0.032			
2.1	A	4 A	Morrowan	318.05	0	Packstone		Skeletal, Cement	Crinoids, Many recrystallized grains		medium gray	109	1.80	-3.59	0.013	0.022	X		
3	A	5 A	Morrowan	318.03	10	Packstone	Skeletal Packstone	Skeletal, Cement, Matrix			light gray						X		
3.5	A	6 A	Morrowan	318.02	10	Packstone	Skeletal Packstone	Skeletal, Cement, Matrix	Crinoids		light gray	111	1.32	-0.87	0.011	0.032	X		
4.7	A	7 A	Morrowan	317.99	10	Packstone		Matrix, Skeletal, Other	Dark grains (possibly quartz or phosphate)	Black grains in very fine carbonate matrix	light gray	74	1.19	-0.55	0.01	0.017			
5.6	A	8 A	Morrowan	317.97	10	Packstone	Skeletal Packstone	Skeletal, Cement	Brachiopods, Crinoids, Intraclasts		medium gray	73	0.91	1.19	0.019	0.027	X		
9	A	9 A	Morrowan	317.90	50	Packstone	Skeletal Packstone	Matrix, Chert	Brachiopods, Sponge spicules	Hand sample is 80% chert with zones of carbonate	light gray/dark gray chert	155	1.02	-2.88	0.012	0.025	X		X
10	A	10 A	Morrowan	317.87	10	Packstone		Matrix, Other	Dark grains (possibly quartz or phosphate)	Very fine grained, Sample was epoxied	light gray	75	1.58	-2.66	0.011	0.028			
11	A	11A	Morrowan	317.85	70	Siltstone													
12	A	12 A	Morrowan	317.83	10	Packstone		Matrix, Other	Dark grains (possibly quartz or phosphate)	Silt throughout sample, Stylolite across sample, Sample was epoxied	light gray	71	-2.18	-8.57	0.016	0.026			
12	B	12 A	Morrowan	317.83	0	Cement - Fracture		Cement		Cement taken from fracture	light gray	96	-13.44	-5.34	0.012	0.02			
13.3	A	1	Morrowan	317.80	5	Packstone	Pelletal-Skeletal Packstone	Skeletal, Matrix	Pellets, Spines, Crinoids, Brachiopods		medium gray	71	0.51	-5.99	0.021	0.02	X		
14.2	A	2	Morrowan	317.78	5	Packstone	Skeletal Packstone	Skeletal, Matrix	Brachiopods, Spines, Crinoids, Trilobite		dark gray	110	0.76	-4.62	0.015	0.032	X		
17.2	A	3	Morrowan	317.71	0	Calcisiltstone		Matrix		Thinly bedded with interbedded sand	dark gray	72	0.80	-4.28	0.02	0.024			
18.2	A	4	Morrowan	317.69	5	Wackestone		Matrix	Crinoids	Hand sample contains orange oxidized grains, Sample was epoxied	medium gray	70	0.96	-4.01	0.01	0.031			
19.4	A	5	Morrowan	317.66	5	Packstone		Matrix, Sand, Skeletal		Hand sample contains a few micro vugs, Very-fine grained sand (2-3%)	light gray		2.25	-3.85	0.008	0.016			
19.4	D	5	Morrowan	317.66	5	Packstone		Matrix, Sand,		Hand sample contains a	light gray	62	2.27	-3.79	0.007	0.017			

APPENDIX A - Continued

Sample (Meter + Letter)		Hand Sample Number	North American Stage	Age GTS 2004	% Silt/Sand	Classification	Expanded Classification	Material Sampled in order of Abundance	Fossils and Clasts	Other Notes (Hand Sample, unless specified)	Color	Powder Weight (ug) for Analysis	$\delta^{13}C$ vs VPDB	$\delta^{18}O$ vs VPDB	$\delta^{13}C$ 1σ	$\delta^{18}O$ 1σ	Thin Section	BSE Image	CL Image
								Skeletal		few micro vugs, Very-fine grained sand (2-3%)									
19.4	D	5	Morrowan	317.66	5	Packstone		Matrix, Sand, Skeletal		Hand sample contains a few micro vugs, Very-fine grained sand (2-3%)	light gray	78	2.24	-3.92	0.009	0.015			
20.2	A	6	Morrowan	317.64	0	Wackestone		Matrix, Skeletal	Crinoids, Brachiopods		dark gray	107	1.73	-4.79	0.017	0.035			
21.2	A	7	Morrowan	317.62	0	Wackestone		Matrix, Skeletal	Brachiopods, spines, crinoids	Burrows	dark gray						X		
22.2	A	8	Morrowan	317.59	0	Packstone		Matrix, Skeletal	Crinoids, Silicified burrows	Chert nodules in hand sample	dark gray	73	1.90	-3.39	0.046	0.038			
23.3	A	9	Morrowan	317.57	100	Wackestone	Dolowackestone	Chert	Brachiopods, Dolomite inclusions in vugs	Calcite filled vugs in hand sample	dark gray						X	X	X
24.2	A	10	Morrowan	317.55	50	Packstone		Matrix, Skeletal	Bryozoans	50% Silt	medium gray	120	1.51	-4.26	0.017	0.028			
25.2	A	11	Morrowan	317.53	40	Wackestone	Sandy Wackestone	Matrix, Sand		Oxidized material in fractures, 40% Silt	dark gray	126	1.60	-5.81	0.042	0.048			
26.8	A	12	Morrowan	317.49	30	Siltstone	Muddy Siltstone	Matrix, Silt			light gray	144	0.99	-2.03	0.013	0.025	X	X	X
27.8	A	13	Morrowan	317.47	30	Wackestone		Pellets	Pellets	30% Silt	light gray	102	1.86	-4.21	0.003	0.013			
28.8	A	14	Morrowan	317.44	5	Wackestone/ Packstone	Skeletal Wackestone	Matrix, Skeletal	Brachiopod, Crinoid, Spines		medium gray	77	-0.33	-8.23	0.011	0.018	X		
30	A	15	Morrowan	317.42	5	Calcisiltstone		Matrix, Skeletal		Evaporite nodules, 2-3% Silt	medium gray	70	1.16	0.08	0.032	0.025			
30	B	15	Morrowan	317.42	0	Cement - Evaporite		Cement		Evaporite nodules	light gray	73	-6.61	-5.17	0.01	0.023			
31.3	A	16	Morrowan	317.39	0	Crystalline		Calcite Spar		Large vugs (1-5 mm)	light gray	79	-4.57	-13.21	0.022	0.014			
32.3	A	17	Morrowan	317.37	15	Packstone		Skeletal, Matrix	Crinoid, Pellets, Brachiopods, Spines, Bryozoans, Gastropods, Intraclasts		medium gray	111	2.11	-5.07	0.022	0.039	X		
33.2	A	18	Morrowan	317.34	60	Siltstone		Silt, Matrix	Crinoids		light gray	194	2.91	-4.55	0.015	0.023	X		
34.2	A	19	Morrowan	317.32	15	Packstone	Skeletal Packstone	Coated grains, Skeletal, Matrix	Coated Grains, Crinoids, Brachiopods	Interbedded siltstone	dark gray	104	2.18	-4.91	0.024	0.032	X		
35.2	A	20	Morrowan	317.30	0	Packstone		Matrix, Cement, Skeletal	Crinoids (65%)		dark gray	106	2.44	-4.56	0.024	0.01			
36.2	A	21	Morrowan	317.28	10	Packstone		Skeletal, Matrix	Brachiopods, Crinoids, Bryozoans	Interbedded siltstone (1 mm beds)	medium gray						X		
37.2	A	22	Morrowan	317.25	30	Packstone		Skeletal, Cement	Crinoids (10%), Pellets (40%)	30% Silt, Skeletal grains have micritized rims	light gray								
38	A	23	Morrowan	317.24	10	Packstone	Skeletal Packstone	Skeletal, Matrix	Crinoid, Brachiopod, Bryozoans	Skeletal grains have micritized rims	medium gray	90	2.16	-4.39	0.008	0.028	X		
38.6	A	24	Morrowan	317.22	10	Packstone		Matrix	Brachiopods (20%), Crinoids (10%)	Pellets (40%), Silt (10%), Sample was epoxied	dark gray	77	2.05	-4.35	0.021	0.014			
40.2	A	25	Morrowan	317.19	10	Packstone	Skeletal Packstone	Matrix, Skeletal	Brachiopods, Crinoids, Bryozoans, Intraclasts		medium gray	75	-0.48	-6.64	0.008	0.029	X		
41	A	26	Morrowan	317.17	5	Packstone	Skeletal Packstone	Skeletal, Matrix	Crinoid, Brachiopod, Spines, Foraminifera		medium gray	93	1.25	-5.65	0.015	0.032	X		
42.5	A	27	Morrowan	317.13	60	Siltstone		Sand, Skeletal,	Brachiopods, Crinoids	60% Silt	medium	192	1.95	-5.12	0.019	0.012			

APPENDIX A - Continued

Sample (Meter + Letter)		Hand Sample Number	North American Stage	Age GTS 2004	% Silt/Sand	Classification	Expanded Classification	Material Sampled in order of Abundance	Fossils and Clasts	Other Notes (Hand Sample, unless specified)	Color	Powder Weight (ug) for Analysis	$\delta^{13}C$ vs VPDB	$\delta^{18}O$ vs VPDB	$\delta^{13}C$ 1σ	$\delta^{18}O$ 1σ	Thin Section	BSE Image	CL Image
44	A	28	Morrowan	317.10	5	Wackestone		Matrix	Crinoids, Brachiopods	Oxidized grains	gray	60	2.22	-4.14	0.024	0.025			
45	A	29	Morrowan	317.08	0	Packstone	Skeletal Packstone	Skeletal, Matrix	Crinoid, Ramose Bryozoans, Brachiopods, Intraclasts, Gastropods		medium gray	70	2.41	-3.97	0.011	0.03	X		
46	A	30	Morrowan	317.05	5	Wackestone		Matrix, Skeletal	Brachiopod, Crinoids, Spines	Sample was epoxied, Possible phosphate?	light gray	84	1.48	-4.86	0.017	0.03	X		
46.6	A	31	Morrowan	317.04	0	Mudstone		Matrix		Sample appears microcrystalline	light gray	77	2.47	-2.44	0.019	0.035			
47.6	A	32	Morrowan	317.02	10	Mudstone		Matrix, Sand		10% Silt	medium gray	75	2.52	-2.75	0.01	0.022			
48.6	A	33	Morrowan	316.99	55	Siltstone	Siltstone	Silt, Matrix	Crinoids, Brachiopods, Intraclasts		light gray	171	1.69	-6.42	0.013	0.053	X		
49.7	A	34	Morrowan	316.97	60	Siltstone	Siltstone	Skeletal, Matrix, Sand	Crinoids, Brachiopods	Thin interbedded packstone beds	light gray	146	1.45	-4.82	0.023	0.023	X		
50.7	A	35	Morrowan	316.95	15	Wackestone		Matrix, Sand	Crinoids	chert nodules (15% silt)	medium gray	98	2.34	-5.28	0.008	0.031			
51.7	A	36	Morrowan	316.92	5	Packstone	Skeletal Packstone	Skeletal, Matrix	Crinoids, Brachiopods, Ramose Bryozoans, Foraminifera		dark gray	66	2.38	-4.59	0.025	0.037	X		
52.7	A	37	Morrowan	316.90	0	Packstone	Skeletal Packstone	Skeletal, Matrix	Crinoids, Brachiopods, Ramose Bryozoans	Sample Contains Stylolites	dark gray	106	2.33	-4.10	0.016	0.021	X		
53.7	A	38	Morrowan	316.88	10	Wackestone		Matrix, Skeletal	Crinoids	Bedding visible, Contains stylolites	medium gray	142	2.76	-4.34	0.029	0.045			
54.7	A	39	Morrowan	316.86	30	Packstone	Silty Skeletal Packstone	Skeletal, Matrix, Silt	Brachiopods, Spines, Crinoids	Possible Phosphate	dark gray	111	2.79	-4.03	0.015	0.032	X		
56	A	40	Morrowan	316.83	0	Packstone	Skeletal Packstone	Skeletal, Matrix	Brachiopods, Fenestrate Bryozoans, Spines, Crinoids		dark gray	106	2.15	-4.23	0.011	0.033	X		
57.5	A	41	Morrowan	316.79	5	Wackestone		Matrix, Skeletal	Crinoids, Pellets		medium gray	76	2.63	-4.50	0.021	0.039			
57.5	B	41	Morrowan	316.79	0	Cement - Fracture		Cement		Blocky cement from fracture	clear	69	-1.57	-12.47	0.009	0.015			
58.5	A	42	Morrowan	316.77	0	Wackestone		Matrix, Skeletal	Crinoids, Brachiopods		medium gray	73	2.16	-4.24	0.021	0.03			
60	A	43	Morrowan	316.74	10	Packstone	Skeletal Packstone	Skeletal, Matrix	Brachiopod, Crinoids, Spines, Silicified Phylloid Algae.	Light gray chert nodules, Sampled next to chert, Contains spicules or algae	dark gray	76	0.77	-5.54	0.01	0.032	X		
62	A	44	Morrowan	316.69	40	Packstone	Silty Skeletal Packstone	Silt, Skeletal, Matrix	Brachiopod, Crinoids, Bryozoans, Coated grains		medium gray	176	2.32	-4.10	0.013	0.037	X		
64	A	45	Morrowan	316.64	90	Crystalline		Calcite Spar, Sand		90% Sand	light gray	314	1.71	-4.66	0.013	0.02			
64.5	A	46	Morrowan	316.63	90	Sandstone		Calcite Spar, Sand	Crinoids (15%)	90% Sand	light gray		2.15	-4.59	0.0195	0.038			
64.5	D	46	Morrowan	316.63	90	Sandstone		Calcite Spar,	Crinoids (15%)	90% Sand	light gray	467	2.21	-4.53	0.024	0.032			

APPENDIX A - Continued

Sample (Meter + Letter)		Hand Sample Number	North American Stage	Age GTS 2004	% Silt/Sand	Classification	Expanded Classification	Material Sampled in order of Abundance	Fossils and Clasts	Other Notes (Hand Sample, unless specified)	Color	Powder Weight (ug) for Analysis	$\delta^{13}C$ vs VPDB	$\delta^{18}O$ vs VPDB	$\delta^{13}C$ 1σ	$\delta^{18}O$ 1σ	Thin Section	BSE Image	CL Image
64.5	D	46	Morrowan	316.63	90	Sandstone		Sand Calcite Spar, Sand	Crinoids (15%)	90% Sand	light gray	491	2.08	-4.66	0.015	0.044			
65	A	47	Morrowan	316.62	10	Wackestone		Matrix, Sand, Skeletal		5% Sand	dark gray	76	2.80	-4.54	0.02	0.031			
66	A	48	Morrowan	316.60	80	Sandstone		Matrix, Sand, Skeletal		80% Sand, Sampled along fracture	dark gray	416	2.52	-4.53	0.019	0.041		X	
69	A	49	Morrowan	316.53	10	Wackestone		Matrix, Skeletal	Crinoids, Brachiopods, Very fine unidentified skeletal grains		medium gray	130	1.49	-6.26	0.02	0.03			
70	A	50	Morrowan	316.51	50	Mudstone		Matrix, Sand			light gray	135	-0.95	-9.75	0.015	0.006			
71	A	51	Morrowan	316.48	5	Wackestone	Skeletal Wackestone	Matrix, Skeletal	Brachiopod, Crinoid, Foraminifera		medium gray	80	2.71	-3.99	0.044	0.03	X		
72	A	52	Morrowan	316.46	20	Crystalline		Spar, Sand			light gray	111	-1.41	-13.48	0.016	0.04			
72	B	52	Morrowan	316.46	0	Cement - Void		Cement		Blocky cement	white	64	-4.57	-5.52	0.015	0.028			
73.5	A	53	Morrowan	316.43	5	Wackestone	Skeletal Wackestone	Matrix, Skeletal	Crinoids, Small brachiopod fragments	Chert nodules, Cement filled voids (1-5 mm wide)	light gray	95	2.14	-3.84	0.021	0.041	X		
74.5	A	54	Morrowan	316.41	5	Wackestone	Skeletal Wackestone	Matrix, Skeletal	Crinoids, Brachiopods, Spines, Horn corals	Wavy laminations, Stylolites	medium gray	74	-0.39	-8.26	0.032	0.017	X		X
75.5	A	55	Morrowan	316.38	10	Wackestone	Wackestone	Matrix, Silt, Chert	Crinoids	Hand sample contains a large fracture (2mm wide) filled with calcite	gray	61	1.58	-2.14	0.021	0.024	X		X
76.5	A	56	Morrowan	316.36	10	Wackestone		Matrix	Crinoids, Brachiopods		medium gray	76	2.62	-4.86	0.013	0.036			
77	A	57	Morrowan	316.35	0	Wackestone	Skeletal Wackestone	Matrix, Skeletal	Brachiopods, Spines, Foraminifera		gray	77	3.37	-4.85	0.018	0.023	X		
78	A	58	Morrowan	316.33	5	Packstone	Skeletal Packstone	Skeletal, Matrix	Brachiopods, Spines, Foraminifera, Bryozoans		dark gray	94	2.88	-6.20	0.017	0.016	X		
79	A	59	Morrowan	316.30	10	Wackestone		Matrix, Sand	Crinoids, Brachiopods		medium gray	64	3.67	-4.27	0.017	0.01			
80	A	60	Morrowan	316.28	90	Sandstone		Matrix, Sand		90% Sand	medium gray	355	2.43	-5.09	0.016	0.03			
81	A	61	Morrowan	316.26	90	Sandstone		Matrix, Sand		90% Sand	medium gray	486	2.56	-5.77	0.017	0.028			
82	A	62	Morrowan	316.23	70	Sandstone		Matrix, Sand		70% Sand	medium gray	284	1.27	-6.20	0.011	0.025			
82.5	A	63	Morrowan	316.22	10	Grainstone	Skeletal Grainstone	Skeletal, Matrix	Crinoid, Pellets, Spines, Brachiopod	Rust colored stylolites, Intraclasts	medium gray	63	3.20	-3.94	0.024	0.034	X		
83.5	A	64	Morrowan	316.20	10	Packstone		Matrix, Skeletal	Crinoids (10%), Brachiopods		medium gray	78	2.55	-4.44	0.038	0.054			
84.5	A	65	Morrowan	316.18	5	Wackestone	Skeletal Wackestone	Matrix, Skeletal	Spines, Brachiopod, Crinoid	Stylolites forming	light gray	101	1.69	-6.51	0.021	0.02	X		
85	A	66	Morrowan	316.17	10	Wackestone	Coral Crinoid Wackestone	Matrix, Skeletal	Crinoids, In-situ corals		gray		1.06	-6.02	0.0295	0.0265			
85	D	66	Morrowan	316.17	10	Wackestone	Coral Crinoid Wackestone	Matrix, Skeletal	Crinoids, In-situ corals		gray	78	1.02	-5.99	0.038	0.028	X		

APPENDIX A - Continued

Sample (Meter + Letter)		Hand Sample Number	North American Stage	Age GTS 2004	% Silt/Sand	Classification	Expanded Classification	Material Sampled in order of Abundance	Fossils and Clasts	Other Notes (Hand Sample, unless specified)	Color	Powder Weight (ug) for Analysis	$\delta^{13}C$ vs VPDB	$\delta^{18}O$ vs VPDB	$\delta^{13}C$ 1σ	$\delta^{18}O$ 1σ	Thin Section	BSE Image	CL Image
85	D	66	Morrowan	316.17	10	Wackestone	Coral Crinoid Wackestone	Matrix, Skeletal	Crinoids, In-situ corals		gray	109	1.11	-6.06	0.021	0.025			
85.5	A	67	Morrowan	316.15	15	Wackestone		Matrix, Sand, Skeletal	Crinoids (1%)	Chert nodules, Very fine grained	medium gray	152	2.87	-2.51	0.022	0.016			
86.5	A	68	Morrowan	316.13	10	Wackestone		Matrix, Sand		Contains evaporites (5% Silt)	light gray		2.39	-0.68	0.0215	0.022			
86.5	D	68	Morrowan	316.13	10	Wackestone		Matrix, Sand		Contains evaporites (5% Silt)	light gray	75	2.44	-0.62	0.025	0.02			
86.5	D	68	Morrowan	316.13	10	Wackestone		Matrix, Sand		Contains evaporites (5% Silt)	light gray	64	2.33	-0.75	0.018	0.024			
86.5	B	68	Morrowan	316.13	0	Cement - Evaporite		Cement		Contains evaporites (5% Silt)	light gray		0.56	-4.17	0.0205	0.034			
86.5	D	68	Morrowan	316.13	0	Cement - Evaporite		Cement		Contains evaporites (5% Silt)	light gray	135	0.50	-4.26	0.014	0.032			
86.5	D	68	Morrowan	316.13	0	Cement - Evaporite		Cement		Contains evaporites (5% Silt)	light gray	73	0.62	-4.09	0.027	0.036			
88	A	69	Morrowan	316.10	0	Wackestone	Cherty Wackestone	Matrix	Crinoids	Evaporites	light gray	92	3.21	-0.88	0.019	0.029	X		
89	A	70	Morrowan	316.08	20	Wackestone		Matrix, Sand, Skeletal		20% Sand	medium gray	191	2.99	-3.87	0.018	0.034			
90	A	71	Morrowan	316.05	0	Wackestone		Matrix	Brachiopods (10%), Crinoids (5%)		light gray	61	3.10	-3.95	0.015	0.013			
91	A	72	Morrowan	316.03	10	Packstone		Skeletal, Matrix, Sand	Crinoids, Brachiopods	Filled fractures (1 mm wide), 10% Silt	medium gray	80	2.74	-4.58	0.014	0.008			
92	A	73	Morrowan	316.01	20	Wackestone	Brachiopod Crinoid Wackestone	Matrix, Skeletal	Crinoids, Brachiopods		light gray	106	1.19	-6.56	0.017	0.022	X		X
93	A	74	Morrowan	315.98	0	Wackestone	Skeletal Wackestone	Matrix, Skeletal	Horn coral, Brachiopod, Crinoids	Sample was epoxied	gray	114	2.55	-3.62	0.017	0.027	X		
94	A	75	Morrowan	315.96	5	Wackestone		Matrix, Sand	Brachiopods, Crinoids	5% Silt	gray	65	1.68	-3.94	0.018	0.035			
94	B	75	Morrowan	315.96	0	Cement - Crinoid		Cement	Cement	Cement from large crinoid	white	68	3.32	-3.26	0.009	0.027			
95	A	76	Morrowan	315.94	20	Packstone	Skeletal Wackestone	Skeletal, Matrix	Brachiopod, Crinoid		medium gray	91	1.65	-4.67	0.016	0.027	X		
96.2	A	77	Morrowan	315.91	5	Packstone	Skeletal Wackestone	Skeletal, Matrix	Crinoid, Brachiopod, Bryozoans		medium gray	113	2.32	-3.03	0.041	0.035	X		
97.5	A	78	Morrowan	315.88	0	Wackestone	Skeletal Wackestone	Skeletal, Matrix	Crinoids, Foraminifera, Brachiopods, Spines		medium gray	111	2.07	-3.57	0.013	0.017	X		
98.5	A	79	Morrowan	315.86	0	Wackestone		Matrix	Brachiopods, Crinoids		gray	67	1.70	-3.83	0.013	0.016			
99.5	A	80	Morrowan	315.84	10	Wackestone	Brachiopod Crinoid Wackestone	Skeletal, Matrix	Brachiopod, Crinoid, Horn corals, Bryozoans	Chert nodules in hand sample	dark gray	93	1.00	-4.71	0.016	0.024	X		
100.5	A	81	Morrowan	315.81	70	Sandstone		Matrix, Sand	Crinoids (5%)	70% Sand	gray	388	2.16	-4.97	0.018	0.026			
101.5	A	82	Morrowan	315.79	5	Wackestone		Matrix, Skeletal, Sand	Crinoids, Brachiopods	5% Sand	light gray	123	2.47	-3.70	0.018	0.039			
102.7	A	83	Morrowan	315.76	30	Packstone	Silty Skeletal Packstone	Silt, Skeletal, Matrix	Crinoids, Brachiopods, Foraminifera, Bryozoans		dark gray	93	2.65	-3.58	0.007	0.021	X		
104	A	84	Morrowan	315.73	5	Wackestone		Matrix, Skeletal, Sand		5% Sand	medium gray	89	2.46	-3.53	0.005	0.032			
105	A	85	Morrowan	315.71	0	Wackestone	Skeletal Wackestone	Matrix, Skeletal	Crinoid, Brachiopod,		gray	89	2.24	-3.64	0.016	0.022	X		

APPENDIX A - Continued

Sample (Meter + Letter)		Hand Sample Number	North American Stage	Age GTS 2004	% Silt/Sand	Classification	Expanded Classification	Material Sampled in order of Abundance	Fossils and Clasts	Other Notes (Hand Sample, unless specified)	Color	Powder Weight (ug) for Analysis	$\delta^{13}C$ vs VPDB	$\delta^{18}O$ vs VPDB	$\delta^{13}C$ 1σ	$\delta^{18}O$ 1σ	Thin Section	BSE Image	CL Image
106	A	86	Morrowan	315.69	10	Wackestone		Matrix, Sand	Bryozoans, Horn corals Crinoids	Chert, Some oxidized grains	dark gray	68	2.17	-3.58	0.018	0.024			
107	A	87	Morrowan	315.67	10	Packstone	Crinoid Brachiopod Packstone	Skeletal, Matrix	Crinoids, Brachiopods, Spines, Foraminifera, Bryozoans	Stylolites forming	dark gray	65	2.25	-3.53	0.015	0.028	X		
108	A	88	Morrowan	315.64	20	Packstone	Skeletal Packstone	Skeletal, Matrix, Silt	Crinoid, Brachiopods		medium gray	125	2.85	-3.83	0.018	0.042	X		
109	A	89	Morrowan	315.62	5	Wackestone		Matrix, Sand	Crinoids	5% Sand	medium gray	126	3.00	-3.69	0.011	0.035			
110	A	90	Morrowan	315.60	40	Wackestone		Matrix, Sand	Brachiopods, Crinoids		medium gray	138	2.91	-4.49	0.021	0.029			
111	A	91	Morrowan	315.57	5	Packstone	Brachiopod Crinoid Bryozoan Packstone	Skeletal, Matrix	Crinoids, Brachiopods, Horn corals, Bryozoans		medium gray	109	1.96	-3.97	0.015	0.054	X		
112	A	92	Morrowan	315.55	0	Wackestone		Matrix	Bryozoans	Vugs	gray	97	1.69	-4.07	0.015	0.023			
113	A	93	Morrowan	315.53	20	Wackestone		Matrix, Sand	Bryozoans (10%), Crinoids (10%)	15% Sand	gray	79	2.51	-3.76	0.014	0.034			
114	A	94	Morrowan	315.51	5	Wackestone	Skeletal Wackestone	Matrix, Skeletal	Crinoid, Brachiopod, Horn coral		medium gray	92	2.24	-3.78	0.008	0.039	X		
114.5	A	95	Morrowan	315.50	5	Wackestone/Packstone	Skeletal Packstone	Skeletal, Matrix	Crinoid, Brachiopod		dark gray	77	1.78	-4.36	0.025	0.02	X		
115.5	A	96	Morrowan	315.47	5	Wackestone	Cherty Wackestone	Matrix, Skeletal	Brachiopod, Crinoid		medium gray	74	2.34	-4.05	0.015	0.029	X		
115.5	B	96	Morrowan	315.47	100	Chert		Chert		Light gray material is the chert	light gray	1216	1.97	-4.16	0.012	0.033	X		
118	A	97	Morrowan	315.42	5	Wackestone		Matrix, Sand	Crinoids	Highly fractured, 5% Silt, Sample was epoxied	medium gray	101	2.65	-3.90	0.014	0.028			
118.5	A	98	Morrowan	315.40	0	Wackestone	Skeletal Wackestone	Matrix, Skeletal	Brachiopods, Crinoids	Large fracture with clear fill in hand sample	light gray	94	1.21	-6.41	0.014	0.042	X		
120	A	99	Morrowan	315.37	5	Wackestone		Matrix, Sand	Crinoids	5% Sand, Microfractures	gray		2.39	-5.81					
120	D	99	Morrowan	315.37	5	Wackestone		Matrix, Sand	Crinoids	5% Sand, Microfractures	gray	80	2.32	-5.86	0.006	0.02			
120	D	99	Morrowan	315.37	5	Wackestone		Matrix, Sand	Crinoids	5% Sand, Microfractures	gray	71	2.45	-5.75	0.005	0.015			
121	A	100	Morrowan	315.35	5	Wackestone		Matrix, Sand	Crinoids (15%)	1% Sand	dark gray	79	2.41	-3.67	0.019	0.027			
122	A	101	Morrowan	315.32	100	Packstone	Skeletal Packstone	Chert	Brachiopods, Crinoids	Mottled/clotted texture, Hand sample was epoxied	dark gray						X		
123	A	102	Morrowan	315.30	5	Packstone		Skeletal, Matrix, Sand	Crinoids (<1 mm), Brachiopods	1% Sand	gray	66	2.69	-4.86	0.017	0.033			
124	A	103	Morrowan	315.28	5	Wackestone		Matrix, Sand	Crinoids (<1%)	3% Sand	dark gray	122	3.03	-3.86	0.016	0.016			
125	A	104	Morrowan	315.26	5	Packstone	Skeletal Packstone	Skeletal, Matrix	Brachiopod, Crinoids		dark gray	111	2.41	-3.71	0.023	0.037	X		
126	A	105	Morrowan	315.23	5	Wackestone	Skeletal Wackestone	Skeletal, Matrix	Crinoid, Brachiopods, Foraminifera	Light gray chert nodules	medium gray	96	2.49	-3.75	0.019	0.018	X		
126.5	A	106	Morrowan	315.22	40	Wackestone		Matrix, Sand	Brachiopod, Crinoids	40% Sand	medium gray	208	2.82	-4.24	0.022	0.049			
127	A	107	Morrowan	315.21	30	Wackestone		Matrix, Sand	Crinoids, Brachiopods	30% Sand	medium gray	151	2.54	-4.15	0.018	0.017			
128	A	108	Morrowan	315.19	5	Wackestone	Skeletal Wackestone	Skeletal, Matrix	Crinoids, Brachiopods, Foraminifera	Oxidized material between grains	dark gray	62	2.31	-4.32	0.015	0.034	X		

APPENDIX A - Continued

Sample (Meter + Letter)		Hand Sample Number	North American Stage	Age GTS 2004	% Silt/Sand	Classification	Expanded Classification	Material Sampled in order of Abundance	Fossils and Clasts	Other Notes (Hand Sample, unless specified)	Color	Powder Weight (ug) for Analysis	$\delta^{13}C$ vs VPDB	$\delta^{18}O$ vs VPDB	$\delta^{13}C$ 1σ	$\delta^{18}O$ 1σ	Thin Section	BSE Image	CL Image
129	A	109	Morrowan	315.17	5	Wackestone		Matrix, Sand	Crinoids (40%)	5% Sand	dark gray		2.06	-3.55	0.011	0.0255			
129	D	109	Morrowan	315.17	5	Wackestone		Matrix, Sand	Crinoids (40%)	5% Sand	dark gray	62	2.02	-3.60	0.015	0.042			
129	D	109	Morrowan	315.17	5	Wackestone		Matrix, Sand	Crinoids (40%)	5% Sand	dark gray	80	2.10	-3.51	0.007	0.009			
129	B	109	Morrowan	315.17	0	Cement - Crinoid		Crinoid			white	100	2.08	-4.86	0.007	0.03			
130	A	110	Morrowan	315.14	5	Wackestone	Skeletal Wackestone	Matrix, Skeletal	Brachiopods, Crinoids, Spines, Horn corals		dark gray	90	1.16	-4.72	0.016	0.014	X		
131	A	111	Morrowan	315.12	10	Wackestone		Matrix, Sand		5% Sand, Hand sample is mostly chert	medium gray/orange	144	0.87	-4.62	0.011	0.035			
132	A	112	Morrowan	315.10	5	Mudstone		Matrix, Sand		(5% Sand), Chert nodules	gray	99	1.92	-0.72	0.012	0.035			
133	A	113	Morrowan	315.07	5	Mudstone		Matrix, Sand		Contains chert nodules, 5% Sand	light gray	73	1.76	-0.35	0.022	0.049			
134.5	A	114	Morrowan	315.04	30	Packstone		Matrix, Sand, Skeletal, Other	Crinoids (30%), Brachiopods, Other = Oxidized stringers	30% Sand, Orange/white stringers between grains	medium gray	127	0.93	-4.54	0.015	0.022			
136	A	115	Morrowan	315.01	10	Packstone	Crinoid Packstone	Skeletal, Matrix	Brachiopods, Crinoids, Spines		medium gray	69	1.95	-4.00	0.018	0.033	X		
137	A	116	Morrowan	314.98	5	Packstone	Intraclasts Packstone	Matrix	Crinoids, Brachiopods, Bryozoans	Interbedded mudstone beds (Drilled mud for analysis)	medium gray	87	0.19	-7.40	0.013	0.026	X		
138	A	117	Morrowan	314.96	10	Wackestone	Skeletal Wackestone	Matrix, Skeletal	Crinoids, Brachiopods		light gray	64	1.27	-7.04	0.009	0.039	X		
139	A	118	Morrowan	314.94	5	Packstone	Skeletal Packstone	Skeletal, Matrix	Crinoids, Brachiopods, Horn corals, Spines		dark gray	107	1.87	-4.18	0.012	0.029	X		
141	A	119	Morrowan	314.89	0	Wackestone	Skeletal Wackestone	Matrix, Skeletal	Crinoids, Brachiopods, Corals, Trilobite fragments		gray	71	1.20	-8.12	0.022	0.049	X		X
142	A	120	Morrowan	314.87	5	Wackestone	Skeletal Wackestone	Matrix, Skeletal	Crinoids, Brachiopods, Coral fragments	Dark organic matter (dead oil?)	gray	94	-1.41	-8.23	0.014	0.039	X		
143	A	121	Morrowan	314.85	5	Wackestone		Matrix, Sand	Crinoids (<2 mm)	Fining upwards, 2% Very fine sand	dark gray	71	2.37	-4.51	0.018	0.038			
144	A	122	Morrowan	314.82	30	Packstone		Matrix, Sand, Skeletal	Crinoids, Pellets	30% Sand	gray	130	2.79	-4.77	0.012	0.021			
145	A	123	Morrowan	314.80	40	Packstone		Skeletal, Sand, Matrix	Crinoids, Brachiopods	40% Sand, Oxidized material around grains	gray	127	1.86	-5.94	0.023	0.023			
146	A	124	Morrowan	314.78	10	Grainstone	Pelletal Grainstone/ Packstone	Skeletal, Matrix	Crinoids, Brachiopods, Pellets, Coral fragments		dark gray	72	3.24	-4.10	0.015	0.03	X		
147	A	125	Morrowan	314.76	5	Grainstone	Skeletal Grainstone	Skeletal, Matrix	Crinoid, Brachiopods, Foraminifera		medium gray	64	2.68	-4.32	0.035	0.036	X		
148	A	126	Morrowan	314.73	5	Packstone	Skeletal Packstone	Skeletal, Matrix	Crinoids, Brachiopods, Bryozoans, Foraminifera		dark gray	61	2.87	-3.98	0.021	0.034	X		
150	A	127	Morrowan	314.69	10	Grainstone	Skeletal Grainstone	Skeletal, Matrix	Crinoids, Brachiopods, Horn corals		gray	61	2.35	-4.28	0.014	0.017	X		
152	A	128	Morrowan	314.64	10	Packstone	Skeletal Packstone	Skeletal, Matrix	Crinoids, Brachiopods, Horn corals, Bryozoans		gray	66	2.26	-4.27	0.019	0.023	X		
153	A	129	Morrowan	314.62	30	Wackestone		Matrix, Sand	Crinoids, Brachiopods	30% Sand	medium gray	139	2.82	-3.56	0.018	0.023			
154	A	130	Morrowan	314.60	45	Sandstone	Sandy Grainstone	Silt, Matrix, Skeletal	Crinoids, Brachiopods		light gray	160	1.70	-5.40	0.018	0.024	X		

APPENDIX A - Continued

Sample (Meter + Letter)		Hand Sample Number	North American Stage	Age GTS 2004	% Silt/Sand	Classification	Expanded Classification	Material Sampled in order of Abundance	Fossils and Clasts	Other Notes (Hand Sample, unless specified)	Color	Powder Weight (ug) for Analysis	$\delta^{13}C$ vs VPDB	$\delta^{18}O$ vs VPDB	$\delta^{13}C$ 1σ	$\delta^{18}O$ 1σ	Thin Section	BSE Image	CL Image
155	A	131	Morrowan	314.57	90	Sandstone		Sand, Matrix		90% Sand	light gray	340	2.43	-5.42	0.012	0.012			
156	A	1 E	Morrowan	314.55	5	Mudstone		Matrix, Sand	Single Ostracod	1-2% Sand	gray	119	3.80	-4.57	0.02	0.022			
157	A	2 E	Morrowan	314.53	5	Mudstone		Matrix, Sand		5% Sand, Highly fractured	medium gray	107	3.64	-4.16	0.025	0.02			
158	A	3 E	Morrowan	314.51	5	Wackestone		Matrix, Sand	Brachiopods, Crinoids	2-3% Sand	medium gray	118	3.83	-3.73	0.018	0.026			
159	B	4 E	Morrowan	314.48	100	Chert		Matrix, Sand		Chert nodules, Sample was epoxied	gray	74	2.68	-6.10	0.06	0.242			
160	A	5 E	Morrowan	314.46	5	Packstone	Skeletal Packstone	Skeletal, Matrix	Brachiopods, Crinoids, Bryozoans		medium gray	70	2.41	-4.48	0.018	0.015	X		
161	A	6 E	Morrowan	314.44	10	Wackestone	Skeletal Wackestone	Skeletal, Matrix	Crinoids, Brachiopods, Horn corals, Bryozoans		dark gray	92	2.50	-3.67	0.004	0.031	X		
162	A	7 E	Morrowan	314.41	5	Wackestone		Matrix, Sand, Skeletal	Crinoids (<2 mm, 10%), Brachiopods (10%)	5% Sand	medium gray	106	2.47	-3.65	0.015	0.015			
163	A	8 E	Morrowan	314.39	50	Wackestone		Matrix, Sand	Crinoids (5%)	50% Sand	dark gray	146	2.78	-4.22	0.013	0.033			
164	A	9 E	Morrowan	314.37	0	Wackestone	Skeletal Wackestone	Matrix, Skeletal	Brachiopods, Crinoids, Spines, Horn corals, Foraminifera		dark gray	64	2.41	-3.36	0.018	0.026	X		X
165	A	10 E	Morrowan	314.35	0	Wackestone	Skeletal Wackestone	Matrix, Skeletal	Brachiopods, Crinoids, Corals, Foraminifera		light gray	112	2.18	-3.55	0.014	0.027	X		
166	A	11 E	Morrowan	314.32	5	Wackestone		Matrix, Skeletal	Bryozoans, Brachiopods, Crinoids	Drill bit broke (Possible contamination)	light gray	124	1.88	-2.84	0.013	0.028			
167	A	12 E	Morrowan	314.30	5	Wackestone		Matrix, Sand, Skeletal	Unidentified skeletal fragments	5% Sand	gray	69	2.90	-4.06	0.015	0.03			
168	A	13 E	Morrowan	314.28	2	Wackestone		Matrix, Sand	Brachiopods	1% Sand, Contains zones of clear cement	light gray	92	2.56	-6.42	0.014	0.022			
169	A	14 E	Morrowan	314.26	20	Wackestone	Skeletal Wackestone	Matrix, Silt, Skeletal	Brachiopods, Crinoids		light gray	109	2.48	-9.20	0.019	0.023	X		
170	A	15 E	Morrowan	314.23	30	Packstone		Skeletal, Matrix, Sand	Pellets (40%), Brachiopods (5%)	30% Sand	gray		3.32	-4.53	0.0235	0.027			
170	D	15 E	Morrowan	314.23	30	Packstone		Skeletal, Matrix, Sand	Pellets (40%), Brachiopods (5%)	30% Sand	gray	145	3.36	-4.48	0.017	0.026			
170	D	15 E	Morrowan	314.23	30	Packstone		Skeletal, Matrix, Sand	Pellets (40%), Brachiopods (5%)	30% Sand	gray	119	3.28	-4.57	0.03	0.028			
176	A	16 E	Morrowan	314.10	25	Packstone	Skeletal Packstone	Silt, Matrix, Skeletal	Crinoids, Spines, Foraminifera		dark gray	121	3.14	-4.06	0.018	0.023	X		
177	A	17 E	Morrowan	314.07	40	Wackestone		Matrix, Sand		40% Sand	gray	172	2.78	-4.17	0.013	0.029			
178	A	18 E	Morrowan	314.05	25	Wackestone		Matrix, Sand		25% Sand	dark gray	109	3.01	-4.18	0.01	0.03			
179	A	19 E	Morrowan	314.03	5	Packstone	Skeletal Packstone	Skeletal, Matrix	Brachiopods, Foraminifera, Crinoids, Spines		dark gray	90	3.03	-3.43	0.014	0.037	X		
180	A	20 E	Morrowan	314.01	20	Wackestone		Matrix, Sand		Sampled from one side of a stylolite, Zones of dissolution on other side of stylolite	medium gray	147	2.27	-3.48	0.007	0.019			
181	A	21 E	Morrowan	313.98	10	Packstone	Skeletal Packstone	Skeletal, Matrix	Crinoids, Foraminifera, Brachiopods, Spines		dark gray	104	2.91	-3.37	0.012	0.035	X		

APPENDIX A - Continued

Sample (Meter + Letter)		Hand Sample Number	North American Stage	Age GTS 2004	% Silt/Sand	Classification	Expanded Classification	Material Sampled in order of Abundance	Fossils and Clasts	Other Notes (Hand Sample, unless specified)	Color	Powder Weight (ug) for Analysis	$\delta^{13}C$ vs VPDB	$\delta^{18}O$ vs VPDB	$\delta^{13}C$ 1σ	$\delta^{18}O$ 1σ	Thin Section	BSE Image	CL Image
183	A	1 F	Morrowan	313.94	15	Packstone	Skeletal Packstone	Skeletal, Matrix	Brachiopods, Spines		dark gray	99	1.96	-3.89	0.014	0.021	X		
184	A	2 F	Morrowan	313.91	5	Wackestone	Brachiopod Wackestone	Matrix, Skeletal	Brachiopods, Spines	Fine matrix	light gray	100	1.32	-6.18	0.008	0.031	X	X	
185	A	3 F	Morrowan	313.89	10	Packstone		Skeletal, Matrix, Sand	Brachiopods (20%), Crinoids (5%)	10% Silt	light gray	61	1.94	-4.63	0.012	0.033			
186	A	4 F	Morrowan	313.87	0	Calcisiltstone		Matrix, Silt		Black chert nodules	light gray	120	1.91	-5.53	0.021	0.048			
187	A	5 F	Morrowan	313.85	0	Mudstone		Matrix		Chert nodules	medium gray		2.09	-4.41					
188	A	6 F	Morrowan	313.82	50	Wackestone		Matrix, Sand	Crinoids (2-3%), Brachiopods	50% Sand	dark gray	199	2.50	-3.49	0.012	0.027			
189	A	7 F	Morrowan	313.80	40	Wackestone		Skeletal, Matrix, Sand	Brachiopods, Crinoids	40% Sand	gray	207	2.43	-3.80	0.006	0.038			
190	A	8 F	Morrowan	313.78	70	Siltstone	Siltstone	Silt, Matrix	Intraclasts, Bryozoans, Ostracods, Crinoids, Algae	Chert	dark gray		1.85	-4.54	0.0165	0.0255	X		
190	D	8 F	Morrowan	313.78	70	Siltstone	Siltstone	Silt, Matrix	Intraclasts, Bryozoans, Ostracods, Crinoids, Algae	Chert	dark gray	352	1.87	-4.45	0.022	0.034			
190	D	8 F	Morrowan	313.78	70	Siltstone	Siltstone	Silt, Matrix	Intraclasts, Bryozoans, Ostracods, Crinoids, Algae	Chert	dark gray	410	1.82	-4.64	0.011	0.017			
190	B	8 F	Morrowan	313.78	60	Siltstone		Silt, Matrix	Intraclasts, Bryozoans, Crinoids	60% Very fine quartz silt	medium gray	241	1.77	-4.69	0.017	0.019	X		
191	A	9 F	Morrowan	313.75	90	Sandstone		Sand, Matrix		90% Sand	dark gray	522	2.23	-3.97	0.016	0.022			
191	D	9 F	Morrowan	313.75	90	Sandstone		Sand, Matrix		90% Sand	dark gray								
191	D	9 F	Morrowan	313.75	90	Sandstone		Sand, Matrix		90% Sand	dark gray								
192	A	10 F	Morrowan	313.73	5	Packstone	Bryozoan Crinoidal Packstone	Matrix, Skeletal	Brachiopods, Crinoids, Bryozoans	Chert nodules	dark gray	70	1.71	-4.79	0.011	0.017	X		
193	A	11 F	Morrowan	313.71	20	Packstone		Skeletal, Matrix	Brachiopods, Spines, Intraclasts, Bryozoans	Silica going after spines, Stylolites forming	dark gray	153	2.95	-3.41	0.009	0.017	X		
194	A	12 F	Morrowan	313.69	80	Sandstone		Sand, Matrix	Crinoids, Brachiopods	80% Sand	gray	210	2.67	-4.34	0.015	0.015			
194	D	12 F	Morrowan	313.69	80	Sandstone		Sand, Matrix	Crinoids, Brachiopods	80% Sand	gray								
194	D	12 F	Morrowan	313.69	80	Sandstone		Sand, Matrix	Crinoids, Brachiopods	80% Sand	gray								
195	A	13 F	Morrowan	313.66	90	Sandstone		Sand, Matrix		90% Sand	light gray	514	1.79	-4.69	0.004	0.03			
195	D	13 F	Morrowan	313.66	90	Sandstone		Sand, Matrix		90% Sand	light gray								
195	D	13 F	Morrowan	313.66	90	Sandstone		Sand, Matrix		90% Sand	light gray								
196	A	14 F	Morrowan	313.64	80	Sandstone		Sand, Matrix	Brachiopods, Crinoids (<2 mm)	80% Sand	medium gray	252	2.19	-4.08	0.014	0.014			
197	A	15 F	Morrowan	313.62	40	Wackestone	Silty Skeletal Wackestone	Silt, Matrix, Skeletal	Ostracods, Foraminifera, Trilobites, Crinoids, Brachiopods	Intraclasts, Silica has partially replaced crinoids	dark gray	237	2.43	-4.09	0.018	0.044	X		
198	A	16 F	Morrowan	313.60	30	Packstone	Packstone/Grainstone	Skeletal, Matrix	Coated grains, Trilobites, Algae, Brachiopods	Coated grains (Possibly silicified)	dark gray	139	2.33	-4.60	0.014	0.029	X		
199	A	17 F	Morrowan	313.57	60	Sandstone		Sand, Matrix	Crinoids (20%)	60% Sand	dark gray	269	1.86	-4.13	0.008	0.033			
199	D	17 F	Morrowan	313.57	60	Sandstone		Sand, Matrix	Crinoids (20%)	60% Sand	dark gray								
199	D	17 F	Morrowan	313.57	60	Sandstone		Sand, Matrix	Crinoids (20%)	60% Sand	dark gray								
200	A	18 F	Morrowan	313.55	5	Wackestone/ Packstone	Skeletal Wackestone	Matrix, Skeletal	Brachiopods, Crinoids		dark gray	70	1.67	-3.74	0.007	0.024	X		X
201	A	19 F	Morrowan	313.53	15	Wackestone		Matrix, Sand	Crinoids (20%), Brachiopods (10%)	15% Sand	dark gray	95	1.80	-3.41	0.009	0.009			

APPENDIX A - Continued

Sample (Meter + Letter)		Hand Sample Number	North American Stage	Age GTS 2004	% Silt/Sand	Classification	Expanded Classification	Material Sampled in order of Abundance	Fossils and Clasts	Other Notes (Hand Sample, unless specified)	Color	Powder Weight (ug) for Analysis	$\delta^{13}C$ vs VPDB	$\delta^{18}O$ vs VPDB	$\delta^{13}C$ 1σ	$\delta^{18}O$ 1σ	Thin Section	BSE Image	CL Image
202	A	20 F	Morrowan	313.50	5	Packstone	Skeletal Packstone	Skeletal, Matrix	Brachiopods, Crinoids, Spines		medium gray	89	1.95	-4.49	0.015	0.022	X		
203	A	21 F	Morrowan	313.48	75	Packstone		Skeletal, Matrix, Sand	Horn corals (30%), Brachiopods (50%)	75% Chert	medium gray	458	1.83	-5.69	0.013	0.019			
203	D	21 F	Morrowan	313.48	75	Packstone		Skeletal, Matrix, Sand	Horn corals (30%), Brachiopods (50%)	75% Chert	medium gray								
203	D	21 F	Morrowan	313.48	75	Packstone		Skeletal, Matrix, Sand	Horn corals (30%), Brachiopods (50%)	75% Chert	medium gray								
204	A	22 F	Morrowan	313.46	5	Wackestone	Skeletal Wackestone	Matrix, Skeletal	Brachiopods, Bryozoans, Corals, Crinoids, Ostracods, Foraminifera		medium gray	62	1.40	-3.52	0.021	0.046	X		
205	A	23 F	Morrowan	313.44	5	Wackestone/ Packstone	Skeletal Wackestone	Matrix, Skeletal	Brachiopods, Bryozoans, Crinoids		medium gray	91	1.40	-4.25	0.014	0.023	X		
206.5	A	24 F	Morrowan	313.40	5	Wackestone	Crinoidal Wackestone	Matrix	Crinoids, Brachiopods, Spines		medium gray		0.59	-7.13	0.02	0.033	X		
206.5	D	24 F	Morrowan	313.40	5	Wackestone	Crinoidal Wackestone	Matrix	Crinoids, Brachiopods, Spines		medium gray	60	0.54	-7.21	0.016	0.021	X		
206.5	D	24 F	Morrowan	313.40	5	Wackestone	Crinoidal Wackestone	Matrix	Crinoids, Brachiopods, Spines		medium gray	66	0.64	-7.05	0.024	0.045	X		
207	A	25 F	Morrowan	313.39	30	Packstone		Sand, Skeletal, Matrix	Brachiopods	30% Sand	light gray	102	2.65	-3.11	0.009	0.009			
208	A	26 F	Morrowan	313.37	10	Wackestone		Matrix, Sand	Crinoids	10% Sand	gray	80	2.98	-3.50	0.012	0.015			
209	A	27 F	Morrowan	313.35	15	Grainstone	Coated Skeletal Grainstone	Skeletal, Matrix	Coated grains, Crinoids, Bryozoans, Brachiopods		medium gray	134	2.78	-3.81	0.019	0.017	X		
210	A	28 F	Morrowan	313.32	20	Wackestone		Matrix, Sand	Crinoids	20% Sand	gray	112	2.87	-3.80	0.009	0.009			
211	A	29 F	Atokan	313.3	5	Packstone		Skeletal, Matrix, Sand	Crinoids, Brachiopods, Bryozoans	1-2% Silt	medium gray	104	2.29	-4.33	0.007	0.031			
211.5	A	30 F	Atokan	313.27	5	Packstone		Skeletal, Matrix, Sand	Crinoids (<2 mm), Brachiopods	1-2% Silt	medium gray	68	1.94	-4.66	0.02	0.02			
212	A	31 F	Atokan	313.24	5	Wackestone	Skeletal Wackestone	Matrix, Skeletal	Crinoids, Bryozoans, Foraminifera, Spines		dark gray	65	1.94	-3.82	0.02	0.024	X		
212.5	A	32 F	Atokan	313.21	40	Siltstone	Crinoidal Siltstone	Matrix, Silt, Skeletal	Crinoids, Bryozoans, Brachiopods		light gray	174	2.42	-5.69	0.015	0.02	X		
213	A	33 F	Atokan	313.17	80	Sandstone		Sand, Matrix	Brachiopods, Crinoids	80% Sand	gray		1.82	-5.31	0.0105	0.0325			
213	D	33 F	Atokan	313.17	80	Sandstone		Sand, Matrix	Brachiopods, Crinoids	80% Sand	gray	429	1.84	-5.33	0.011	0.021			
213	D	33 F	Atokan	313.17	80	Sandstone		Sand, Matrix	Brachiopods, Crinoids	80% Sand	gray	414	1.81	-5.30	0.01	0.044			
213.5	A	34 F	Atokan	313.14	70	Siltstone		Sand, Skeletal, Matrix		70% Silt	gray	295	2.31	-4.82	0.022	0.022			
214	A	35 F	Atokan	313.11	20	Packstone	Pelletal Grainstone	Skeletal, Matrix	Crinoids, Foraminifera, Bryozoans, Coated grains		dark gray	110	2.64	-4.60	0.01	0.029	X		
214.5	A	36 F	Atokan	313.08	5	Packstone	Skeletal Packstone	Skeletal, Matrix	Foraminifera, Brachiopods, Spines, Phylloid algae	Wavy Laminations	dark gray	88	3.10	-3.74	0.015	0.013	X		
215	A	37 F	Atokan	313.05	5	Packstone	Algal Skeletal Packstone	Skeletal, Matrix	Foraminifera, Spines, Brachiopods, Red algae	Wavy Laminations	dark gray	64	3.09	-3.04	0.01	0.029	X		
215	B	37 F	Atokan	313.05	5	Packstone	Algal Skeletal Packstone	Algae	Algae (Possibly red algae)	Wavy Laminations	white	97	-5.54	-3.28	0.016	0.023	X		

APPENDIX A - Continued

Sample (Meter + Letter)	Hand Sample Number	North American Stage	Age GTS 2004	% Silt/Sand	Classification	Expanded Classification	Material Sampled in order of Abundance	Fossils and Clasts	Other Notes (Hand Sample, unless specified)	Color	Powder Weight (ug) for Analysis	$\delta^{13}C$ vs VPDB	$\delta^{18}O$ vs VPDB	$\delta^{13}C$ 1σ	$\delta^{18}O$ 1σ	Thin Section	BSE Image	CL Image
215.5 A	38 F	Atokan	313.02	25	Wackestone	Skeletal Wackestone	Matrix, Sand		20% Silt	gray	155	1.73	-5.32	0.016	0.022			
216 A	39 F	Atokan	312.99	15	Wackestone	Skeletal Wackestone	Sand, Skeletal, Matrix		10% Silt, Interbedded with thin bedded mudstone	dark gray	68	2.66	-3.72	0.005	0.005			
216.5 A	40 F	Atokan	312.95	5	Packstone		Skeletal, Matrix, Sand	Coated grains	5% Silt, Black material between grains	dark gray	103	2.95	-3.35	0.017	0.031			
217 A	41 F	Atokan	312.92	20	Packstone		Matrix, Sand	Coated grains, Pellets, Red algae	20% Silt, Black material between grains	dark gray	178	3.13	-4.03	0.012	0.041			
217.5 A	42 F	Atokan	312.89	10	Grainstone	Pelletal Grainstone	Pellets, Matrix, Skeletal	Coated bioclasts, Pellets, Crinoids, Brachiopods, Red algae	Stylolite	dark gray	60	2.77	-4.30	0.023	0.019	X		
218 A	43 F	Atokan	312.86	30	Packstone	Skeletal Packstone	Skeletal, Matrix, Silt	Coated bioclasts, Pellets, Crinoids, Spines, Foraminifera, Brachiopods, Red algae		dark gray	121	3.67	-3.43	0.017	0.019	X		
218.5 A	44 F	Atokan	312.83	5	Packstone	Skeletal Packstone	Skeletal, Matrix	Foraminifera, Crinoids, Ostracods, Red algae	Small fractures	medium gray	71	3.60	-4.08	0.013	0.024	X		
219 A	45 F	Atokan	312.80	5	Packstone	Skeletal Packstone	Skeletal, Matrix	Foraminifera, Brachiopods, Fine skeletal grains, Red algae	Small fractures	medium gray	108	3.46	-4.45	0.017	0.021	X		
219.5 A	46 F	Atokan	312.77	10	Wackestone	Skeletal Wackestone	Matrix, Skeletal	Crinoids, Unidentified skeletal fragments		tan	77	-1.16	-9.02	0.02	0.027	X		
220 A	47 F	Atokan	312.73	0	Calcisiltstone		Matrix		Cement filled voids (Possible exposure)	light gray	93	3.37	-3.65	0.016	0.032			
220.5 A	48 F	Atokan	312.70	0	Calcisiltstone		Matrix		Cement filled voids (Possible exposure)	gray	73	3.49	-3.79	0.025	0.025			
221 A	49 F	Atokan	312.67	0	Mudstone		Matrix	Foraminifera		gray	106	3.38	-4.03	0.016	0.034			
221.5 A	50 F	Atokan	312.64	5	Wackestone	Algal Wackestone	Matrix, Skeletal	Crinoids, Bryozoans, Fenestral bryozoans, Red algae		medium gray	84	3.35	-3.55	0.009	0.027	X		
222 A	51 F	Atokan	312.61	5	Wackestone	Algal Wackestone	Matrix, Clear Cement	Crinoids, Foraminifera, Red algae		medium gray	63	3.41	-3.65	0.019	0.024	X		
222.5 A	52 F	Atokan	312.58	0	Mudstone		Matrix		Sample was epoxied	gray	70	3.15	-3.68	0.015	0.015			
222.5 B	52 F	Atokan	312.58	0	Cement - Crinoid		Cement	Crinoids	Cement from crinoid	gray	100	3.37	-3.76	0.012	0.036			
223 A	53 F	Atokan	312.55	0	Wackestone		Matrix, Fracture Fill	Crinoids (25%)	Highly fractured	light gray	108	3.22	-3.83	0.012	0.011			
224 A	54 F	Atokan	312.48	5	Packstone	Skeletal Packstone	Matrix, Skeletal	Crinoids, Abundant foraminifera, Ostracods		dark gray	104	3.16	-3.58	0.008	0.02	X		
225 A	55 F	Atokan	312.42	70	Sandstone		Sand, Matrix		70% Sand	medium gray	304	2.10	-2.15	0.011	0.019			
225.5 A	56 F	Atokan	312.39	5	Packstone		Skeletal, Matrix	Brachiopods, Crinoids	5% Sand	medium gray	62	1.70	-3.65	0.017	0.017			
226 A	57 F	Atokan	312.36	5	Wackestone/ Packstone	Brachiopod Wackestone	Matrix, Skeletal	Brachiopods, Spines, Bryozoans		light gray	66	1.82	-3.62	0.016	0.03	X		
226.5 A	58 F	Atokan	312.33	5	Wackestone	Skeletal Wackestone	Matrix, Skeletal	Spines, Brachiopods, Crinoids, Gastropods		light gray		1.66	-3.31			X		
226.5 B	58 F	Atokan	312.33	0	Cement - Gastropod		Cement, Matrix		Clear cement from 2-3	clear	60	2.46	-3.71	0.012	0.024	X		

APPENDIX A - Continued

Sample (Meter + Letter)		Hand Sample Number	North American Stage	Age GTS 2004	% Silt/Sand	Classification	Expanded Classification	Material Sampled in order of Abundance	Fossils and Clasts	Other Notes (Hand Sample, unless specified)	Color	Powder Weight (ug) for Analysis	$\delta^{13}C$ vs VPDB	$\delta^{18}O$ vs VPDB	$\delta^{13}C$ 1σ	$\delta^{18}O$ 1σ	Thin Section	BSE Image	CL Image
										mm gastropod									
227	A	59 F	Atokan	312.30	0	Packstone		Skeletal, Matrix	Brachiopods, Crinoids	Sample was epoxied	gray	119	1.58	-3.45	0.028	0.013			
227.5	A	60 F	Atokan	312.26	0	Packstone		Skeletal, Matrix	Brachiopods, Crinoids	Some oxidized material in hand sample	gray	66	1.60	-3.64	0.008	0.008			
229	A	62 F	Atokan	312.17	5	Wackestone		Matrix, Sand		1-2% Silt, Dark carbonate between grains	dark gray	108	2.26	-3.93	0.014	0.046			
229.5	A	63 F	Atokan	312.14	5	Packstone	Skeletal Packstone	Skeletal, Matrix	Crinoids, Brachiopods, Spines, Foraminifera, Bryozoans	Large Bryozoans, Excellent specimen	dark gray	90	2.22	-3.72	0.006	0.027	X		
230	A	64 F	Atokan	312.11	5	Packstone	Skeletal Packstone	Skeletal, Matrix	Crinoids, Brachiopods, Spines, Ostracods, Foraminifera		medium gray	72	2.17	-3.79	0.015	0.035	X		
230.5	A	65 F	Atokan	312.08	15	Packstone		Skeletal, Matrix, Sand	Brachiopod, Pellets, Crinoids	15% Silt	medium gray	96	2.00	-5.01	0.013	0.013			
231	A	66 F	Atokan	312.04	50	Packstone		Sand, Matrix		50% Sand	gray	153	0.95	-4.63	0.011	0.012			
232	A	67 F	Atokan	311.98	50	Packstone		Sand, Matrix	Crinoids	50% Sand	gray	140	2.32	-3.56	0.021	0.035			
233	A	68 F	Atokan	311.92	10	Grainstone	Pelletal Grainstone	Pellets, Cement	Pellets, Brachiopod fragments with micritized rims		medium gray	84	2.44	-4.01	0.01	0.029	X		
234	A	69 F	Atokan	311.86	5	Grainstone	Pelletal Grainstone	Oncolite, Cement	Pellets		medium gray	68	2.41	-4.02	0.01	0.031	X		
235	A	70 F	Atokan	311.79	5	Packstone	Pelletal Packstone	Other, Cement	Pellets, Ostracods		light gray	109	2.60	-3.68	0.014	0.028	X		
235.5	A	71 F	Atokan	311.76	10	Wackestone		Matrix, Sand		10 Silt	dark gray	90	2.61	-3.23	0.017	0.028			
236	A	72 F	Atokan	311.73	10	Packstone		Skeletal, Matrix, Sand	Crinoids, Brachiopods	10% Silt, Dark black material between grains	medium gray	75	2.28	-3.61	0.01	0.01			
237.5	A	73 F	Atokan	311.64	30	Packstone		Sand, Matrix, Skeletal	Brachiopods	30% Sand, Some oxidized grains visible	medium gray	169	1.73	-3.59	0.016	0.019			
238	A	74 F	Atokan	311.60	0	Grainstone		Skeletal, Matrix	Brachiopods (80%), Spines		medium gray	67	1.37	-3.54	0.011	0.011			
238.5	A	75 F	Atokan	311.57	5	Packstone	Skeletal Packstone	Skeletal, Matrix	Brachiopods, Spines, Oncolites, Bivalves?		medium gray	61	1.35	-3.46	0.022	0.037	X		
239	A	76 F	Atokan	311.54	30	Wackestone		Matrix, Sand, Skeletal	Crinoids, Brachiopods, Spines	30% Silt	medium gray	152	0.96	-3.36	0.012	0.025			
239.5	A	77 F	Atokan	311.51	15	Wackestone		Matrix, Sand	Crinoids	15% Silt	medium gray		1.28	-3.43	0.0135	0.0255			
239.5	D	77 F	Atokan	311.51	15	Wackestone		Matrix, Sand	Crinoids	15% Silt	medium gray	117	1.27	-3.46	0.015	0.035			
239.5	D	77 F	Atokan	311.51	15	Wackestone		Matrix, Sand	Crinoids	15% Silt	medium gray	100	1.29	-3.40	0.012	0.016			
240	A	78 F	Atokan	311.48	50	Siltstone		Silt, Matrix, Skeletal	Foraminifera, Bryozoans	50% Silt	medium gray	168	1.90	-4.71	0.011	0.027	X		
240.5	A	79 F	Atokan	311.45	30	Wackestone/ Packstone	Skeletal Packstone	Skeletal, Matrix	Brachiopods, Spines, Coated grains	Stylolites forming	dark gray	111	1.66	-4.17	0.019	0.048	X		
241	A	80 F	Atokan	311.42	10	Wackestone	Cherty Skeletal Wackestone	Matrix, Skeletal	Bryozoans, Bivalves, Brachiopods	Black chert nodules, Analysis was done near exposure surface due to chert	light gray	102	1.23	-3.64	0.02	0.017	X		

APPENDIX A - Continued

Sample (Meter + Letter)		Hand Sample Number	North American Stage	Age GTS 2004	% Silt/Sand	Classification	Expanded Classification	Material Sampled in order of Abundance	Fossils and Clasts	Other Notes (Hand Sample, unless specified)	Color	Powder Weight (ug) for Analysis	$\delta^{13}C$ vs VPDB	$\delta^{18}O$ vs VPDB	$\delta^{13}C$ 1σ	$\delta^{18}O$ 1σ	Thin Section	BSE Image	CL Image
241.5	A	81 F	Atokan	311.38	0	Wackestone	Skeletal Wackestone	Calcisilt, Skeletal	Brachiopods, Spines	Possible vadose zone exposure	light gray	87	1.39	-3.14	0.011	0.022			
242	A	82 F	Atokan	311.35	0	Wackestone		Matrix, Skeletal	Brachiopods, Spines	Coarsening upwards	brown/gray	62	0.96	-3.92	0.011	0.011			
242.5	A	83 F	Atokan	311.32	10	Wackestone	Skeletal Wackestone	Matrix, Skeletal	Crinoids, Bryozoans, Brachiopods, Bivalves	Black chert nodules	light gray	148	0.65	-4.10	0.017	0.026	X		
243	A	84 F	Atokan	311.29	30	Wackestone		Matrix, Sand, Skeletal	Crinoids	30% Silt	medium gray	150	1.40	-3.88	0.025	0.026			
243.5	A	85 F	Atokan	311.26	10	Mudstone	Silty Mudstone	Matrix, Sand		10% Silt	medium gray	62	1.06	-3.38	0.016	0.033			
244	A	86 F	Atokan	311.23	40	Wackestone		Matrix, Sand		40% Silt	medium gray	142	1.60	-3.87	0.016	0.016			
244.5	A	87 F	Atokan	311.20	30	Packstone		Matrix, Skeletal, Sand		30% Silt	medium gray	112	1.16	-3.29	0.02	0.028			
245	A	88 F	Atokan	311.16	5	Wackestone	Skeletal Wackestone	Matrix, Skeletal	Crinoids, Spines, Brachiopods, Foraminifera, Phylloid algae		medium gray	113	1.87	-2.85	0.023	0.028	X		
245.5	A	89 F	Atokan	311.13	5	Wackestone	Skeletal Wackestone	Matrix, Skeletal	Crinoids, Spines, Brachiopods, Bivalves, Bryozoans		light gray	76	2.10	-3.32	0.011	0.021	X		
247	A	90 F	Atokan	311.04	20	Wackestone	Skeletal Wackestone	Matrix, Silt, Sand	Crinoids, Spines		dark gray	146	2.08	-2.93	0.016	0.025	X		
248	A	91 F	Atokan	310.98	0	Wackestone		Matrix, Skeletal	Spines, Brachiopods		dark gray	71	1.20	-4.36	0.017	0.017			
249	A	92 F	Atokan	310.91	0	Packstone		Calcisilt, Skeletal	Crinoids, Brachiopods, Spines	Wavy Bedding	gray	94	1.47	-4.35	0.014	0.027			
249.5	A	93 F	Atokan	310.88	10	Wackestone	Skeletal Wackestone	Matrix, Skeletal	Crinoids, Brachiopods, Spines		dark gray	69	1.68	-3.47	0.018	0.03	X		
251	A	94 F	Atokan	310.79	30	Packstone	Silty Skeletal Packstone	Skeletal, Matrix	Crinoids, Bryozoans, Algae, Pellets, Bryozoans		medium gray	141	2.48	-4.00	0.019	0.033	X		
252.5	A	95 F	Atokan	310.69	20	Wackestone		Matrix, Sand, Skeletal	Crinoids	20% Silt	medium gray	103	2.99	-3.44	0.023	0.029			
254	A	96 F	Atokan	310.60	20	Packstone	Silty Skeletal Packstone	Skeletal, Matrix, Silt	Foraminifera, Crinoids, Bryozoans		medium gray	101	2.25	-5.32	0.021	0.024	X		
255.5	A	97 F	Atokan	310.50	90	Sandstone		Sand, Cement		90% Very fine sand	light gray		2.15	-4.68	0.011	0.0325			
255.5	D	97 F	Atokan	310.50	90	Sandstone		Sand, Cement		90% Very fine sand	light gray	564	2.23	-4.55	0.009	0.027			
255.5	D	97 F	Atokan	310.50	90	Sandstone		Sand, Cement		90% Very fine sand	light gray	489	2.08	-4.80	0.013	0.038			
257	A	98 F	Atokan	310.41	50	Siltstone	Siltstone	Matrix, Silt	Foraminifera, Crinoids, Pellets		light gray	169	2.43	-4.18	0.007	0.019	X		
258	A	99 F	Atokan	310.35	20	Packstone	Silty Skeletal Packstone	Skeletal, Matrix, Silt	Pellets, Crinoids, Foraminifera		medium gray		2.58	-3.81	0.01	0.0265	X		
258	D	99 F	Atokan	310.35	20	Packstone	Silty Skeletal Packstone	Skeletal, Matrix, Silt	Pellets, Crinoids, Foraminifera		medium gray	116	2.57	-3.80	0.005	0.028			
258	D	99 F	Atokan	310.35	20	Packstone	Silty Skeletal Packstone	Skeletal, Matrix, Silt	Pellets, Crinoids, Foraminifera		medium gray	99	2.60	-3.83	0.015	0.025			
259	A	100 F	Atokan	310.29	30	Wackestone		Sand, Matrix, Skeletal		30% Sand	gray	92	2.51	-4.01	0.006	0.006			
260	A	101 F	Atokan	310.22	40	Packstone	Silty Skeletal	Skeletal, Silt,	Pellets, Crinoids,		light gray	180	2.44	-3.93	0.022	0.025	X		

APPENDIX A - Continued

Sample (Meter + Letter)		Hand Sample Number	North American Stage	Age GTS 2004	% Silt/Sand	Classification	Expanded Classification	Material Sampled in order of Abundance	Fossils and Clasts	Other Notes (Hand Sample, unless specified)	Color	Powder Weight (ug) for Analysis	$\delta^{13}C$ vs VPDB	$\delta^{18}O$ vs VPDB	$\delta^{13}C$ 1σ	$\delta^{18}O$ 1σ	Thin Section	BSE Image	CL Image
							Packstone	Matrix	Foraminifera										
265.5	A	102 F	Atokan	309.88	40	Sandstone		Matrix, Sand, Skeletal	Crinoids, Brachiopods	Chert nodules, 50% Sand	gray	175	2.00	-3.71	0.008	0.022			
266	A	103 F	Atokan	309.85	20	Wackestone	Wackestone	Matrix, Silt	Crinoids, Foraminifera, Brachiopods		light gray	119	2.21	-3.64	0.025	0.023	X		
266.5	A	104 F	Atokan	309.81	40	Wackestone		Matrix, Sand, Skeletal	Crinoids, Brachiopods	40% Silt	gray	136	2.24	-3.62	0.015	0.015			
267	A	105 F	Atokan	309.78	10	Grainstone	Skeletal Grainstone	Skeletal, Cement, Matrix	Crinoids, Brachiopods, Foraminifera, Pellets		medium gray	105	2.09	-3.66	0.013	0.027	X		
267.5	A	106 F	Atokan	309.75	35	Wackestone		Matrix, Pellets, Sand	Pellets	35% Silt	gray	166	1.68	-3.81	0.01	0.026			
268	A	107 F	Atokan	309.72	60	Siltstone		Sand, Matrix	Brachiopods	30% Silt	gray	256	1.75	-5.36	0.014	0.029			
269	A	108 F	Atokan	309.66	30	Wackestone		Matrix, Sand	Crinoids	Oxidized material between grains, 60% Silt	medium gray	94	1.28	-3.62	0.013	0.013			
270	A	109 F	Atokan	309.59	30	Packstone	Silty Skeletal Packstone	Skeletal, Matrix	Brachiopods, Crinoids, Spines		light gray	182	1.03	-5.66	0.015	0.021	X		
271	A	110 F	Atokan	309.53	5	Wackestone	Skeletal Wackestone	Matrix	In-situ colonial corals, Crinoids		dark gray	102	0.87	-3.90	0.021	0.027	X		
271.5	A	1B	Desmoinesian	309.5	15	Wackestone/ Packstone	Skeletal Wackestone	Matrix, Skeletal, Silt	Crinoids, Brachiopods	Dark organic matter	light gray	100	-0.03	-6.00	0.01	0.028	X		
272	A	2 B	Desmoinesian	309.49	10	Wackestone		Matrix, Sand	Crinoids	10% Silt	dark gray	112	0.91	-4.20	0.024	0.035			
274	A	3 B	Desmoinesian	309.44	20	Wackestone		Calcisilt, Sand, Skeletal	Crinoids	Highly fractured, 20% Silt, Sampled from covered interval	brown/gray		1.39	-4.93	0.02	0.0215			
274	D	3 B	Desmoinesian	309.44	20	Wackestone		Calcisilt, Sand, Skeletal	Crinoids	Highly fractured, 20% Silt, Sampled from covered interval	brown/gray	117	1.42	-4.77	0.023	0.023			
274	D	3 B	Desmoinesian	309.44	20	Wackestone		Calcisilt, Sand, Skeletal	Crinoids	Highly fractured, 20% Silt, Sampled from covered interval	brown/gray	174	1.37	-5.08	0.017	0.02			
277	A	4 B	Desmoinesian	309.37	15	Wackestone	Silty Skeletal Wackestone	Matrix, Skeletal	Brachiopods, Bivalves	Dark organic matter	light gray	143	1.18	-6.83	0.025	0.036	X	X	X
278	A	5 B	Desmoinesian	309.35	10	Wackestone		Matrix, Sand	Brachiopods, Spines		brown		0.58	-6.81					
279	A	6 B	Desmoinesian	309.32	40	Wackestone		Matrix, Sand, Skeletal	Brachiopods, Spines	2 distinct textures visible, Brown/orange material visible between grains	gray	138	1.72	-6.48	0.022	0.024			
280	A	7 B	Desmoinesian	309.30	10	Wackestone		Matrix, Sand	Brachiopods, Crinoids, Spines		light gray	96	0.46	-7.53	0.019	0.026			
281	A	8 B	Desmoinesian	309.27	60	Siltstone		Sand, Matrix		60% Silt	light gray		0.39	-8.36					
281.5	A	9 B	Desmoinesian	309.26	30	Wackestone		Matrix, Sand	Brachiopods, Spines	30% Silt	light gray	114	-1.78	-8.50	0.012	0.036			
286	A	10 B	Desmoinesian	309.16	50	Wackestone		Matrix, Sand		50% silt	gray	138	2.53	-4.79	0.012	0.028			
287	A	11 B	Desmoinesian	309.13	10	Grainstone	Pelletal Grainstone	Pellets, Matrix	Pellets, Coated grains		medium gray	78	3.44	-4.22	0.028	0.007	X		
288	A	12 B	Desmoinesian	309.11	10	Grainstone	Pelletal Grainstone/ Packstone	Matrix, Sand	Pellets	10% Silt	dark gray	98	3.56	-3.96	0.02	0.047			
290	A	14 B	Desmoinesian	309.06	30	Siltstone		Matrix, Sand		30% Silt	medium	95	3.59	-3.71	0.034	0.03			

APPENDIX A - Continued

Sample (Meter + Letter)		Hand Sample Number	North American Stage	Age GTS 2004	% Silt/Sand	Classification	Expanded Classification	Material Sampled in order of Abundance	Fossils and Clasts	Other Notes (Hand Sample, unless specified)	Color	Powder Weight (ug) for Analysis	$\delta^{13}C$ vs VPDB	$\delta^{18}O$ vs VPDB	$\delta^{13}C$ 1σ	$\delta^{18}O$ 1σ	Thin Section	BSE Image	CL Image
291	A	15 B	Desmoinesian	309.04	5	Grainstone	Pelletal Grainstone	Pellets, Matrix	Pellets, Coated grains, Bryozoans, Foraminifera fragments		gray medium gray	71	3.54	-3.53	0.013	0.044	X		
292	A	16 B	Desmoinesian	309.01	5	Mudstone		Matrix, Sand		5% Silt	dark gray	73	2.68	-3.42	0.01	0.008			
293	A	17 B	Desmoinesian	308.99	30	Packstone	Silty Skeletal Wackestone	Skeletal, Matrix	Crinoids, Foraminifera, Corals		medium gray	77	1.89	-3.84	0.008	0.034	X		
294	A	18 B	Desmoinesian	308.97	10	Wackestone/ Packstone	Skeletal Wackestone	Matrix, Skeletal	Crinoids, Brachiopods	Large chert nodule and stylolite	dark gray	102	1.72	-3.13	0.024	0.016	X		
294.5	A	19 B	Desmoinesian	308.96	5	Grainstone		Skeletal, Matrix, Sand	Pellets	5% Silt	medium gray	60	3.48	-3.72	0.025	0.033			
295	A	20 B	Desmoinesian	308.94	20	Packstone		Skeletal, Matrix, Sand	Brachiopods, Pellets, Crinoids	20% Silt	gray	142	2.56	-3.40	0.007	0.016			
295.5	A	21 B	Desmoinesian	308.93	5	Wackestone	Skeletal Wackestone	Matrix, Skeletal	Crinoids, Brachiopods		light gray	91	1.93	-2.23	0.024	0.028	X		
296.5	A	23 B	Desmoinesian	308.91	5	Wackestone	Coral Wackestone	Matrix	Pellets, Crinoids, Brachiopods	5% Silt, Chert nodules	gray	76	3.04	-3.84	0.022	0.015	X		
296.5	B	23 B	Desmoinesian	308.91	0	Cement - Coral		Calcite from Horn Coral	In-situ horn corals		white	64	1.27	-5.10	0.012	0.022	X		
296.5	C	23 B	Desmoinesian	308.91	5	Packstone		Skeletal, Matrix	Pellets, Crinoids, Brachiopods	5% Silt, Chert nodules	gray	105	0.97	-5.15	0.008	0.019	X		
297	A	24 B	Desmoinesian	308.90	60	Sandstone	Sandstone	Sand, Skeletal, Matrix	Brachiopods	60% Silt	light gray	253	2.46	-4.31	0.021	0.036			
297.5	A	25 B	Desmoinesian	308.88	40	Grainstone		Skeletal, Matrix	Foraminifera, Coated bioclasts, Phylloid algae		medium gray	177	2.84	-4.07	0.008	0.023	X		
298	A	26 B	Desmoinesian	308.87	80	Sandstone		Sand, Matrix, Skeletal	Crinoids	80% Very fine sand	gray	310	3.15	-3.97	0.013	0.024			
298.5	A	27 B	Desmoinesian	308.86	70	Sandstone		Sand, Matrix	Brachiopods	70% sand, Oxidized material between grains	gray		2.65	-3.08	0.0165	0.027			
298.5	D	27 B	Desmoinesian	308.86	70	Sandstone		Sand, Matrix	Brachiopods	70% sand, Oxidized material between grains	gray	370	2.65	-3.97	0.016	0.03			
298.5	D	27 B	Desmoinesian	308.86	70	Sandstone		Sand, Matrix	Brachiopods	70% sand, Oxidized material between grains	gray	279	2.65	-2.20	0.017	0.024			
298.5	B	27 B	Desmoinesian	308.86	0	Cement - Void		Cement		Fibrous white cement taken from large pore	white	62	3.29	-4.66	0.014	0.016			
299	A	28 B	Desmoinesian	308.85	30	Wackestone	Sandy Wackestone	Matrix, Silt	Brachiopods		medium gray	92	2.96	-3.17	0.013	0.022	X		
299.5	A	29 B	Desmoinesian	308.84	0	Wackestone	Skeletal Wackestone	Matrix, Skeletal	Brachiopods, Foraminifera, Spines, Crinoids, Bryozoans, Phylloid algae		medium gray	100	2.96	-3.03	0.011	0.019	X		
300	A	30 B	Desmoinesian	308.82	20	Wackestone		Matrix, Sand	Brachiopods	20% Silt	medium gray	103	3.32	-3.37	0.014	0.044			
300.5	A	31 B	Desmoinesian	308.81	5	Mudstone		Matrix	Crinoids	1-2% Silt, Highly fractured	gray	97	2.58	-2.88	0.013	0.033			
301	A	32 B	Desmoinesian	308.80	5	Packstone		Matrix, Skeletal, Sand	Brachiopods, Crinoids	5% Silt	gray	76	3.07	-3.10	0.018	0.022			
301.5	A	33 B	Desmoinesian	308.79	5	Packstone	Skeletal Packstone	Skeletal, Matrix	Spines, Brachiopod	Grainy texture	light gray	62	-0.52	-6.42	0.012	0.033	X		

APPENDIX A - Continued

Sample (Meter + Letter)		Hand Sample Number	North American Stage	Age GTS 2004	% Silt/Sand	Classification	Expanded Classification	Material Sampled in order of Abundance	Fossils and Clasts	Other Notes (Hand Sample, unless specified)	Color	Powder Weight (ug) for Analysis	$\delta^{13}C$ vs VPDB	$\delta^{18}O$ vs VPDB	$\delta^{13}C$ 1σ	$\delta^{18}O$ 1σ	Thin Section	BSE Image	CL Image
									fragments										
302	A	34 B	Desmoinesian	308.78	10	Packstone		Matrix, Skeletal, Sand	Brachiopods, Crinoids	10% Silt	gray	98	1.82	-4.29	0.024	0.041			
305	A	35 B	Desmoinesian	308.71	5	Wackestone	Bryozoan Brachiopod Wackestone	Matrix	Brachiopods, Spines, Bryozoans		light gray	112	-0.10	-5.65	0.023	0.03	X		X
306	A	36 B	Desmoinesian	308.68	80	Sandstone		Sand, Matrix		80% Very fine sand	light gray	304	0.97	-3.90	0.017	0.029			
307.5	A	37 B	Desmoinesian	308.65	80	Sandstone		Sand, Matrix		8% Silt	medium gray		1.02	-4.10	0.02	0.038			
307.5	D	37 B	Desmoinesian	308.65	80	Sandstone		Sand, Matrix		8% Silt	medium gray	465	1.05	-4.03	0.013	0.046			
307.5	D	37 B	Desmoinesian	308.65	80	Sandstone		Sand, Matrix		8% Silt	medium gray	402	1.00	-4.17	0.027	0.03			
309	A	38 B	Desmoinesian	308.61	80	Sandstone		Sand, Matrix		Chert nodules (2-10 cm)	light gray	262	0.58	-6.34	0.01	0.021			
312	A	40 B	Desmoinesian	308.54	25	Grainstone	Skeletal Grainstone	Skeletal, Matrix	Foraminifera, Brachiopods, Crinoids		light gray	103	2.21	-3.06	0.019	0.018	X		
313	A	41 B	Desmoinesian	308.52	10	Wackestone		Skeletal, Matrix	Brachiopods, Crinoids	10% Silt	gray	94	1.30	-4.18	0.009	0.035			
314	A	42 B	Desmoinesian	308.49	70	Siltstone		Sand, Matrix		70% Silt	gray	202	1.22	-3.82	0.021	0.084			
315	A	43 B	Desmoinesian	308.47	10	Packstone	Foraminifera Packstone	Skeletal, Matrix	Foraminifera, Brachiopods		medium gray	109	1.49	-3.12	0.011	0.04	X		
316	A	44 B	Desmoinesian	308.45	70	Siltstone		Sand, Matrix	Brachiopods, Crinoids	70% Silt	light gray	359	0.45	-7.48	0.012	0.028			
319	A	45 B	Desmoinesian	308.37	5	Calcisiltstone		Matrix, Calcisilt, Sand		5% Silt	light gray	68	1.30	-7.92	0.013	0.014			
321	A	46 B	Desmoinesian	308.33	0	Wackestone		Matrix, Skeletal			gray	68	0.56	-4.62	0.016	0.058			
322	A	47 B	Desmoinesian	308.30	70	Siltstone		Sand, Matrix		White chert nodules, 70% Silt	gray		-0.13	-5.78	0.025	0.0285			
322	D	47 B	Desmoinesian	308.30	70	Siltstone		Sand, Matrix		White chert nodules, 70% Silt	gray	244	-0.12	-6.64	0.023	0.037			
322	D	47 B	Desmoinesian	308.30	70	Siltstone		Sand, Matrix		White chert nodules, 70% Silt	gray	296	-0.14	-4.92	0.027	0.02			
323	A	48 B	Desmoinesian	308.28	20	Mudstone	Silty Mudstone	Matrix, Silt			light gray	120	-1.33	-7.22	0.008	0.033	X		
324	A	49 B	Desmoinesian	308.26	85	Siltstone		Sand, Matrix		Black chert, 85%	gray		-0.66	-6.61	0.023	0.049			
324	D	49 B	Desmoinesian	308.26	85	Siltstone		Sand, Matrix		Black chert, 85%	gray	549	-0.74	-6.80	0.026	0.049			
324	D	49 B	Desmoinesian	308.26	85	Siltstone		Sand, Matrix		Black chert, 85%	gray	462	-0.58	-6.41	0.02	0.049			
325	A	50 B	Desmoinesian	308.23	90	Sandstone		Sand, Matrix		90% Sand, Chert nodules	light gray	409	-0.66	-6.29	0.018	0.013			
327	A	52 B	Desmoinesian	308.19	80	Siltstone		Sand, Matrix		80% Very fine sand, Black chert nodules	medium gray	446	0.18	-4.90	0.02	0.031			
328	A	53 B	Desmoinesian	308.16	75	Siltstone		Sand, Matrix		75% Very fine sand	medium gray	289	0.11	-5.29	0.011	0.012			
328.5	A	54 B	Desmoinesian	308.15	5	Wackestone	Skeletal Wackestone	Matrix, Skeletal	Crinoids, Bryozoans, Foraminifera		medium gray	103	1.01	-3.11	0.003	0.014	X		
329	A	55 B	Desmoinesian	308.14	15	Wackestone		Matrix, Sand	Brachiopods	15% Silt	light gray	152	0.77	-4.05	0.015	0.026			
329.5	A	56 B	Desmoinesian	308.13	40	Wackestone		Sand, Matrix		40% Silt	gray	139	0.85	-4.45	0.016	0.01			
330	A	57 B	Desmoinesian	308.11	100	Wackestone	Rugos Coral Wackestone	Chert	Horn corals		dark gray						X		
333	A	58 B	Desmoinesian	308.04	15	Wackestone		Matrix, Skeletal, Sand	Brachiopods, Foraminifera	15% Silt, Highly fractured	gray	144	1.76	-3.89	0.016	0.028			

APPENDIX A - Continued

Sample (Meter + Letter)		Hand Sample Number	North American Stage	Age GTS 2004	% Silt/Sand	Classification	Expanded Classification	Material Sampled in order of Abundance	Fossils and Clasts	Other Notes (Hand Sample, unless specified)	Color	Powder Weight (ug) for Analysis	$\delta^{13}C$ vs VPDB	$\delta^{18}O$ vs VPDB	$\delta^{13}C$ 1σ	$\delta^{18}O$ 1σ	Thin Section	BSE Image	CL Image
333.5	A	59 B	Desmoinesian	308.03	5	Wackestone	Skeletal Wackestone	Matrix, Skeletal	Brachiopods, Crinoids, Spines, Algae?		medium gray	80	1.94	-4.87	0.019	0.031	X		
334	A	60 B	Desmoinesian	308.02	50	Packstone		Matrix, Sand		50% Silt	gray	120	2.29	-3.48	0.014	0.015			
334.5	A	61 B	Desmoinesian	308.01	5	Wackestone	Foraminifera Wackestone	Matrix, Skeletal	Foraminifera, Brachiopods, Crinoids		light gray	107	2.39	-3.45	0.016	0.015	X		
335	A	62 B	Desmoinesian	308.00	5	Wackestone		Matrix, Skeletal, Sand		2-3% Silt	dark gray	110	1.78	-3.72	0.007	0.031			
335.5	A	63 B	Desmoinesian	307.98	10	Calcisiltstone		Calcisilt, Silt		10% Silt, Bedding visible (1-10 cm)	gray	63	2.00	-4.96	0.011	0.02			
336	A	64 B	Desmoinesian	307.97	5	Wackestone	Skeletal Wackestone	Matrix, Skeletal	Foraminifera, Brachiopods	Silt	light gray	64	3.00	-2.82	0.006	0.034	X		
336.5	A	65 B	Desmoinesian	307.96	0	Wackestone		Matrix, Skeletal	Brachiopod, Spines	Highly fractured	light gray	107	2.46	-3.32	0.018	0.025			
337	A	66 B	Desmoinesian	307.95	50	Wackestone		Matrix, Sand		50% Silt	gray		2.58	-3.64	0.0205	0.029			
337	D	66 B	Desmoinesian	307.95	50	Wackestone		Matrix, Sand		50% Silt	gray	135	2.60	-3.63	0.025	0.029			
337	D	66 B	Desmoinesian	307.95	50	Wackestone		Matrix, Sand		50% Silt	gray	131	2.56	-3.66	0.016	0.029			
337.5	A	67 B	Desmoinesian	307.94	15	Packstone		Matrix, Skeletal	Coated grains, Foraminifera, Crinoids, Brachiopods, Bivalves	early stage pressure solution seams	medium gray	101	2.59	-3.92	0.02	0.038	X		
338	A	68 B	Desmoinesian	307.92	50	Siltstone	Siltstone	Silt, M		Silt	medium gray	160	1.89	-5.20	0.025	0.025	X		
339	A	69 B	Desmoinesian	307.90	75	Siltstone		Sand, K, M	Crinoids	75% Silt, Epoxied	gray	456	1.99	-5.60	0.012	0.046			
340	A	70 B	Desmoinesian	307.88	40	Wackestone		Matrix, Sand		40%, Black chert nodules	dark gray	130	1.51	-4.31	0.014	0.009			
341	A	1 C	Desmoinesian	307.85	10	Mudstone		Matrix					2.26	-3.73					
342	A	2 C	Desmoinesian	307.83	10	Packstone	Skeletal Packstone	Fine Black Matrix, Skeletal	Foraminifera, Crinoids, Brachiopod fragments, Spines, Algae, Silt					-4.28			X		
343	A	3 C	Desmoinesian	307.81	50	Mudstone		Matrix, Sand	Brachiopods, Spines, Colonial corals	Possible In-situ colonial corals, Sample was epoxied	dark gray	101	2.85	-3.29	0.019	0.023	X		
343	A	3 C	Desmoinesian	307.81	50	Mudstone		Matrix, Sand	Brachiopods, Spines, Colonial corals	Possible In-situ colonial corals, Sample was epoxied	dark gray		0.45	-4.52					
343	D	3 C	Desmoinesian	307.81	50	Mudstone		Matrix, Sand	Brachiopods, Spines, Colonial corals	Possible In-situ colonial corals, Sample was epoxied	dark gray		0.53	-4.62					
343	D	3 C	Desmoinesian	307.81	50	Mudstone		Matrix, Sand	Brachiopods, Spines, Colonial corals	Possible In-situ colonial corals, Sample was epoxied	dark gray		0.37	-4.41					
344	A	4 C	Desmoinesian	307.78	40	Mudstone	Cherty Mudstone	Matrix	10% Quartz silt	Chert nodules in black mud, Fracture filled with calcite			2.27	-3.48			X		X
345	A	5 C	Desmoinesian	307.76	10	Siltstone		Matrix		Chert nodules in black mud			1.56	-5.39			X		
346	A	6 C	Desmoinesian	307.73	0	Packstone	Brachiopod Packstone	Matrix, Skeletal	Brachiopods, Crinoids, Fenestrate bryozoan, Foraminifera				2.71	-3.73			X		X
346	B	6 C	Desmoinesian	307.73	0	Cement - Fracture		Cement		Possibly gathered 15%			0.40	-13.74					X

APPENDIX A - Continued

Sample (Meter + Letter)		Hand Sample Number	North American Stage	Age GTS 2004	% Silt/Sand	Classification	Expanded Classification	Material Sampled in order of Abundance	Fossils and Clasts	Other Notes (Hand Sample, unless specified)	Color	Powder Weight (ug) for Analysis	$\delta^{13}C$ vs VPDB	$\delta^{18}O$ vs VPDB	$\delta^{13}C$ 1σ	$\delta^{18}O$ 1σ	Thin Section	BSE Image	CL Image
										matrix with cement									
346	D	6 C	Desmoinesian	307.73	0	Cement - Fracture		Cement		Possibly gathered 15% matrix with cement			0.44	-13.86			X		X
346	D	6 C	Desmoinesian	307.73	0	Cement - Fracture		Cement		Possibly gathered 15% matrix with cement			0.36	-13.62			X		X
347	A	7 C	Desmoinesian	307.71	40	Mudstone		Matrix					2.83	-4.97					
348	A	8 C	Desmoinesian	307.69	40	Mudstone		Matrix		Stylolites in black mud			2.10	-4.53					
349	A	9 C	Desmoinesian	307.66	40	Mudstone		Matrix		Contains cement filled fractures			2.50	-4.68					
349	D	9 C	Desmoinesian	307.66	40	Mudstone		Matrix		Contains cement filled fractures			2.62	-3.79					
349	D	9 C	Desmoinesian	307.66	40	Mudstone		Matrix		Contains cement filled fractures			2.38	-5.57					
350	A	10 C	Desmoinesian	307.64	20	Mudstone	Mudstone	Matrix	20% Quartz silt, Clasts of calcite	Black mud with quartz and calcite clasts			2.84	-4.67			X		
351	A	11 C	Desmoinesian	307.62	10	Wackestone	Mud Wackestone	Matrix	Crinoids, Foraminifera, Quartz silt, Spines, Fenestrate bryozoan	Analysis taken from mud			3.02	-3.54			X		
352	A	12 C	Desmoinesian	307.59	30	Siltstone		Matrix	Crinoids, Burrows	Analysis taken from black mud			2.49	-5.13			X		
352	D	12 C	Desmoinesian	307.59	30	Siltstone		Matrix	Crinoids, Burrows	Analysis taken from black mud			2.36	-5.38			X		
352	D	12 C	Desmoinesian	307.59	30	Siltstone		Matrix	Crinoids, Burrows	Analysis taken from black mud			2.62	-4.89			X		
353	A	13 C	Desmoinesian	307.57	20	Mudstone	Silty Mudstone	Matrix		Silty gray carbonate with growths, Quartz intergrowths			2.86	-1.03			X		
353	D	13 C	Desmoinesian	307.57	20	Mudstone	Silty Mudstone	Matrix		Silty gray carbonate with growths			2.81	-1.03			X		
353	D	13 C	Desmoinesian	307.57	20	Mudstone	Silty Mudstone	Matrix		Silty gray carbonate with growths			2.92	-1.04			X		
354	A	14 C	Desmoinesian	307.55	40	Mudstone		Matrix		Black Mud			1.77	-4.77					
354.5	A	15 C	Desmoinesian	307.53	10	Wackestone	Crinoidal Brachiopod Wackestone	Matrix, Sand	Crinoids, Brachiopods, Spines	Sandy matrix			3.12	-3.27			X		
354.5	D	15 C	Desmoinesian	307.53	10	Wackestone	Crinoidal Brachiopod Wackestone	Matrix, Sand	Crinoids, Brachiopods, Spines	Sandy matrix			3.13	-3.39			X		
354.5	D	15 C	Desmoinesian	307.53	10	Wackestone	Crinoidal Brachiopod Wackestone	Matrix, Sand	Crinoids, Brachiopods, Spines	Sandy matrix			3.11	-3.14			X		
355	A	16 C	Desmoinesian	307.52	20	Wackestone/ Packstone	Crinoidal Wackestone /Packstone	Mud, Matrix	Crinoids, Spines, Foraminifera	70% Packstone, 30% Wackestone, Black mud			2.22	-3.76			X		
355.5	A	17 C	Desmoinesian	307.51	65	Siltstone	Quartz Siltstone	Sand, Cement		Quartz silt			1.09	-5.17			X		
356	A	18 C	Desmoinesian	307.50	35	Packstone	Sandy Packstone	Sand, Skeletal, Matrix	Brachiopods, Unidentified skeletal grains	50% Fine Sand			-0.82	-8.63			X		
356	D	18 C	Desmoinesian	307.50	35	Packstone	Sandy Packstone	Sand, Skeletal, Matrix	Brachiopods, Unidentified skeletal grains	50% Fine Sand			-0.71	-8.50			X		
356	D	18 C	Desmoinesian	307.50	35	Packstone	Sandy Packstone	Sand, Skeletal,	Brachiopods, Unidentified	50% Fine Sand			-0.94	-8.76			X		

APPENDIX A - Continued

Sample (Meter + Letter)		Hand Sample Number	North American Stage	Age GTS 2004	% Silt/Sand	Classification	Expanded Classification	Material Sampled in order of Abundance	Fossils and Clasts	Other Notes (Hand Sample, unless specified)	Color	Powder Weight (ug) for Analysis	$\delta^{13}C$ vs VPDB	$\delta^{18}O$ vs VPDB	$\delta^{13}C$ 1σ	$\delta^{18}O$ 1σ	Thin Section	BSE Image	CL Image
								Matrix	skeletal grains										
356.5	A	19 C	Desmoinesian	307.49	50	Packstone	Sandy Packstone	Sandy, Matrix	Micrite, Foraminifera, Algae	50% or more medium grained sand			1.30	-4.61			X		
357	A	20 C	Desmoinesian	307.47	65	Packstone	Quartz-dominated Packstone	Sandy, Skeletal, Matrix	Crinoids, Foraminifera	very sandy, lots of skeletal fragments			1.53	-4.79			X		
358	A	21 C	Desmoinesian	307.45	35	Packstone	Silty Bioclastic Packstone	Matrix, Sand	Foraminifera, Unidentified skeletal fragments	Very silty, Sampled mud			0.98	-4.01			X		
362	A	22 C	Desmoinesian	307.36	20	Mudstone		Matrix					0.34	-4.56					
362	D	22 C	Desmoinesian	307.36	20	Mudstone		Matrix					0.33	-4.63					
362	D	22 C	Desmoinesian	307.36	20	Mudstone		Matrix					0.35	-4.49					
363	A	23 C	Desmoinesian	307.33	20	Mudstone	Carbonate Mudstone	Matrix, Skeletal	Unidentified skeletal fragments	Fractured			1.43	-4.35			X		
364	A	24 C	Desmoinesian	307.31	25	Wackestone	Silty Brachiopod Wackestone	Sand, Skeletal, Matrix	Brachiopods, Crinoids	15% Very fine quartz silt			1.05	-5.37			X		
365	A	25 C	Desmoinesian	307.28	40	Wackestone		Matrix, Sand		Fine grained	gray		1.15	-5.16					
365	D	25 C	Desmoinesian	307.28	40	Wackestone		Matrix, Sand		Fine grained	gray		1.06	-5.15					
365	D	25 C	Desmoinesian	307.28	40	Wackestone		Matrix, Sand		Fine grained	gray		1.24	-5.16					
366	A	26 C	Desmoinesian	307.26	20	Wackestone	Fractured Wackestone	Matrix, Sand	Foraminifera	Large calcite filled fractures, 20% Quartz silt			1.78	-3.85			X		X
368	A	27 C	Desmoinesian	307.21	30	Mudstone		Matrix		Sampled black fine mud			-0.70	-6.36					
368	D	27 C	Desmoinesian	307.21	30	Mudstone		Matrix		Sampled black fine mud			-0.71	-6.37					
368	D	27 C	Desmoinesian	307.21	30	Mudstone		Matrix		Sampled black fine mud			-0.69	-6.34					
369	A	28 C	Desmoinesian	307.19	40	Mudstone		Matrix		Sampled black/gray fine mud			1.87	-4.13					
370	A	29 C	Desmoinesian	307.17	70	Siltstone	Quartz Siltstone	Sand, Matrix	Crinoids, Unidentified skeletal fragments	Quartz range from silt to medium sized grains			2.52	-5.01			X		
371	A	30 C	Desmoinesian	307.14	55	Mudstone	Sandy Mudstone	Matrix, Sand	Unidentified skeletal fragments	Sample was layered with lots of sand			2.69	-4.51			X		
372	A	31 C	Desmoinesian	307.12	45	Wackestone	Sandy Wackestone	Matrix, Skeletal	Crinoids, Bryozoans, Foraminifera	50% Skeletal, 50% Mud,			3.32	-5.35			X		
373	A	32 C	Desmoinesian	307.10	20	Packstone	Skeletal Packstone	Skeletal, Matrix	Foraminifera, Brachiopods, Crinoids, Bryozoans	50-70% skeletal grains			1.75	-5.10			X		
373	D	32 C	Desmoinesian	307.10	20	Packstone	Skeletal Packstone	Skeletal, Matrix	Foraminifera, Brachiopods, Crinoids, Bryozoans	50-70% skeletal grains			1.71	-5.73			X		
373	D	32 C	Desmoinesian	307.10	20	Packstone	Skeletal Packstone	Skeletal, Matrix	Foraminifera, Brachiopods, Crinoids, Bryozoans	50-70% skeletal grains			1.78	-4.47			X		
374	A	33 C	Desmoinesian	307.07	5	Mudstone	Brachiopod Mudstone	Matrix, Sand	Brachiopods, Crinoids	Minor amounts of sand				-4.18			X		
375	A	34 C	Desmoinesian	307.05	30	Mudstone		Matrix		Sampled gray fine matrix			0.47	-7.34					
375	D	34 C	Desmoinesian	307.05	30	Mudstone		Matrix		Sampled gray fine matrix			0.54	-6.83					
375	D	34 C	Desmoinesian	307.05	30	Mudstone		Matrix		Sampled gray fine matrix			0.40	-7.85					
377	A	35 C	Desmoinesian	307.00	20	Wackestone	Vuggy Wackestone	Matrix		Vuggy with tertiary calcite filled fractures,			1.92	-7.01			X		X

APPENDIX A - Continued

Sample (Meter + Letter)		Hand Sample Number	North American Stage	Age GTS 2004	% Silt/Sand	Classification	Expanded Classification	Material Sampled in order of Abundance	Fossils and Clasts	Other Notes (Hand Sample, unless specified)	Color	Powder Weight (ug) for Analysis	$\delta^{13}C$ vs VPDB	$\delta^{18}O$ vs VPDB	$\delta^{13}C$ 1σ	$\delta^{18}O$ 1σ	Thin Section	BSE Image	CL Image
378	A	36 C	Desmoinesian	306.98	30	Mudstone		Matrix	gray, upper non-layered part	Sampled gray fine mud Sampled upper non-layered part	gray		1.08	-6.46					
380	A	37 C	Desmoinesian	306.93	20	Wackestone	Crinoidal Wackestone	Skeletal, Matrix	Crinoids, Micritized ooids/pellets, Foraminifera, Bryozoans, Algae				2.99	-3.84			X		
380.5	A	38 C	Desmoinesian	306.92	20	Wackestone		Matrix	gray matrix, away from concretions	Sample was epoxied			4.02	-3.75					
381	A	39 C	Desmoinesian	306.91	1	Wackestone	Vuggy Wackestone	Matrix	Bryozoans, Foraminifera, Algae, Quartz	Sampled in matrix and avoided chert nodules, Large calcite filled vugs			1.31				X		X
382	A	40 C	Desmoinesian	306.88	5	Wackestone	Vuggy Micritized Wackestone	Matrix	Foraminifera, Brachiopods, Algae	Vuggy, Micritized grains			3.59	-4.15			X		
383	A	41 C	Desmoinesian	306.86	10	Packstone	Crinoidal Packstone	Skeletal, Matrix	Crinoids, Brachiopods, Arthropod legs, Foraminifera	Sample is fractured			3.36	-3.38			X		
384	A	42 C	Desmoinesian	306.83	5	Wackestone	Wackestone	Matrix	Algae, Brachiopods, Bryozoans	Sampled mud, Contains calcite intergrowths			2.76	-6.18			X		X
386	A	43 C	Desmoinesian	306.79	15	Packstone	Brachiopod Packstone	Matrix, Skeletal	Brachiopods, Bryozoans, Crinoids, Foraminifera	Stylolites			2.49	-4.38			X		
387	A	44 C	Desmoinesian	306.76	5	Wackestone	Algal Wackestone	Matrix	Algae, Bryozoans, Foraminifera, Brachiopods, Quartz	Sample is fractured			2.74				X		
388	A	45 C	Desmoinesian	306.74	5	Wackestone	Muddy Wackestone	Matrix	Brachiopods, Crinoids	Micrite			2.40	-3.76			X		X
390	A	46 C	Desmoinesian	306.69	5	Wackestone	Foraminifera Brachiopod Bryozoan Wackestone	Matrix	Foraminifera, Brachiopods, Bryozoans, Crinoids, Arthropod legs	Sampled Mud			2.41	-3.32			X		
391	A	47 C	Desmoinesian	306.67	5	Wackestone/ Packstone	Foraminifera Crinoidal Packstone and Skeletal Wackestone	Matrix, Skeletal	Foraminifera, Crinoids, Brachiopods, Bryozoans	Sample contains fractures, Sampling avoided fractures			2.35	-3.48			X		X
392	A	48 C	Desmoinesian	306.65	0	Wackestone	Fractured Wackestone	Matrix, Skeletal, Microfractures	Crinoids, Bryozoans	Highly fractured			2.73	-1.83			X		
392	D	48 C	Desmoinesian	306.65	0	Wackestone	Fractured Wackestone	Matrix, Skeletal, Microfractures	Crinoids, Bryozoans	Highly fractured			2.65	-1.97			X		
392	D	48 C	Desmoinesian	306.65	0	Wackestone	Fractured Wackestone	Matrix, Skeletal, Microfractures	Crinoids, Bryozoans	Highly fractured			2.82	-1.69			X		
393	A	49 C	Desmoinesian	306.62	30	Mudstone		Matrix		Sampled medium gray fine matrix	medium gray		1.76	-3.97					
394	A	50 C	Desmoinesian	306.60	40	Wackestone	Sandy Wackestone	Sand, Matrix	Crinoids, Green Algae, Brachiopods, Foraminifera	Very Sandy			1.68	-4.23			X		
395	A	51 C	Desmoinesian	306.57	25	Wackestone	Silty Wackestone	Silt, Matrix	Crinoids, Foraminifera,	Silty, Highly altered			2.57	-5.53			X		

APPENDIX A - Continued

Sample (Meter + Letter)		Hand Sample Number	North American Stage	Age GTS 2004	% Silt/Sand	Classification	Expanded Classification	Material Sampled in order of Abundance	Fossils and Clasts	Other Notes (Hand Sample, unless specified)	Color	Powder Weight (ug) for Analysis	$\delta^{13}C$ vs VPDB	$\delta^{18}O$ vs VPDB	$\delta^{13}C$ 1σ	$\delta^{18}O$ 1σ	Thin Section	BSE Image	CL Image
									Brachiopods, Unidentified fragments										
396	A	52 C	Desmoinesian	306.55	45	Wackestone	Crinoidal Wackestone	Matrix, Sand, Cement, Skeletal	Crinoids	Sandy, Cement			1.85	-6.99			X		X
397	A	53 C	Desmoinesian	306.53	40	Packstone	Bryozoan Packstone	Matrix	Bryozoans, Crinoids, Brachiopods	Sample contains fractures			2.74	-3.69			X		
397	B	53 C	Desmoinesian	306.53	0	Cement - Void		Cement		Calcite nodules				-2.94			X		
398	A	54 C	Desmoinesian	306.50	15	Wackestone/ Packstone	Sandy Crinoidal Wackestone/ Packstone	Skeletal, Sand, Matrix	Crinoids, Bryozoans	Sandy, 30% Skeletal			2.76	-4.23			X		
399	A	55 C	Desmoinesian	306.48	10	Wackestone	Bryozoan Brachiopod Wackestone	Matrix, Sand, Skeletal	Brachiopods, Bryozoans, Crinoids	Sampled sandy wackestone (30% skeletal grains)			2.89	-4.98			X		
400	A	56 C	Desmoinesian	306.46	40	Wackestone		Matrix		Drilled black/brown mud away from dark altered material			2.92	-4.38					
401	A	57 C	Desmoinesian	306.43	35	Wackestone	Bryozoan Wackestone/ Mudstone	Matrix, Skeletal, Fractures	Bryozoans	Lots of microfractures, 30% Skeletal			2.49	-4.01			X		
402	A	58 C	Desmoinesian	306.41	20	Wackestone	Wackestone	Matrix, Sand	Bryozoans, Brachiopods, Crinoids	Sampled sandy gray mud			2.15	-4.86			X		
402	D	58 C	Desmoinesian	306.41	20	Wackestone	Wackestone	Matrix, Sand	Bryozoans, Brachiopods, Crinoids	Sampled sandy gray mud			2.12	-4.77			X		
402	D	58 C	Desmoinesian	306.41	20	Wackestone	Wackestone	Matrix, Sand	Bryozoans, Brachiopods, Crinoids, Foraminifera	Sampled sandy gray mud			2.18	-4.96			X		
403	A	59 C	Desmoinesian	306.38	20	Wackestone		Matrix			gray		2.88	-1.04					
404	A	60 C	Desmoinesian	306.36	5	Wackestone	Calcite Wackestone	Matrix	Crinoids, Calcite nodules, Brachiopods	Hand sample contains chert nodules	gray		-0.19	-6.41			X	X	X
404	D	60 C	Desmoinesian	306.36	5	Wackestone	Calcite Wackestone	Matrix	Crinoids, Calcite nodules, Brachiopods	Hand sample contains chert nodules	gray		-0.21	-6.76			X	X	X
404	D	60 C	Desmoinesian	306.36	5	Wackestone	Calcite Wackestone	Matrix	Crinoids, Calcite nodules, Brachiopods	Hand sample contains chert nodules	gray		-0.16	-6.05			X	X	X
405	A	61 C	Desmoinesian	306.34	5	Packstone	Crinoidal Bryozoan Packstone	Skeletal	Crinoids, Bryozoans, Algae, Foraminifera, Unidentified skeletal grains, Gastropods				3.05	-3.93			X		
406	A	62 C	Desmoinesian	306.31	2	Packstone	Crinoidal Algal Packstone	Skeletal	Crinoids, Algae, Bryozoans, Spines, Foraminifera, Unidentified skeletal grains, Gastropods	100% Skeletal			3.07	-3.80			X		X
407	A	63 C	Desmoinesian	306.29	10	Packstone	Silty Bryozoan Crinoidal Packstone	Skeletal	Bryozoans, Crinoids, Brachiopods, Foraminifera, Unidentified skeletal grains	100% Skeletal, Bottom is siltstone			2.13	-3.88			X		X
407	D	63 C	Desmoinesian	306.29	10	Packstone	Silty Bryozoan Crinoidal Packstone	Skeletal	Bryozoans, Crinoids, Brachiopods,	100% Skeletal, Bottom is siltstone			2.18	-3.85			X		X

APPENDIX A - Continued

Sample (Meter + Letter)		Hand Sample Number	North American Stage	Age GTS 2004	% Silt/Sand	Classification	Expanded Classification	Material Sampled in order of Abundance	Fossils and Clasts	Other Notes (Hand Sample, unless specified)	Color	Powder Weight (ug) for Analysis	$\delta^{13}C$ vs VPDB	$\delta^{18}O$ vs VPDB	$\delta^{13}C$ 1σ	$\delta^{18}O$ 1σ	Thin Section	BSE Image	CL Image
407	D	63 C	Desmoinesian	306.29	10	Packstone	Silty Bryozoan Crinoidal Packstone	Skeletal	Foraminifera, Unidentified skeletal grains Bryozoans, Crinoids, Brachiopods, Foraminifera, Unidentified skeletal grains	100% Skeletal, Bottom is siltstone			2.07	-3.92			X		X
408	A	64 C	Desmoinesian	306.27	5	Wackestone	Nodular Calcite Wackestone	Matrix, Skeletal	Crinoids, Bryozoans, Brachiopods	Hand sample contains evaporite nodules in very fine wackestone			1.19	-6.85			X		X
408	B	64 C	Desmoinesian	306.27	0	Cement - Evaporite	Calcite Nodule	Cement		Sampled calcite from evaporite nodule							X		X
408	D	64 C	Desmoinesian	306.27	5	Wackestone	Nodular Calcite Wackestone	Matrix, Skeletal	Crinoids, Bryozoans, Brachiopods	Hand sample contains evaporite nodules in very fine wackestone			1.33	-6.84			X		X
408	D	64 C	Desmoinesian	306.27	5	Wackestone	Nodular Calcite Wackestone	Matrix, Skeletal	Crinoids, Bryozoans, Brachiopods	Hand sample contains evaporite nodules in very fine wackestone			1.05	-6.86			X		X
409	A	65 C	Desmoinesian	306.24	5	Wackestone	Muddy Wackestone	Sand, Matrix	Brachiopods, Crinoids, Bryozoans	Sandy, Possibly altered			-0.15	-7.18			X		
409	D	65 C	Desmoinesian	306.24	5	Wackestone	Muddy Wackestone	Sand, Matrix	Brachiopods, Crinoids, Bryozoans	Sandy, Possibly altered			-0.01	-7.32			X		
409	D	65 C	Desmoinesian	306.24	5	Wackestone	Muddy Wackestone	Sand, Matrix	Brachiopods, Crinoids, Bryozoans	Sandy, Possibly altered			-0.28	-7.05			X		
410	A	66 C	Desmoinesian	306.22	2	Packstone	Brachiopod Packstone	Skeletal, Matrix	Brachiopods, Spines, Crinoids, Foraminifera, Unidentified skeletal grains	Drilled gray mud along bedding			3.02	-3.86			X		
411	A	67 C	Desmoinesian	306.19	10	Mudstone		Matrix		Drilled gray mud along bedding			2.92	-4.15					
412	A	68 C	Desmoinesian	306.17	10	Mudstone		Matrix		Drilled gray mud along bedding			0.69	-8.46					
412	D	68 C	Desmoinesian	306.17	10	Mudstone		Matrix		Drilled gray mud along bedding			0.79	-8.62					
412	D	68 C	Desmoinesian	306.17	10	Mudstone		Matrix		Drilled gray mud along bedding			0.76	-8.32					
412	D	68 C	Desmoinesian	306.17	10	Mudstone		Matrix		Drilled gray mud along bedding			0.52	-8.45					
413	A	69 C	Desmoinesian	306.15	15	Wackestone	Muddy Wackestone	Matrix, Skeletal	Bryozoan, Crinoids	Drilled mud with about 10% skeletal fragments			1.81	-5.22			X		
414	A	70 C	Desmoinesian	306.12	2	Wackestone	Wackestone	Matrix	Intraclasts, Foraminifera, Bryozoans, Coral fragments	50% of hand sample is chert that has replaced calcite, Includes intergrowths of calcite and micrite			4.60	-4.64			X		
415	A	71 C	Desmoinesian	306.10	1	Wackestone	Wackestone	Matrix	Pellets, Brachiopods, Bryozoans, Foraminifera	Hand sample contains cement filled fractures and voids			4.17	-6.76			X		

APPENDIX A - Continued

Sample (Meter + Letter)		Hand Sample Number	North American Stage	Age GTS 2004	% Silt/Sand	Classification	Expanded Classification	Material Sampled in order of Abundance	Fossils and Clasts	Other Notes (Hand Sample, unless specified)	Color	Powder Weight (ug) for Analysis	$\delta^{13}C$ vs VPDB	$\delta^{18}O$ vs VPDB	$\delta^{13}C$ 1σ	$\delta^{18}O$ 1σ	Thin Section	BSE Image	CL Image
416	A	72 C	Desmoinesian	306.08	3	Packstone	Pelletal Packstone	Matrix	Pellets, Foraminifera, Bryozoans, Brachiopods	Hand sample contains cement filled fractures, Contains gypsum and coarse calcite			4.82	-4.42			X		X
417	A	73 C	Desmoinesian	306.05	1	Wackestone	Pelletal Foraminifera Wackestone	Calcite	Pellets, Foraminifera, Crinoids, Brachiopods	Hand sample contains cement filled fractures, Contains calcite intergrowths			4.37	-3.42			X		
418	A	74 C	Desmoinesian	306.03	7	Packstone	Crinoidal Packstone	Skeletal, Matrix	Crinoids, Foraminifera, Brachiopods, Bryozoans				3.78	-5.28			X		
418	D	74 C	Desmoinesian	306.03	7	Packstone	Crinoidal Packstone	Skeletal, Matrix	Crinoids, Foraminifera, Brachiopods, Bryozoans				3.73				X		
418	D	74 C	Desmoinesian	306.03	7	Packstone	Crinoidal Packstone	Skeletal, Matrix	Crinoids, Foraminifera, Brachiopods, Bryozoans				3.84	-5.28			X		
419	A	75 C	Desmoinesian	306.01	1	Packstone	Foraminifera Packstone	Matrix, Skeletal	Foraminifera, Algae, Crinoids				4.38	-2.88			X		X
420	A	76 C	Desmoinesian	305.98	5	Packstone	Brachiopod Foraminifera Packstone	Skeletal, Matrix, Microfractures	Brachiopods, Foraminifera, Crinoids, Bryozoans	Hand sample contains microfractures, 50% Skeletal			3.51	-3.71			X		
421	A	77 C	Desmoinesian	305.96	10	Mudstone		Matrix		Drilled lighter gray material (finer grained)									
421	B	77 C	Desmoinesian	305.96	0	Cement - Fracture		Cement		Cement from fracture fill			3.26						
422	A	78 C	Desmoinesian	305.93	30	Mudstone		Matrix		Drilled dark gray mud	dark gray		3.63	-3.50					
423	A	79 C	Desmoinesian	305.91	30	Mudstone		Matrix		Drilled darker mudstone above lighter mudstone			3.55	-3.97					
424	A	80 C	Desmoinesian	305.89	35	Mudstone		Matrix		Drilled dark gray mud			3.75	-3.09					
425	A	81 C	Desmoinesian	305.86	40	Mudstone		Matrix		Hand sample contains fractures			3.56	-3.99					
425	B	81 C	Desmoinesian	305.86	0	Cement - Fracture		Cement		Analysis of fracture fill			3.62	-4.61					
426	A	82 C	Desmoinesian	305.84	5	Mudstone	Micritic Mudstone	Matrix	Bryozoans				3.80	-4.34			X		
426	D	82 C	Desmoinesian	305.84	5	Mudstone	Micritic Mudstone	Matrix	Bryozoans				3.82	-4.70			X		
426	D	82 C	Desmoinesian	305.84	5	Mudstone	Micritic Mudstone	Matrix	Bryozoans				3.78	-3.99			X		
427	A	83 C	Desmoinesian	305.82	30	Mudstone		Matrix		Sample gray mud, Avoided white material			3.20	-5.26					
428	A	84 C	Desmoinesian	305.79	1	Wackestone	Fractured Micritic Wackestone	Matrix	Foraminifera, Crinoids	Hand sample contains fractures			3.66	-4.96			X		
429	A	85 C	Desmoinesian	305.77	5	Packstone	Sandy Packstone	Sand, Matrix	Crinoids, Pellets, Sponge spicules?	Sandy			3.56	-4.23			X		X
429	C	85 C	Desmoinesian	305.77	5	Wackestone	Micritic Wackestone	Matrix	Foraminifera, Brachiopods, Crinoids, Gastropods, Sponge spicules?	Stylolites			1.88	-6.29			X		X
430	A	86 C	Desmoinesian	305.74	0	Wackestone	Micritic Wackestone	Matrix		Hand sample contains calcite and silica filled veins			3.43	-4.86			X		
431	A	87 C	Desmoinesian	305.72	35	Wackestone	Sandy Wackestone	Matrix, Skeletal	Bryozoans	Sandy			0.91	-6.24			X		
432	A	88 C	Desmoinesian	305.70	2	Wackestone	Wackestone	Matrix, Skeletal	Dark organic matter	Drilled micrite with			0.00	-7.57			X		

APPENDIX A - Continued

Sample (Meter + Letter)		Hand Sample Number	North American Stage	Age GTS 2004	% Silt/Sand	Classification	Expanded Classification	Material Sampled in order of Abundance	Fossils and Clasts	Other Notes (Hand Sample, unless specified)	Color	Powder Weight (ug) for Analysis	$\delta^{13}C$ vs VPDB	$\delta^{18}O$ vs VPDB	$\delta^{13}C$ 1σ	$\delta^{18}O$ 1σ	Thin Section	BSE Image	CL Image
432	D	88 C	Desmoinesian	305.70	2	Wackestone	Wackestone	Matrix, Skeletal		about 10% skeletal, Lots of calcite intergrowths Drilled micrite with about 10% skeletal, Lots of calcite intergrowths			0.01	-7.79			X		
432	D	88 C	Desmoinesian	305.70	2	Wackestone	Wackestone	Matrix, Skeletal		Drilled micrite with about 10% skeletal, Lots of calcite intergrowths			0.06	-7.60			X		
432	D	88 C	Desmoinesian	305.70	2	Wackestone	Wackestone	Matrix, Skeletal		Drilled micrite with about 10% skeletal, Lots of calcite intergrowths			-0.07	-7.33			X		
433	A	89 C	Desmoinesian	305.67	10	Wackestone	Bryozoan Wackestone	Matrix	Bryozoans, Dead oil	Drilled micrite with about 10% skeletal, Bryozoans replaced with silica			1.91	-6.47			X		
433	D	89 C	Desmoinesian	305.67	10	Wackestone	Bryozoan Wackestone	Matrix	Bryozoans, Dead oil	Drilled micrite with about 10% skeletal, Bryozoans replaced with silica			2.10	-6.96			X		
433	D	89 C	Desmoinesian	305.67	10	Wackestone	Bryozoan Wackestone	Matrix	Bryozoans, Dead oil	Drilled micrite with about 10% skeletal, Bryozoans replaced with silica			1.71	-5.97			X		
434	A	90 C	Missourian	305.65	2	Wackestone	Bryozoan Wackestone	Matrix, Skeletal	Bryozoans, Dark organic matter in pores	Drilled micrite with about 10% skeletal			1.33	-5.93			X		
434	D	90 C	Missourian	305.65	2	Wackestone		Matrix, Skeletal	Bryozoans	Drilled micrite with about 10% skeletal			1.39	-5.98			X		
434	D	90 C	Missourian	305.65	2	Wackestone		Matrix, Skeletal	Bryozoans	Drilled micrite with about 10% skeletal			1.28	-5.87			X		
435	A	91 C	Missourian	305.64	5	Packstone		Silt, Cement	Crinoids	Dolomite (30% dolomite inclusions), Epoxied	gray	76	2.91	-1.13	0.004	0.031	X		
436	A	92 C	Missourian	305.62	30	Packstone	Bryozoan Packstone	Matrix, Skeletal	Bryozoans, Crinoids, Brachiopods, Foraminifera				2.44	-4.16			X		
437	A	93 C	Missourian	305.61	10	Packstone		Skeletal, Matrix	Bryozoans, Crinoids	Sample was epoxied	dark gray	108	2.50	-3.17	0.014	0.015	X		
438	A	94 C	Missourian	305.59	10	Packstone		Skeletal, Matrix	Foraminifera, Bryozoans, Brachiopods, Spines	Sample was epoxied, Early stylolite formation	dark gray	61	2.83	-2.12	0.01	0.04	X		X
439	A	95 C	Missourian	305.58	5	Wackestone	Bryozoan Wackestone	Matrix, Sand	Bryozoans, Crinoids	30% Silt			1.41	-6.15					X
439	D	95 C	Missourian	305.58	5	Wackestone	Bryozoan Wackestone	Matrix, Sand	Bryozoans, Crinoids	30% Silt			1.41	-6.83			X		
439	D	95 C	Missourian	305.58	5	Wackestone	Bryozoan Wackestone	Matrix, Sand	Bryozoans, Crinoids	30% Silt			1.42	-5.48			X		
440	A	96 C	Missourian	305.56	50	Wackestone	Silicified Wackestone	Matrix	Crinoids, Bryozoans	Mostly silicified			2.75	-1.52			X		
441.5	A	97 C	Missourian	305.54	55	Wackestone	Silicified Wackestone	Chert, Matrix	Crinoids, Bryozoans	Mostly replaced by chert, Drilled softer area, Some bedding visible			2.85	-2.37			X		

APPENDIX A - Continued

Sample (Meter + Letter)		Hand Sample Number	North American Stage	Age GTS 2004	% Silt/Sand	Classification	Expanded Classification	Material Sampled in order of Abundance	Fossils and Clasts	Other Notes (Hand Sample, unless specified)	Color	Powder Weight (ug) for Analysis	$\delta^{13}C$ vs VPDB	$\delta^{18}O$ vs VPDB	$\delta^{13}C$ 1σ	$\delta^{18}O$ 1σ	Thin Section	BSE Image	CL Image
443	A	98 C	Missourian	305.52	15	Packstone	Bryozoan Crinoidal Packstone	Chert, Matrix	Bryozoans, Crinoids, Brachiopods, Spines, Foraminifera, Detrital plagioclase	Mostly Chert, Phosphate grains, Some grains rimmed with iron			1.89	-5.44					
443	D	98 C	Missourian	305.52	15	Packstone	Bryozoan Crinoidal Packstone	Chert, Matrix	Bryozoans, Crinoids, Brachiopods, Spines, Foraminifera, Detrital plagioclase	Mostly Chert, Phosphate grains, Some grains rimmed with iron			1.92	-5.63			X		
443	D	98 C	Missourian	305.52	15	Packstone	Bryozoan Crinoidal Packstone	Chert, Matrix	Bryozoans, Crinoids, Brachiopods, Spines, Foraminifera, Detrital plagioclase	Mostly Chert, Phosphate grains, Some grains rimmed with iron			1.86	-5.24					
444.5	A	99 C	Missourian	305.50	15	Packstone	Bryozoan Packstone	Skeletal, Matrix	Bryozoans, Crinoids, Brachiopods, Algae	80-90% Skeletal			2.68	-4.45			X		
446	A	100 C	Missourian	305.48	5	Packstone	Bryozoan Packstone	Skeletal, Matrix	Bryozoans, Crinoids, Foraminifera, Brachiopods	80-90% Skeletal			2.52	-4.31			X		
447.5	A	101 C	Missourian	305.45	10	Packstone	Cherty Packstone	Skeletal, Matrix	Crinoids, Foraminifera, Brachiopods, Bryozoans	Finer grained, Less crinoids, 70% Skeletal			2.08	-5.10					
447.5	C	101 C	Missourian	305.45	10	Packstone	Crinoidal Packstone	Skeletal, Matrix	Crinoids, Foraminifera, Brachiopods, Bryozoans	Less fine grained, Chert cemented, Crinoids, 90% skeletal			1.82	-4.19					
447.5	D	101 C	Missourian	305.45	10	Packstone	Cherty Packstone	Skeletal, Matrix	Crinoids, Foraminifera, Brachiopods, Bryozoans	Finer grained, Less crinoids, 70% Skeletal			1.94	-6.12			X		
447.5	D	101 C	Missourian	305.45	10	Packstone	Crinoidal Packstone	Skeletal, Matrix	Crinoids, Foraminifera, Brachiopods, Bryozoans	Less fine grained, Chert cemented, Crinoids, 90% skeletal			2.21	-4.08			X		
447.5	D	101 C	Missourian	305.45	10	Packstone	Crinoidal Packstone	Skeletal, Matrix	Crinoids, Foraminifera, Brachiopods, Bryozoans	Less fine grained, Chert cemented, Crinoids, 90% skeletal			2.06	-3.97			X		
447.5	D	101 C	Missourian	305.45	10	Packstone	Cherty Packstone	Skeletal, Matrix	Crinoids, Foraminifera, Brachiopods, Bryozoans	Finer grained, Less crinoids, 70% Skeletal			1.57	-4.41			X		
449	A	102 C	Missourian	305.43	10	Wackestone		Skeletal, Matrix	Unidentified skeletal fragments				1.53	-5.94					
449	D	102 C	Missourian	305.43	10	Wackestone		Skeletal, Matrix	Unidentified skeletal fragments				1.50	-5.89					
449	D	102 C	Missourian	305.43	10	Wackestone		Skeletal, Matrix	Unidentified skeletal fragments				1.56	-5.99					
449	D	102 C	Missourian	305.43	10	Wackestone		Skeletal, Matrix	Unidentified skeletal fragments				1.52	-5.64					
450	A	103 C	Missourian	305.42	20	Packstone	Bryozoan Crinoidal Packstone	Skeletal, Matrix	Crinoids, Bryozoans, Foraminifera	60-70% Skeletal			2.45	-4.91			X		
451	A	104 C	Missourian	305.40	5	Packstone		Skeletal, Matrix	Foraminifera, Bryozoans		brown	92	2.48	-4.59	0.016	0.018	X		
452	A	105 C	Missourian	305.39	5	Packstone		Skeletal, Matrix	Crinoids, Bryozoans, Foraminifera		medium gray	60	2.76	-3.14	0.017	0.025	X		
453	A	106 C	Missourian	305.37	10	Wackestone		Matrix, Skeletal		Sampled dark gray micrite			2.69	-2.40					
453	D	106 C	Missourian	305.37	10	Wackestone		Matrix, Skeletal		Sampled dark gray			2.65	-2.42					

APPENDIX A - Continued

Sample (Meter + Letter)		Hand Sample Number	North American Stage	Age GTS 2004	% Silt/Sand	Classification	Expanded Classification	Material Sampled in order of Abundance	Fossils and Clasts	Other Notes (Hand Sample, unless specified)	Color	Powder Weight (ug) for Analysis	$\delta^{13}C$ vs VPDB	$\delta^{18}O$ vs VPDB	$\delta^{13}C$ 1σ	$\delta^{18}O$ 1σ	Thin Section	BSE Image	CL Image
										micrite									
453	D	106 C	Missourian	305.37	10	Wackestone		Matrix, Skeletal		Sampled dark gray micrite			2.72	-2.38					
454	A	107 C	Missourian	305.36	10	Wackestone		Matrix, Skeletal		Sampled Micrite			0.95	-6.60					
454	D	107 C	Missourian	305.36	10	Wackestone		Matrix, Skeletal		Sampled Micrite			0.93	-6.80					
454	D	107 C	Missourian	305.36	10	Wackestone		Matrix, Skeletal		Sampled Micrite			0.96	-6.40					
454	D	107 C	Missourian	305.36	10	Wackestone		Matrix, Skeletal		Sampled Micrite			0.93	-6.40					
455	A	108 C	Missourian	305.35	10	Wackestone		Matrix, Skeletal		Sampled Micrite			2.98	-2.58					
455	D	108 C	Missourian	305.35	10	Wackestone		Matrix, Skeletal		Sampled Micrite			2.89						
455	D	108 C	Missourian	305.35	10	Wackestone		Matrix, Skeletal		Sampled Micrite			3.08	-2.58					
456	A	109 C	Missourian	305.33	10	Wackestone		Matrix, Skeletal		Sampled Micrite			2.91	-3.69					
457	A	110 C	Missourian	305.32	10	Wackestone	Bryozoan Wackestone	Matrix, Skeletal	Bryozoans	Sampled mud, One bed visible			2.17	-5.17			X		
459	A	Mike's Algae	Missourian	305.29	10	Wackestone		Matrix, Skeletal			dark gray	68	3.53	-2.99	0.02	0.032	X		X
459	B	Mike's Algae	Missourian	305.29	0	Cement - Evaporite		Cement	Crinoids	White evaporite nodule	white	111	-10.76	-3.43	0.014	0.026	X		X
459	A	111 C	Missourian	305.29	10	Boundstone	Bryozoan Boundstone/ Wackestone	Matrix, Skeletal	Bryozoans, Gastropods, Pellet filled burrows	About 40% mud, 60% skeletal			3.40	-3.45			X		X
460	A	112 C	Missourian	305.27	5	Wackestone	Crinoidal Wackestone	Matrix	Crinoids, Brachiopods, Bryozoans, Foraminifera	Sampled black mud			3.66	-3.72			X		
461	A	113 C	Missourian	305.26	10	Mudstone		Matrix		Sampled black mud			2.63	-3.90					
462	A	114 C	Missourian	305.24	10	Mudstone		Matrix		Sampled black mud			3.08	-3.43					
466	A	115 C	Missourian	305.19	15	Mudstone		Matrix		Sample gray mud				-5.39					
467	A	116 C	Missourian	305.17	25	Mudstone		Matrix		Contained gray sand			3.02	-4.60					
468	A	117 C	Missourian	305.16	20	Mudstone		Matrix		Contained black sand			2.26	-4.77					
469	A	118 C	Missourian	305.14	15	Mudstone		Matrix		Contained gray sand			3.05	-5.63					
470	A	119 C	Missourian	305.13	10	Mudstone		Matrix		Avoided fractures when sampling			0.65	-7.04					
470	D	119 C	Missourian	305.13	10	Mudstone		Matrix		Avoided fractures when sampling			0.66	-6.93					
470	D	119 C	Missourian	305.13	10	Mudstone		Matrix		Avoided fractures when sampling			0.64	-7.14					
471	A	120 C	Missourian	305.11	15	Mudstone		Matrix					3.87	-4.18					
472	A	121 C	Missourian	305.10	15	Mudstone		Matrix		Sampled black mud			3.92	-4.27					
473	A	122 C	Missourian	305.08	10	Mudstone		Matrix		Sampled black mud			3.72	-4.47					
474	A	123 C	Missourian	305.07	10	Mudstone		Matrix		Sampled black mud			3.29	-4.17					
475	A	124 C	Missourian	305.06	15	Wackestone		Matrix		Sample gray mud			2.81	-4.99					
476	A	125 C	Missourian	305.04	15	Wackestone	Crinoidal Wackestone	Matrix, Skeletal	Crinoids, Foraminifera, Bryozoans, Brachiopods	Chert nodules, Sampled zones with least amount of skeletal grains			3.17	-1.97			X		
477	A	126 C	Missourian	305.03	10	Wackestone		Matrix		Sampled mud			3.17	-1.92					
478	A	127 C	Missourian	305.01	5	Wackestone	Bryozoan Wackestone	Matrix, Cement	Bryozoan, Crinoids, Brachiopods	Some calcite and silica filled fractures, Edges of brachiopods are silicified			1.69	-6.04					
478	D	127 C	Missourian	305.01	5	Wackestone	Bryozoan Wackestone	Matrix, Cement	Bryozoan, Crinoids, Brachiopods	Some calcite and silica filled fractures, Edges of brachiopods are silicified			1.80	-6.13			X		

APPENDIX A - Continued

Sample (Meter + Letter)		Hand Sample Number	North American Stage	Age GTS 2004	% Silt/Sand	Classification	Expanded Classification	Material Sampled in order of Abundance	Fossils and Clasts	Other Notes (Hand Sample, unless specified)	Color	Powder Weight (ug) for Analysis	$\delta^{13}C$ vs VPDB	$\delta^{18}O$ vs VPDB	$\delta^{13}C$ 1σ	$\delta^{18}O$ 1σ	Thin Section	BSE Image	CL Image
478	D	127 C	Missourian	305.01	5	Wackestone	Bryozoan Wackestone	Matrix, Cement	Bryozoan, Crinoids, Brachiopods	Some calcite and silica filled fractures, Edges of brachiopods are silicified			1.57	-5.94			X		
479	A	128 C	Missourian	305.00	5	Wackestone		Matrix, Skeletal	Crinoids	Sample was epoxied	tan	98	1.08	-6.74	0.017	0.033	X		
480	A	129 C	Missourian	304.98	10	Wackestone		Matrix, Skeletal	Brachiopods, Spines, Crinoids, Bryozoans	Sample was epoxied	light gray	64	2.96	-4.56	0.013	0.023	X		
481	A	130 C	Missourian	304.97	10	Wackestone	Micritic Wackestone	Matrix	Crinoids	Some graded bedding visible	light gray		2.17	-7.50			X		
481	D	130 C	Missourian	304.97	10	Wackestone	Micritic Wackestone	Matrix	Crinoids	Some graded bedding visible	light gray		2.34	-7.60			X		
481	D	130 C	Missourian	304.97	10	Wackestone	Micritic Wackestone	Matrix	Crinoids	Some graded bedding visible	light gray		2.00	-7.40			X		
482	A	131 C	Missourian	304.95	30	Packstone	Sandy Packstone	Matrix	Unidentified skeletal fragments, Crinoids, Brachiopods, Trilobite fragments, Pellets	Sandy, Sampled dark gray mud			3.32	-3.87			X		
483	A	132 C	Missourian	304.94	20	Wackestone	Fractured Wackestone	Matrix	Pellets, Micritic algae, Bryozoans, Trilobite fragments, Bivalves	Contained silicified zones, Sample very fine gray mud			3.75	-4.79			X		
484	A	133 C	Missourian	304.92	1	Boundstone	Phylloid Algae Boundstone	Matrix	Phylloid algae, Pellets, Dolomite Rhombs, Gastropods				3.83	-5.25			X		X
485	A	134 C	Missourian	304.91	2	Wackestone	Fractured Wackestone	Matrix	Pellets, Foraminifera, Crinoids, Dolomite Rhombs	Hand sample was fractured, Contains silicified zones, Analysis on gray mud			3.26	-6.37			X		
486	A	135 C	Missourian	304.90	10	Mudstone		Matrix		very hard/siliceous	light gray		3.87	-5.48					
487	A	136 C	Missourian	304.88	1	Packstone	Foraminifera Packstone	Skeletal, Matrix	Foraminifera, Brachiopods	Sampled black mud			4.46	-4.29			X		
488	A	137 C	Missourian	304.87	3	Packstone	Micritized Packstone	Skeletal, Matrix	40% Micritized skeletal fragments, Intraclasts, Crinoids, Gastropods				3.90						
490	A	139 C	Missourian	304.84	2	Packstone	Micritic Packstone	Matrix	Pellets, Foraminifera, Bryozoans	Mostly mud sampled , Avoided oxidized grains/clasts			3.59	-6.03			X		
491	A	140 C	Missourian	304.82	10	Mudstone		Matrix, Silt	Phylloid algae	Highly fractured, Stayed in gray matrix, Silt (10-20%)			3.74	-5.76					
492	A	141 C	Missourian	304.81	0	Wackestone		Matrix, Skeletal	Crinoids, Foraminifera, Brachiopods, Bryozoans, Phylloid algae	Sample was epoxied	medium gray	105	3.89	-3.65	0.022	0.027	X		
493	A	142 C	Missourian	304.79	10	Wackestone		Matrix	Phylloid algae	Sampled mud			4.30	-4.98					
493	C	142 C	Missourian	304.79	10	Packstone		Skeletal, Matrix	Phylloid algae	Highly fractured			4.35	-5.05					
494	A	143 C	Missourian	304.78	3	Wackestone	Foraminifera Crinoidal Packstone	Matrix	Foraminifera, Crinoids, Brachiopods, Intraclasts, Bivalves	Drilled mud			4.04	-4.93			X		
495	A	144 C	Missourian	304.77	15	Wackestone	Crinoidal Brachiopod	Matrix	Crinoids, Brachiopods	Drilled mud			2.21	-7.80			X		

APPENDIX A - Continued

Sample (Meter + Letter)		Hand Sample Number	North American Stage	Age GTS 2004	% Silt/Sand	Classification	Expanded Classification	Material Sampled in order of Abundance	Fossils and Clasts	Other Notes (Hand Sample, unless specified)	Color	Powder Weight (ug) for Analysis	$\delta^{13}C$ vs VPDB	$\delta^{18}O$ vs VPDB	$\delta^{13}C$ 1σ	$\delta^{18}O$ 1σ	Thin Section	BSE Image	CL Image
495	D	144 C	Missourian	304.77	15	Wackestone	Wackestone Crinoidal Brachiopod Wackestone	Matrix	Crinoids, Brachiopods	Drilled mud			2.16	-7.80			X		
495	D	144 C	Missourian	304.77	15	Wackestone	Crinoidal Brachiopod Wackestone	Matrix	Crinoids, Brachiopods	Drilled mud			2.26				X		
497	A	1 D	Missourian	304.74	0	Calcisiltstone		Matrix, Skeletal	Small skeletal fragments	Really thin sample, alteration possible.	light gray	103	1.09	-8.07	0.018	0.012			
498	A	2 D	Missourian	304.72	30	Mudstone		Matrix, Sand		30% Silt	gray	107	2.90	1.68	0.013	0.023			
499	A	3 D	Missourian	304.71	60	Siltstone		Sand, Matrix		60% Silt	light gray	251	0.84	-8.21	0.021	0.02			
500	A	4 D	Missourian	304.69	10	Calcisiltstone		Matrix, Sand		10% Silt	light gray	71	-0.03	-7.97	0.023	0.048			
501	A	5 D	Missourian	304.68	50	Siltstone	Crinoidal Siltstone	Silt, Skeletal, Matrix	Crinoids, Brachiopod, Bryozoans		medium gray						X		
504	A	6 D	Missourian	304.63	40	Wackestone		Matrix, Sand		40% Silt	medium gray	138	2.14	-4.71	0.016	0.021			
505	A	7 D	Missourian	304.62	10	Packstone	Brachiopod Packstone	Skeletal, Matrix	Brachiopods, Spines		gray	107	1.40	-4.57	0.008	0.023	X		
506	A	8 D	Missourian	304.61	40	Packstone	Silty Skeletal Packstone	Silt, Matrix, Skeletal	Bryozoans, Trilobite fragments		medium gray	131	1.89	-2.68	0.018	0.024			X
507	A	9 D	Missourian	304.59	40	Wackestone		Matrix, Sand, Skeletal	Bryozoans, Brachiopods, Crinoids	40% Silt	light gray	148	0.80	-5.39	0.011	0.02			
508	A	10 D	Missourian	304.58	90	Sandstone		Sand, Matrix, Skeletal	Crinoids, Brachiopods	Chert nodules, 90% Sand, Fractures	gray	500	1.27	-3.67	0.014	0.042			
509	A	11 D	Missourian	304.56	25	Wackestone	Silty Wackestone	Matrix, Silt	Bryozoans, Foraminifera, Brachiopods	Sample contains highly oxidized orange spots	gray	140	2.01	-5.28	0.012	0.017	X		
510	A	12 D	Missourian	304.55	5	Mudstone		Matrix, Sand		5% Silt	medium gray	65	2.70	-4.01	0.012	0.041			
511	A	13 D	Missourian	304.53	10	Wackestone		Matrix, Skeletal, Sand	Crinoids	10% Silt	gray	70	2.58	-3.71	0.019	0.028			
512	A	14 D	Missourian	304.52	30	Wackestone		Matrix, Cement, Skeletal	Crinoids	30% Silt, Orange cement between grains	gray/orange	92	2.00	-5.52	0.017	0.014			
513	A	15 D	Missourian	304.50	40	Wackestone		Matrix, Sand		40% Silt	gray	150	2.34	-4.92	0.007	0.022			
514	A	16 D	Missourian	304.49	30	Wackestone		Matrix, Sand, Skeletal	Crinoids	30% Silt, White cement between grains	light gray	106	0.37	-7.61	0.009	0.026			
515	A	17 D	Missourian	304.48	80	Siltstone		Sand, Matrix		80% Silt	light gray	401	-0.22	-8.09	0.003	0.02			
515.5	A	18 D	Missourian	304.47	30	Wackestone /Packstone	Silty Skeletal Wackestone	Silt, Matrix	Crinoids, Bryozoans		medium gray	120	1.92	-6.11	0.014	0.026	X		
516	A	19 D	Missourian	304.46	90	Siltstone		Sand, Matrix	Crinoids	90% Silt	tan	494	-2.22	-11.19	0.004	0.016			
517	A	20 D	Missourian	304.45	10	Wackestone	Skeletal Wackestone	Matrix, Skeletal	Crinoids, Bryozoans, Brachiopods		dark gray	106	2.04	-5.24	0.029	0.036	X		
518	A	21 D	Missourian	304.43	70	Siltstone	Siltstone	Silt, Matrix	Brachiopods		medium gray	314	-0.38	-6.88	0.011	0.027	X		
519	A	22 D	Missourian	304.42	50	Packstone		Matrix, Sand		50% Sand	gray	132	2.12	-4.52	0.014	0.014			
520	A	23 D	Missourian	304.40	40	Packstone		Matrix, Skeletal, Sand		40% Sand	dark gray	133	1.25	-5.20	0.011	0.03			
521	A	24 D	Missourian	304.39	20	Packstone	Skeletal Packstone	Skeletal, Matrix	Crinoids, Bryozoans, Foraminifera, Brachiopods		dark gray	141	1.75	-4.53	0.02	0.026	X		
522	A	25 D	Missourian	304.37	25	Packstone		Matrix,	Crinoids, Spines,	25% Silt	gray								

APPENDIX A - Continued

Sample (Meter + Letter)		Hand Sample Number	North American Stage	Age GTS 2004	% Silt/Sand	Classification	Expanded Classification	Material Sampled in order of Abundance	Fossils and Clasts	Other Notes (Hand Sample, unless specified)	Color	Powder Weight (ug) for Analysis	$\delta^{13}C$ vs VPDB	$\delta^{18}O$ vs VPDB	$\delta^{13}C$ 1σ	$\delta^{18}O$ 1σ	Thin Section	BSE Image	CL Image
523	A	26 D	Missourian	304.36	30	Packstone		Skeletal, Sand Matrix, Skeletal, Sand	Brachiopods, Bryozoans Crinoids, Brachiopods, Bryozoans	30% Silt	gray								
524	A	27 D	Missourian	304.34	5	Wackestone		Matrix, Sand	Crinoids, Brachiopods	5% Silt	medium gray								
525	A	28 D	Missourian	304.33	20	Wackestone/ Packstone		Matrix, Skeletal	Brachiopod, Bryozoans, Crinoids		dark gray	94	1.98	-4.02	0.014	0.036	X		
526	A	29 D	Missourian	304.32	0	Mudstone	Brecciated Mudstone	Matrix	Crystal silt	Breccia with fine grained fill. Likely exposed in vadose zone	medium gray	115	2.36	-4.09	0.018	0.018	X		
527	A	30 D	Missourian	304.30	10	Wackestone		Matrix, Sand	Crinoids	10% Silt	dark gray								
528	A	31 D	Missourian	304.29	50	Wackestone		Sand, Matrix		50% Silt	gray								
530	A	32 D	Missourian	304.26	60	Siltstone	Siltstone	Silt, Matrix		Contains intraclasts	gray	233	2.50	-6.46	0.014	0.019	X		
534	A	33 D	Missourian	304.20	30	Wackestone	Silty Skeletal Wackestone	Matrix, Silt	Crinoids, Bryozoans		light gray	127	1.27	-6.27	0.018	0.02	X		
538	A	34 D	Missourian	304.14	65	Siltstone		Sand, Matrix	Crinoids	65% Silt	tan								
539	A	35 D	Missourian	304.13	60	Siltstone		Matrix, Sand		60% Silt	tan								
540	A	36 D	Missourian	304.11	15	Wackestone	Silty Skeletal Wackestone	Matrix, Silt	Bryozoans		gray	104	3.07	-4.51	0.004	0.016	X		
541	A	37 D	Missourian	304.10	10	Wackestone		Matrix, Sand		10% Silt, Zones of dissolution have been filled with cement	gray								
542	A	38 D	Missourian	304.08	5	Mudstone		Matrix, Sand		Zones filled with clear blocky cement, Highly fractured, Stylolites	gray								
542	B	38 D	Missourian	304.08	0	Cement - Void		Cement		Blocky clear cement	gray	80	3.08	-4.82	0.012	0.016			
543	A	39 D	Missourian	304.07	5	Mudstone		Matrix, Sand		Highly fractured, 5% Silt	gray								
544	A	40 D	Missourian	304.05	25	Wackestone		Matrix, Sand		25% Silt	gray								
545	A	41 D	Missourian	304.04	15	Mudstone		Matrix, Sand		15% Silt	gray								
546	A	42 D	Missourian	304.03	10	Mudstone		Matrix, Sand, Cement		10% Silt, Highly fractured, Fractures filled with white cement	gray								
547	A	43 D	Missourian	304.01	50	Wackestone		Sand, Matrix		50% Silt, Highly fractured, Sample was epoxied	medium gray								
548	A	44 D	Missourian	304.00	15	Mudstone	Mudstone	Matrix, Silt			gray		3.16	-4.67	0.014	0.028	X		
548	D	44 D	Missourian	304.00	15	Mudstone	Mudstone	Matrix, Silt			gray	143	3.16	-4.67	0.014	0.028	X		
548	D	44 D	Missourian	304.00	15	Mudstone	Mudstone	Matrix, Silt			gray	116	3.12	-4.69	0.017	0.029	X		
549	A	45 D	Missourian	303.98	40	Wackestone	Silty Skeletal Wackestone	Silt, Matrix	Bryozoans, Crinoids, Trilobites		tan	123	0.23	-7.45	0.021	0.034	X		
550	A	46 D	Missourian	303.97	40	Wackestone	Silty Skeletal Wackestone	Matrix, Silt	Bryozoans, Bivalves		tan	186	-0.86	-8.54	0.021	0.042	X		
553	A	48 D	Missourian	303.92	50	Siltstone		Sand, Matrix		50% Silt, Orange stringers between grains	gray								
554	A	49 D	Missourian	303.91	35	Mudstone	Silty Mudstone	Matrix, Silt		Silica filled molds	light gray	113	1.37	-6.50	0.02	0.017	X		X
555	A	50 D	Missourian	303.89	90	Siltstone		Sand, Matrix		90% Silt	light gray								
556	A	51 D	Missourian	303.88	35	Mudstone	Silty Mudstone	Matrix, Silt		Dark chert nodules with	light gray	151	0.75	-7.49	0.016	0.016	X		

APPENDIX A - Continued

Sample (Meter + Letter)		Hand Sample Number	North American Stage	Age GTS 2004	% Silt/Sand	Classification	Expanded Classification	Material Sampled in order of Abundance	Fossils and Clasts	Other Notes (Hand Sample, unless specified)	Color	Powder Weight (ug) for Analysis	$\delta^{13}C$ vs VPDB	$\delta^{18}O$ vs VPDB	$\delta^{13}C$ 1σ	$\delta^{18}O$ 1σ	Thin Section	BSE Image	CL Image
										dolomite inclusions									
557	A	52 D	Missourian	303.87	80	Siltstone		Sand, Matrix		80% Silt	gray								
558	A	53 D	Missourian	303.85	60	Siltstone		Sand, Matrix		Some spots of orange oxidized material, 60% Silt	orange/tan								
558	A	53 D	Missourian	303.85	75	Siltstone		Silt, Matrix		Some spots of orange oxidized material, 60% Silt	orange/tan								
559	A	54 D	Missourian	303.84	70	Siltstone		Silt, Matrix		70% Silt	light gray								
560	A	55 D	Missourian	303.82	40	Wackestone		Matrix, Silt	Crinoids	40% Silt, Thin bedding visible	gray								
561	A	56 D	Missourian	303.81	25	Wackestone	Silty Skeletal Wackestone	Matrix, Silt	Crinoids, Foraminifera, Bivalves		medium gray	93	3.06	-4.78	0.014	0.034	X		
562	A	57 D	Missourian	303.79	5	Wackestone	Skeletal Wackestone	Matrix	Trilobites, Foraminifera, Crinoids, Bryozoans		medium gray	94	3.07	-4.91	0.009	0.019	X		
563	A	58 D	Missourian	303.78	5	Mudstone		Matrix, Silt		5% Silt, Highly fractured	medium gray								
564	A	59 D	Missourian	303.76	20	Wackestone	Silty Skeletal Wackestone	Matrix, Silt		Intraclasts	medium gray	90	3.38	-4.71	0.011	0.035	X		
565	A	60 D	Missourian	303.75	15	Mudstone		Matrix, Silt		15% Silt	gray	113	3.03	-5.02	0.006	0.034			
566	A	61 D	Missourian	303.74	15	Mudstone		Matrix, Silt		15% Silt	medium gray	94	4.60	-1.73	0.01	0.012			
567	A	62 D	Missourian	303.72	10	Mudstone		Matrix, Silt		10% Silt	medium gray	67	3.92	-4.09	0.019	0.019			
568	A	63 D	Missourian	303.71	20	Wackestone		Matrix, Silt		Two textures(siltstone-tan, mudstone-gray)	tan	97	3.38	-4.11	0.019	0.028			
569	A	64 D	Missourian	303.69	30	Wackestone	Silty Wackestone	Matrix, Silt	Crinoids		gray	177	1.84	-5.92	0.019	0.023	X		
570	A	65 D	Missourian	303.68	30	Wackestone		Matrix, Silt, Skeletal	Brachiopods, Crinoids, Spines	30% Silt	gray	93	2.79	-4.57	0.012	0.024			
571	A	66 D	Missourian	303.66	50	Packstone		Sand, Matrix, Skeletal	Crinoids, Brachiopods	50% Silt	light gray	144	1.68	-6.52	0.015	0.021			
572	A	67 D	Missourian	303.65	5	Mudstone		Matrix, Silt		5% Silt, Highly fractured	medium gray	72	2.87	-4.37	0.013	0.012			
573	A	68 D	Missourian	303.63	5	Wackestone	Skeletal Wackestone	Matrix, Skeletal	Foraminifera, Crinoids, Brachiopods		medium gray	64	2.81	-4.24	0.006	0.03	X		
574	A	69 D	Missourian	303.62	5	Mudstone		Matrix, Silt		5% Silt	medium gray	80	2.91	-4.84	0.015	0.018			
575	A	70 D	Missourian	303.60	30	Wackestone		Matrix, Silt		30% Silt	gray								
576	A	71 D	Missourian	303.59	60	Siltstone		Silt, Matrix		60% Silt	light gray	192	3.01	-2.46	0.019	0.029			
577	A	72 D	Missourian	303.58	15	Wackestone	Skeletal Wackestone	Matrix, Silt			gray	146	3.40	-4.36	0.013	0.034	X		
578	A	73 D	Missourian	303.56	20	Mudstone		Matrix, Silt		20% Silt, Highly fractured	gray	105	3.64	-4.06	0.021	0.019			
578.5	A	74 D	Missourian	303.55	5	Mudstone		Matrix, Silt		5% Silt	dark gray	64	3.74	-3.90	0.026	0.009			
579	A	75 D	Missourian	303.55	5	Mudstone		Matrix, Silt		5% Silt	dark gray	80	3.86	-3.86	0.007	0.015			
580	A	76 D	Missourian	303.53	10	Mudstone		Matrix, Silt		10% Silt	medium gray	68	3.81	-3.82	0.021	0.023			
581	A	77 D	Missourian	303.52	50	Siltstone	Laminated Siltstone	Silt, Matrix		Thin bedding, Wavy	gray	129	3.35	-4.69	0.022	0.037	X		

APPENDIX A - Continued

Sample (Meter + Letter)		Hand Sample Number	North American Stage	Age GTS 2004	% Silt/Sand	Classification	Expanded Classification	Material Sampled in order of Abundance	Fossils and Clasts	Other Notes (Hand Sample, unless specified)	Color	Powder Weight (ug) for Analysis	$\delta^{13}C$ vs VPDB	$\delta^{18}O$ vs VPDB	$\delta^{13}C$ 1σ	$\delta^{18}O$ 1σ	Thin Section	BSE Image	CL Image
582	A	78 D	Missourian	303.50	15	Wackestone		Matrix, Silt		15% Silt	medium gray	104	3.23	-4.23	0.015	0.016			
583	A	79 D	Missourian	303.49	50	Siltstone		Silt, Matrix	Crinoids	Skeletal intraclasts	light gray	188	0.49	-6.84	0.015	0.023	X		
584	A	80 D	Missourian	303.47	5	Mudstone		Matrix, Silt		5% Silt	dark gray	68	2.83	-3.87	0.013	0.035			
585	A	81 D	Missourian	303.46	10	Wackestone	Skeletal Wackestone	Matrix, Skeletal	Bryozoans, Brachiopods, Spines, Crinoids	Stylolite forming	dark gray	73	2.45	-3.84	0.036	0.039	X		
586	A	82 D	Missourian	303.45	5	Mudstone		Matrix, Silt		5% Silt, Highly fractured	dark gray	76	2.44	-4.16	0.013	0.024			
586	B	82 D	Missourian	303.45	0	Cement - Fracture		fracture cement		Fracture fill	white	63	1.63	-4.36	0.021	0.032			
587	A	83 D	Missourian	303.43	0	Wackestone	Skeletal Wackestone	Matrix	Foraminifera	Skeletal intraclasts, Orange oxidized grains	dark gray	105	3.06	-3.78	0.011	0.028	X		
588	A	84 D	Missourian	303.42	10	Wackestone		Matrix, Silt, Skeletal	Brachiopods	10% Silt, Sample is fractured	dark gray	73	2.87	-4.01	0.026	0.023			
589	A	85 D	Missourian	303.40	0	Wackestone	Skeletal Wackestone	Matrix	Bryozoans	Other skeletal intraclasts	dark gray	68	2.80	-4.10	0.015	0.038	X		
590	A	86 D	Missourian	303.39	5	Mudstone		Matrix, Silt		2-3% Silt, Sample is fractured	dark gray	76	2.78	-3.21	0.012	0.027			
591	A	87 D	Missourian	303.37	25	Wackestone	Silty Skeletal Wackestone	Matrix, Silt, Skeletal	Crinoids, Brachiopods		dark gray	134	2.68	-4.06	0.013	0.032	X		
592	A	88 D	Missourian	303.36	5	Mudstone		Matrix, Silt		2-3% Silt, Zones of black organic matter	dark gray	61	2.82	-4.17	0.013	0.022			
593	A	89 D	Missourian	303.34	5	Wackestone	Skeletal Wackestone	Matrix	Foraminifera		dark gray	77	2.93	-3.94	0.015	0.041	X		
594	A	90 D	Missourian	303.33	5	Wackestone	Skeletal Wackestone	Matrix	Brachiopods, Foraminifera		dark gray	94	1.50	-4.12	0.011	0.024	X	X	X
595	A	91 D	Missourian	303.31	30	Wackestone		Matrix, Silt		30% Silt, Light colored stringers through parts of hand sample	medium gray	104	-0.45	-5.87	0.024	0.035			
596	A	92 D	Missourian	303.30	30	Wackestone	Silty Skeletal Wackestone	Matrix	Bryozoans, Brachiopods		dark gray	93	-0.19	-6.73	0.022	0.039	X		X

APPENDIX B

THIN SECTIONS FROM GALLAGHER PEAK, IDAHO. THE NUMBER IDENTIFIES SAMPLE AND STRATIGRAPHIC LEVEL OF EACH SAMPLE.

APPENDIX B - Continued

APPENDIX B - Continued

APPENDIX B - Continued

APPENDIX B - Continued

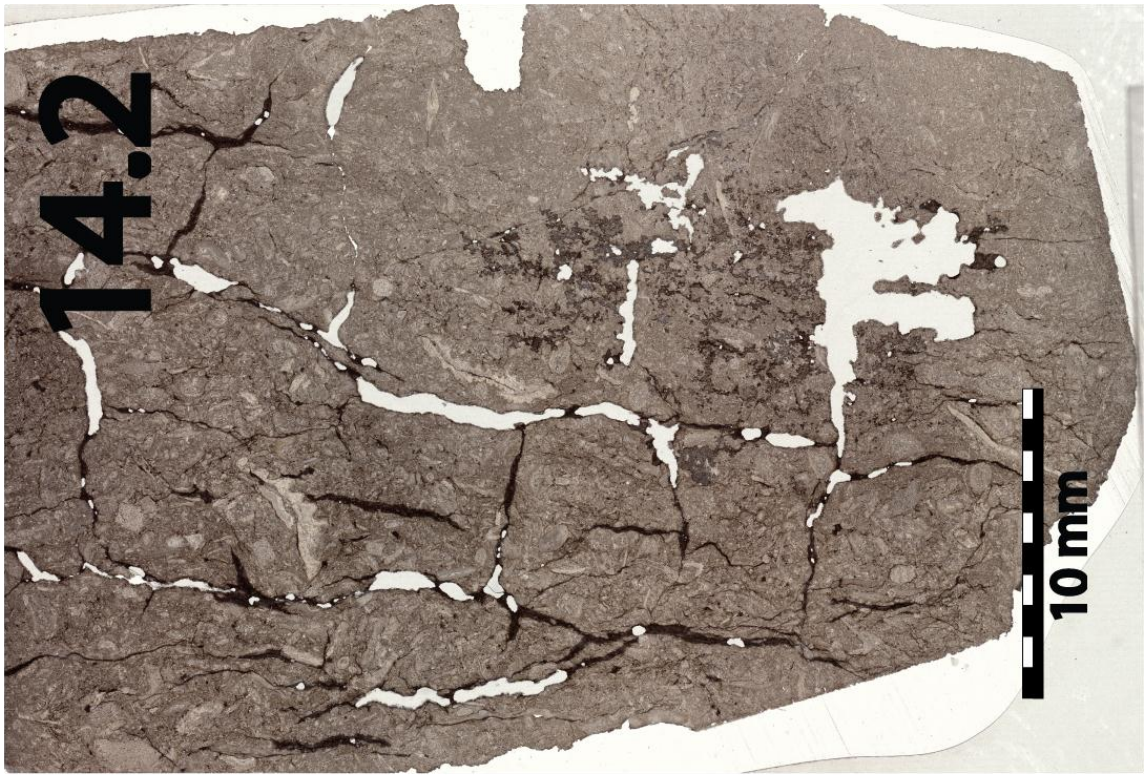

APPENDIX B - Continued

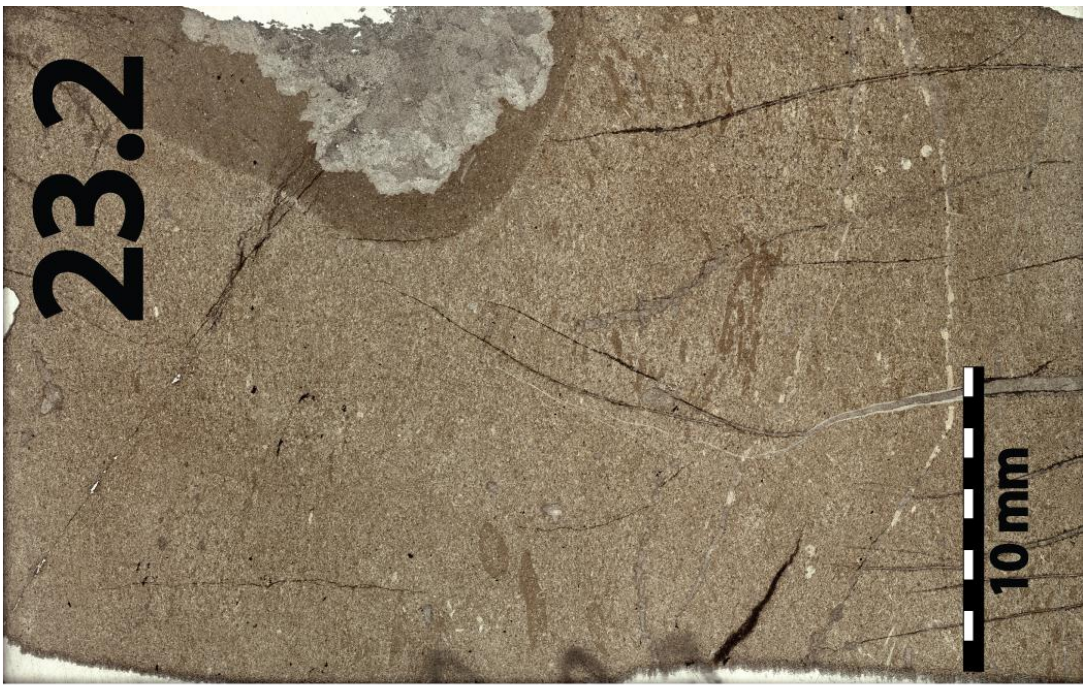

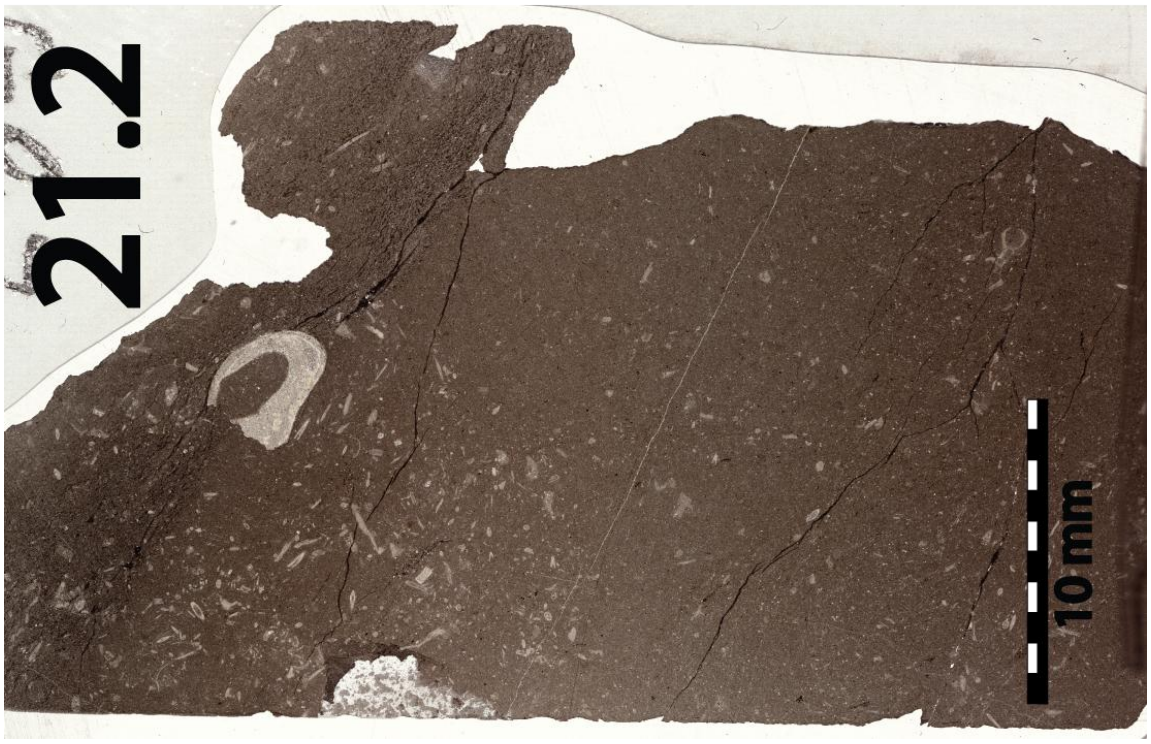

APPENDIX B - Continued

APPENDIX B - Continued

APPENDIX B - Continued

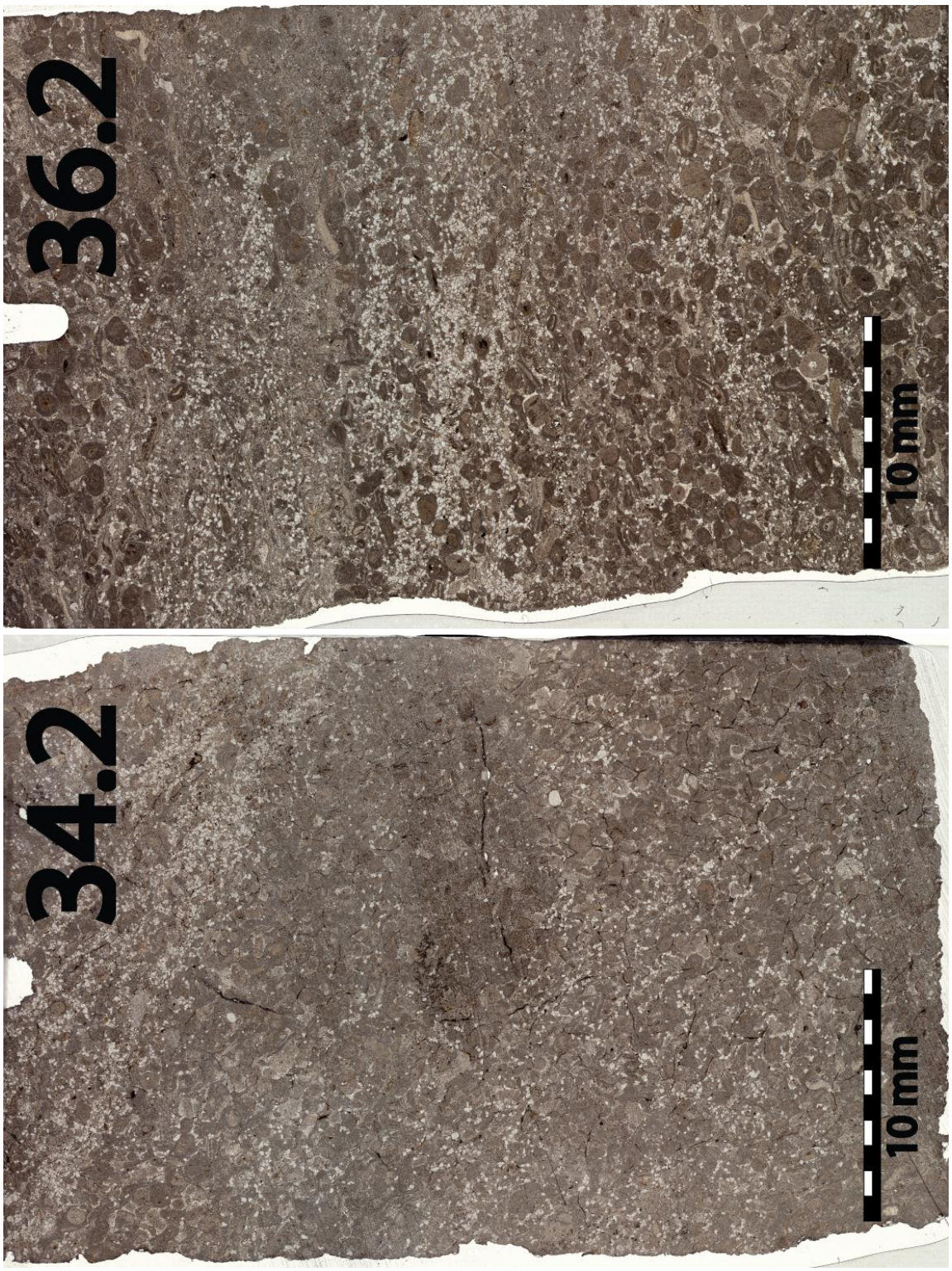

APPENDIX B - Continued

APPENDIX B - Continued

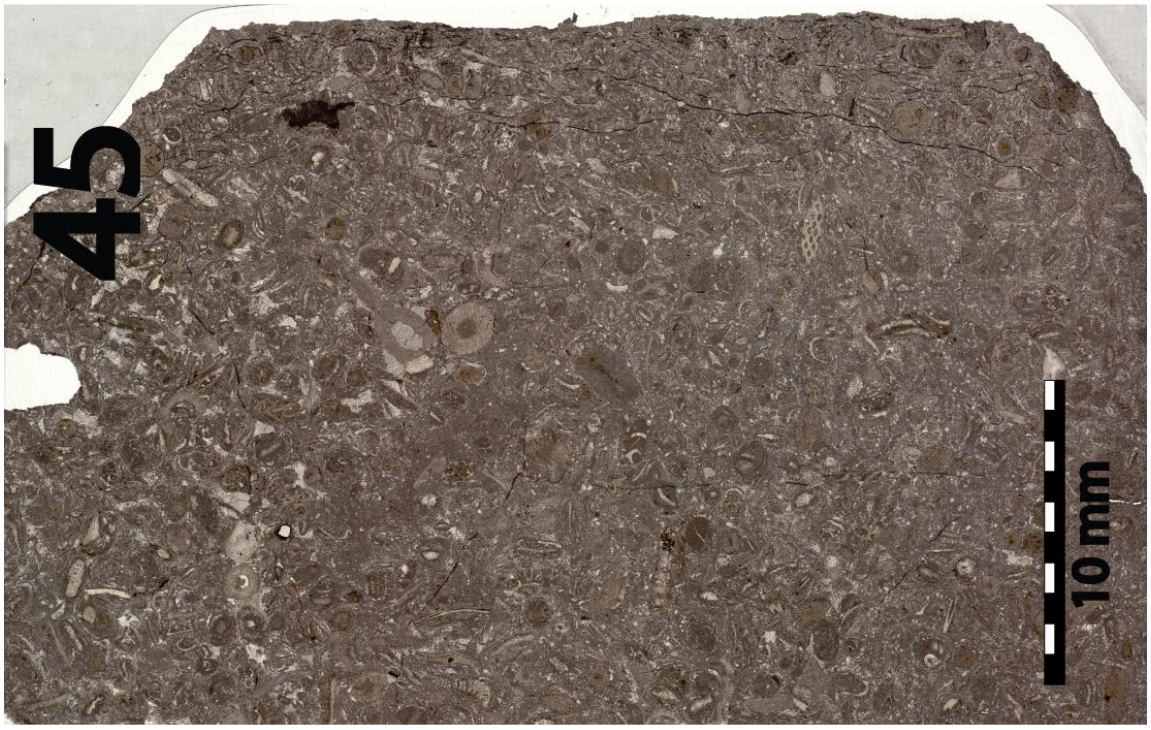

APPENDIX B - Continued

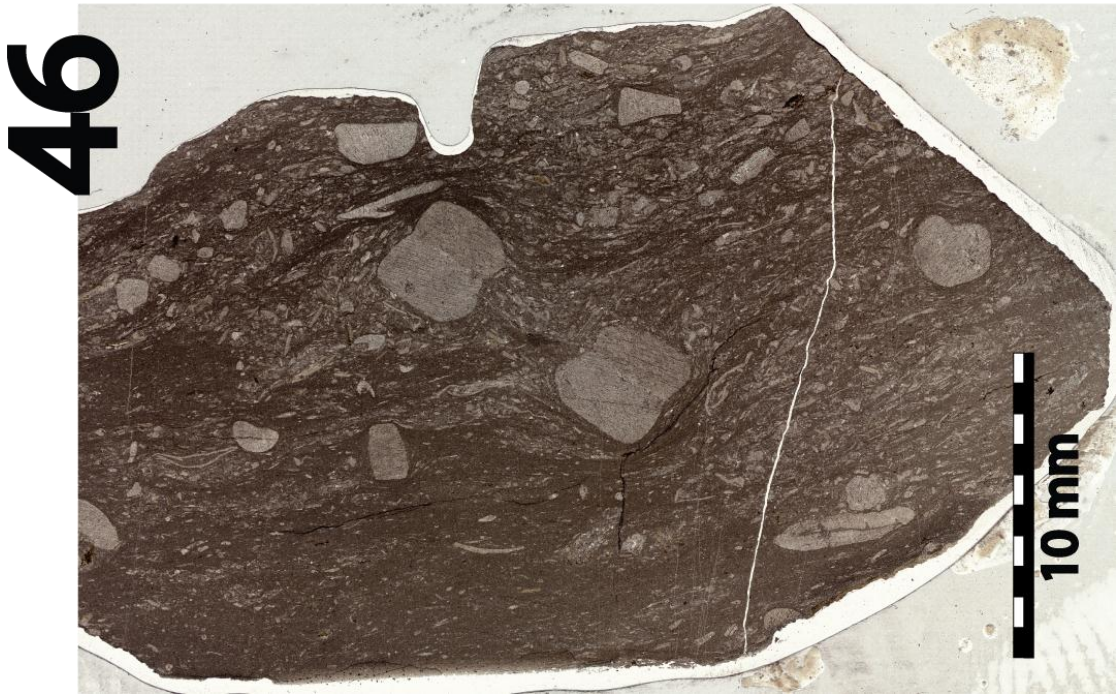

APPENDIX B - Continued

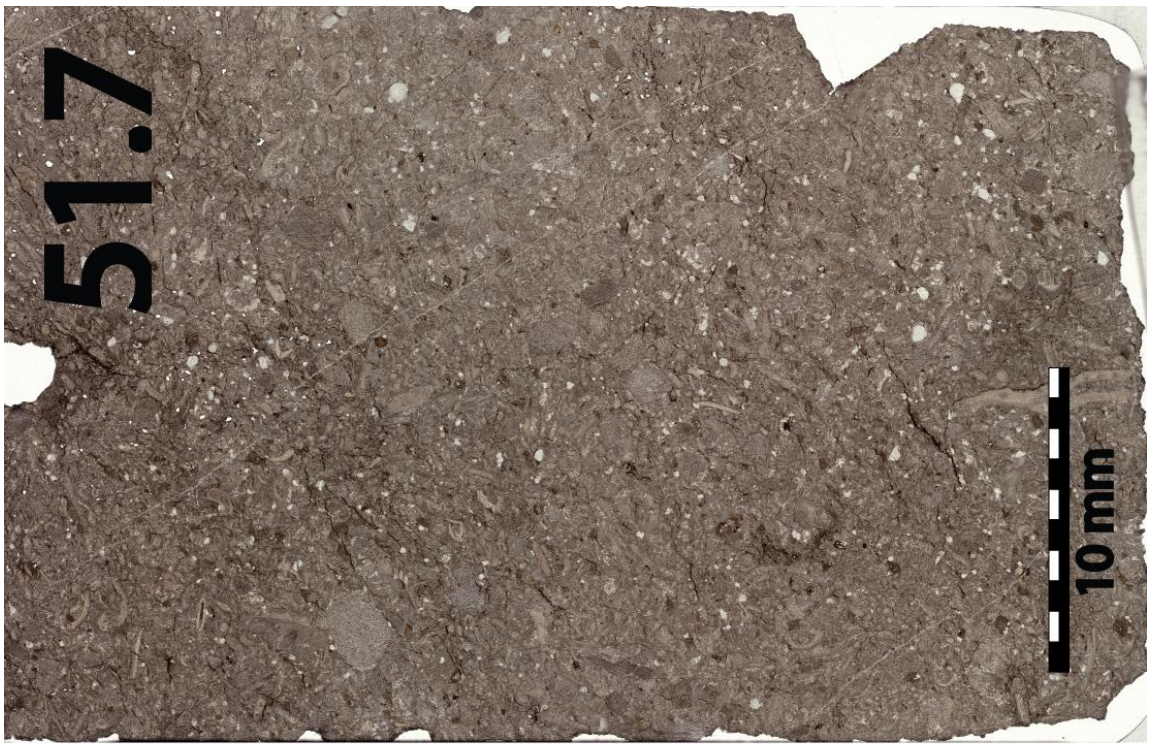

APPENDIX B - Continued

APPENDIX B - Continued

APPENDIX B - Continued

5

APPENDIX B - Continued

APPENDIX B - Continued

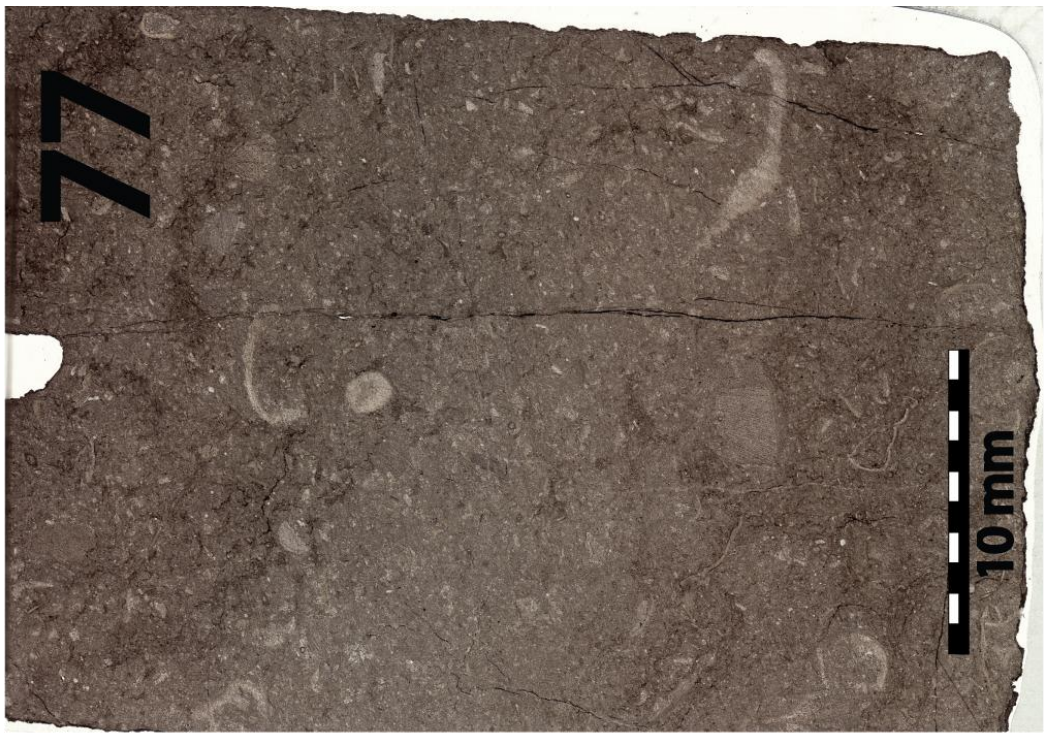

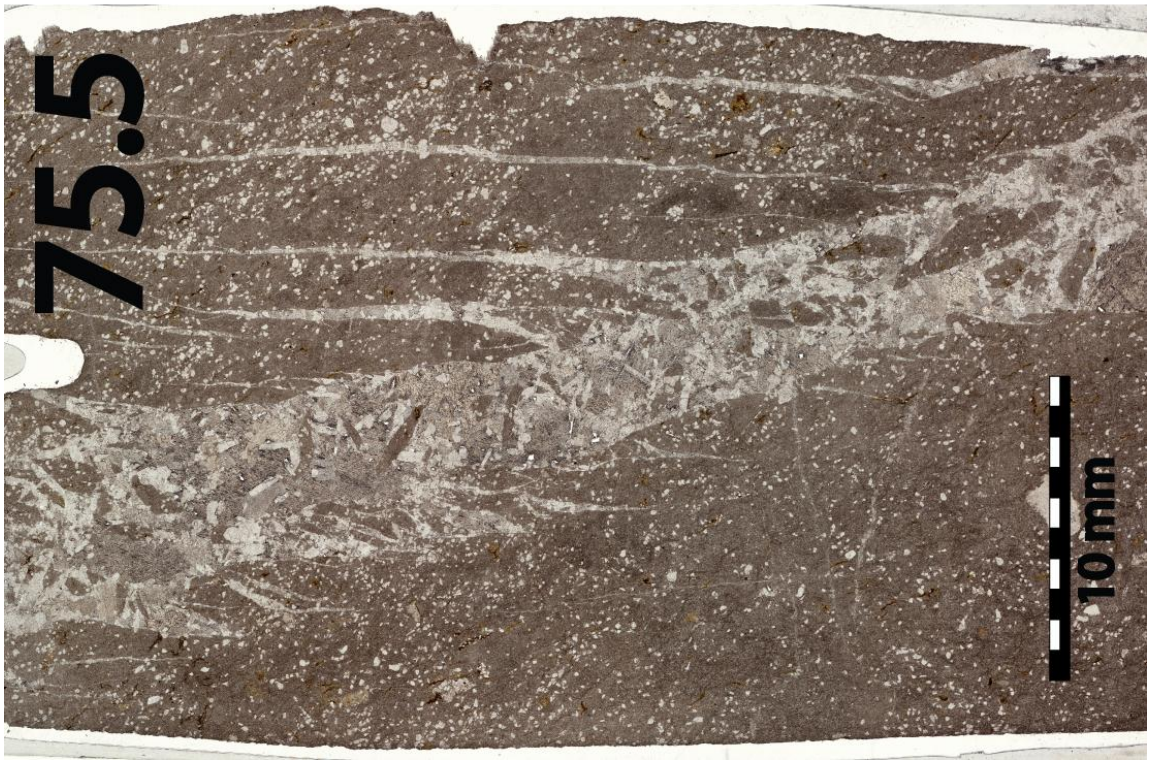

APPENDIX B - Continued

APPENDIX B - Continued

APPENDIX B - Continued

APPENDIX B - Continued

APPENDIX B - Continued

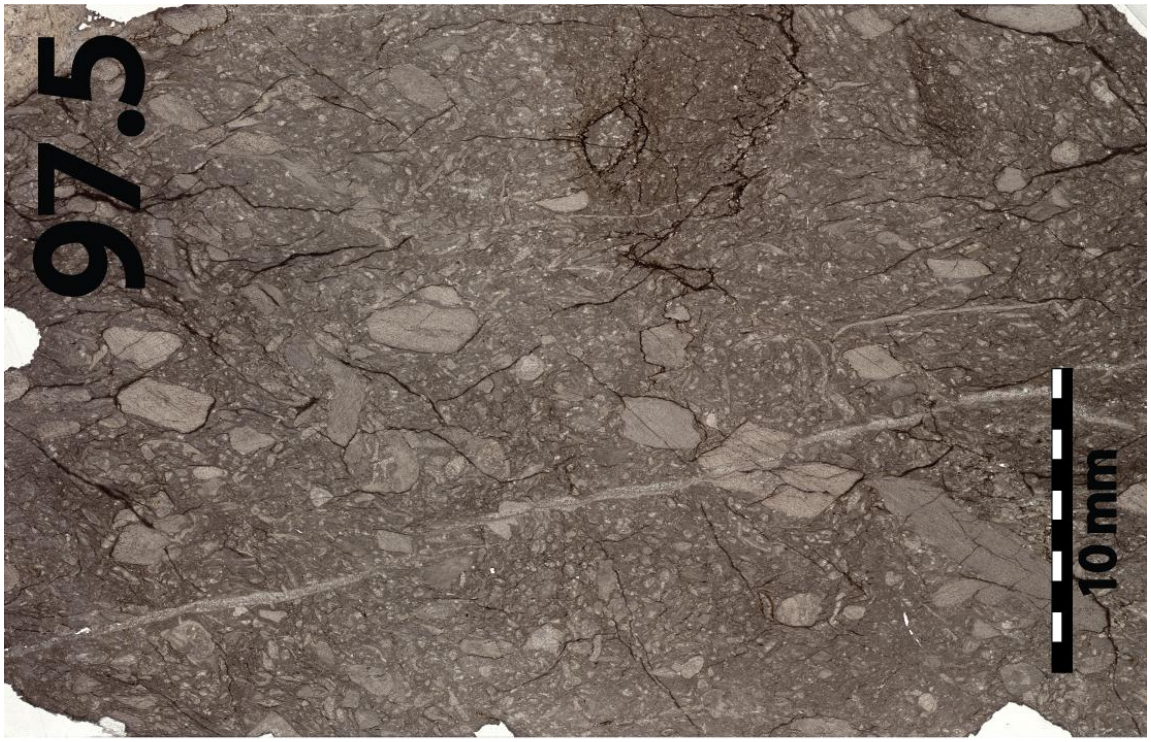

APPENDIX B - Continued

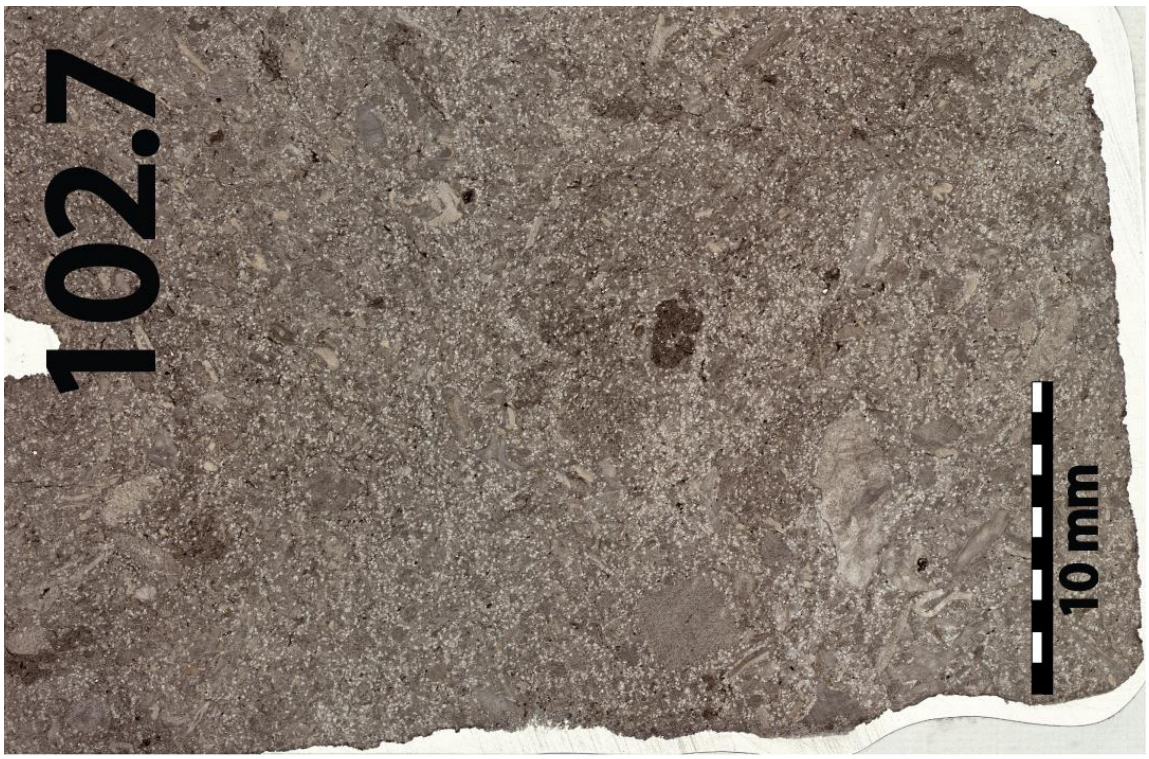

APPENDIX B - Continued

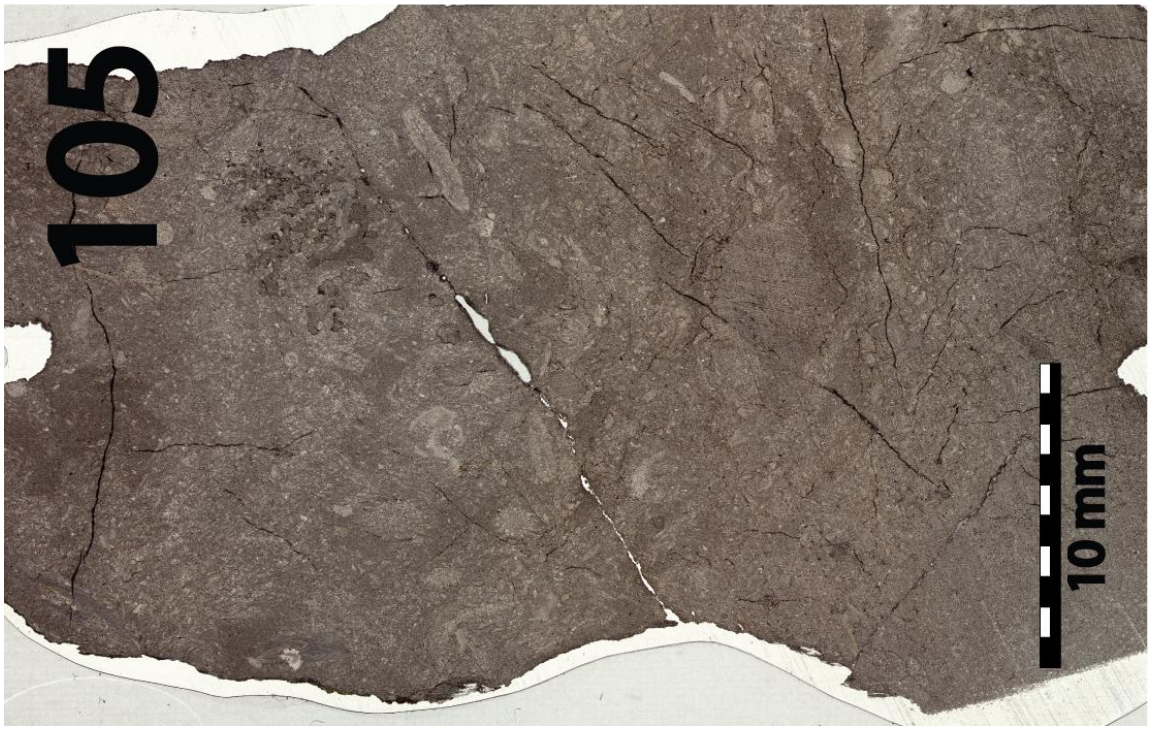

APPENDIX B - Continued

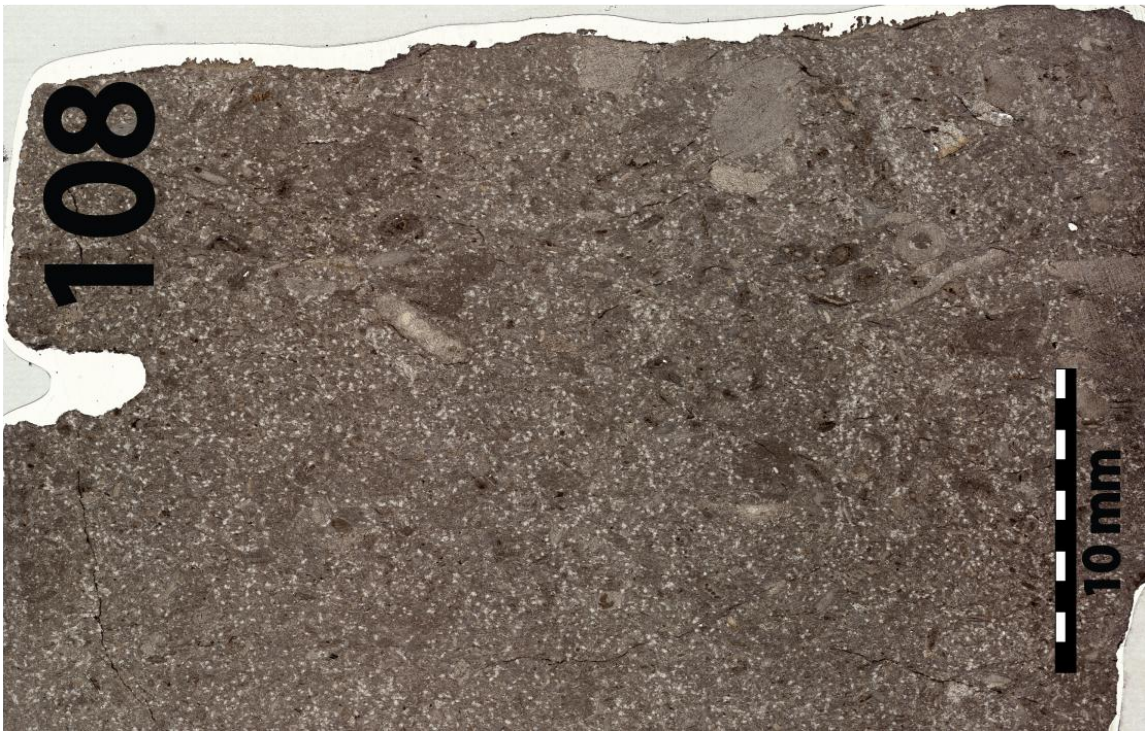

APPENDIX B - Continued

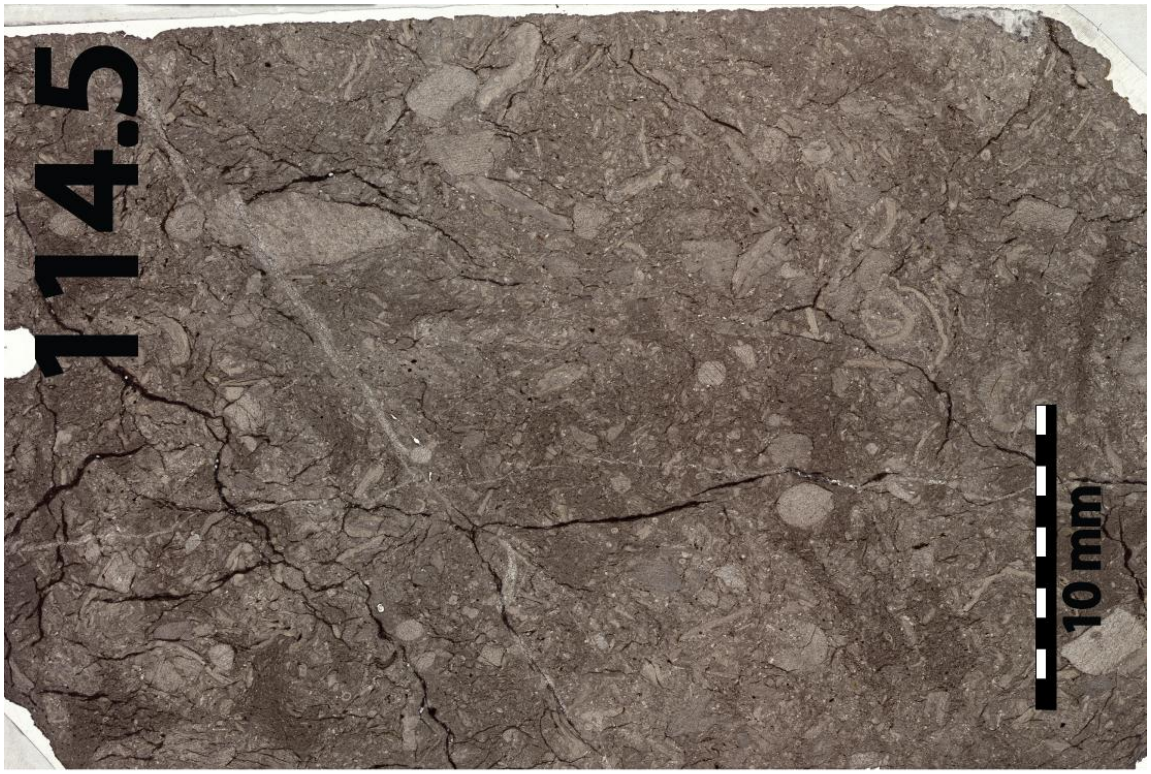

APPENDIX B - Continued

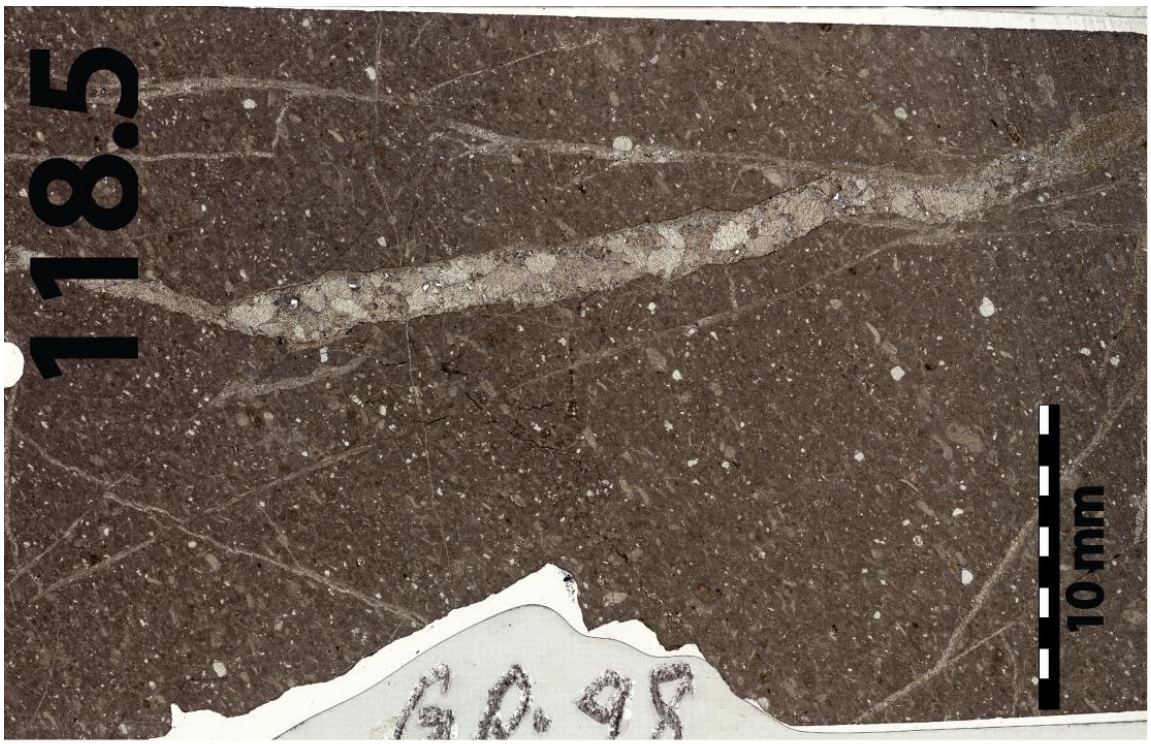

APPENDIX B - Continued

APPENDIX B - Continued

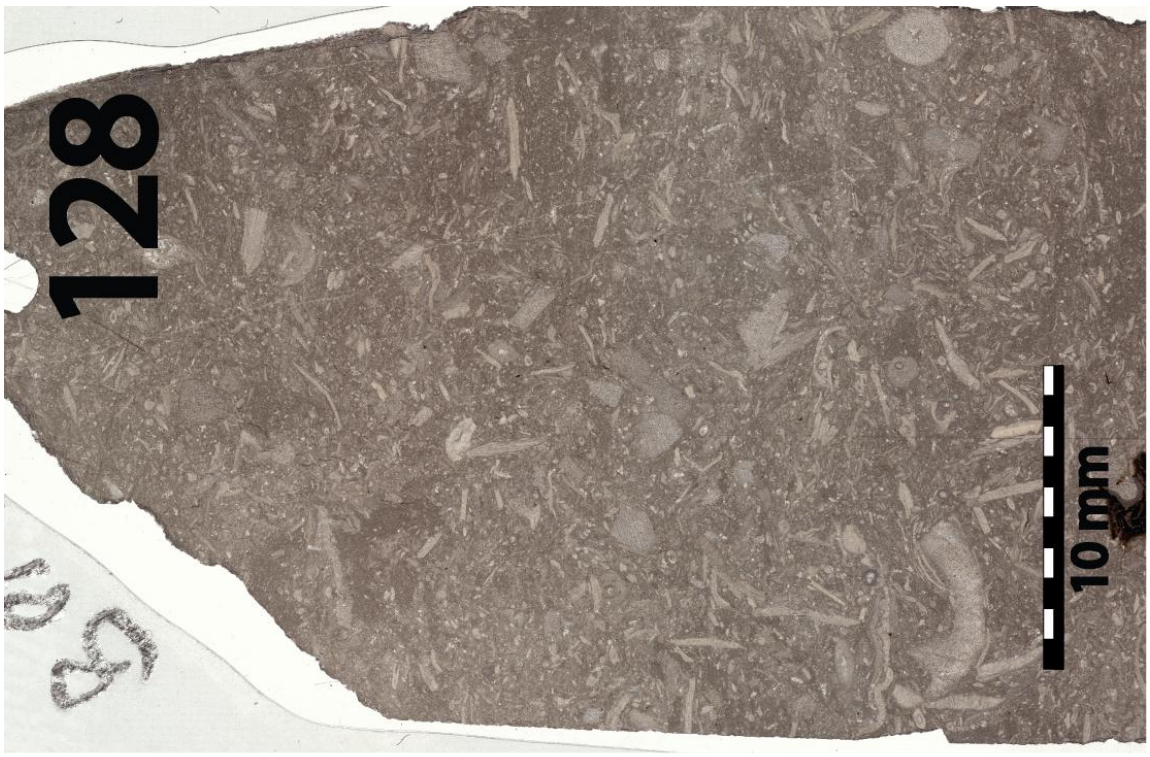

APPENDIX B - Continued

APPENDIX B - Continued

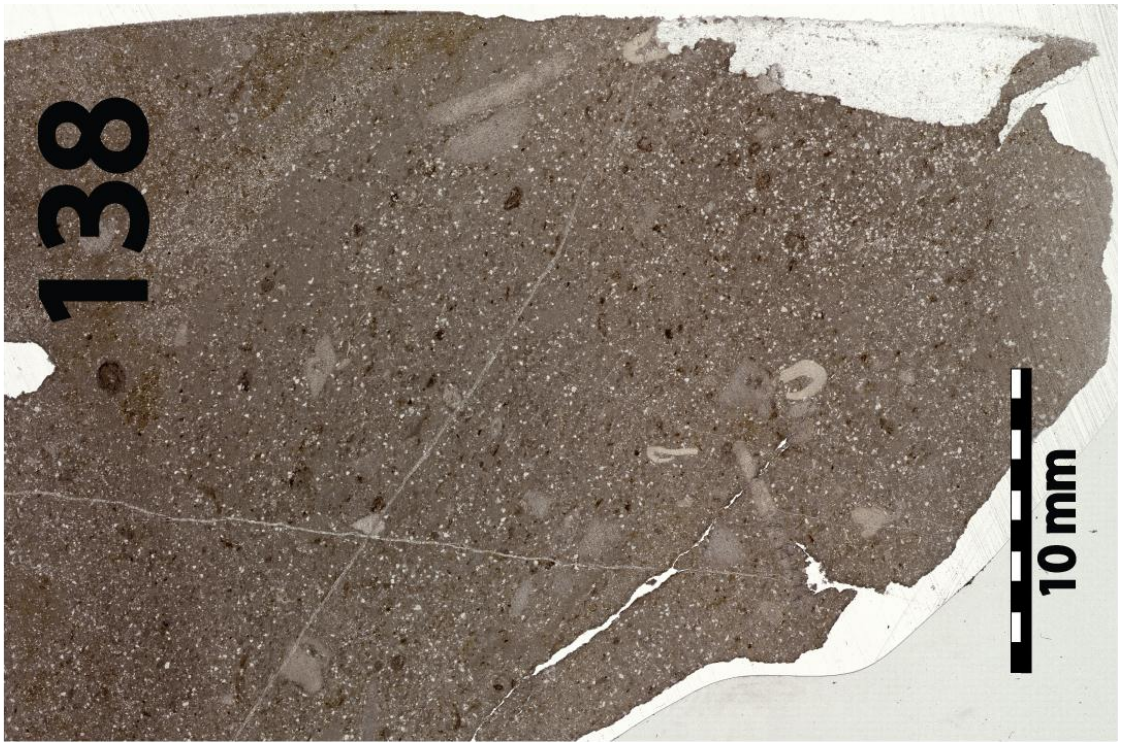

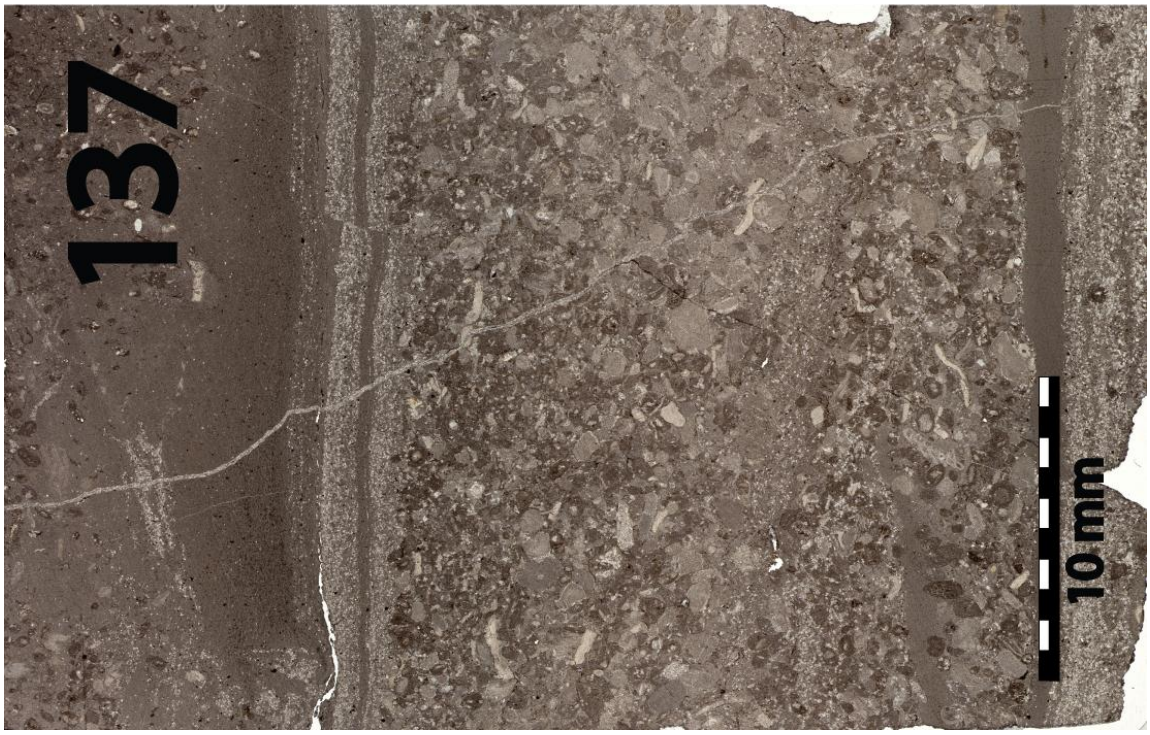

APPENDIX B - Continued

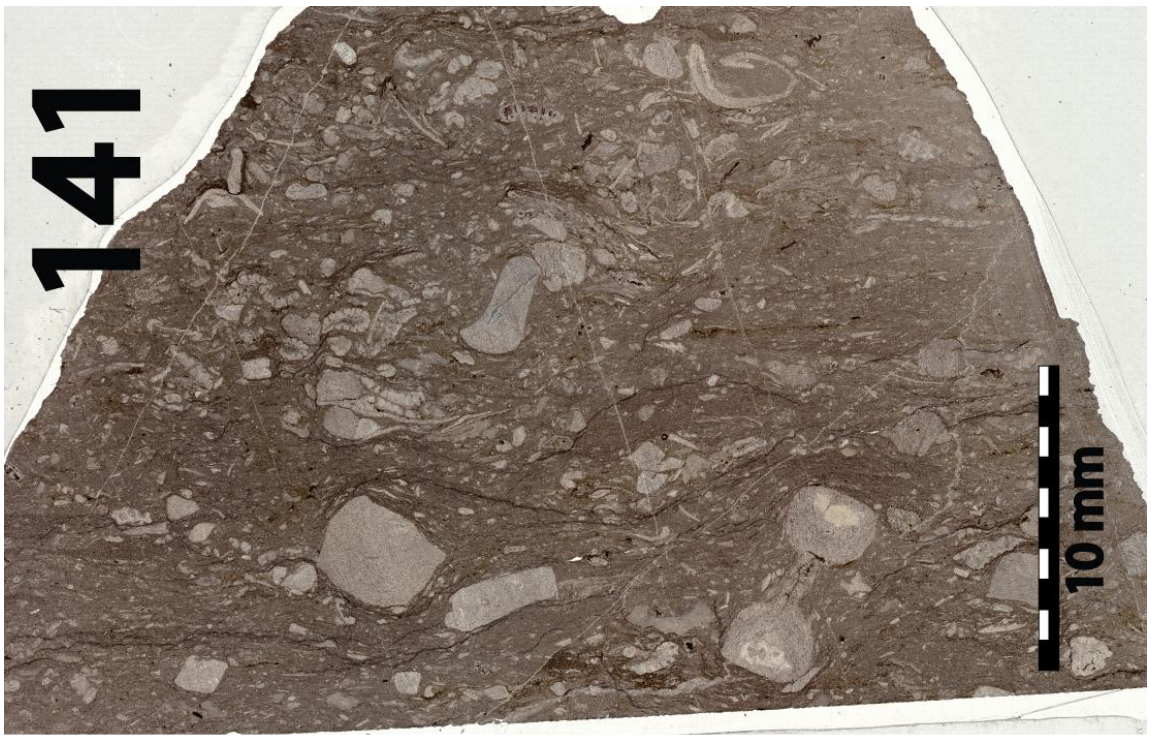

APPENDIX B - Continued

APPENDIX B - Continued

APPENDIX B - Continued

APPENDIX B - Continued

APPENDIX B - Continued

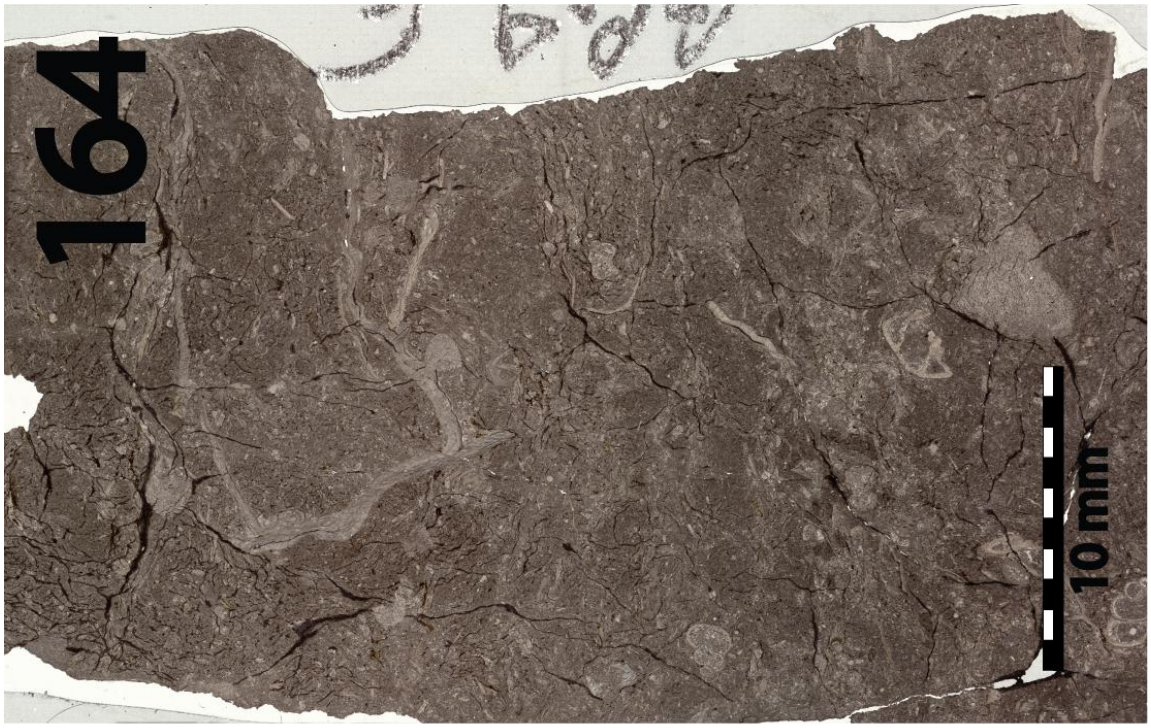

APPENDIX B - Continued

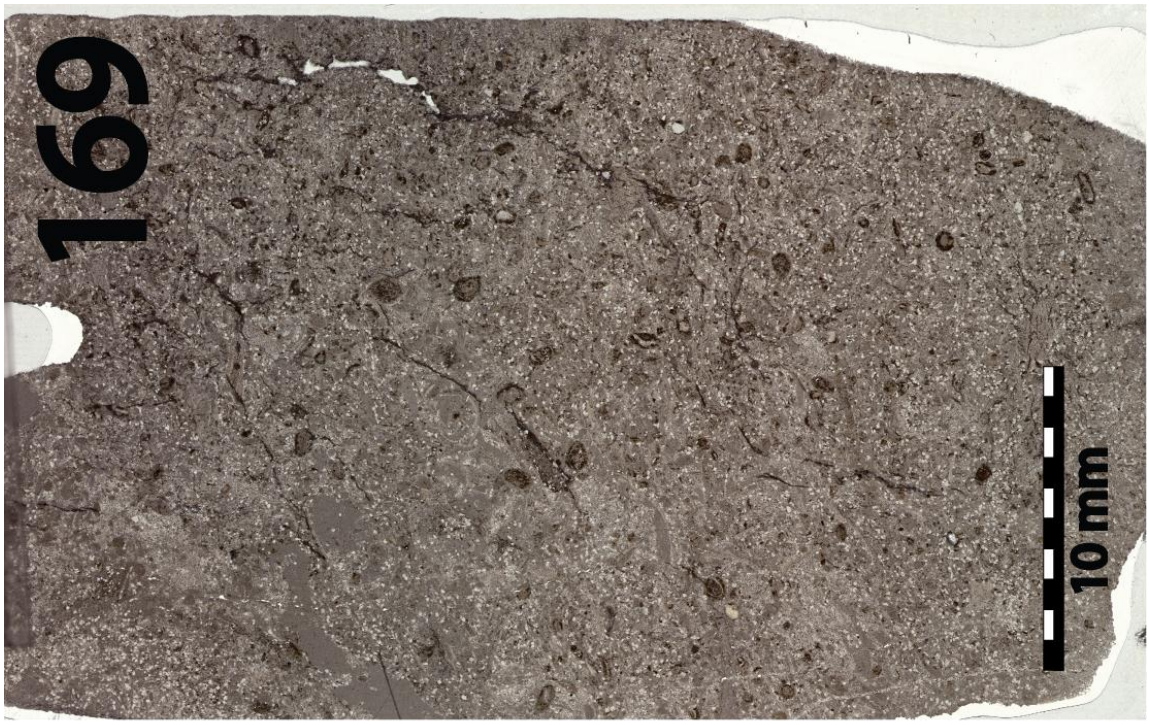

APPENDIX B - Continued

APPENDIX B - Continued

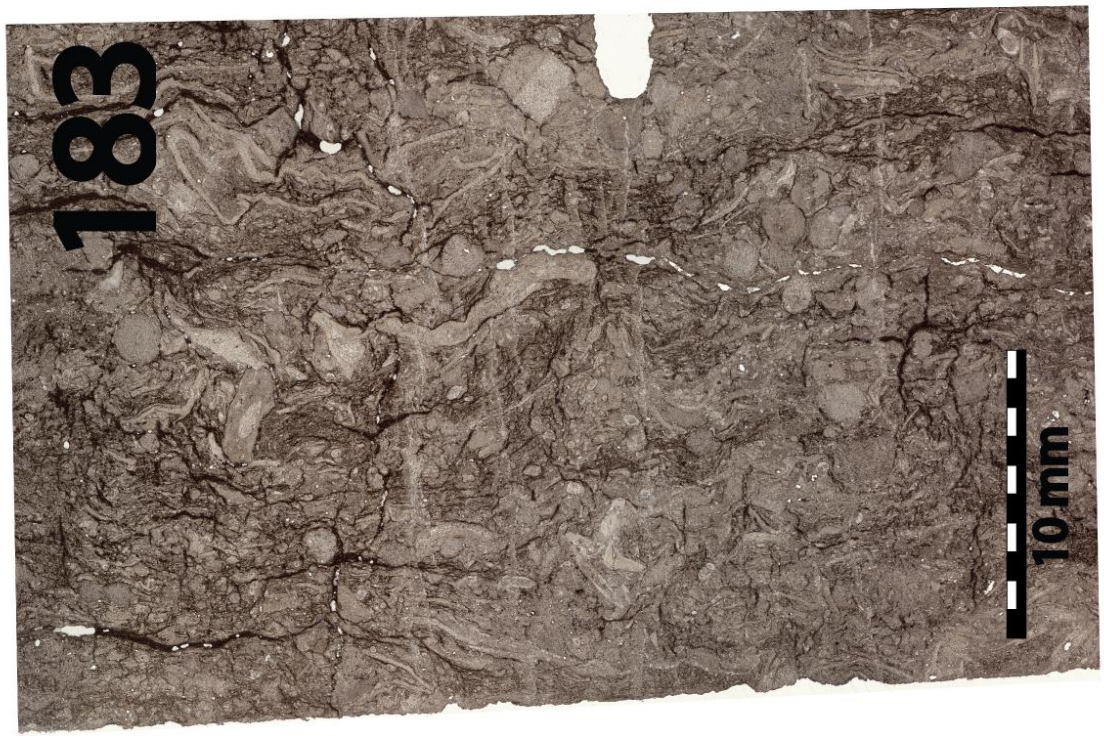

APPENDIX B - Continued

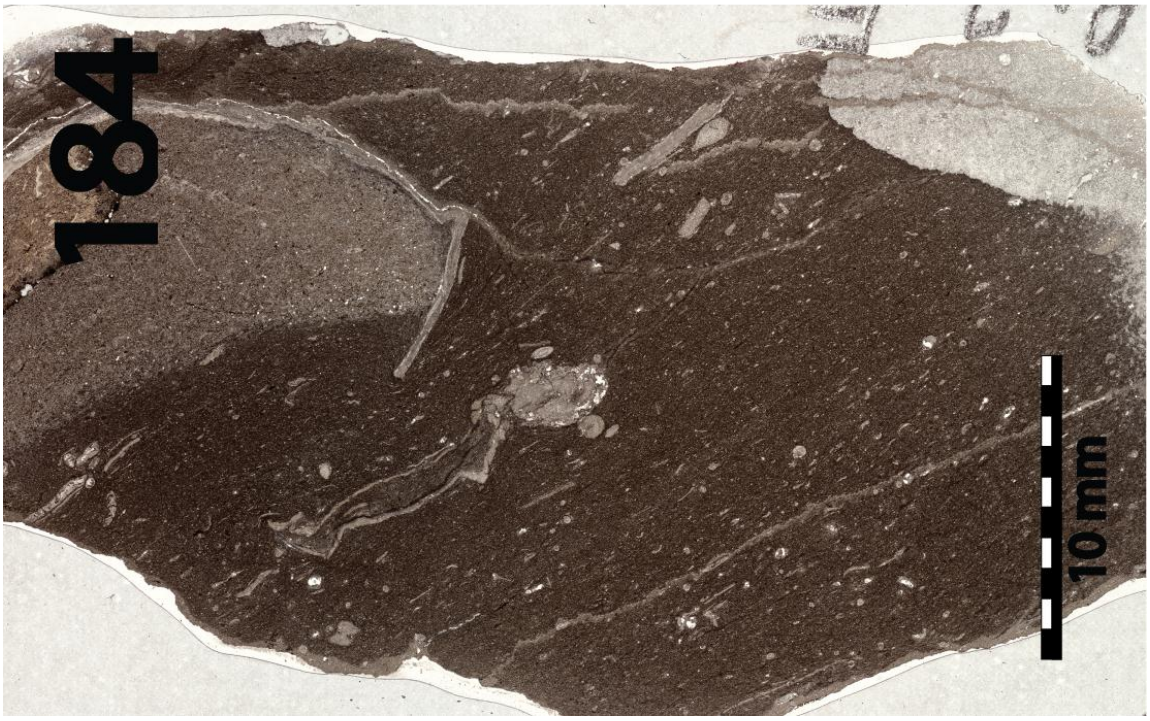

APPENDIX B - Continued

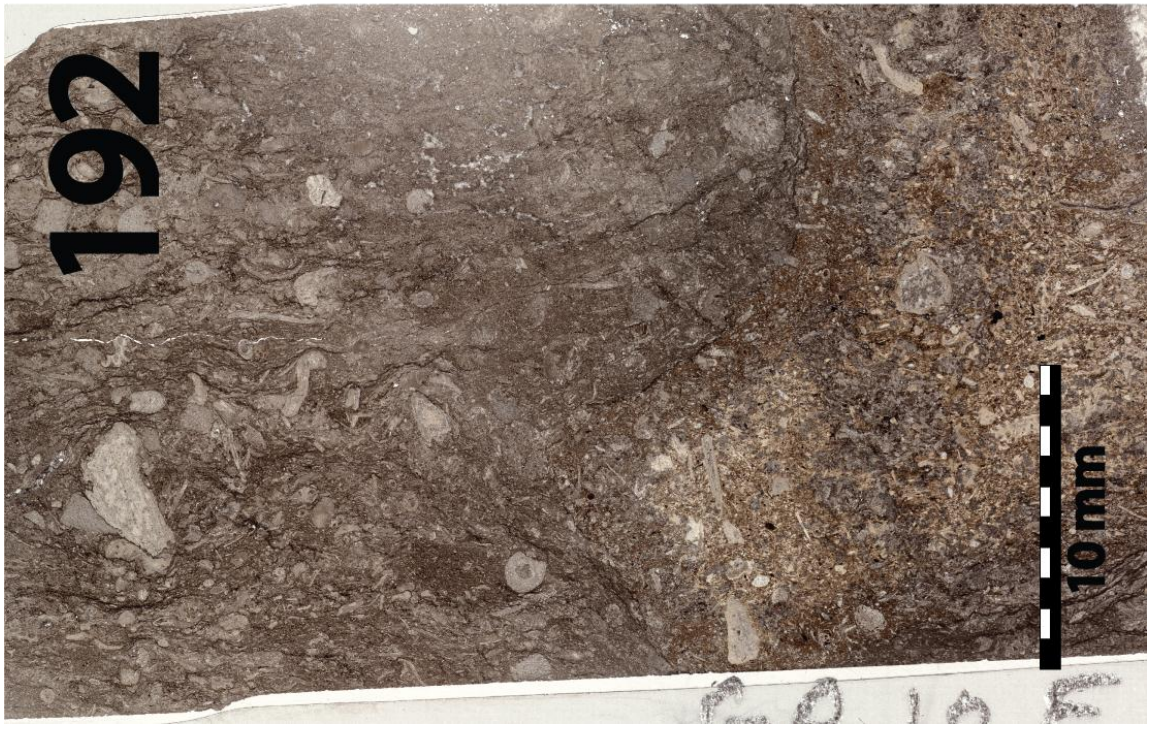

APPENDIX B - Continued

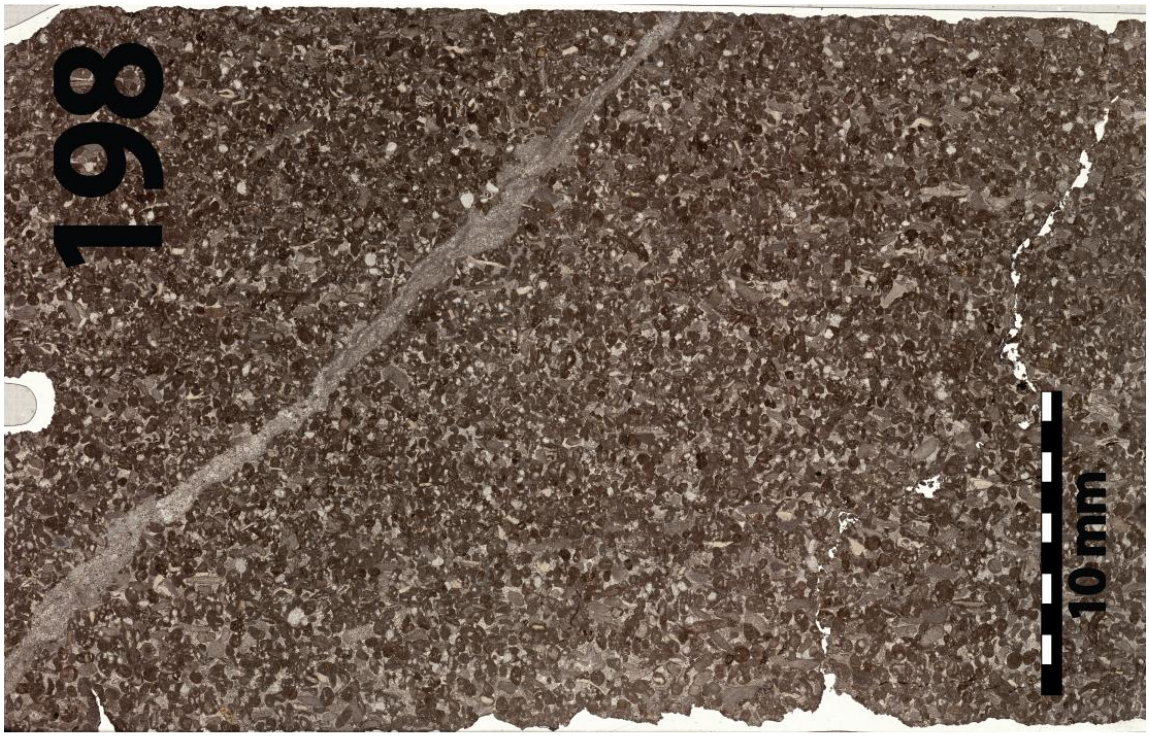

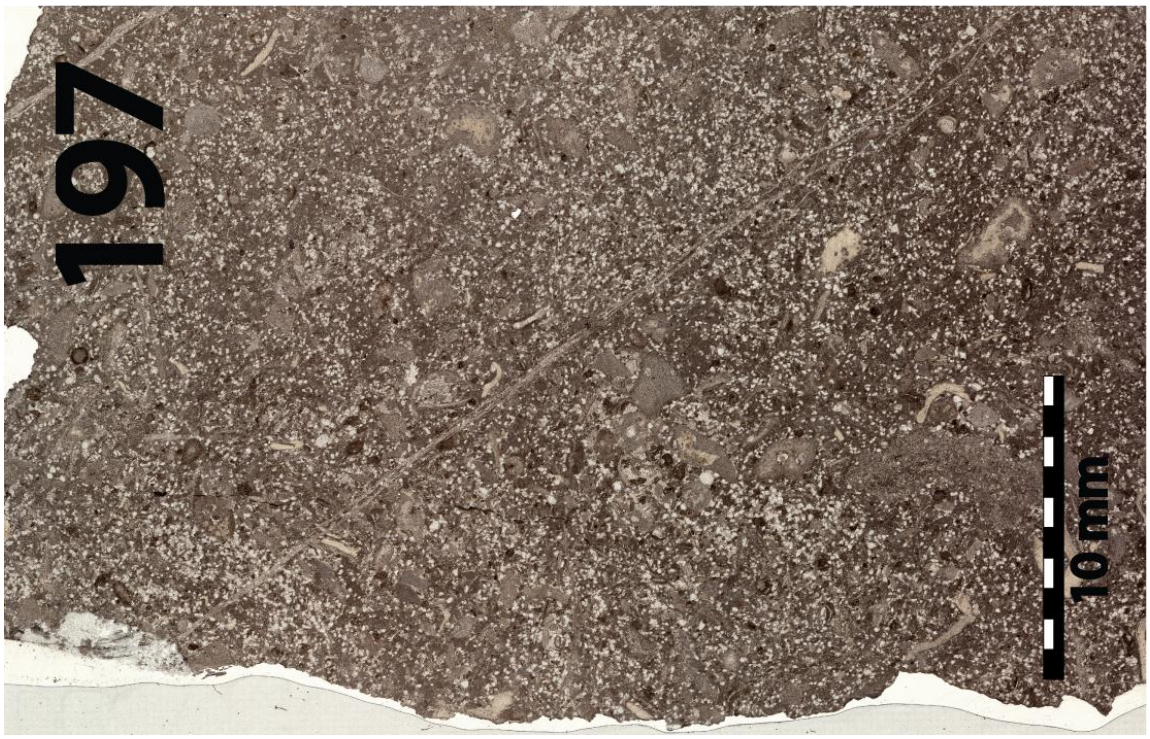

APPENDIX B - Continued

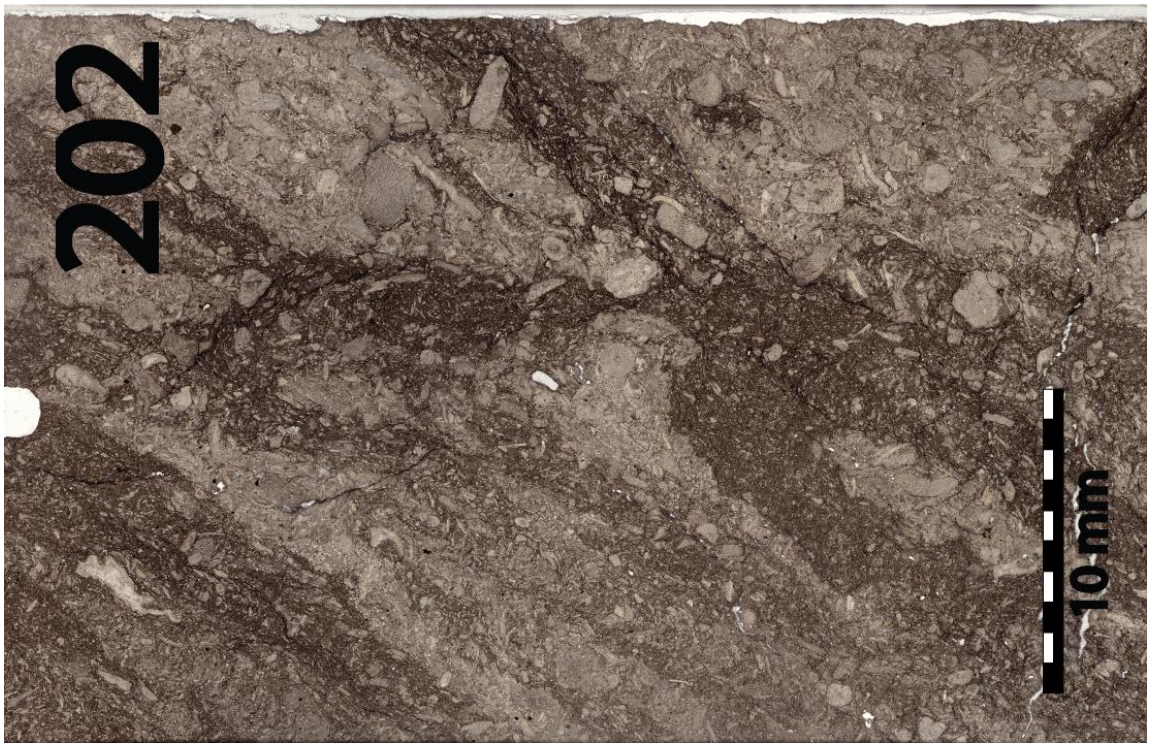

APPENDIX B - Continued

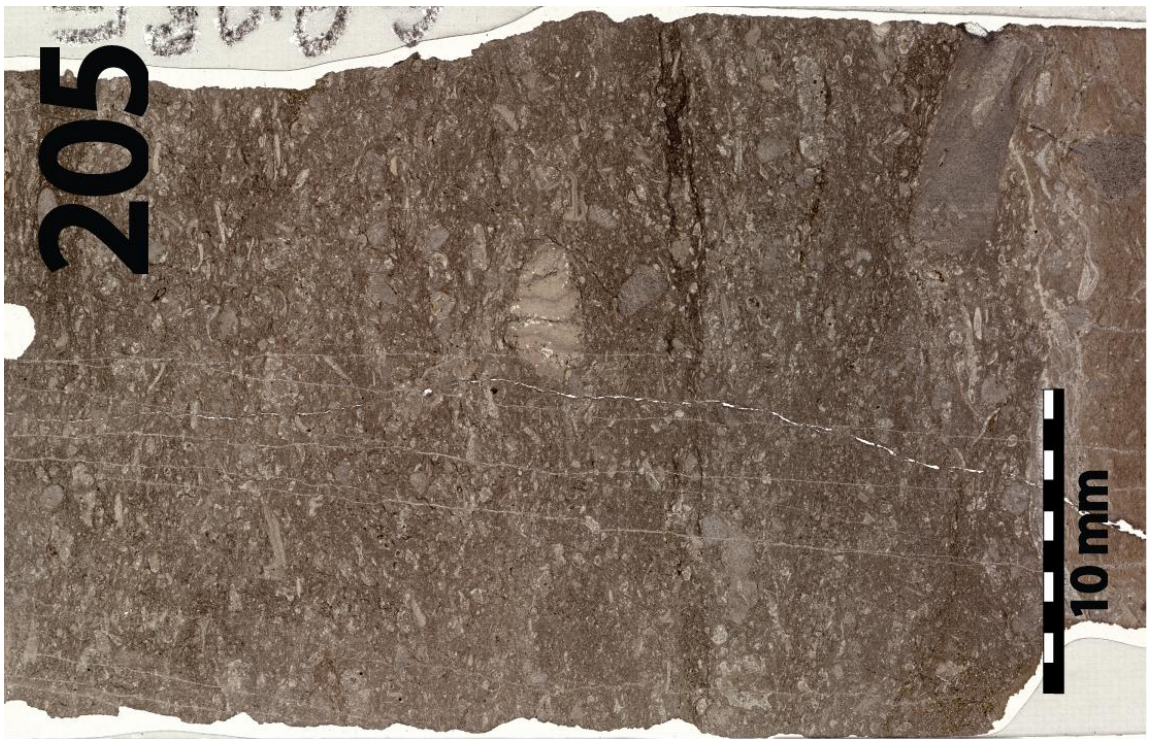

APPENDIX B - Continued

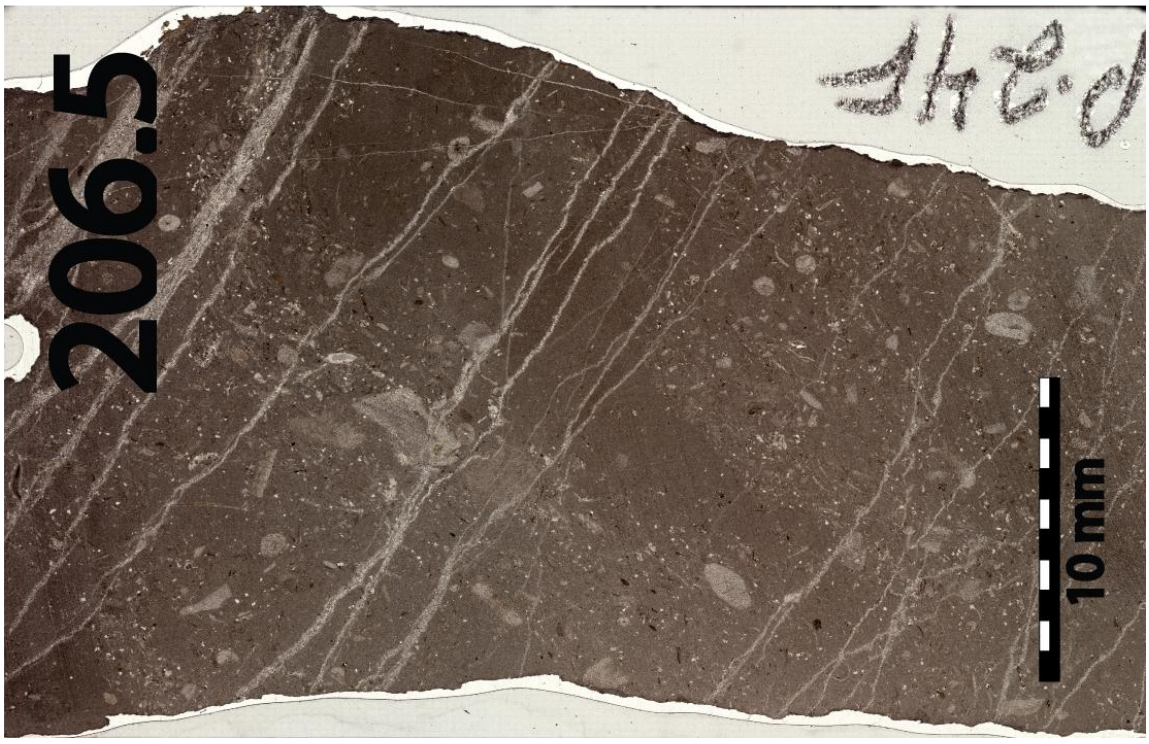

APPENDIX B - Continued

APPENDIX B - Continued

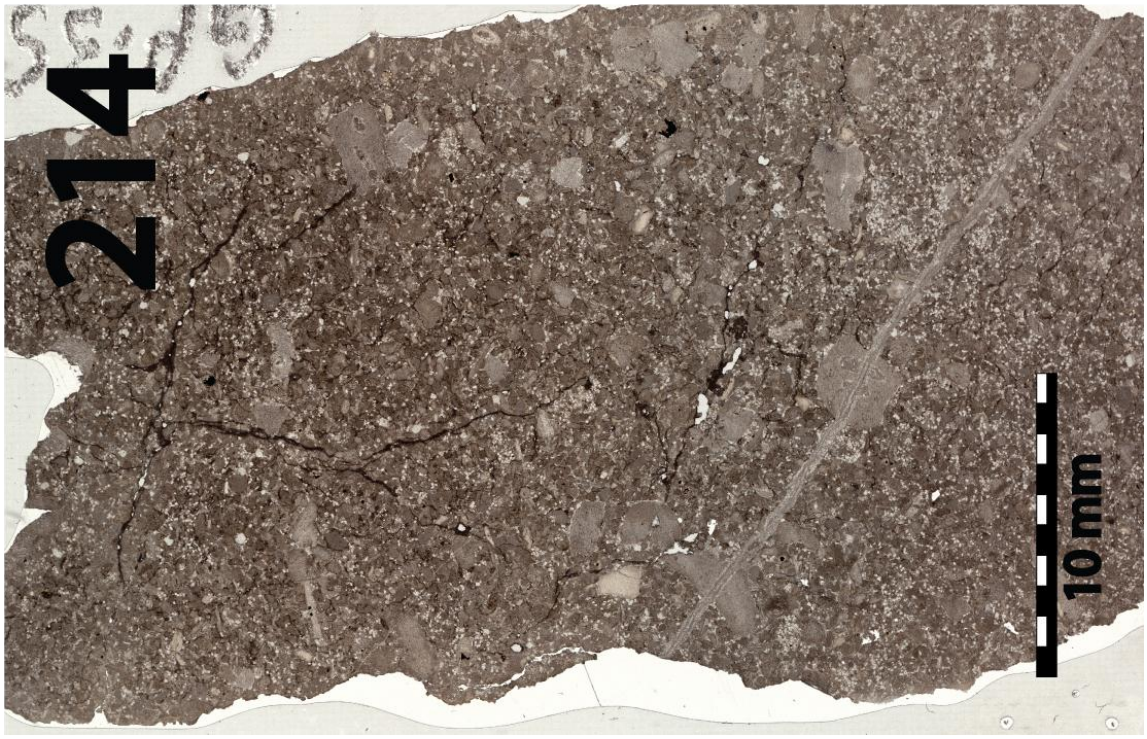

APPENDIX B - Continued

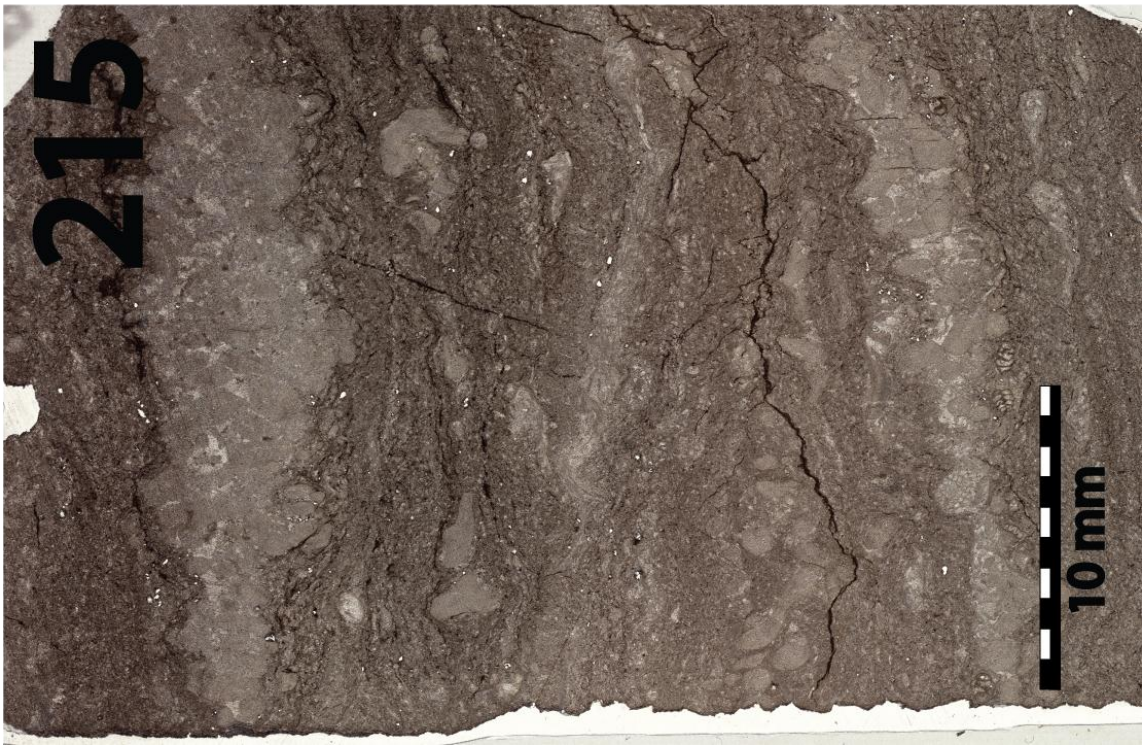

APPENDIX B - Continued

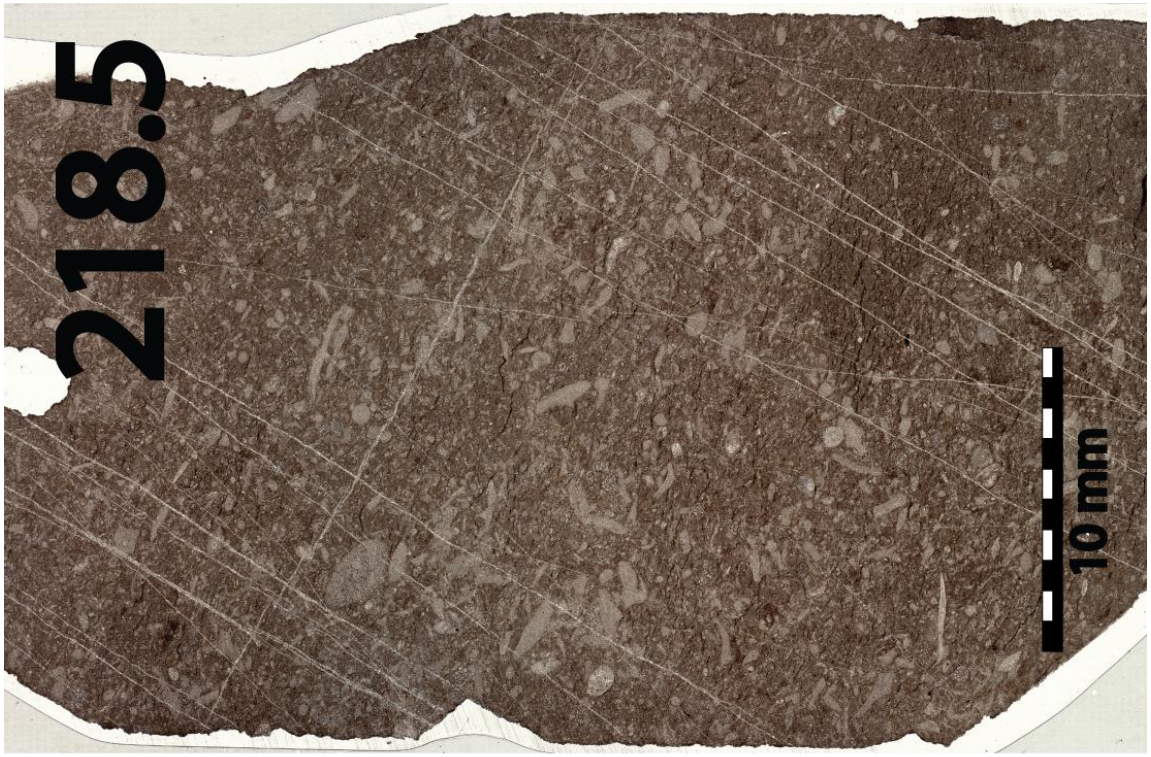

APPENDIX B - Continued

APPENDIX B - Continued

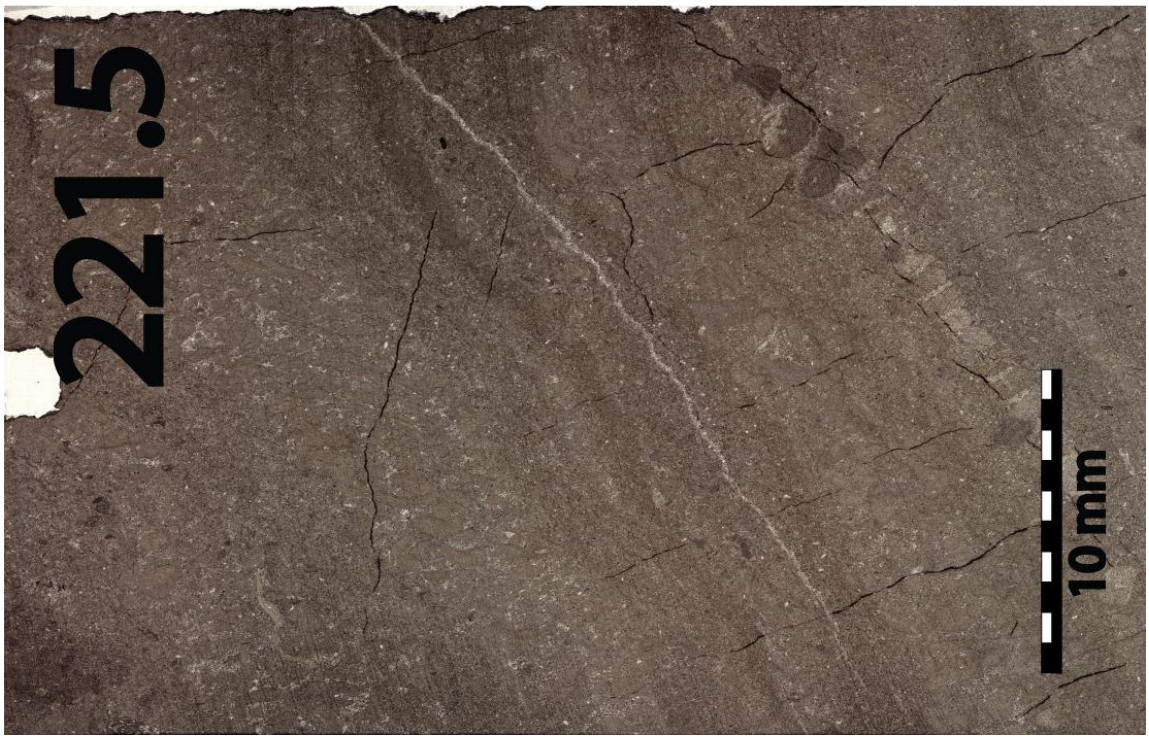

APPENDIX B - Continued

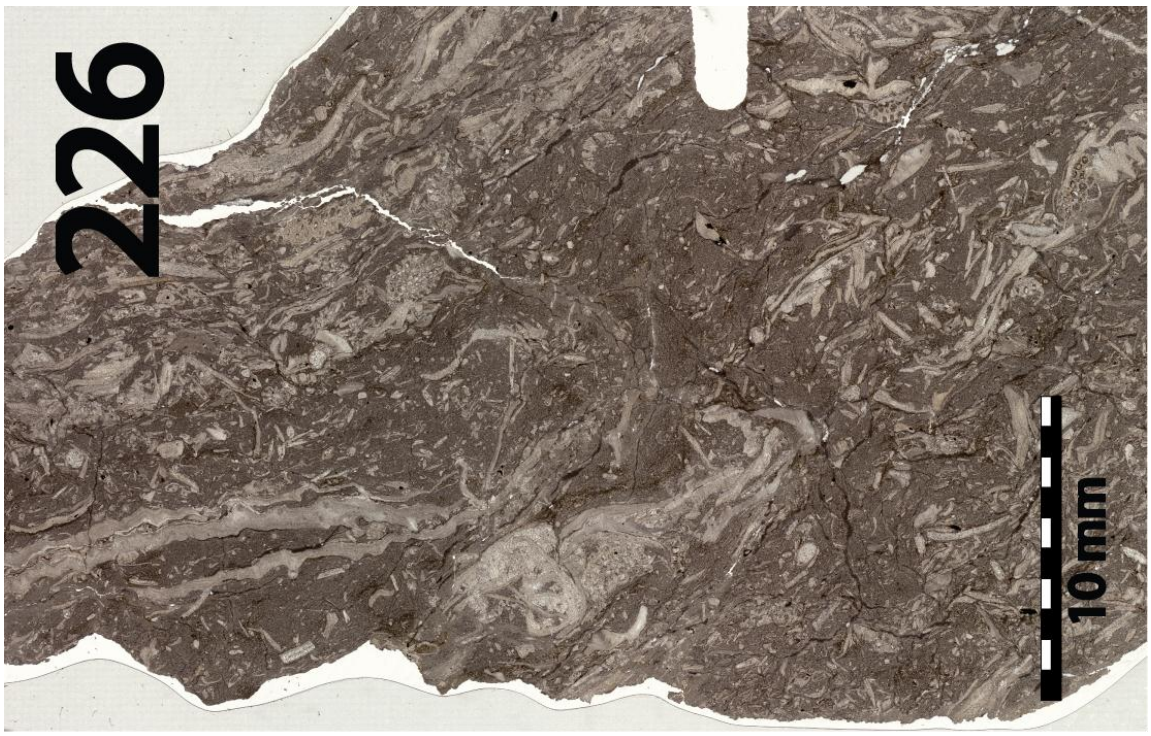

APPENDIX B - Continued

APPENDIX B - Continued

APPENDIX B - Continued

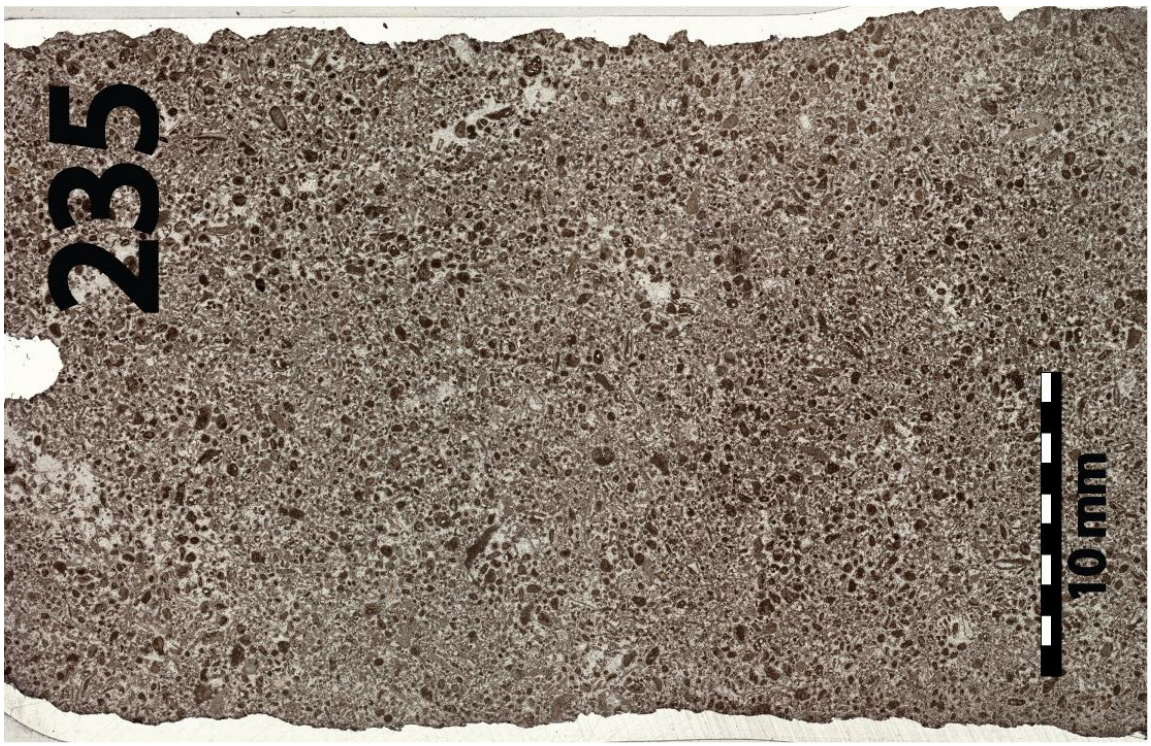

APPENDIX B - Continued

APPENDIX B - Continued

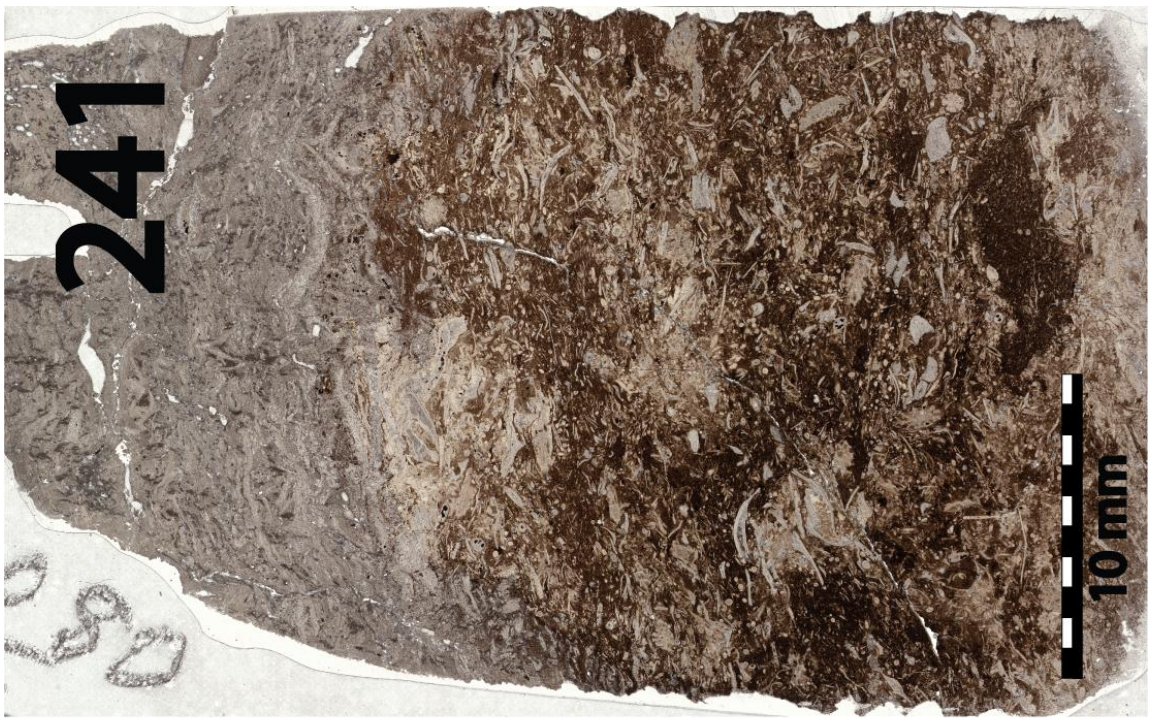

APPENDIX B - Continued

APPENDIX B - Continued

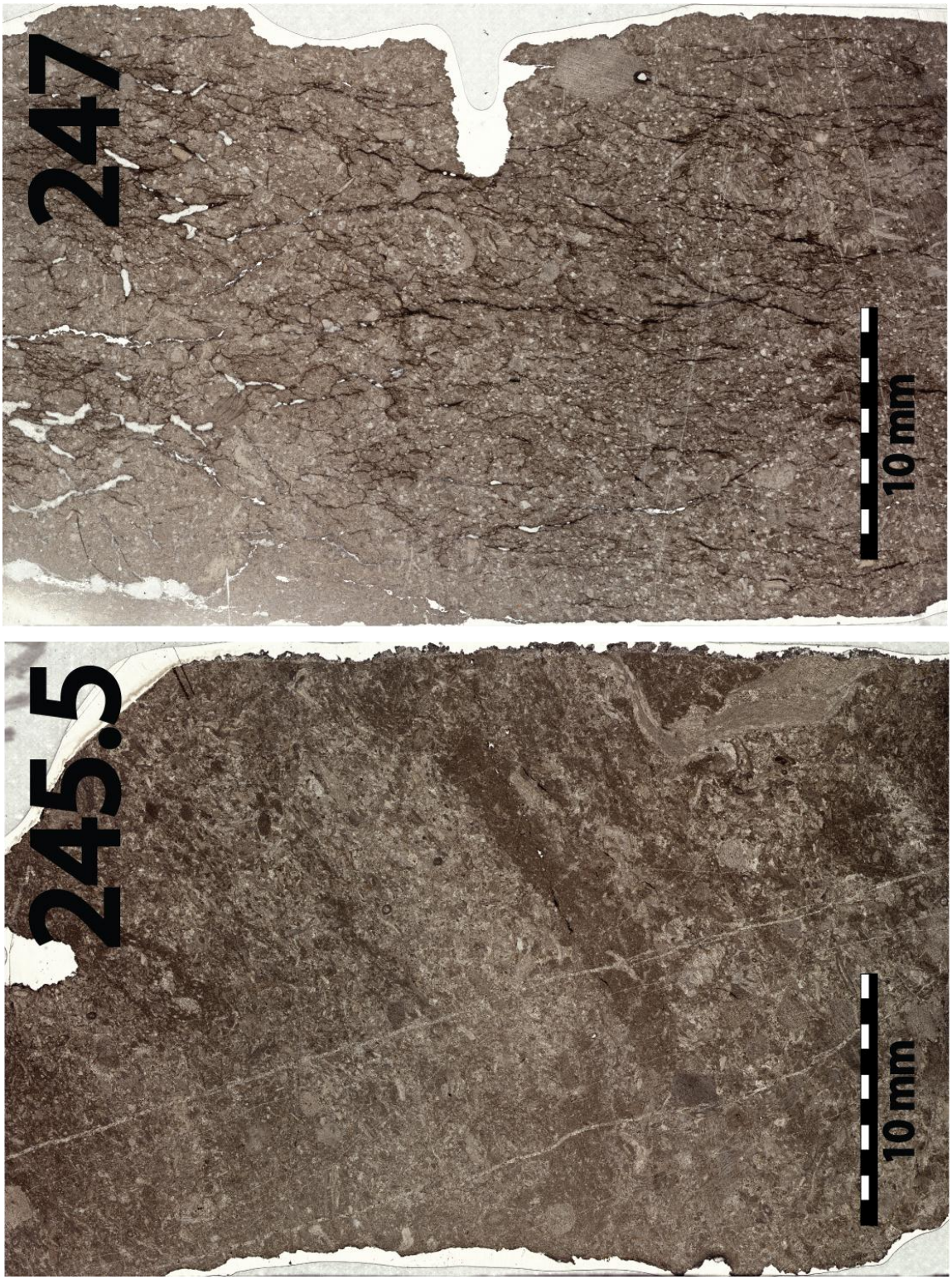

APPENDIX B - Continued

APPENDIX B - Continued

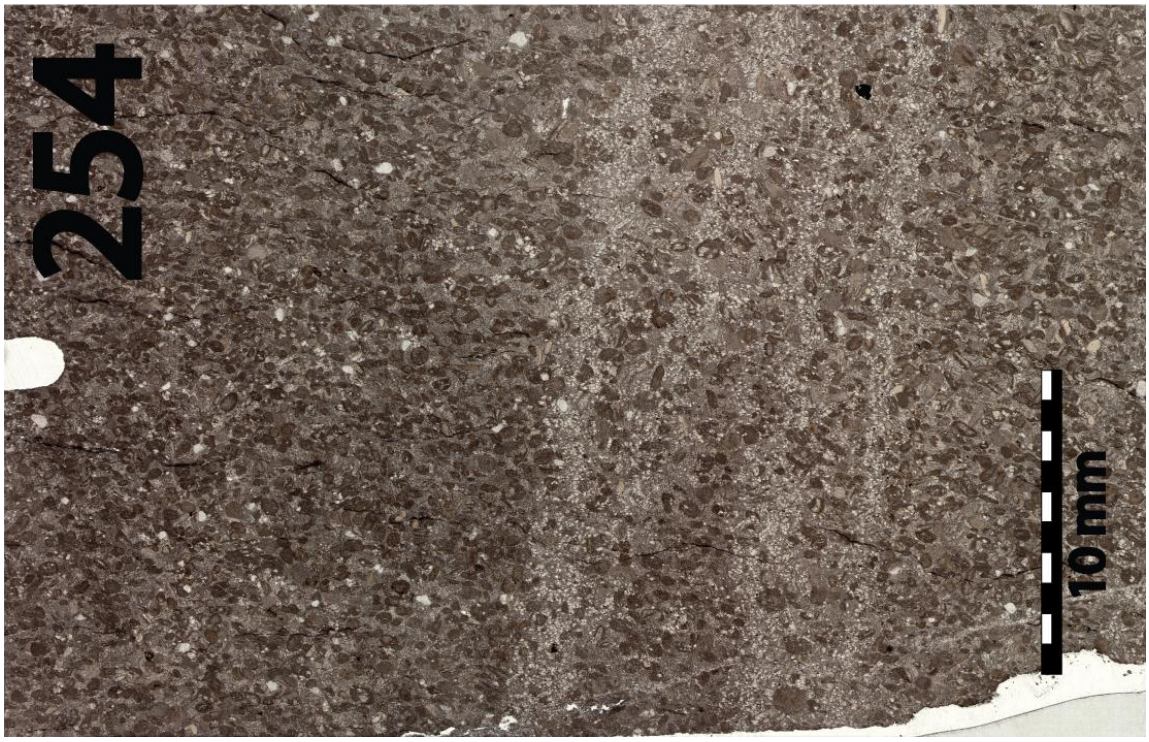

APPENDIX B - Continued

APPENDIX B - Continued

APPENDIX B - Continued

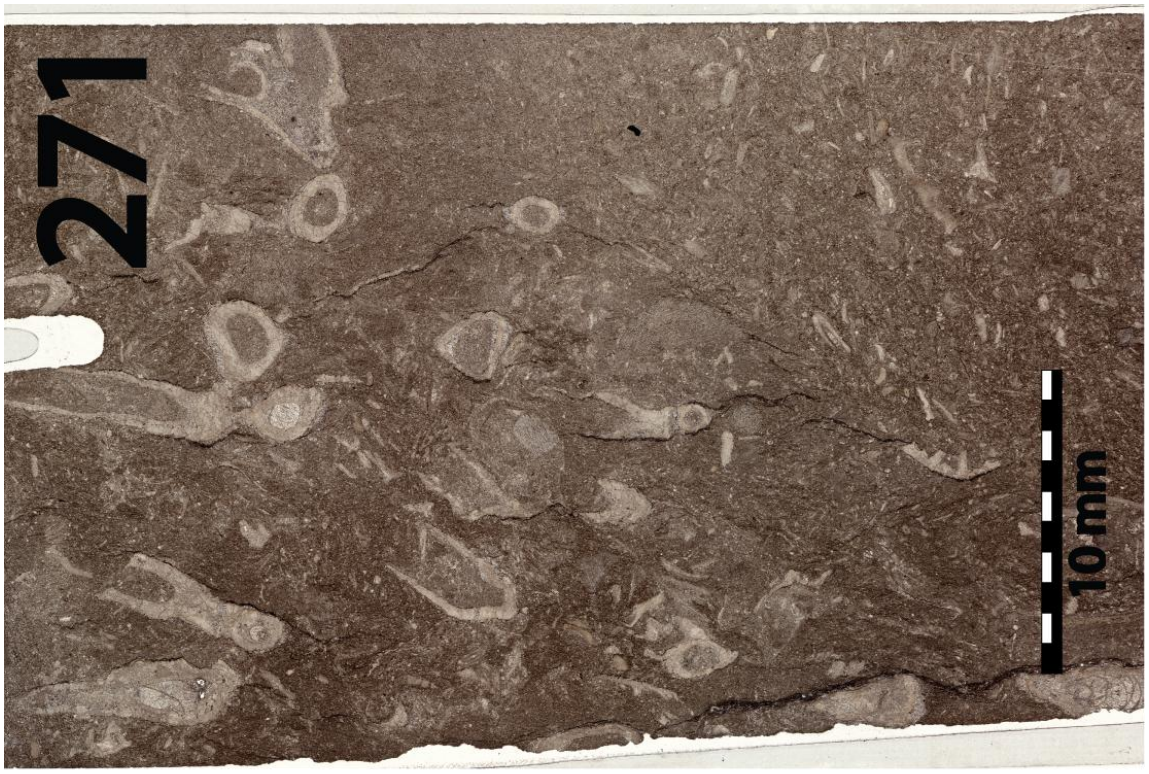

APPENDIX B - Continued

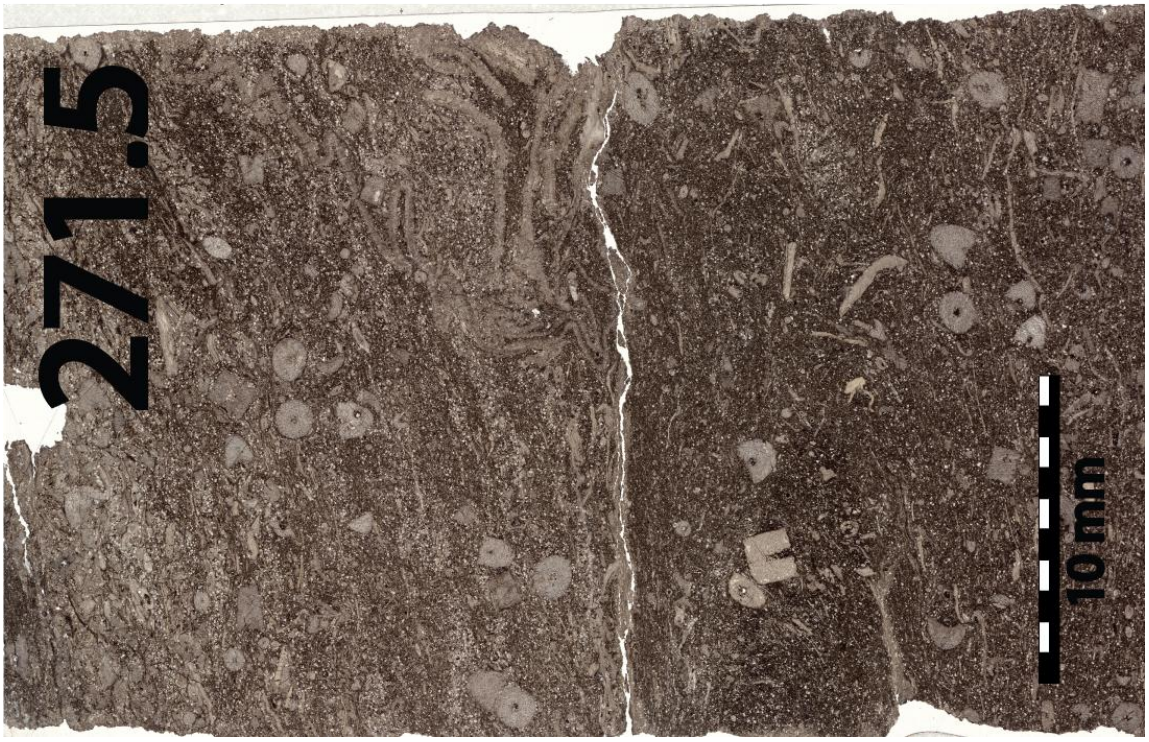

APPENDIX B - Continued

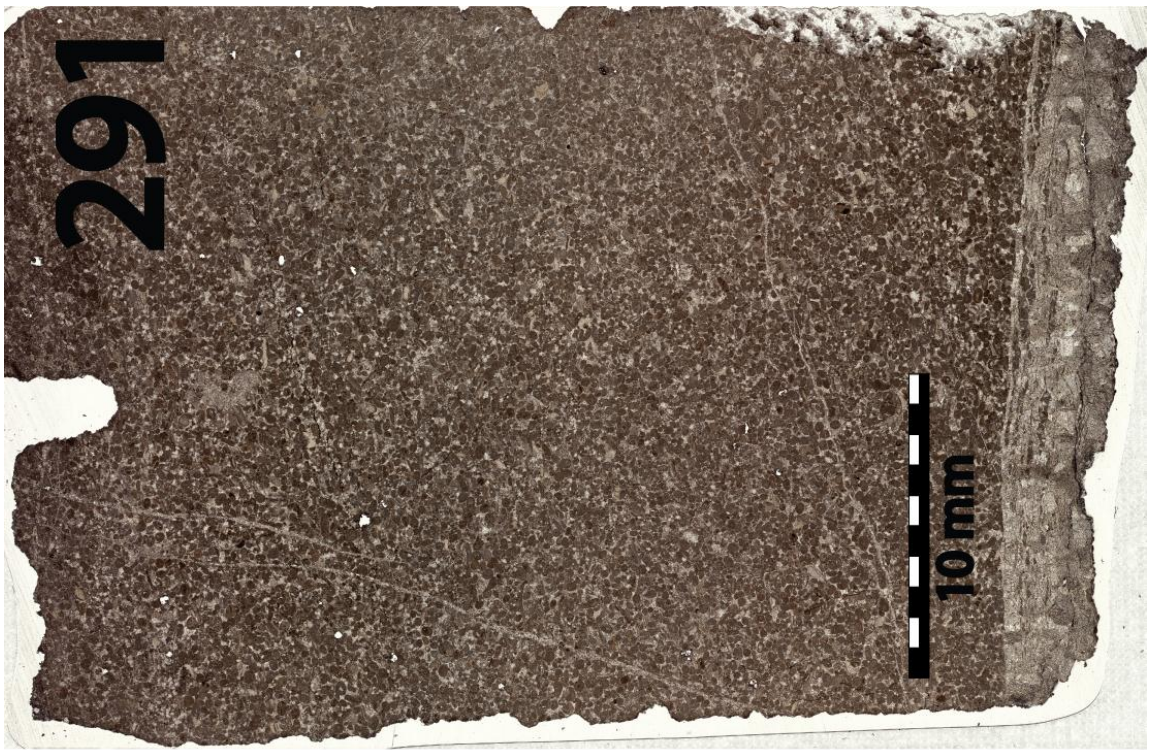

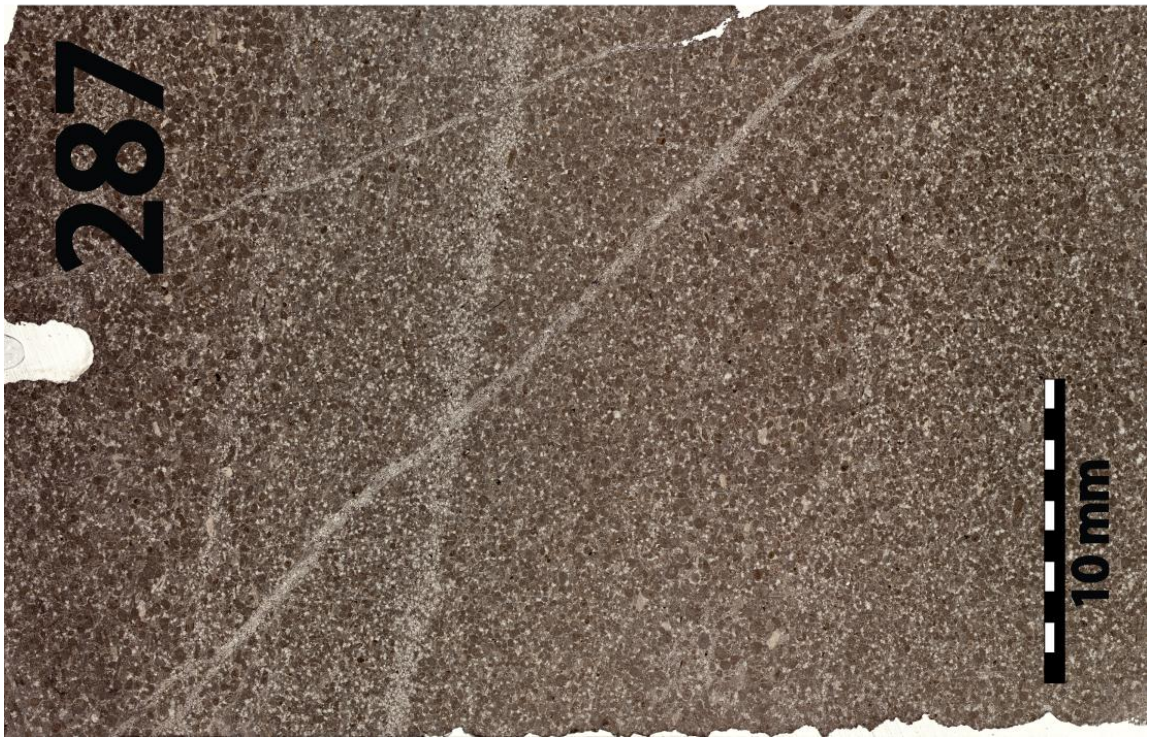

APPENDIX B - Continued

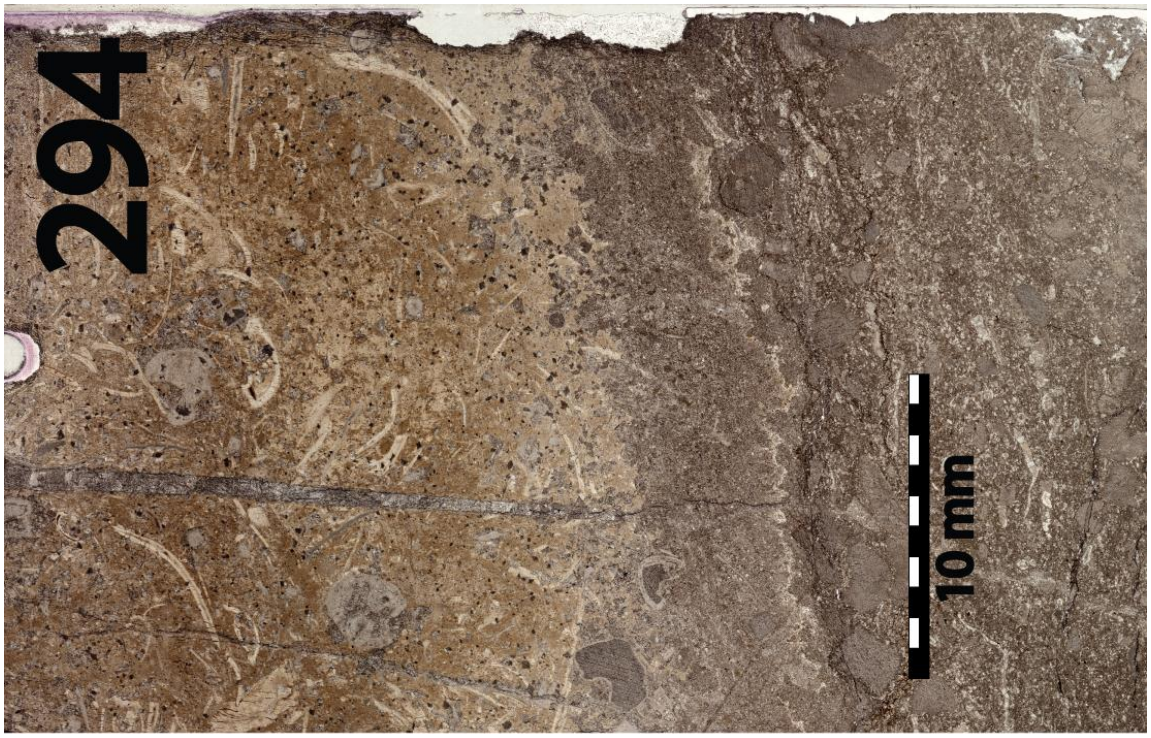

APPENDIX B - Continued

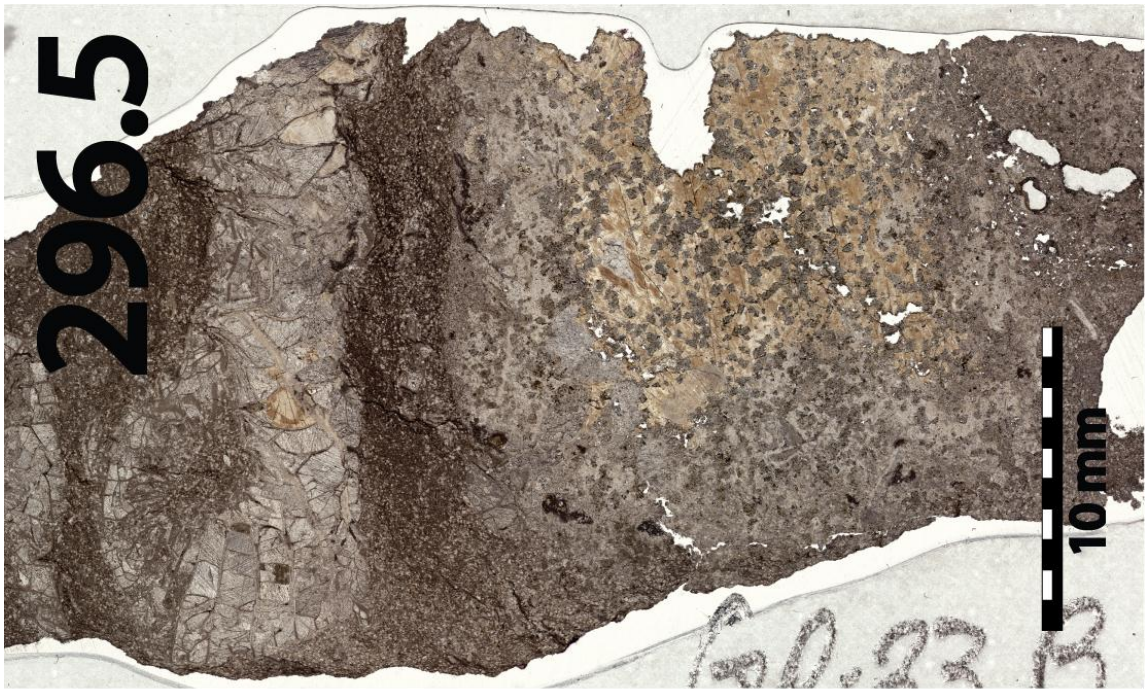

APPENDIX B - Continued

APPENDIX B - Continued

APPENDIX B - Continued

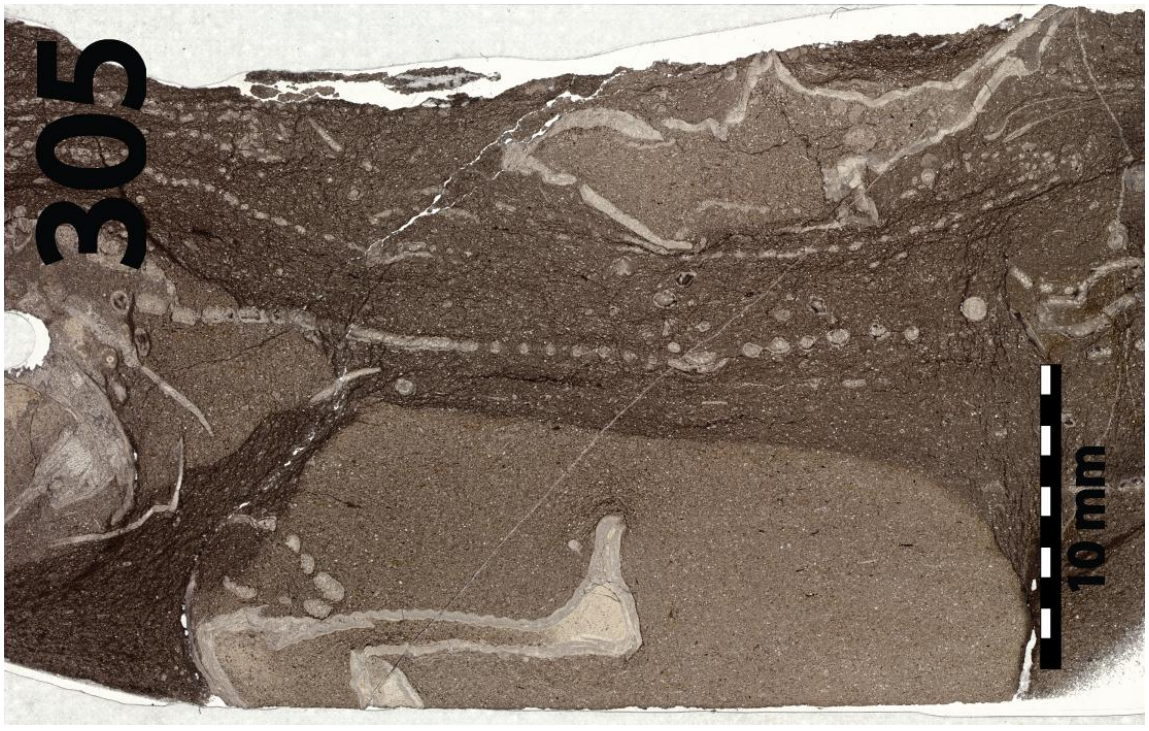

APPENDIX B - Continued

APPENDIX B - Continued

APPENDIX B - Continued

APPENDIX B - Continued

APPENDIX B - Continued

APPENDIX B - Continued

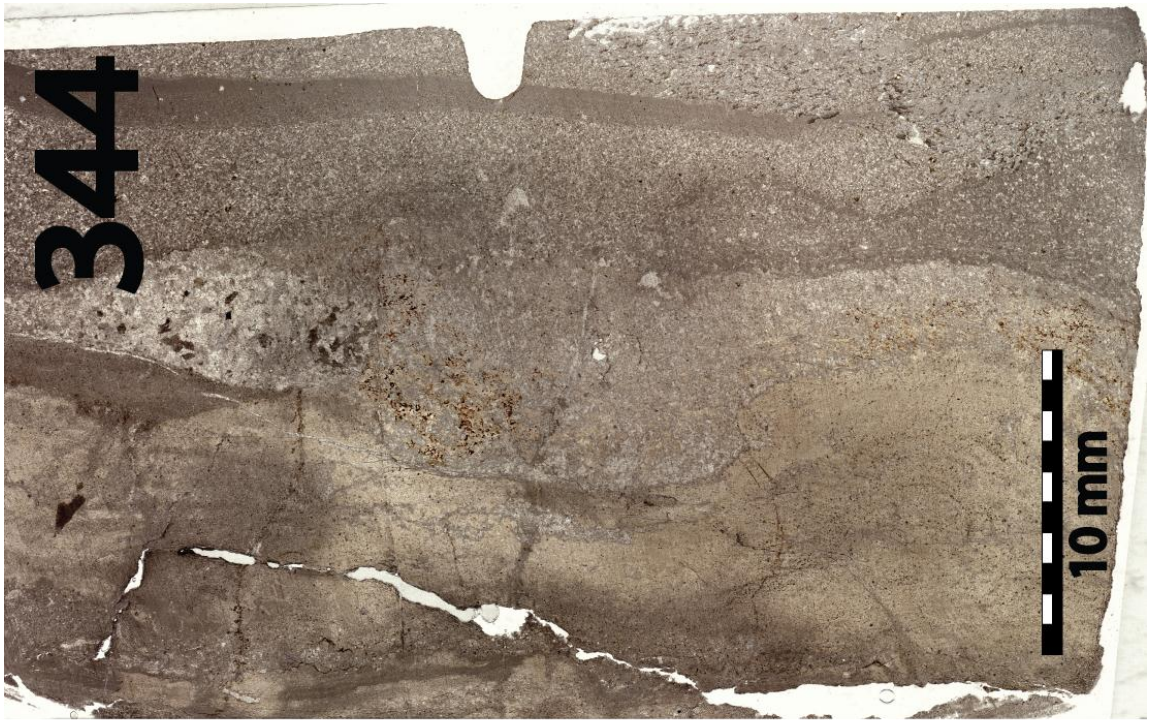

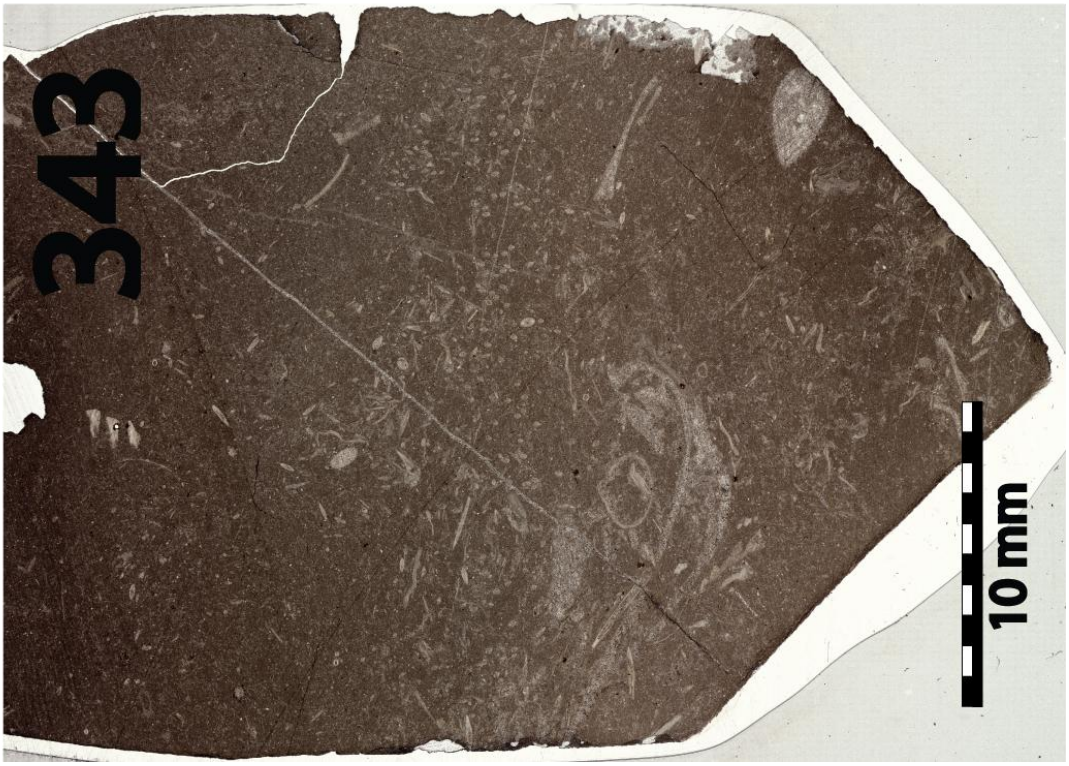

APPENDIX B - Continued

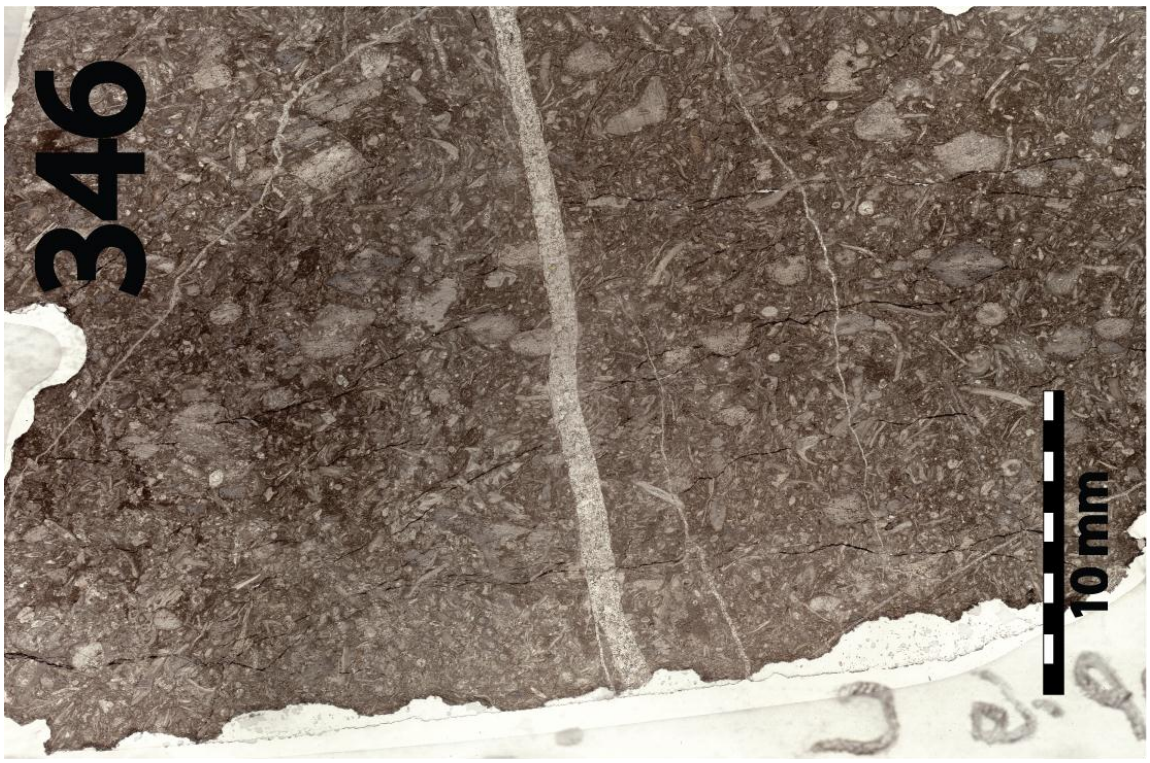

APPENDIX B - Continued

APPENDIX B - Continued

APPENDIX B - Continued

APPENDIX B - Continued

APPENDIX B - Continued

APPENDIX B - Continued

APPENDIX B - Continued

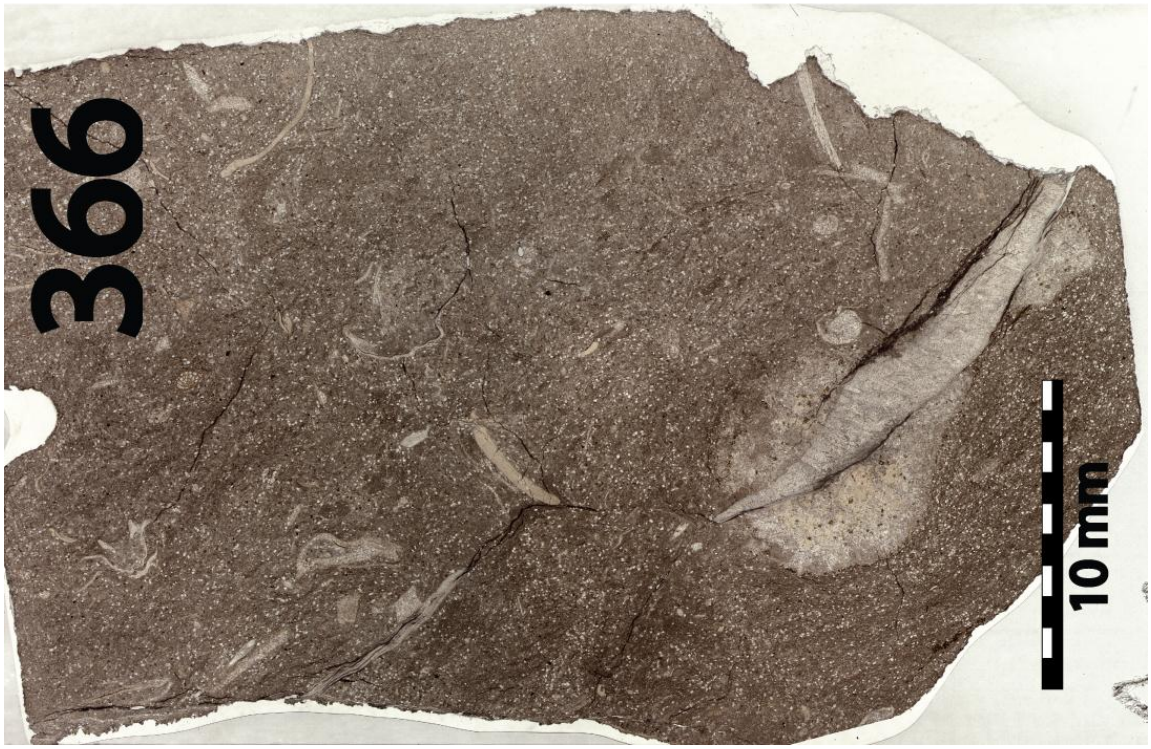

APPENDIX B - Continued

APPENDIX B - Continued

APPENDIX B - Continued

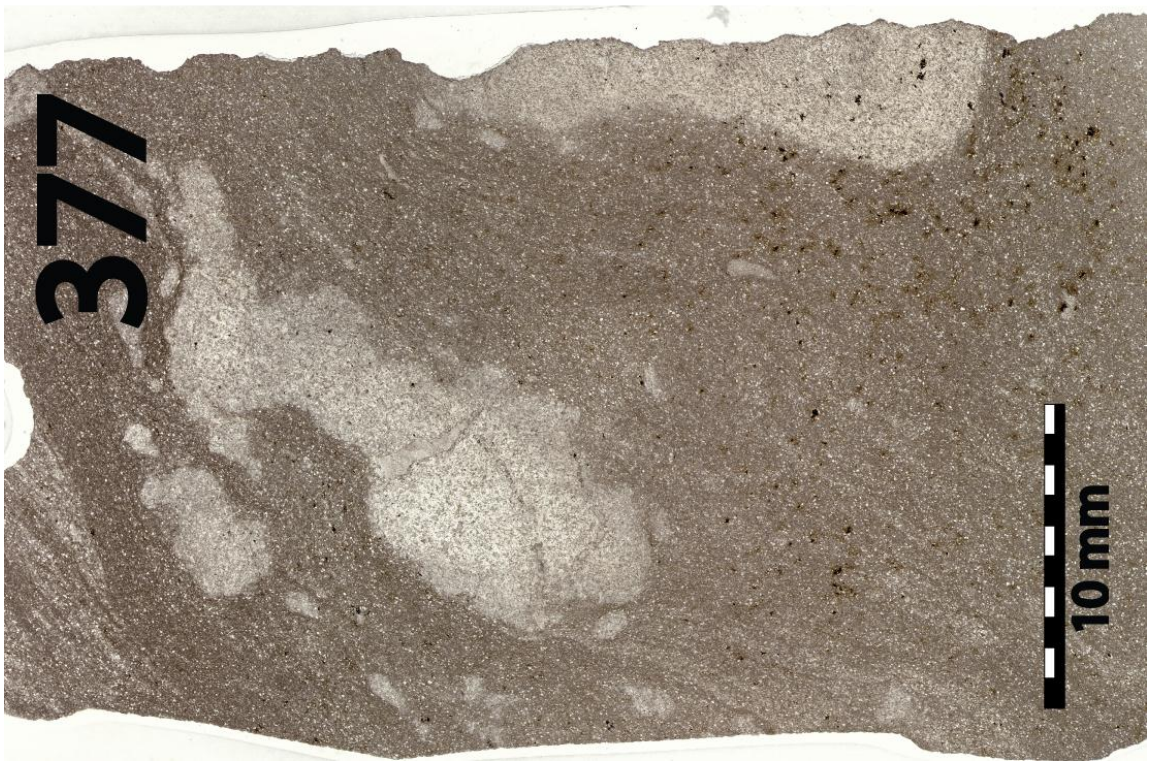

APPENDIX B - Continued

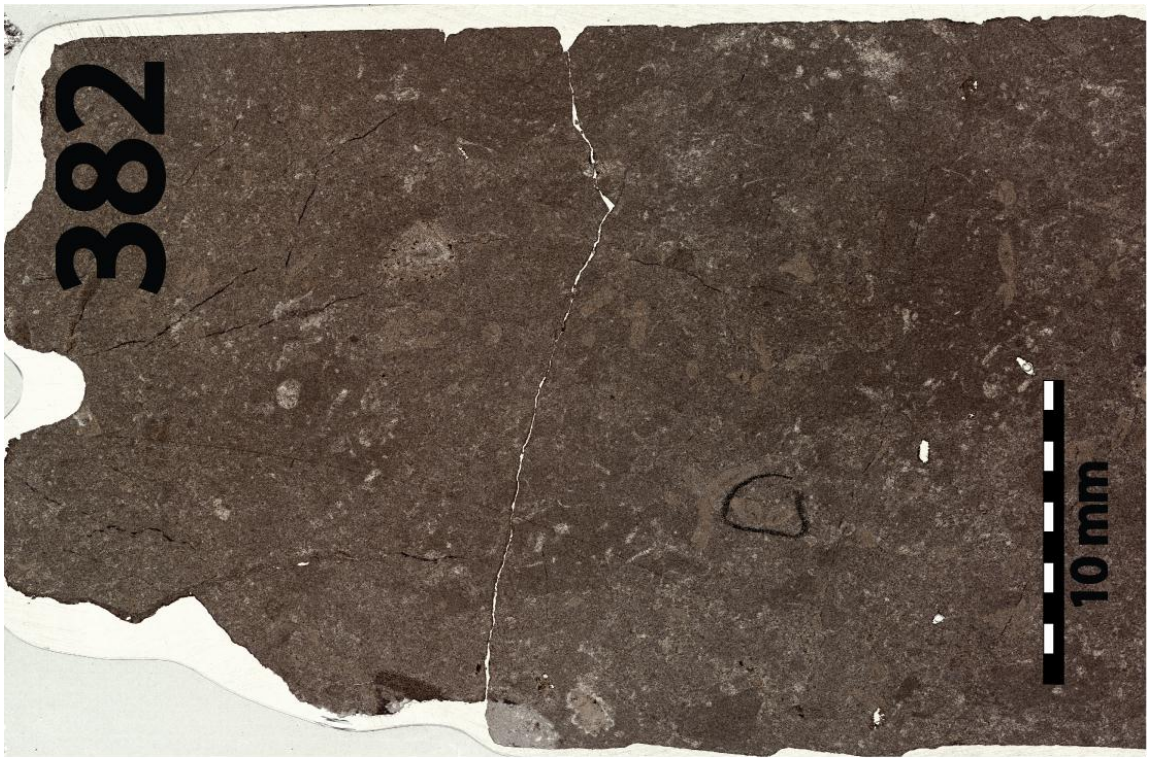

APPENDIX B - Continued

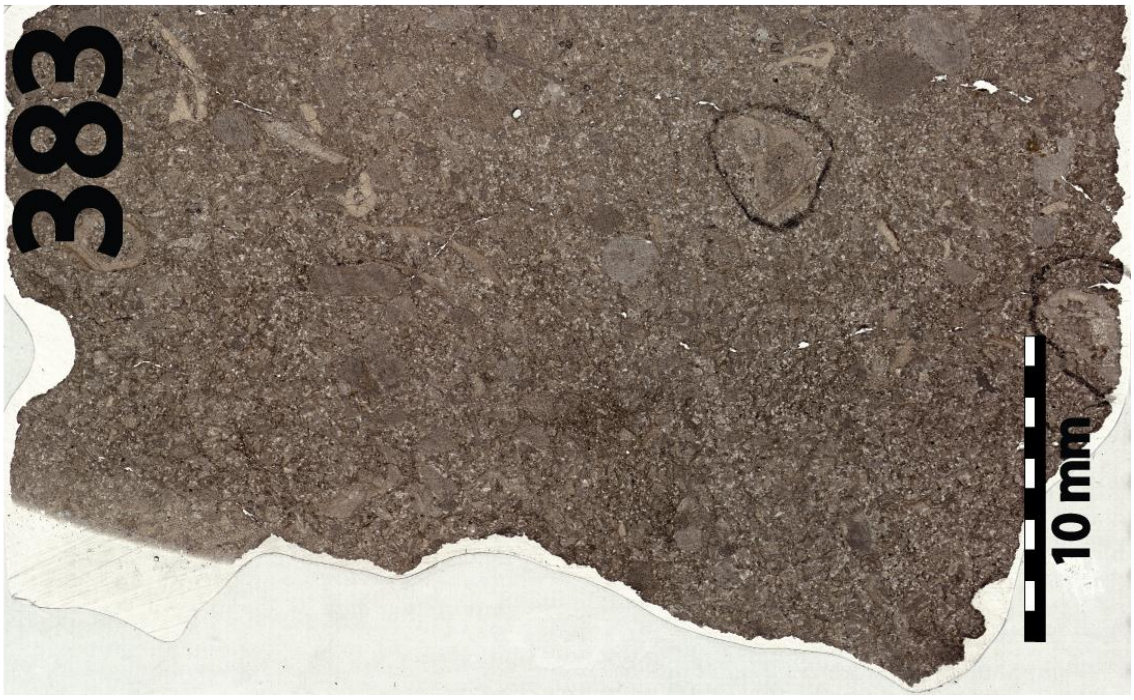

APPENDIX B - Continued

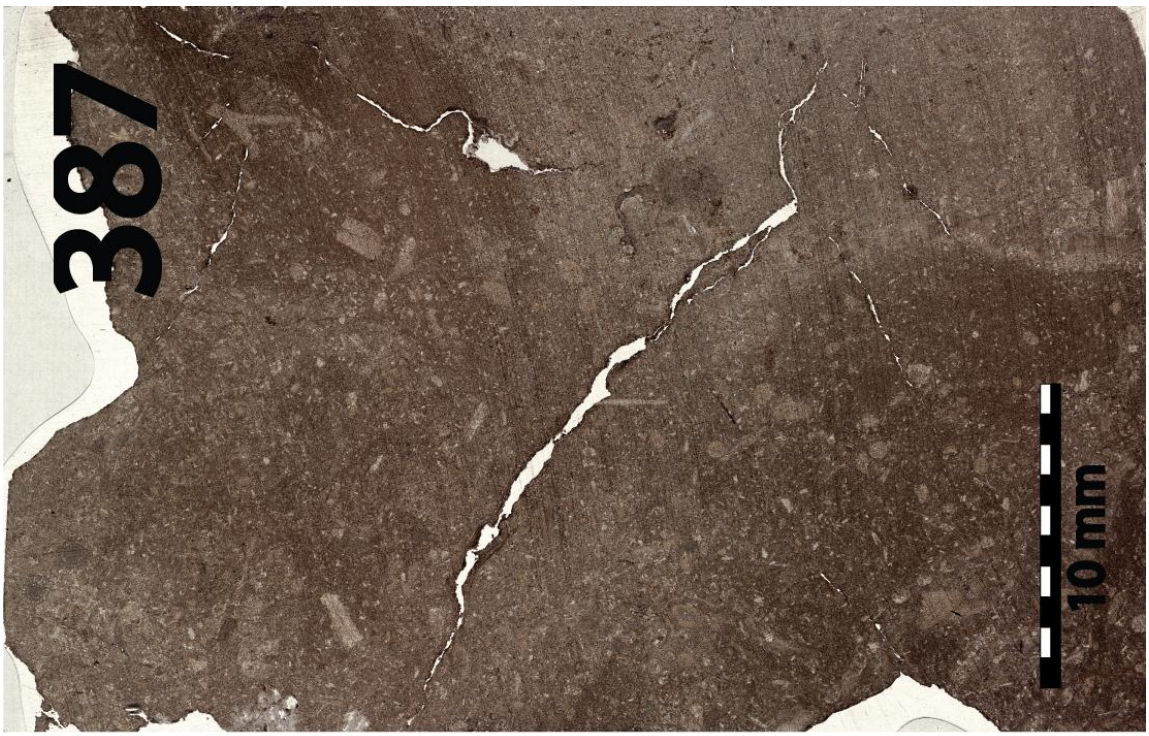

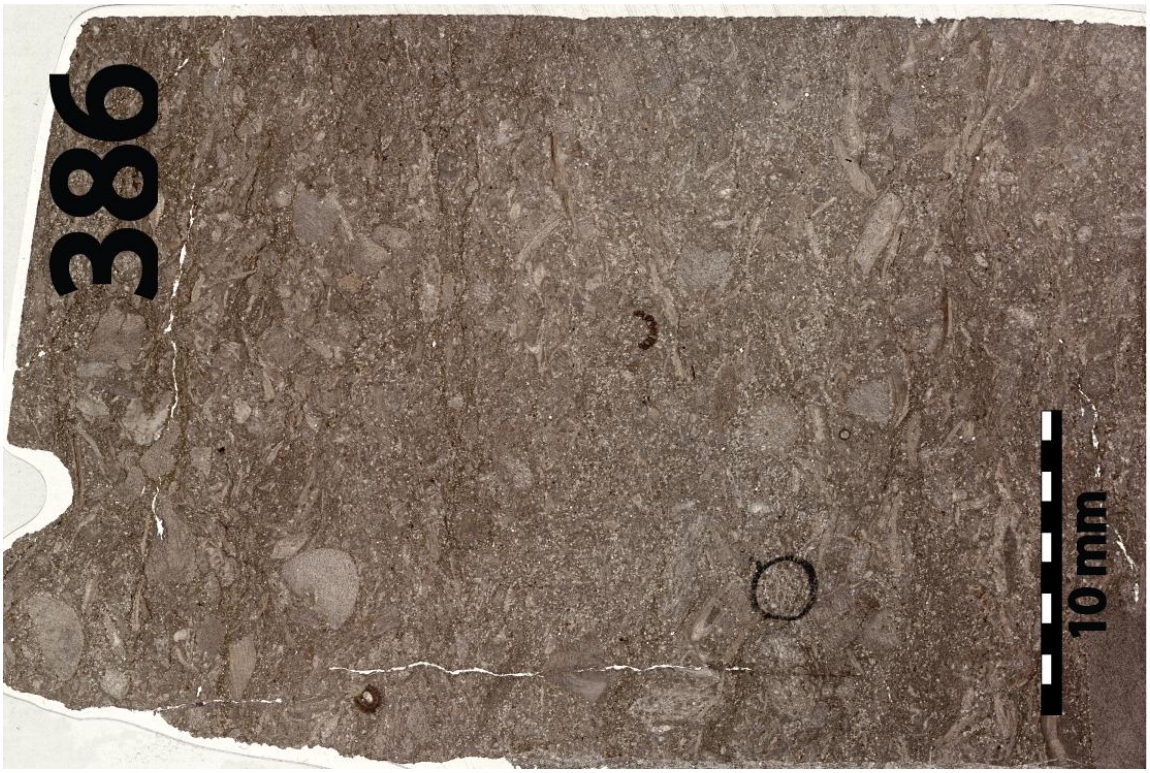

APPENDIX B - Continued

APPENDIX B - Continued

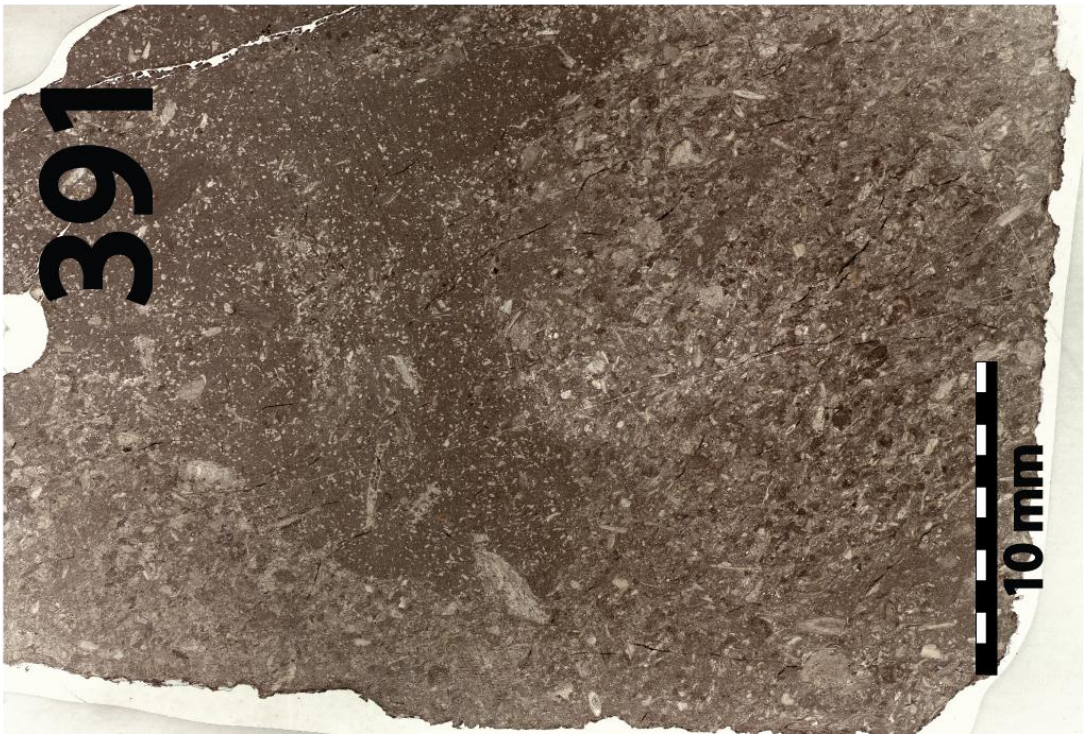

APPENDIX B - Continued

APPENDIX B - Continued

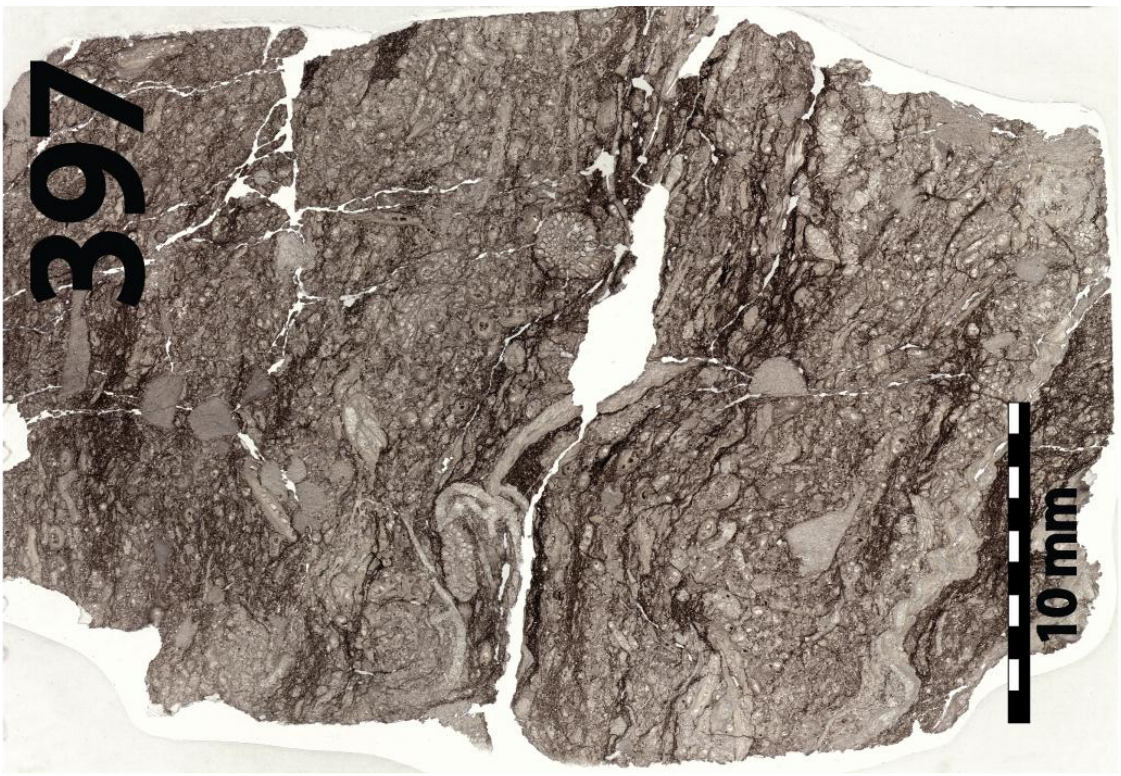

APPENDIX B - Continued

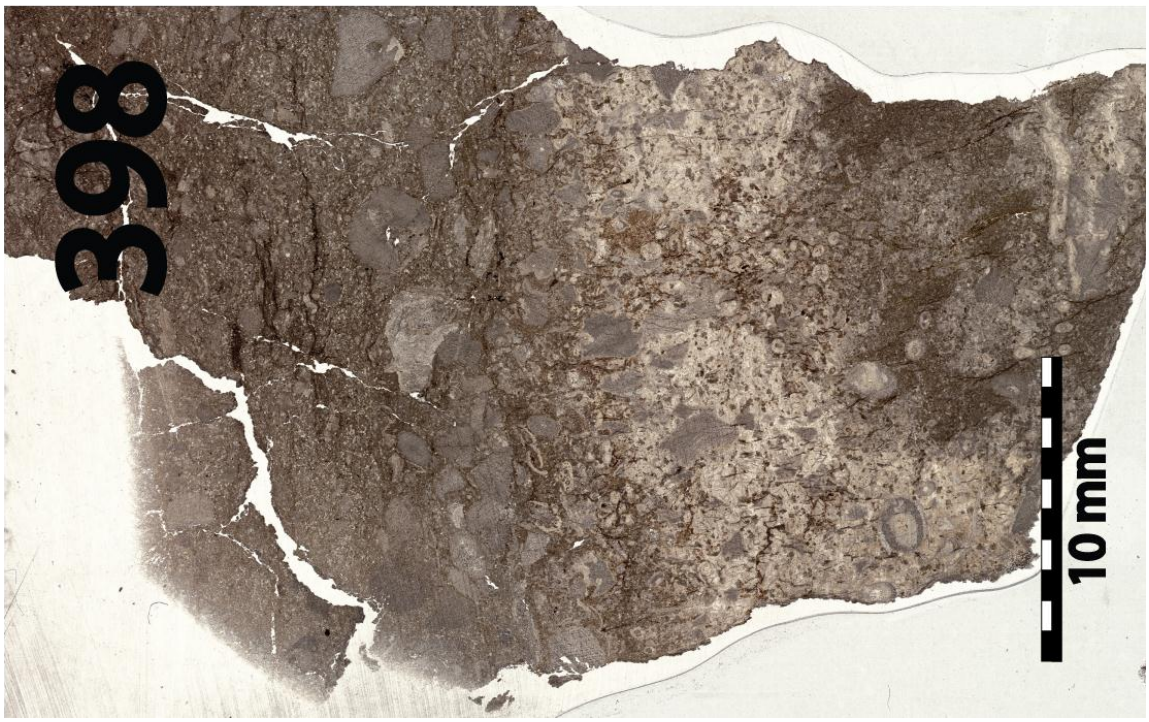

APPENDIX B - Continued

APPENDIX B - Continued

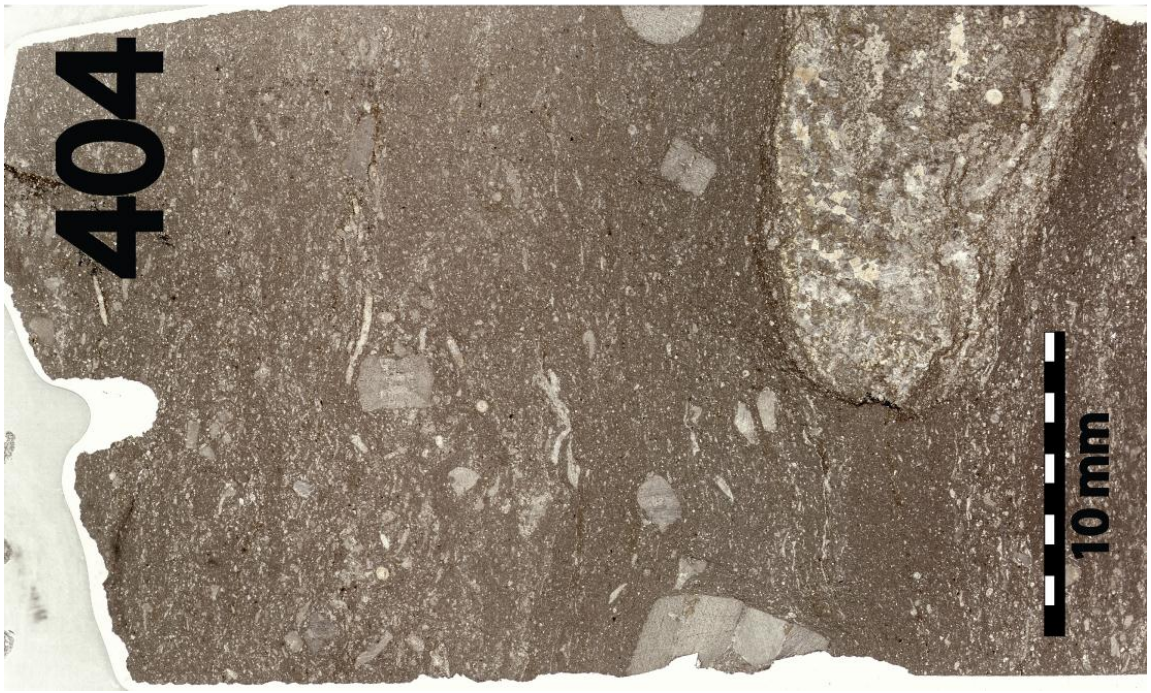

APPENDIX B - Continued

APPENDIX B - Continued

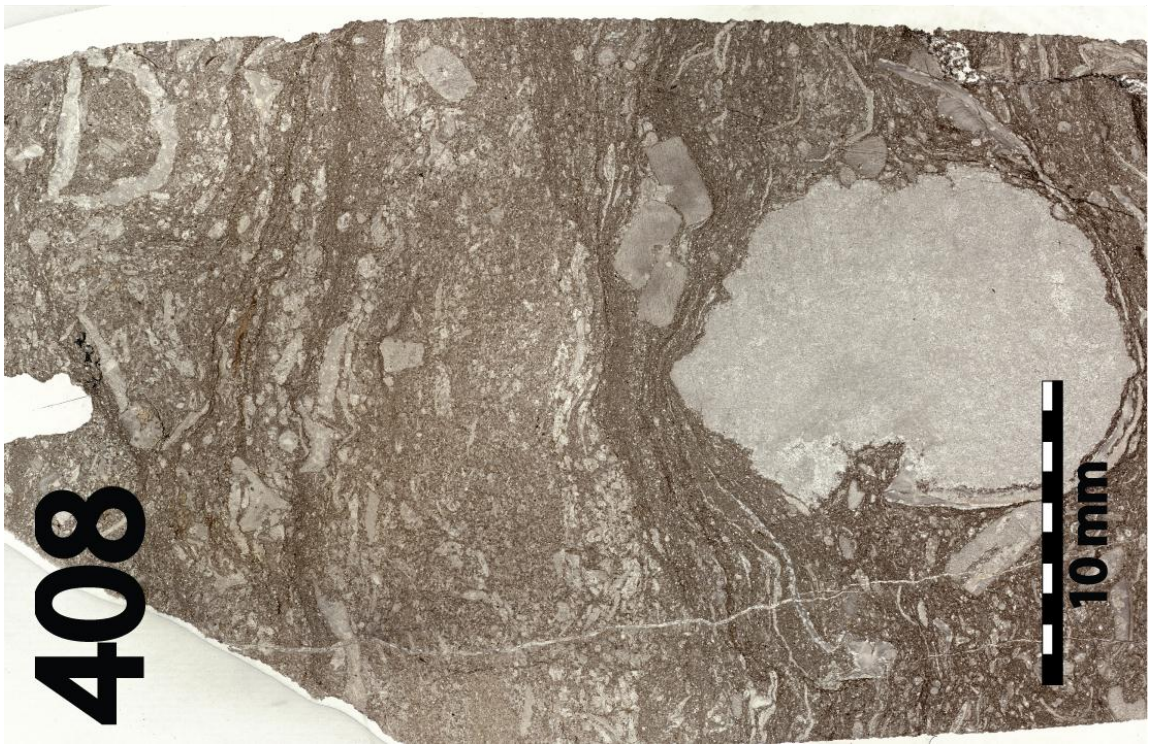

APPENDIX B - Continued

APPENDIX B - Continued

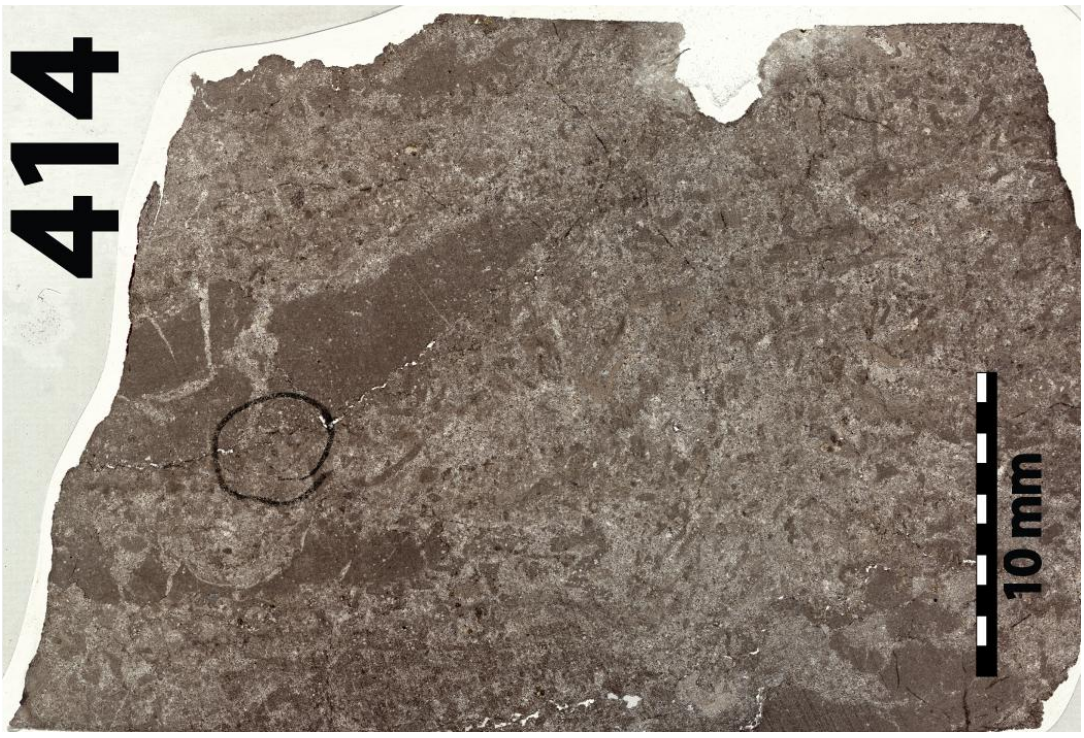

APPENDIX B - Continued

APPENDIX B - Continued

APPENDIX B - Continued

APPENDIX B - Continued

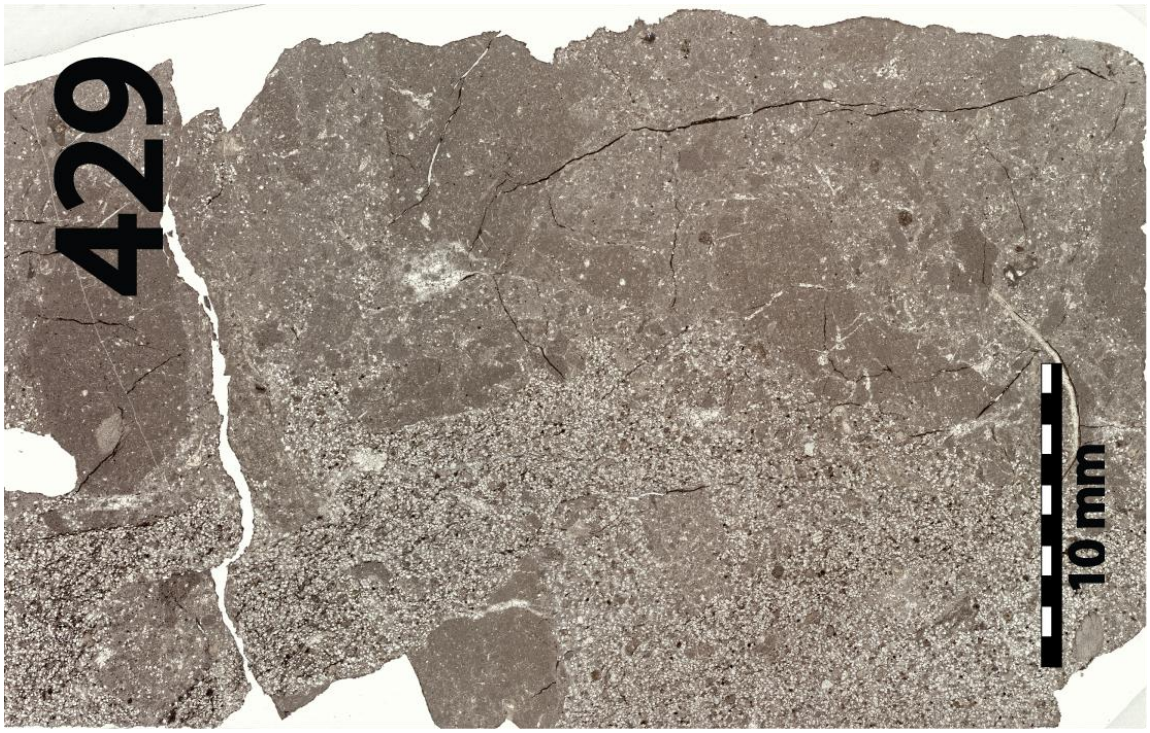

APPENDIX B - Continued

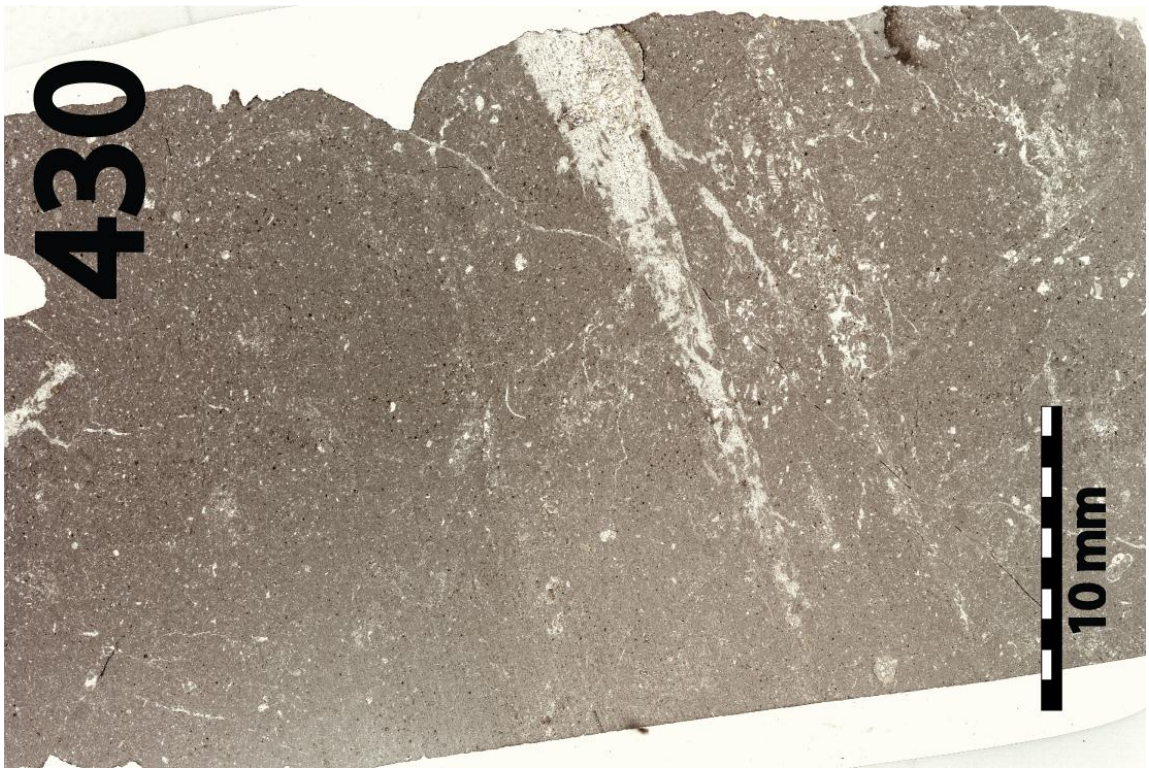

APPENDIX B - Continued

APPENDIX B - Continued

APPENDIX B - Continued

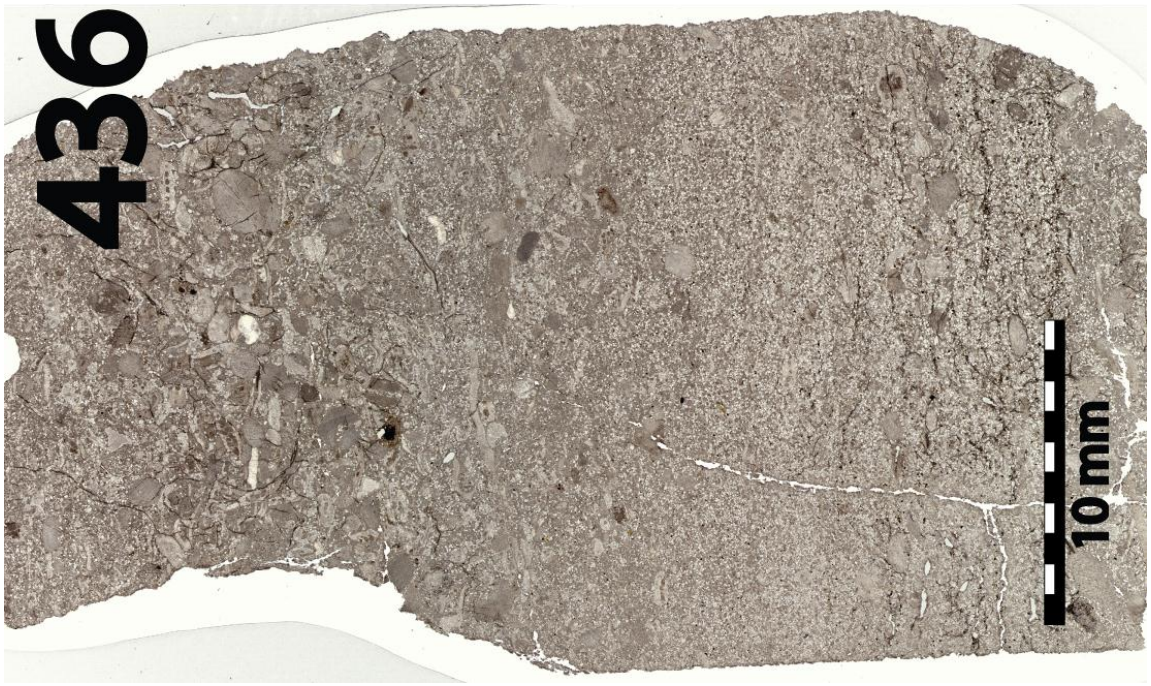

APPENDIX B - Continued

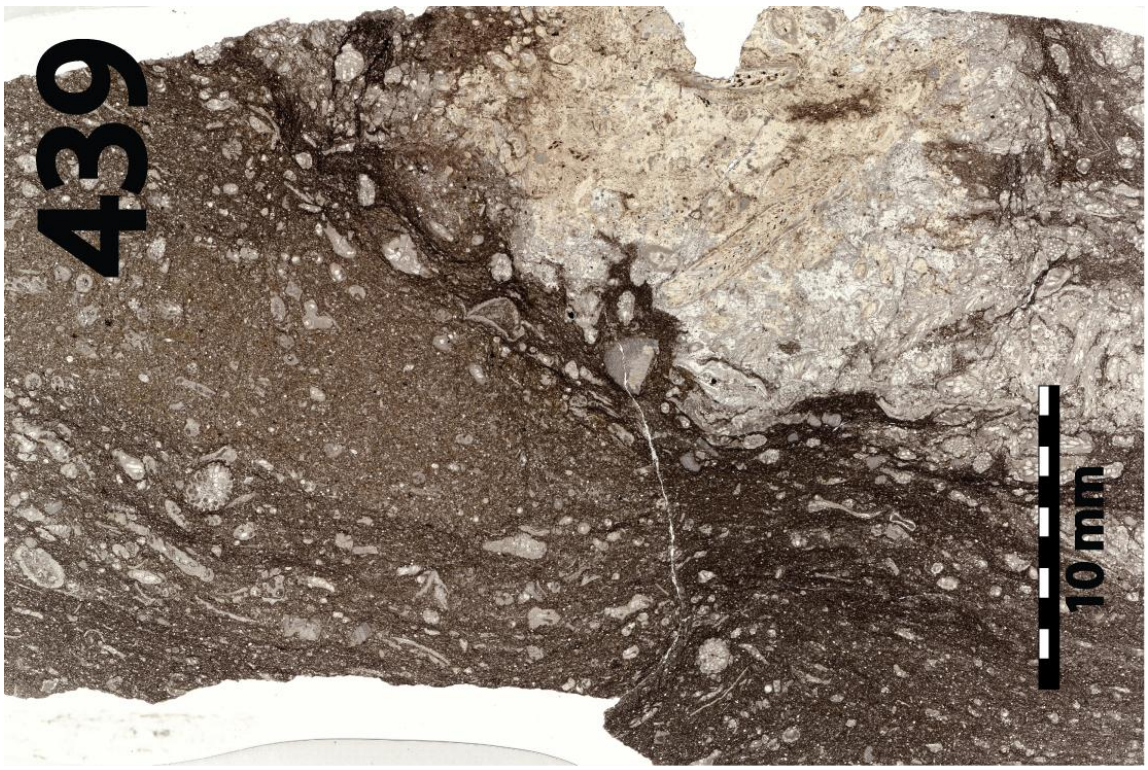

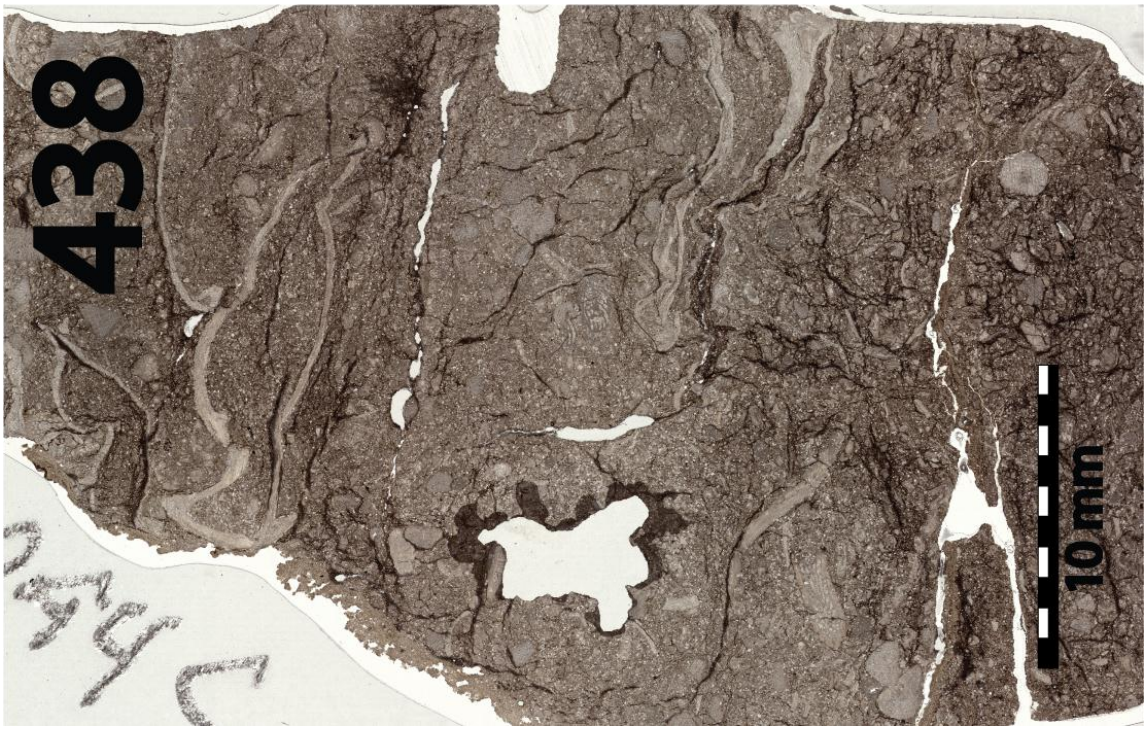

APPENDIX B - Continued

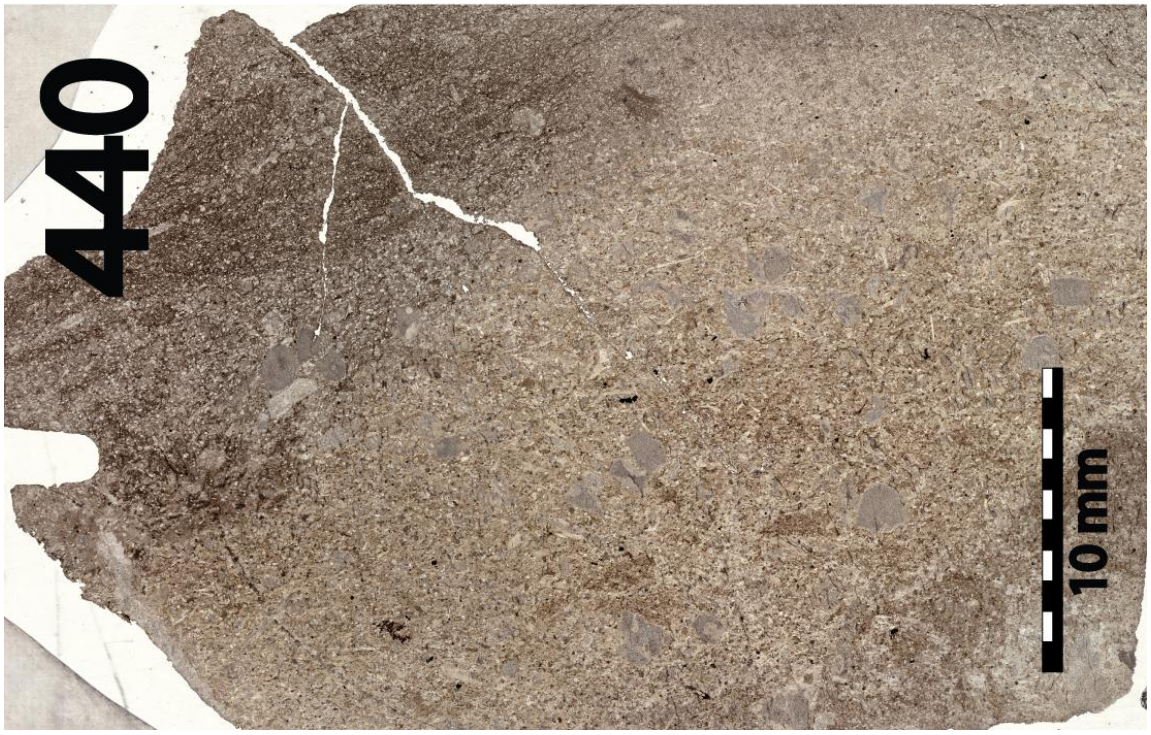

APPENDIX B - Continued

APPENDIX B - Continued

APPENDIX B - Continued

APPENDIX B - Continued

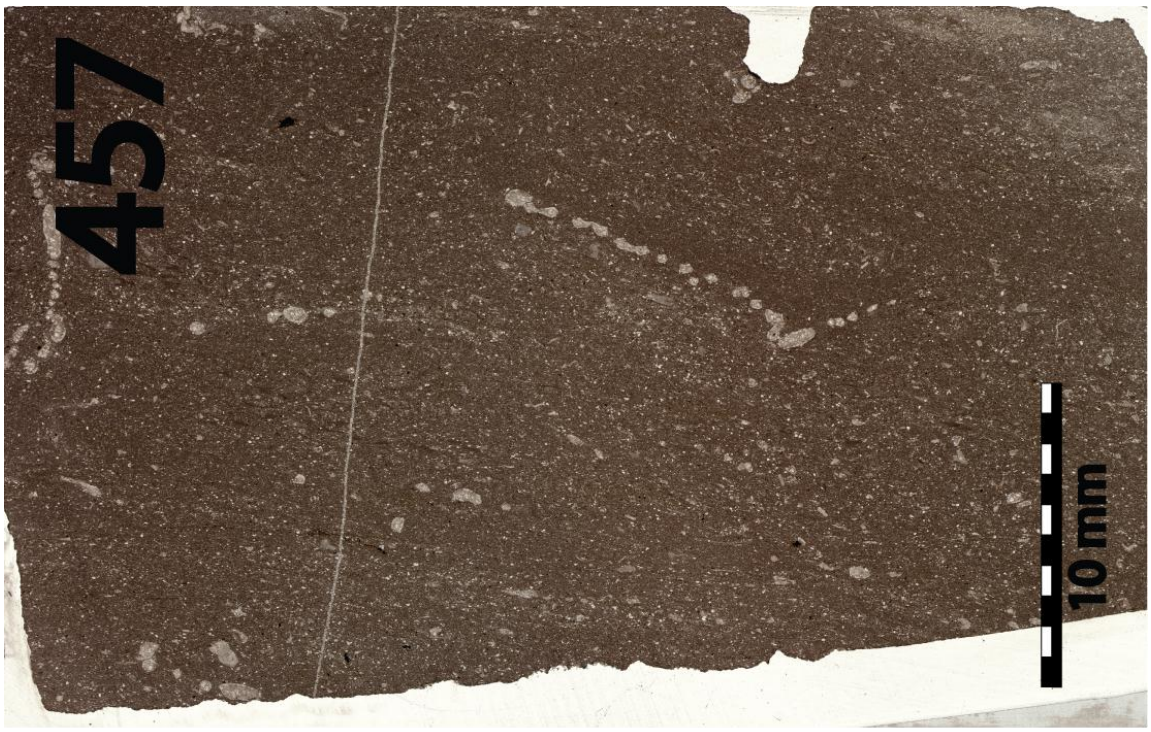

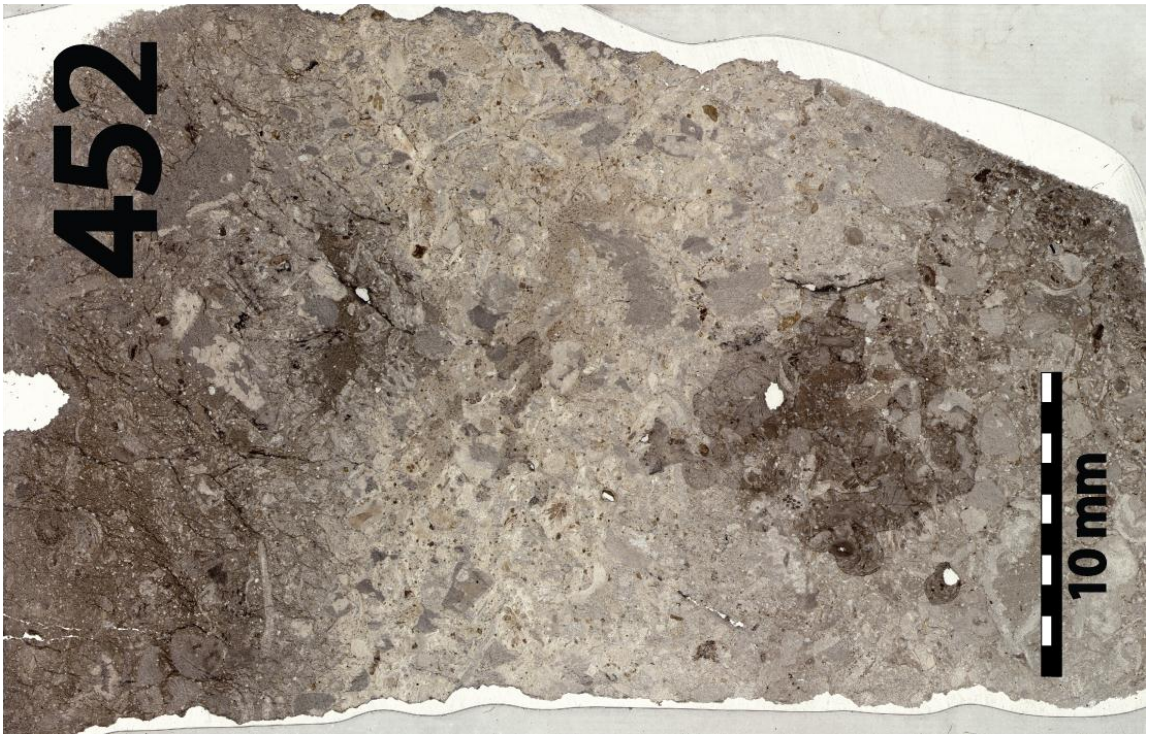

APPENDIX B - Continued

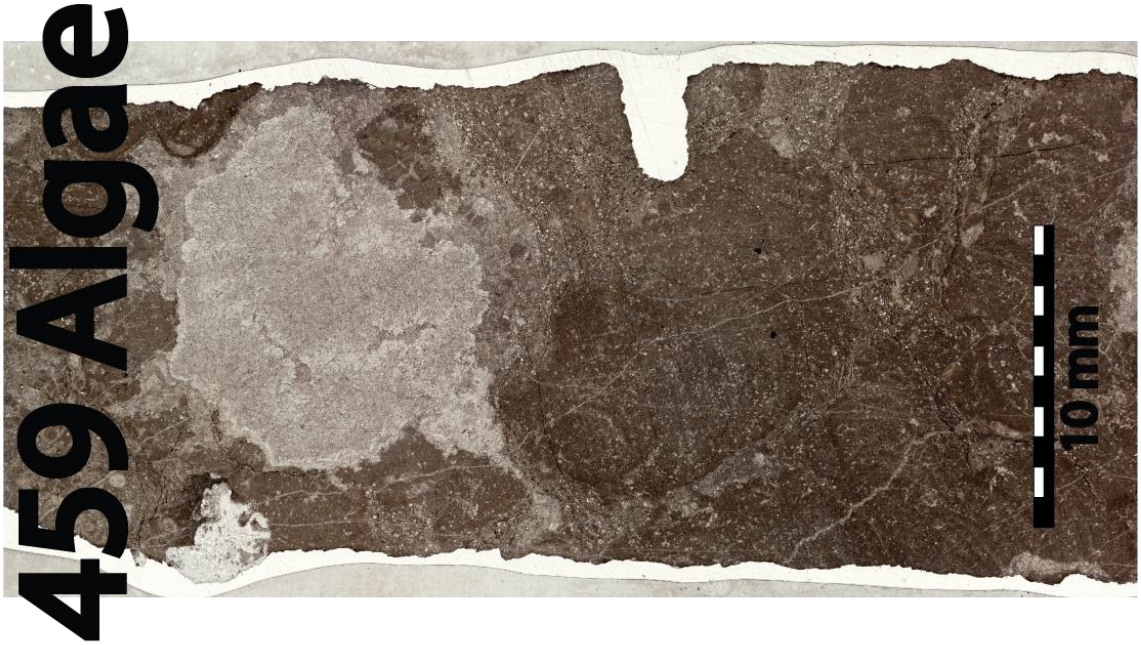

APPENDIX B - Continued

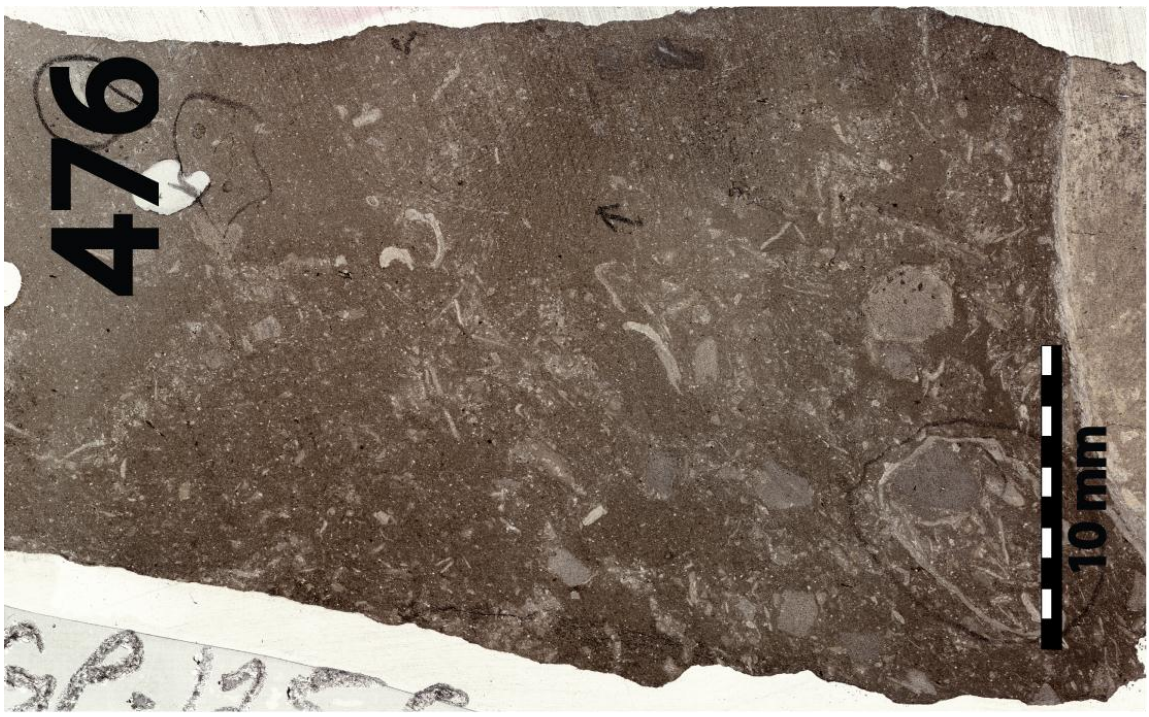

APPENDIX B - Continued

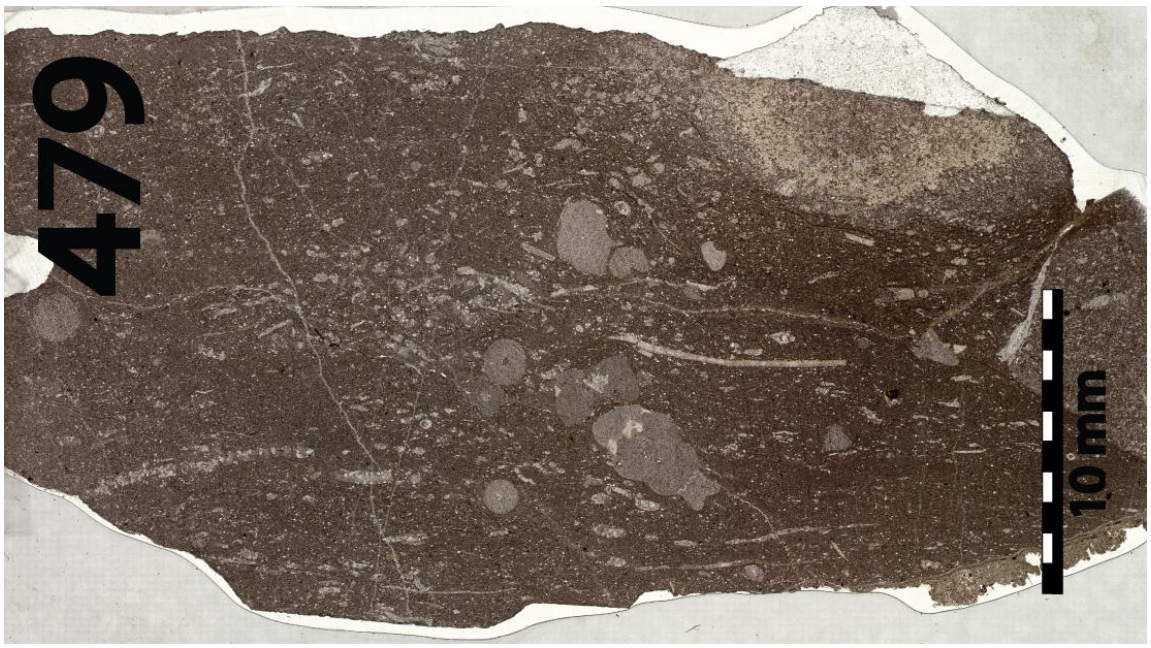

APPENDIX B - Continued

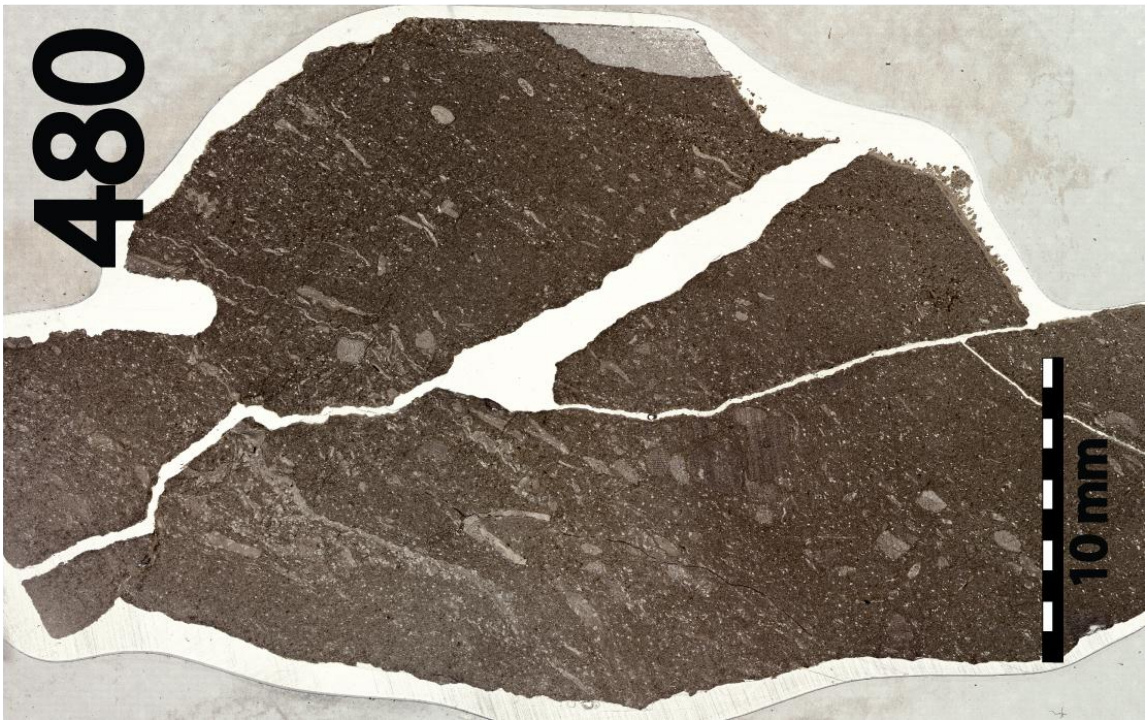

APPENDIX B - Continued

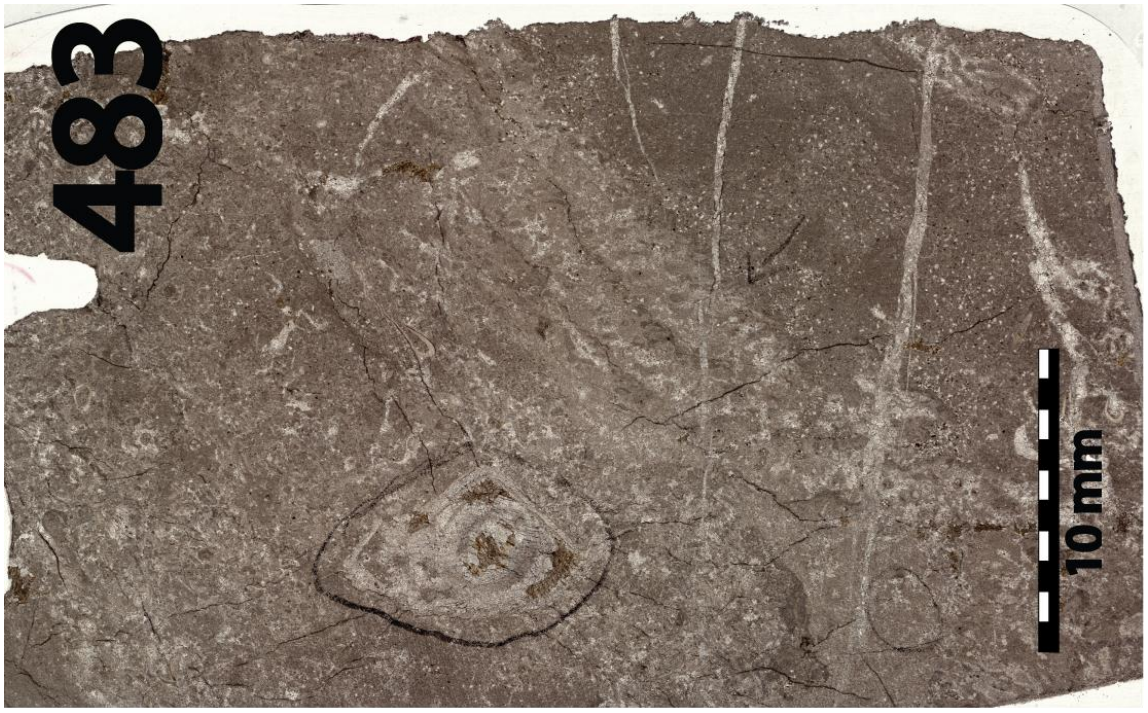

APPENDIX B - Continued

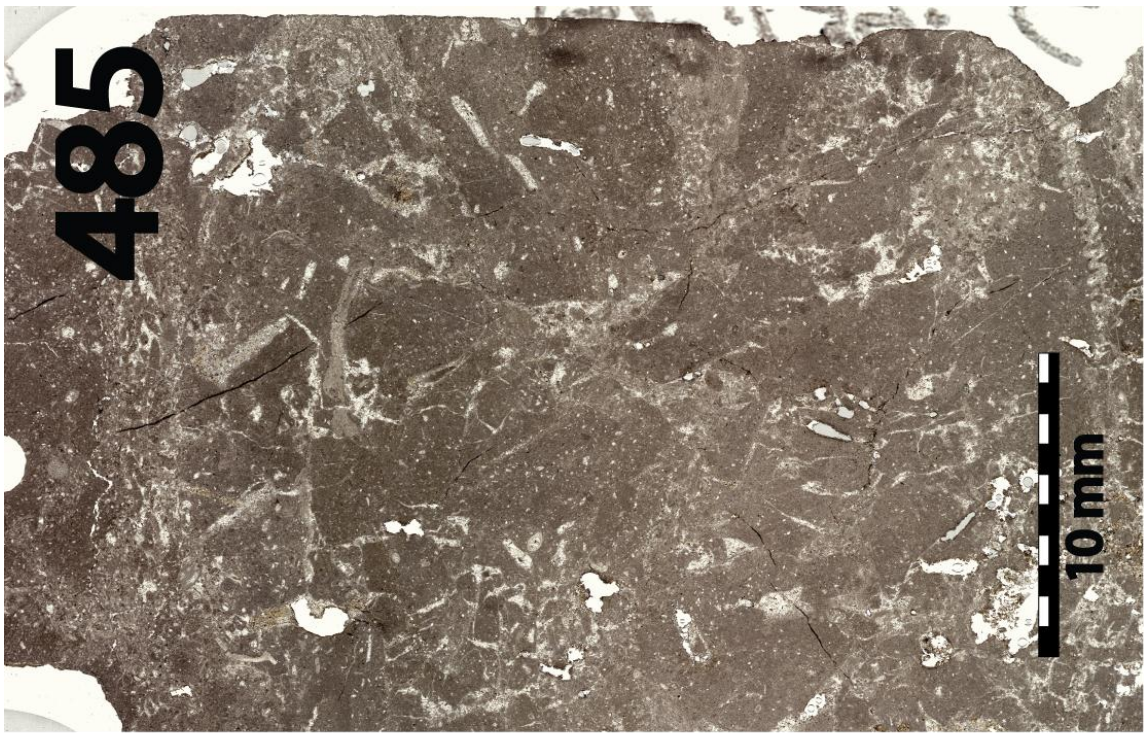

APPENDIX B - Continued

APPENDIX B - Continued

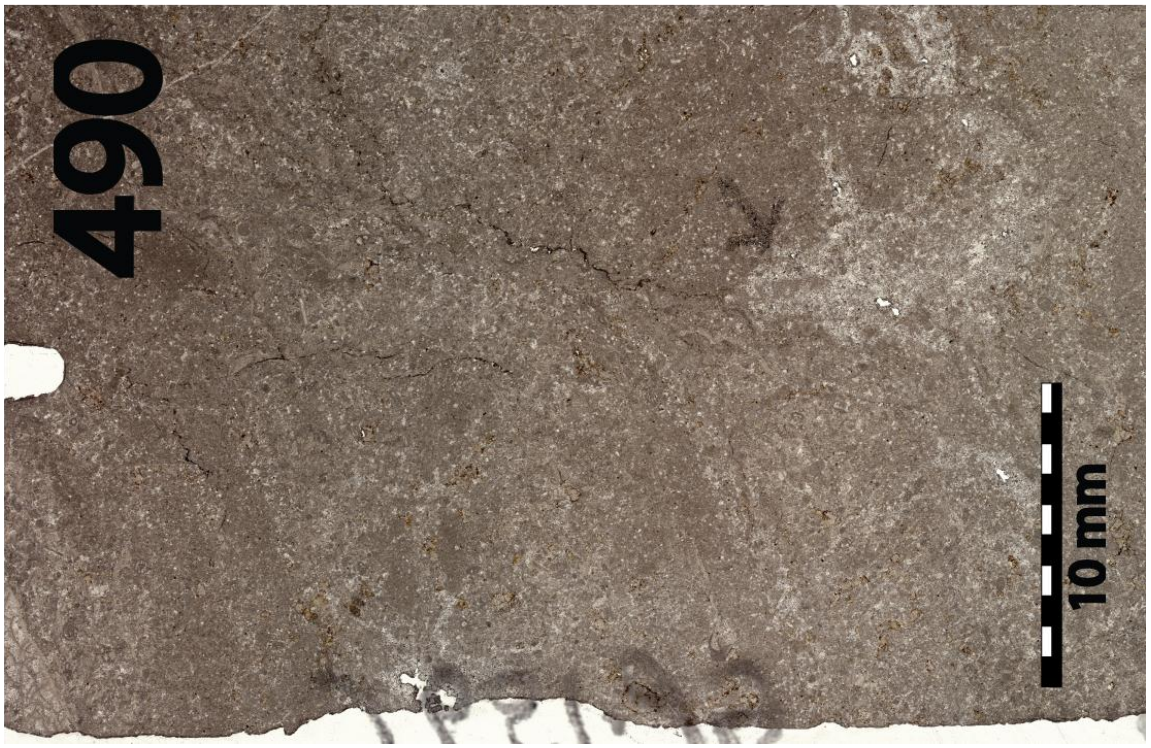

APPENDIX B - Continued

APPENDIX B - Continued

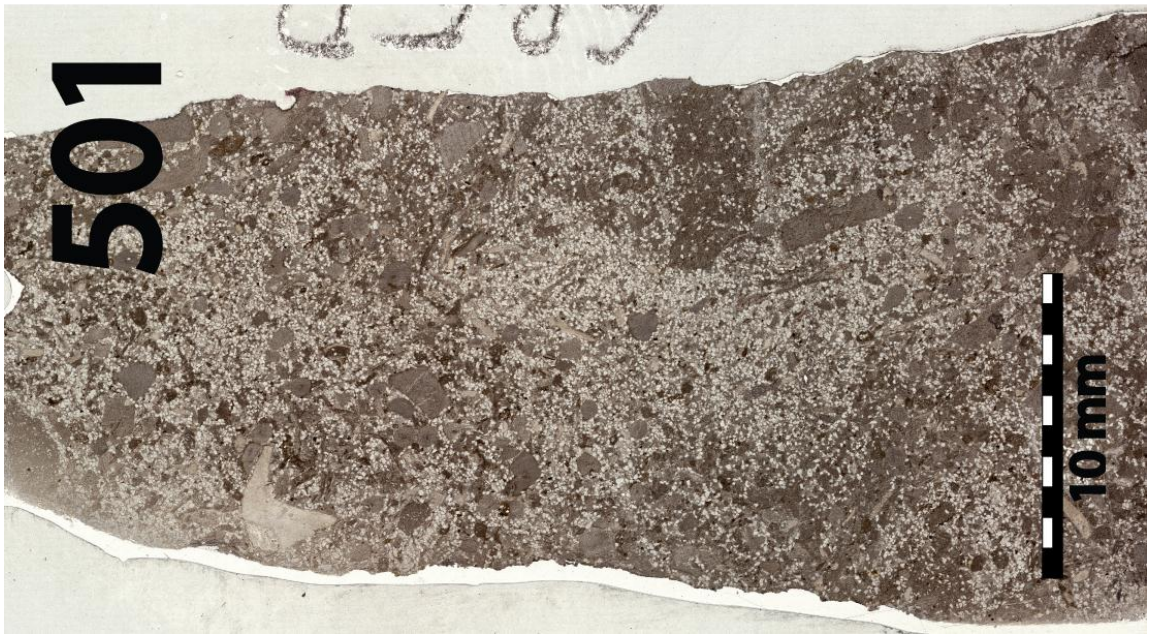

APPENDIX B - Continued

APPENDIX B - Continued

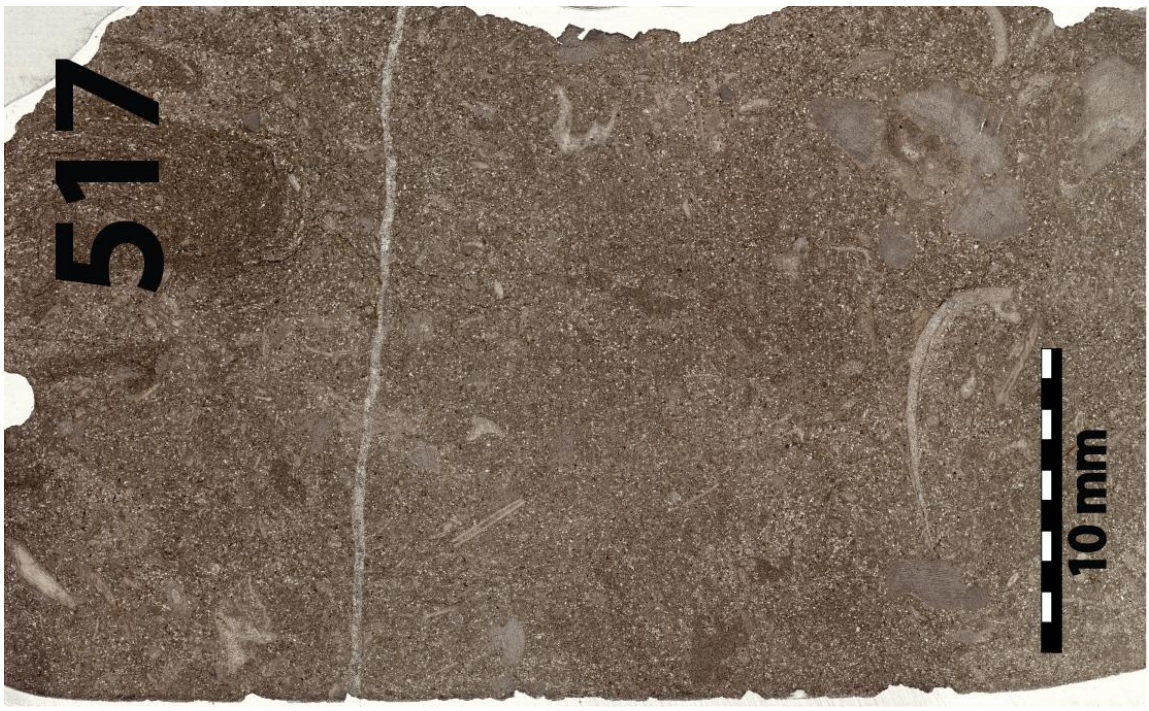

APPENDIX B - Continued

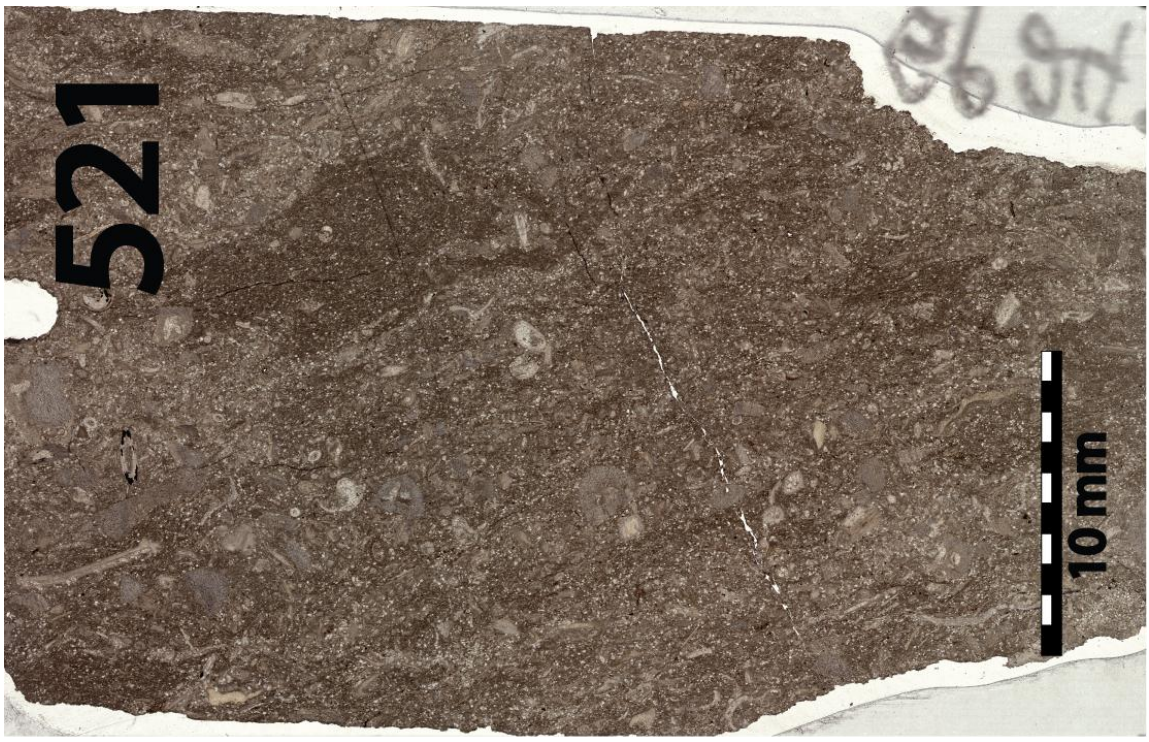

APPENDIX B - Continued

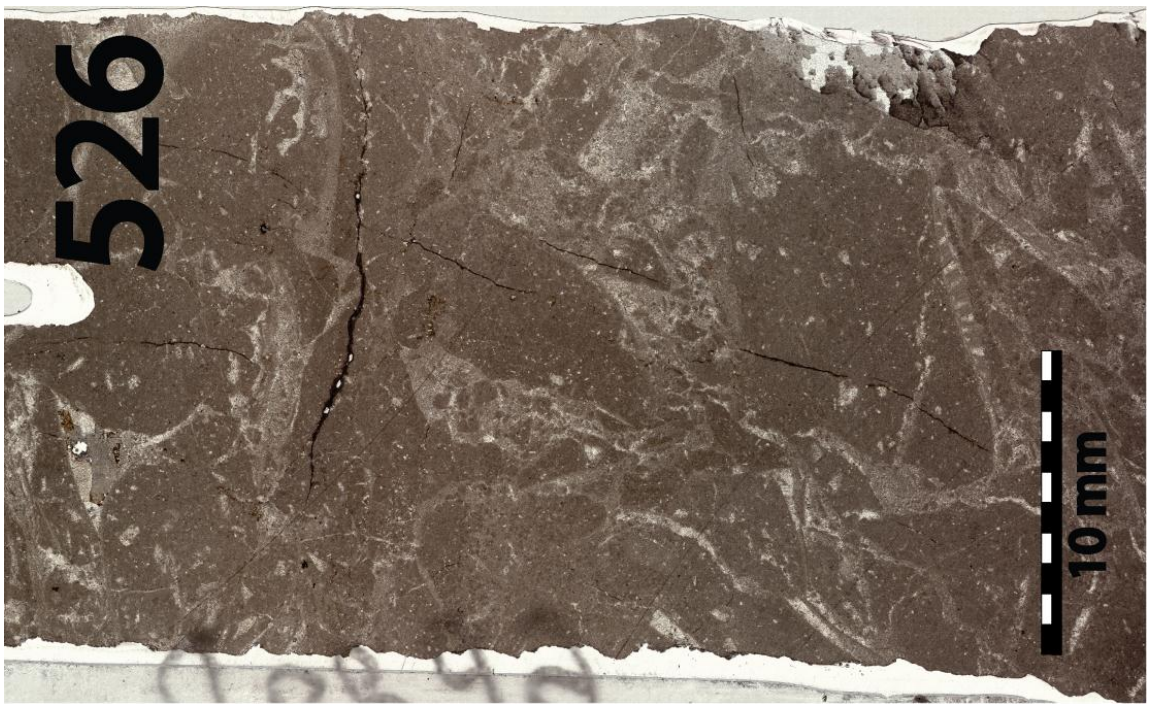

APPENDIX B - Continued

APPENDIX B - Continued

APPENDIX B - Continued

APPENDIX B - Continued

APPENDIX B - Continued

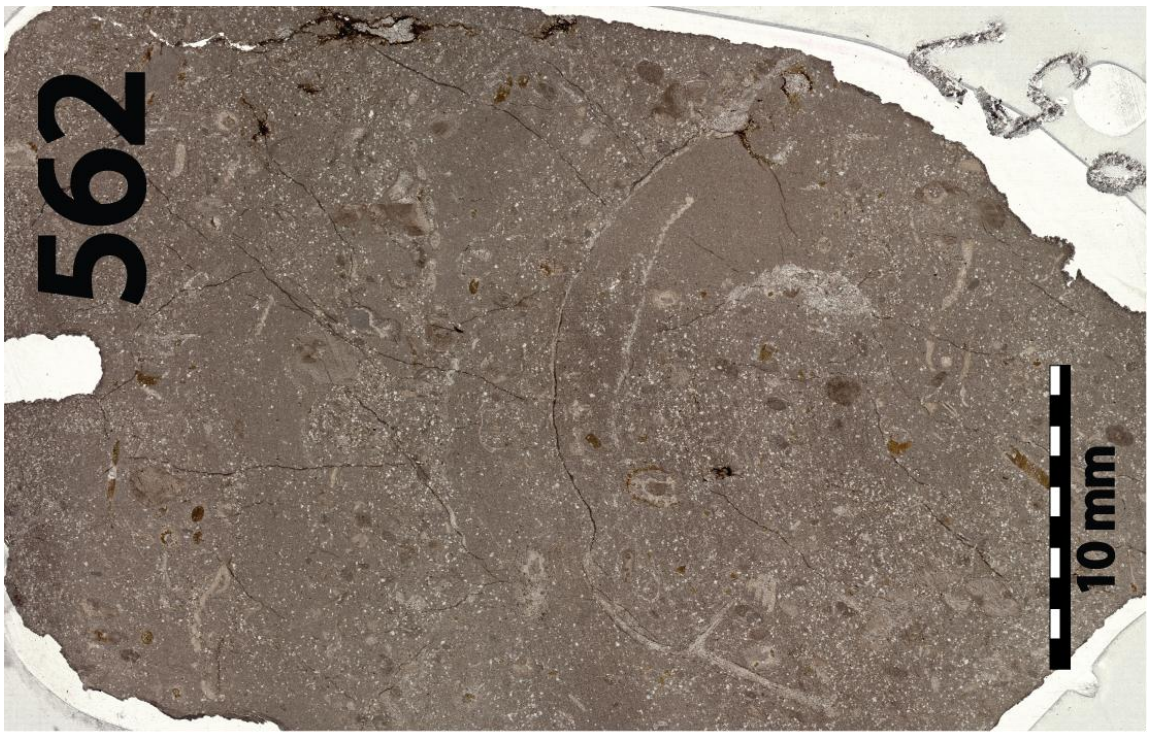

APPENDIX B - Continued

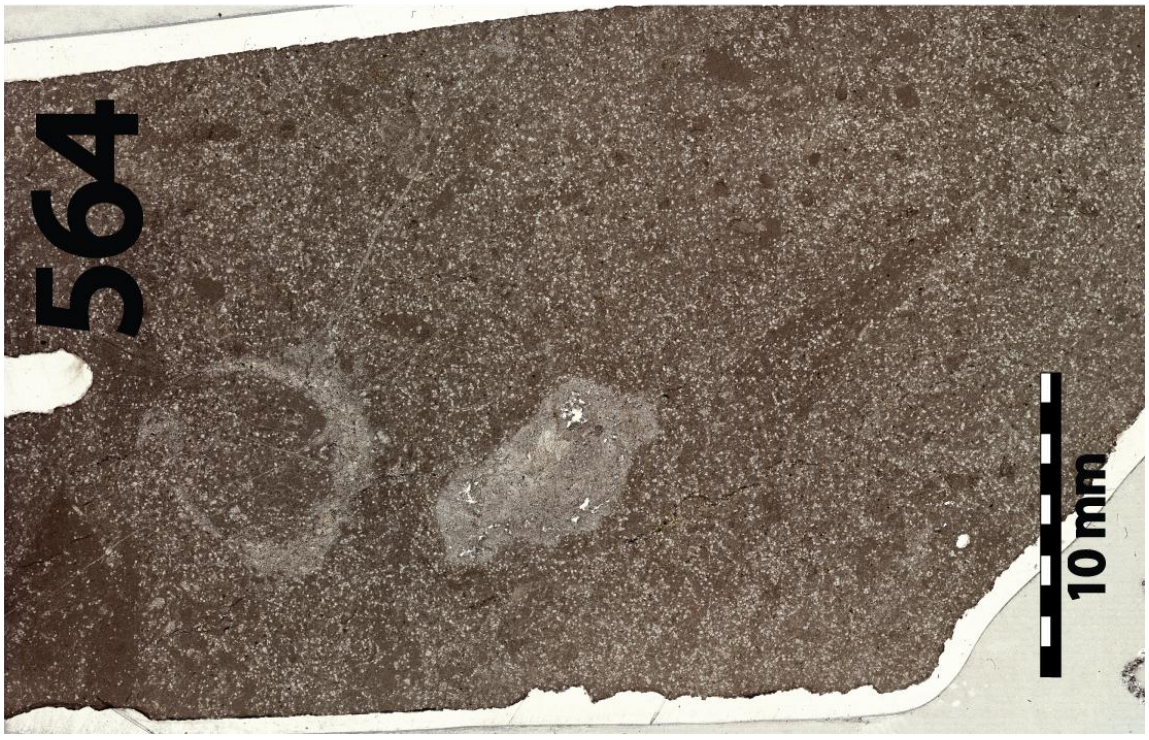

APPENDIX B - Continued

APPENDIX B - Continued

APPENDIX B - Continued

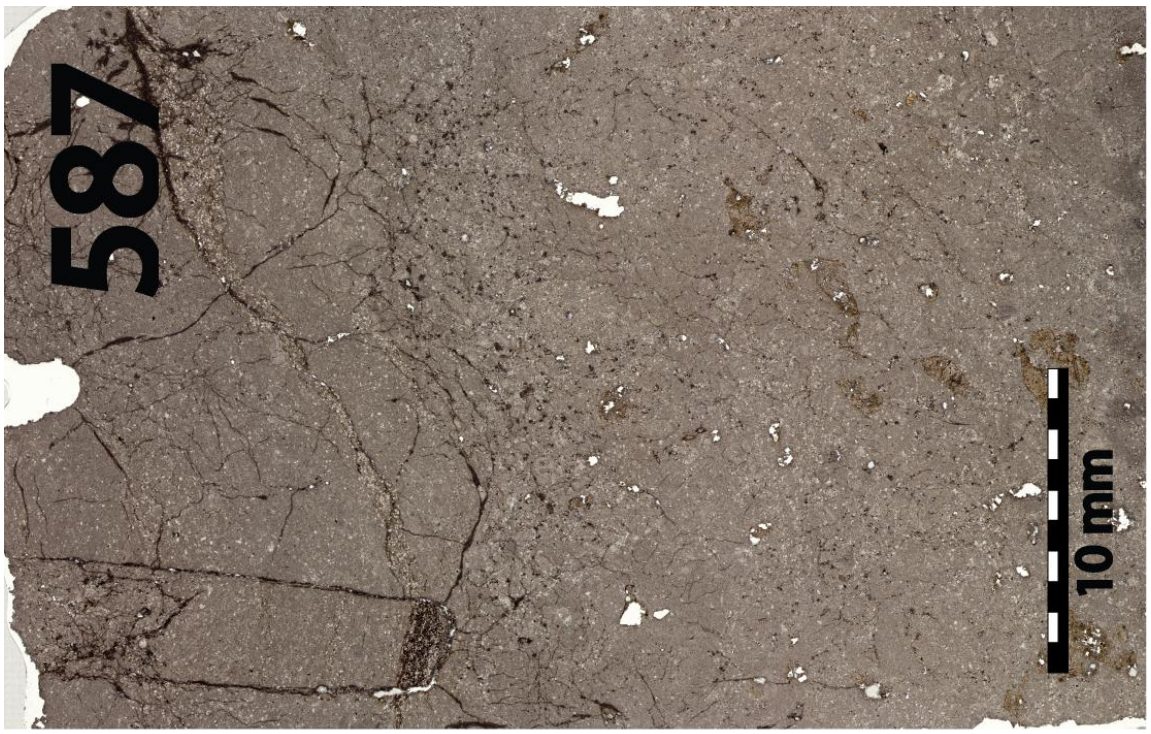

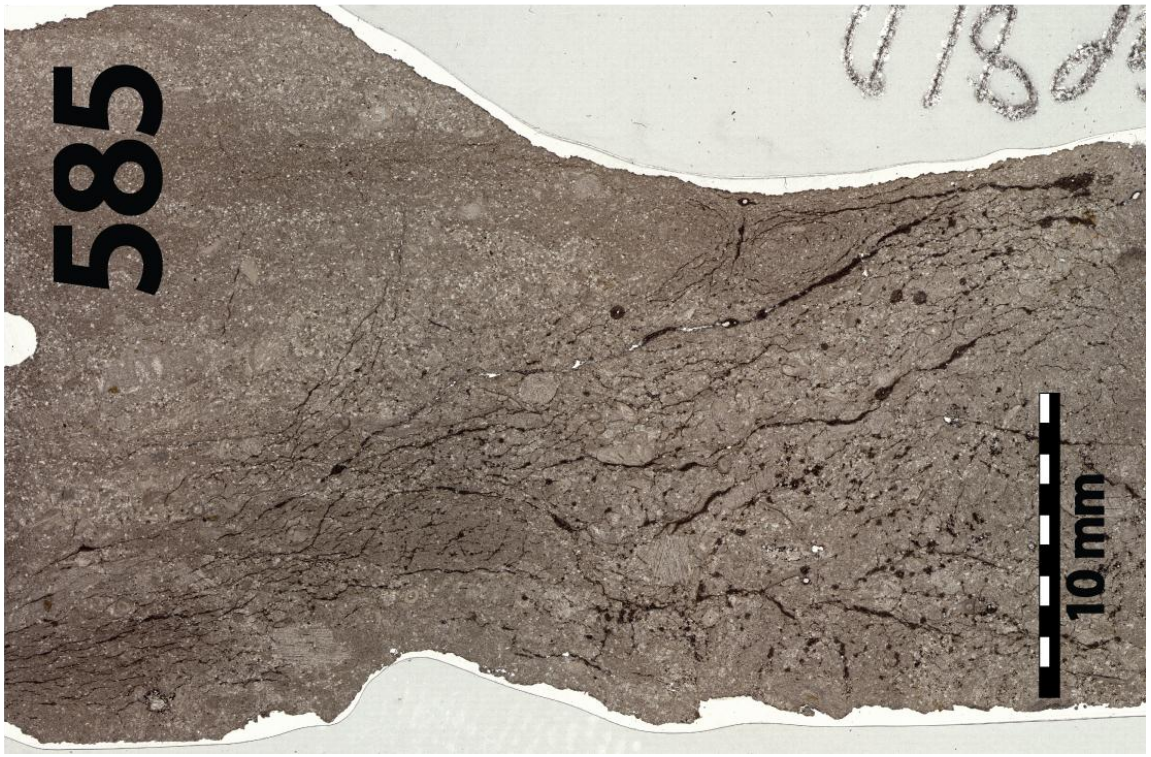

APPENDIX B - Continued

APPENDIX B - Continued

APPENDIX B - Continued

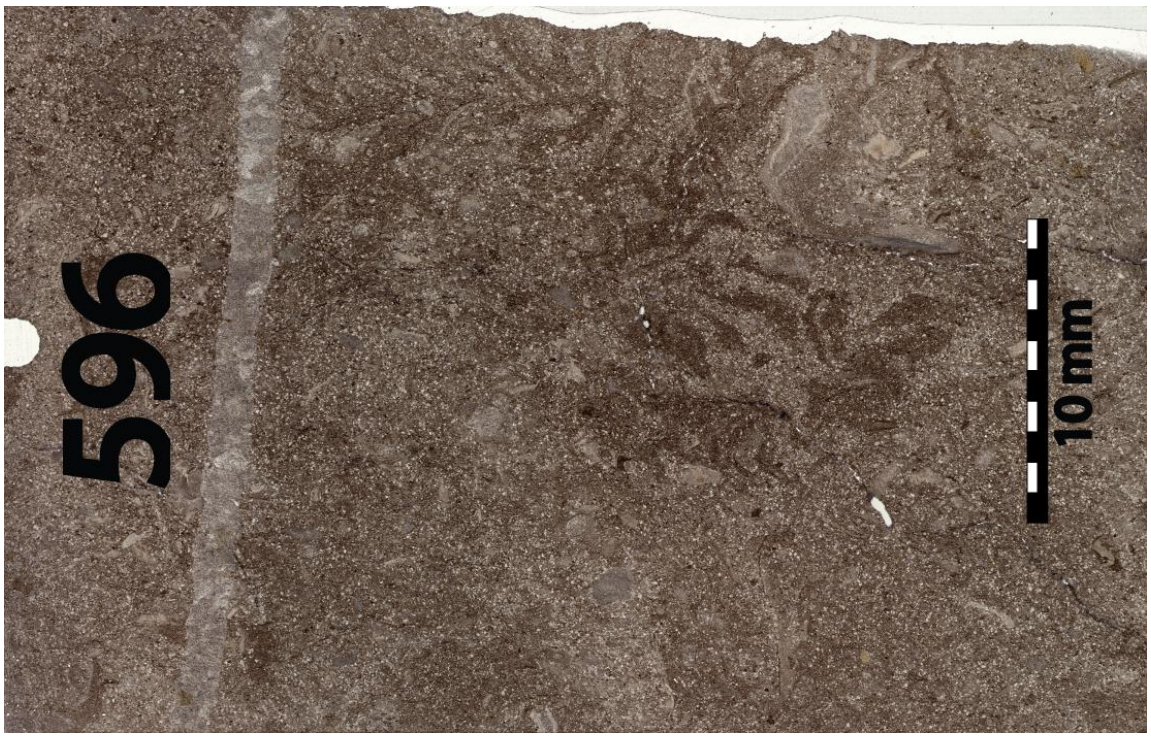

APPENDIX C

FIVE-POINT RUNNING AVERAGE OF DATA FROM IDAHO COVERING NEARLY THE ENTIRE CARBONIFEROUS. TIMESCALE IS ACCORDING TO GRADSTEIN ET AL. (2004). THE UPPER HALF OF THE PROFILE IS FROM GALLAGHER PEAK (PENNSYLVANIAN), WHILE THE BOTTOM HALF IS FROM TAYLOR MOUNTAIN, ANTELOPE CREEK, AND ARCO HILLS (BATT ET AL., 2007).

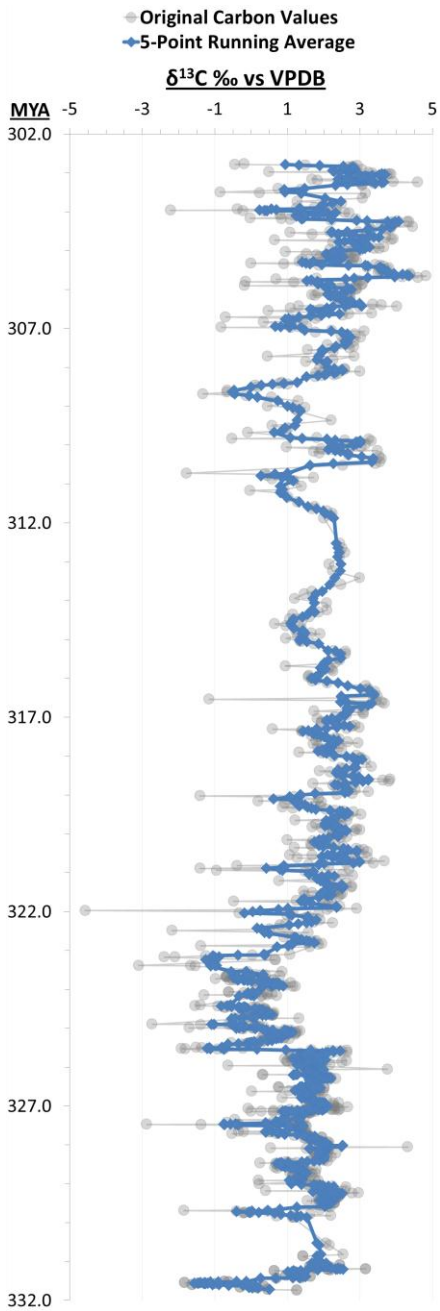

APPENDIX D

BACKSCATTER ELECTRON (BSE) IMAGES AND CATHODOLUMINESCENCENSE (CL) IMAGES TAKEN DURING ELECTRON MICROPROBE ANALYSES. SAMPLE NUMBER IS LOCATED IN THE UPPER LEFT CORNER AND SCALE BAR IS IN THE LOWER LEFT.

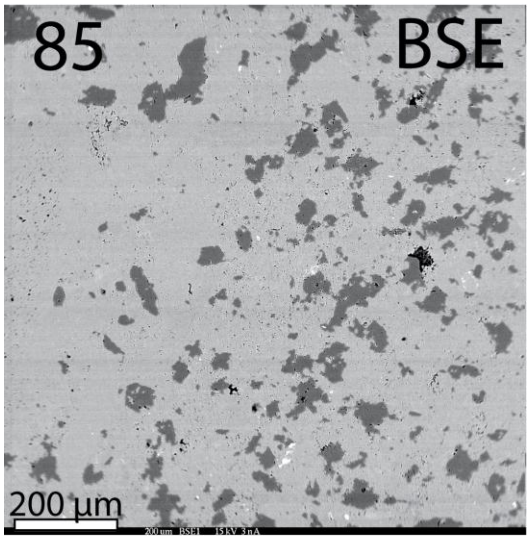

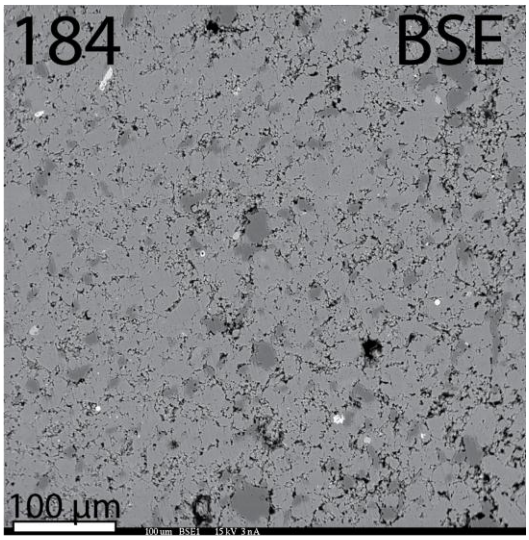

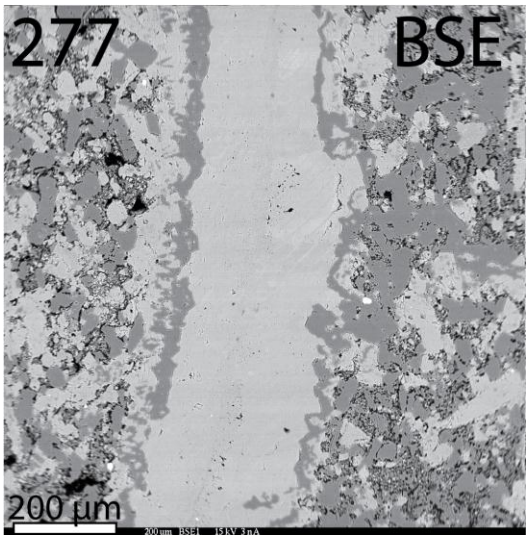

APPENDIX D - Continued

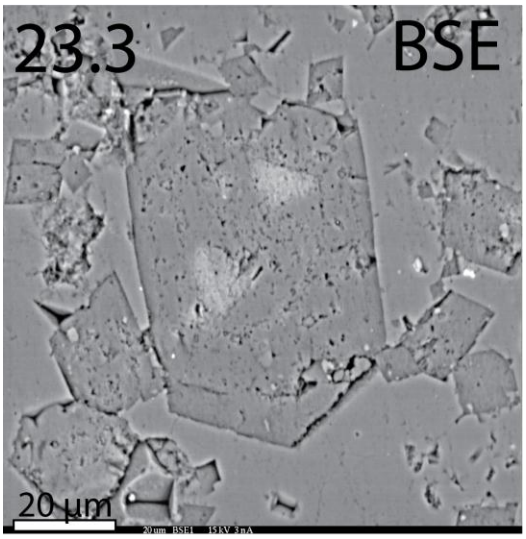

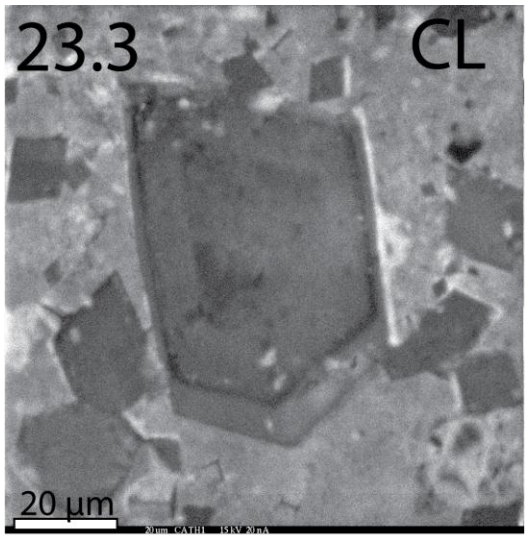

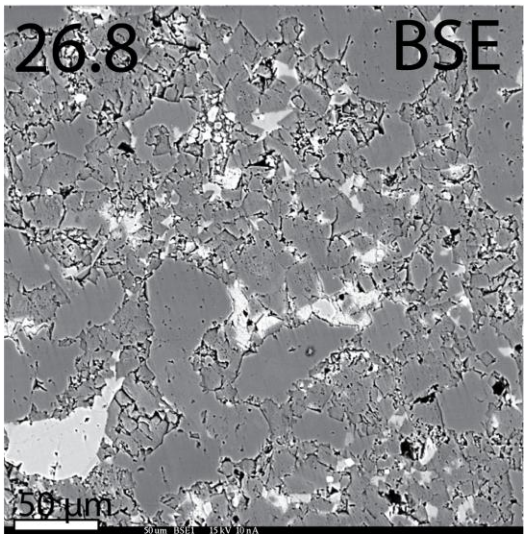

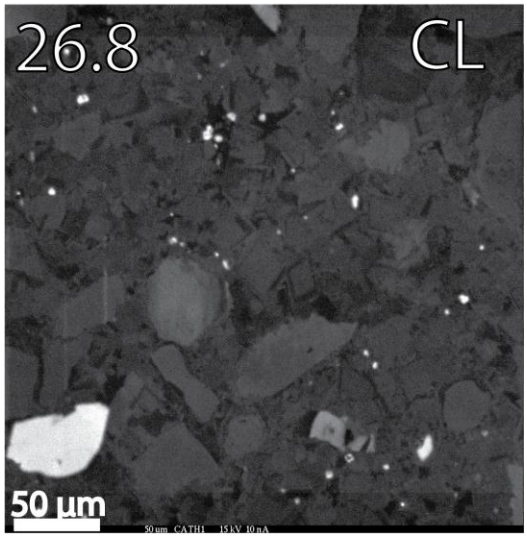

APPENDIX D - Continued

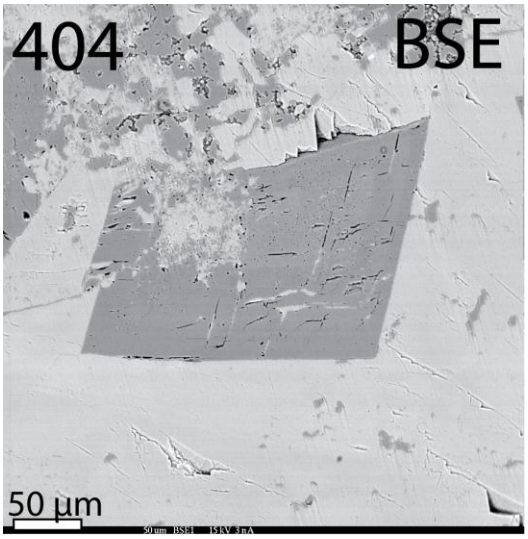

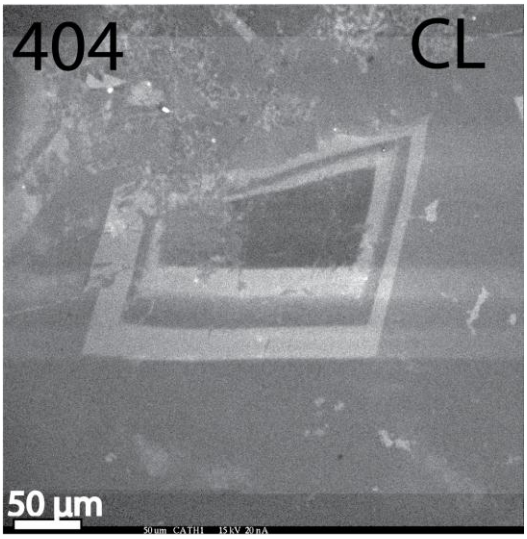

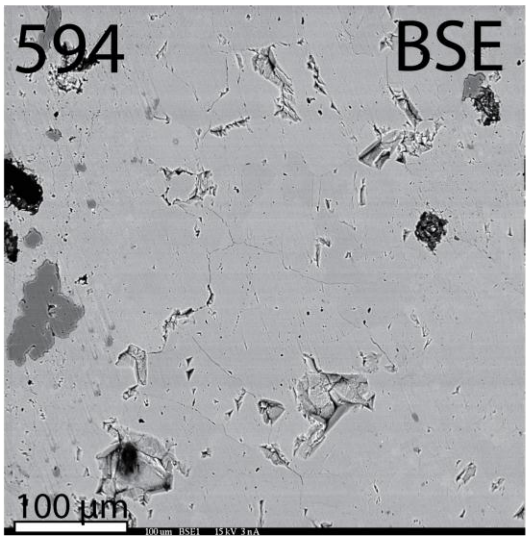

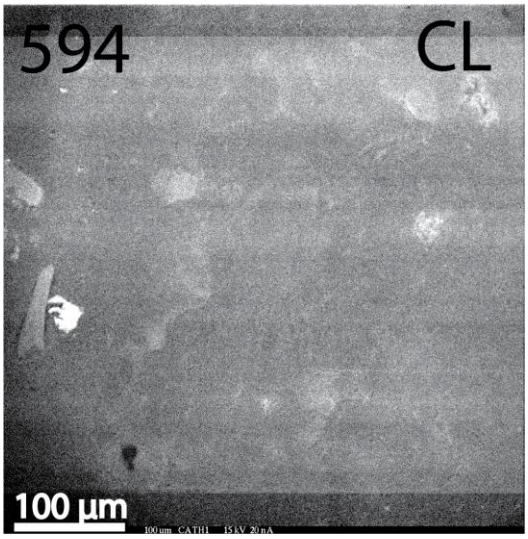

APPENDIX E

FIVE-POINT RUNNING AVERAGE OF PERCENT SAND/SILT AT GALLAGHER PEAK, IDAHO, NEXT TO A SEA LEVEL CURVE FROM ARROW CANYON, NEVADA (HEATH ET AL., 1967), AND A COMPARISON OF $\delta^{13}C$ PROFILES FROM ARROW CANYON (SALTZMAN, 2003) AND GALLAGHER PEAK (THIS STUDY). PERCENT QUARTZ SILT/SAND IS BASED ON VISUAL ESTIMATES MADE FROM THIN SECTIONS AND HAND SAMPLES. GLACIAL EVENTS ARE ACCORDING TO FIELDING ET AL. (2008; WHITE BOXES) AND ISBELL ET AL., 2003 (MODIFIED BY MONTANEZ ET AL., 2007; GRAY BOXES).

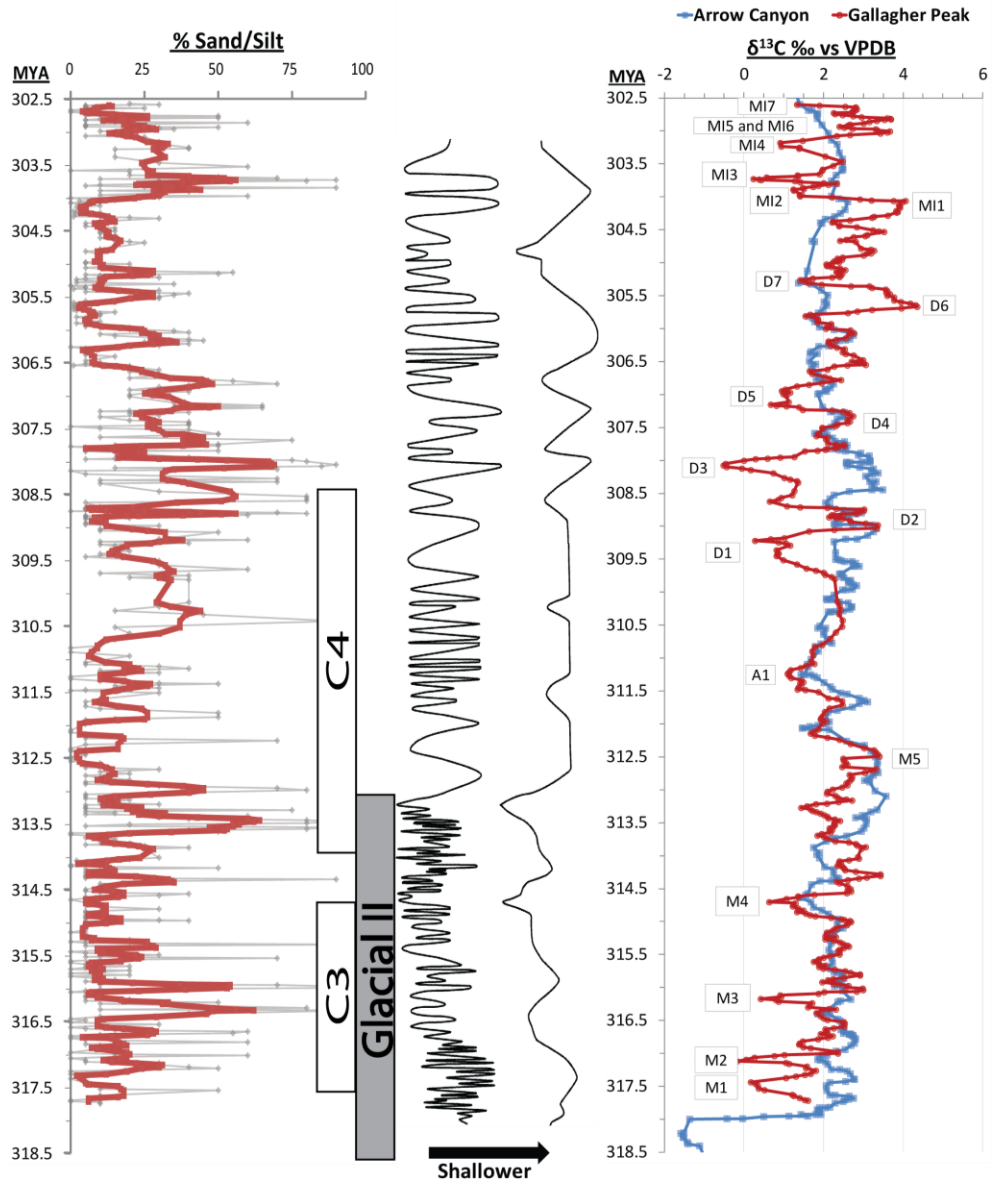

APPENDIX F

SEQUENCE BOUNDARIES AND MAXIMUM FLOODING SURFACES COMPARED TO THE PERCENT SAND/SILT, $\delta^{18}O$, AND $\delta^{13}C$ OF GALLAGHER PEAK, IDAHO. PERCENT SAND/SILT, $\delta^{18}O$, AND $\delta^{13}C$ ARE ALL BASED ON FIVE-POINT RUNNING AVERAGES, WITH ORIGINAL VALUES PLOTTED IN GRAY.

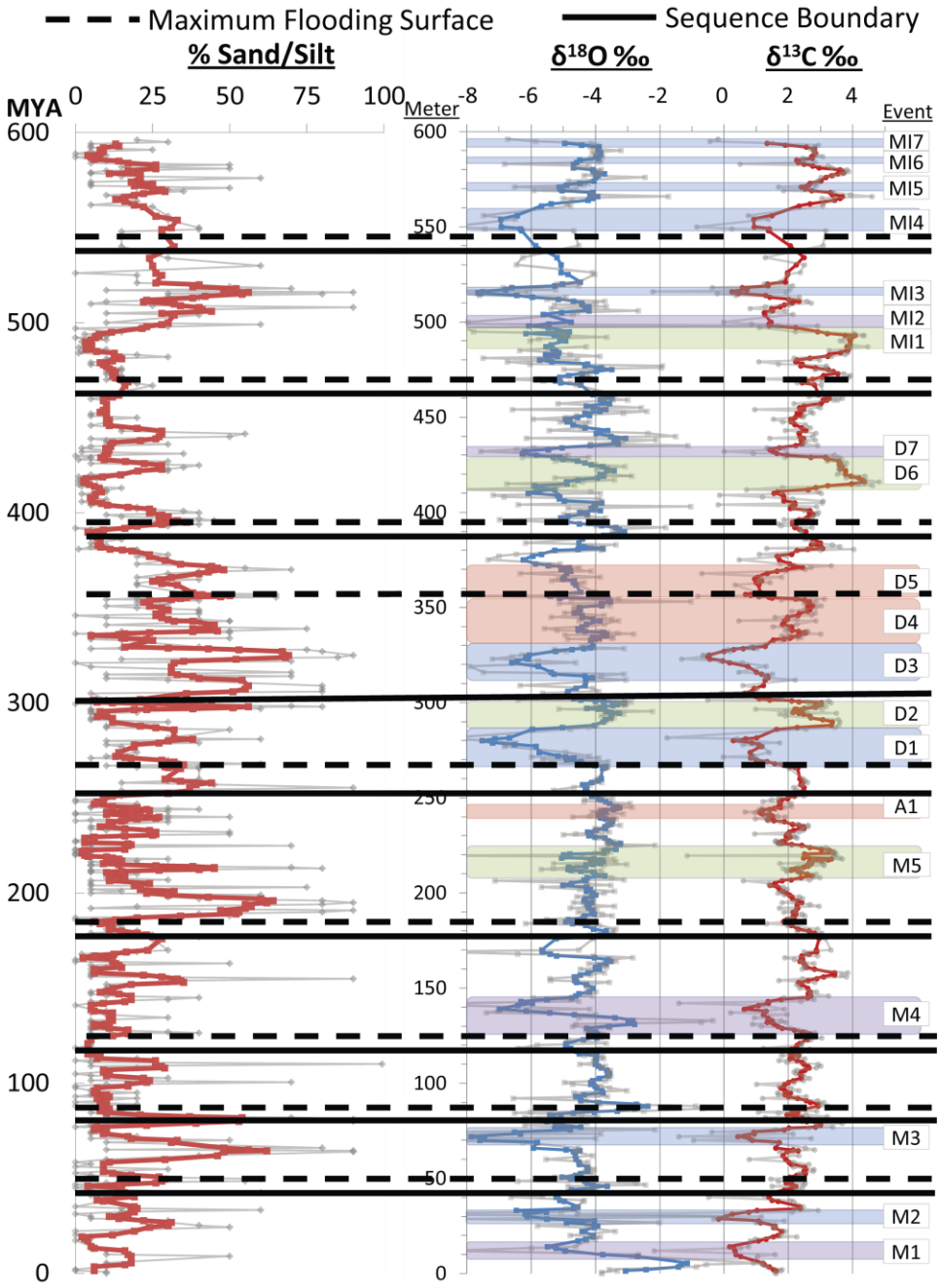

APPENDIX G

FIVE-POINT RUNNING AVERAGES OF $\delta^{13}C$ FROM GALLAGHER PEAK, IDAHO, AND ARROW CANYON, NEVADA NEXT TO $\delta^{13}C$ CURVES OF GALLAGHER PEAK THAT EXCLUDE SAMPLES WITH LOW $\delta^{18}O$ VALUES. THE PLOT ON THE RIGHT ILLUSTRATES HOW SHORT TERM DIAGENETIC EXCURSIONS DROP OUT OF THE PROFILE. THIS ALSO ILLUSTRATES THAT THERE IS LITTLE DIFFERENCE BETWEEN FILTERING SAMPLES WITH $\delta^{18}O$ VALUES LESS THAN -5 VERSES -6‰.

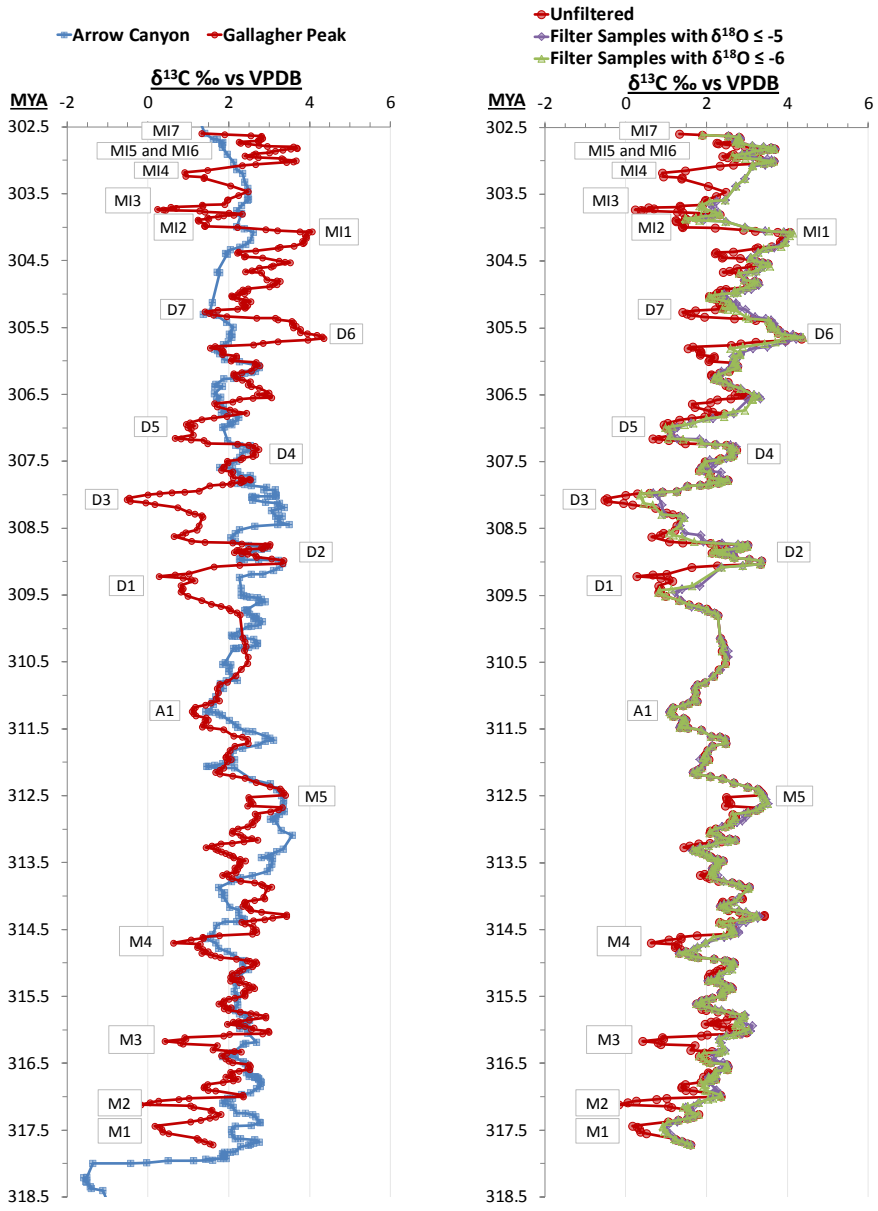

VITA

Name:	Casey Gibson Jolley
Address:	c/o Mike Pope Department of Geology and Geophysics MS 3115, Texas A&M University College Station, Texas 77843-3115
Email Address:	caseyj1202@gmail.com

Education:	B.S., Accounting, Brigham Young University, 2009 Minor, Geology, Brigham Young University, 2009 M.S., Geology, Texas A&M University, 2012
Interests:	Stable isotope geochemistry, Carbonate rocks, Snorkeling, Mountain biking, Scouting, Scuba diving, Camping, Traveling, Piano, Guitar, and Tasting new foods.